APPLICATION OF HYDROPHILIC INTERACTION LIQUID CHROMATOGRAPHY IN ENVIRONMENTAL HEALTH AND PHARMACOTHERAPY STUDIES

Helena Plešnik

Doctoral Dissertation
Jožef Stefan International Postgraduate School
Ljubljana, Slovenia

Supervisor: Assoc. Prof. Dr. Tina Kosjek, IPS and Jožef Stefan Institute, Ljubljana, Slovenia

Evaluation Board:
Prof. Dr. Milena Horvat, Chair, IPS and Jožef Stefan Institute, Ljubljana, Slovenia
Asst. Prof. Dr. Jurij Trontelj, Member, Faculty of Pharmacy, University of Ljubljana, Ljubljana, Slovenia
Prof. Dr. Matej Orešič, Member, School of Medical Sciences, Örebro University, Örebro, Sweden, and Turku Centre for Biotechnology, University of Turku, Finland

MEDNARODNA PODIPLOMSKA ŠOLA JOŽEFA STEFANA
JOŽEF STEFAN INTERNATIONAL POSTGRADUATE SCHOOL



Helena Plešnik

APPLICATION OF HYDROPHILIC INTERACTION LIQUID CHROMATOGRAPHY IN ENVIRONMENTAL HEALTH AND PHARMACOTHERAPY STUDIES

Doctoral Dissertation

UPORABA HIDROFILNE INTERAKCIJSKE TEKOČINSKE KROMATOGRAFIJE V OKOLJSKO ZDRAVSTVENIH IN FARMAKOTERAPEVTSKIH RAZISKAVAH

Doktorska disertacija

Supervisor: Assoc. Prof. Dr. Tina Kosjek

Ljubljana, Slovenia, June 2026

"Little by little, one travels far."

— J. R. R. Tolkien

Acknowledgments

First of all, I would like to express my sincere gratitude to my supervisor, dr. Tina Kosjek. Thank you for your guidance, trust, and support throughout this doctoral journey. Your scientific rigor, critical thinking, and ability to approach problems with clarity have shaped not only this dissertation, but also the way I think as a researcher. I am grateful for the freedom you gave me to develop my own ideas, while always being available when direction or perspective was needed.

My sincere thanks also go to the members of the evaluation committee: Prof. Dr. Milena Horvat, Assoc. Prof. Dr. Jurij Trontelj, and Prof. Dr. Matej Orešič, for accepting this role and for the time and expertise devoted to evaluating this work. I would also like to acknowledge the many collaborators who contributed to different parts of this dissertation. Special thanks to Angelika Vižintin for the collaboration related to bleomycin and electroporation work, and to colleagues at the Faculty of Electrical Engineering, University of Ljubljana, the Veterinary Faculty, University of Ljubljana, the Institute of Oncology Ljubljana, and the Division of Obstetrics and Gynecology, University Medical Centre Ljubljana, whose expertise and support were essential to the studies presented here. My gratitude also extends to collaborators within the European Partnership for the Assessment of Risks from Chemicals project; although too numerous to name individually, their contribution to the broader scientific environment in which this work developed has been highly valuable. Part of this work was also shaped through research exchanges and external collaborations. I would like to thank Jack Steed for hosting me during my visit at SCIEX and for sharing valuable analytical insight. My sincere thanks also go to Tarek Moufawad, Corentin Huet, and dr. Jean-Philippe Antignac for welcoming me at LABERCA and for making my exchange period in France scientifically enriching and personally memorable.

A very special thank you goes to my colleagues at the Jožef Stefan Institute and to former colleagues who remain an important part of this journey: dr. Ana Kovačič, Christoforos Freris, dr. Eirini Andreasidou, dr. Tjaša Gornik, Mohammad Nausad, Brina Pavlovič, Žan Rekar, dr. Žiga Tkalec, dr. Taja Verovšek. Thank you for the discussions, advice, shared frustrations, and many moments that made everyday work lighter. Some of you became much more than colleagues, and that is something I deeply value.

To my friends — thank you for your patience, encouragement, and for reminding me that life exists beyond deadlines, data processing, and unfinished manuscripts. Your support often mattered more than you probably realized. To my family — my parents, Jože and Jožica, my brothers Filip and Florijan, Patricija, and little Bernardka — thank you for being my constant foundation throughout this process. Your support, patience, and quiet confidence carried me through periods when the work felt uncertain, exhausting, or difficult to sustain. Knowing that I could always rely on your encouragement gave me stability far beyond words.

Domen, thank you for your presence, encouragement, and understanding during the final stage of this work. Your support brought calm and perspective at a time when both were especially valuable, and your belief in me meant more than you probably realize.

Abstract

Chemical space coverage remains a major challenge in analytical chemistry. Even with modern instruments and data-processing tools, only a small percentage of all existing organic compounds is detected, let alone identified. Broad range of molecular polarity is one of the main factors influencing this: the most hydrophilic and hydrophobic compounds are often missed, especially in non-targeted workflows that seek broad coverage. This thesis focuses on highly polar compounds analysis and demonstrates the potential of hydrophilic interaction liquid chromatography (HILIC), an increasingly popular but underutilized chromatographic technique.

The work explores HILIC-based LC–MS across three fields: exposure science, metabolomics, and pharmacotherapy. Despite their differences, all three involve analytes that are often poorly retained by conventional reversed-phase (RP) chromatography. This thesis shows that incorporating HILIC into analytical workflows can meaningfully improve their detection and expand the accessible chemical space.

Two studies demonstrated the complementarity of HILIC and RP-based analyses of biologically relevant compounds in non-targeted profiling. An exposure-science-focused study was performed on an ovarian-cancer cohort, applying a fractionation-based sample-preparation approach and discovering 106 exposure biomarkers, six of which differed across groups. HILIC's contribution was assessed as significant since it accounted for 23% of the annotations. The second study, also combining HILIC- and RP-based analysis, was focused both on metabolomics as well as exposure science, analyzing serum and urine samples of women with polycystic ovary syndrome (PCOS), with the aim to identify potential biomarkers of exposure and effect. The analysis revealed alterations in lipids, amino acids, and steroid-related metabolites, spanning a wide polarity range, again supporting the rationale behind the two-column analytical approach.

The pharmacotherapy section of the thesis focuses on bleomycin (BLM), an extremely polar cytostatic drug that has very limited number of published quantitative analytical methods. Two methodological papers are presented, introducing two high-performance analytical methods: one was developed and validated for the quantification of BLM in clinically relevant concentrations and matrices (blood-derived samples), and the other for the quantification of intracellular BLM to support in vitro experiments in the optimization of electrochemotherapy procedures. To the best of our knowledge, these studies represent the first validated analytical methods enabling reliable quantification of bleomycin in the respective experimental and clinical contexts. Beyond the analytical methods themselves, both studies also address practical considerations and common analytical challenges associated with the measurement of highly polar and structurally complex compounds.

The studies in this thesis demonstrate that incorporating HILIC into LC–MS workflows can substantially improve access to the polar end of chemical space across biomedical and environmental applications. The work provides validated methods, transferable workflows, and practical guidance that support more comprehensive analytical strategies in both targeted and non-targeted settings.

Povzetek

Pokritost kemijskega prostora ostaja eden večjih izzivov analizne kemije. Kljub naprednim instrumentom in orodjem za obdelavo podatkov je še vedno mogoče določiti le manjši delež vseh obstoječih organskih spojin. Eden izmed omejujočih dejavnikov je polarnost, saj najbolj hidrofilne in hidrofobne spojine pogosto ostanejo spregledane. To je še posebej očitno pri netarčnih pristopih, ki stremijo k čim širši pokritosti kemijskega prostora. Moja disertacija se osredotoča na zelo polarne spojine ter preučuje potencial hidrofilne interakcijske tekočinske kromatografije (HILIC), vse bolj priljubljene, a premalo izkoriščene kromatografske tehnike.

Prikazana je uporaba HILIC kromatografije na treh področjih: v študijah izpostavljenosti, metabolomiki in farmakoterapiji. Čeprav se področja razlikujejo, jih povezuje skupen analitski izziv: številni pomembni analiti (metaboliti, kontaminanti in terapevtiki) so zelo polarni in se slabo zadržujejo na konvencionalnih reverznofaznih kolonah (RP), zato jih s slednjimi ni mogoče ustrezno določiti. Disertacija skozi aplikativne primere pokaže, kako vključitev HILIC-a v LC–MS protokole izboljša detekcijo polarnih spojin ter razširi dostopni kemijski prostor.

Njegovo uporabnost v študijah izpostavljenosti smo prikazali z razvojem analizne metode za profiliranje biomarkerjev izpostavljenosti v urinu, uporabljene na vzorcih kohorte bolnic z rakom jajčnikov. Z metodo priprave vzorcev na podlagi frakcioniranja smo iz enega alikvota urina dobili dva komplementarna ekstrakta – za HILIC in RP –, kar je bistveno razširilo kemijsko pokritost brez večje porabe vzorca. Skupno smo anotirali 106 biomarkerjev izpostavljenosti, med njimi šest s statistično značilnimi razlikami med bolnimi in zdravimi osebami. Prispevek HILIC metode je bil pomemben, saj je prispeval 23 % anotacij, ki jih z RP kromatografijo nismo zaznali.

V drugi študiji, ki je prav tako združevala HILIC in RP, smo analizirali vzorce seruma in urina žensk s sindromom policističnih jajčnikov (PCOS) z namenom identifikacije potencialnih endogenih in eksogenih biomarkerjev. Rezultati so ponovno potrdili smiselnost analitskega pristopa z dvema kolonama ter pokazali spremembe v vsebnosti lipidov, aminokislin in steroidnih metabolitov.

Del disertacije, ki obravnava podporo farmakoterapiji, se osredotoča na bleomicin (BLM), izredno polaren citostatik, za katerega doslej, z izjemo naše, še ni bilo objavljenih selektivnih analiznih metod za kvantitativno določanje. Predstavljena sta dva metodološka članka: ena metoda je bila razvita in validirana za kvantifikacijo BLM v klinično relevantnih koncentracijah in krvnih vzorcih, druga pa za kvantifikacijo znotrajceličnega BLM pri optimizaciji postopkov elektrokemoterapije in vitro. Kolikor je razvidno iz literature, predstavljata ti metodi prve validirane pristope za zanesljivo kvantifikacijo bleomicina v navedenih kontekstih. Obe študiji poleg razvoja metod obravnavata tudi praktične analitske ovire pri analizi visoko polarnih in strukturno kompleksnih spojin.

Rezultati te naloge potrjujejo, da vključitev HILIC v LC–MS analize v biomedicinskem in okoljskem kontekstu bistveno olajša analizo polarnih spojin. Predstavljene so validirane metode ter praktična priporočila za izvajanje tarčnih in netarčnih analiz z uporabo HILIC kromatografije.

Contents

List of Figures **xv**

Abbreviations **xvii**

1 Introduction **1**
1.1 Bioanalytics and Polar Compounds 1
1.1.1 Chemical space as a concept 1
1.1.2 Chemical space coverage 2
1.1.3 Polarity coverage and small polar compounds in liquid chromatography coupled to mass spectrometry (LC-MS) 3
1.2 Fundamentals of HILIC 4
1.2.1 HILIC: retention mechanisms, stationary and mobile phases 4
1.2.2 Advantages and challenges of using HILIC in LC-MS analyses 6
1.2.3 Current applications of HILIC-based methods 7
1.3 Metabolomics: Analysis of Polar Metabolites 7
1.3.1 Basics of metabolomics: role, scope, biomarkers 7
1.3.2 Analytical needs and challenges in metabolomics 8
1.3.3 Polar metabolome and HILIC in metabolomics 10
1.3.4 RP/HILIC complementarity and benefits 11
1.4 Exposure Science and Exposomics: Analysis of Polar Biomarkers of Exposure 11
1.4.1 Human exposure to chemicals 11
1.4.2 Analytical needs and challenges in metabolomics and exposure science 12
1.4.3 Polar BoEs and HILIC in exposure science 14
1.5 Data Processing, Quality Assurance and Quality Control (QA/QC) in Non-Targeted Studies 15
1.6 Pharmacotherapy and Therapeutic Drug Monitoring (TDM) 19
1.6.1 Analytical roles of LC–MS in support to pharmacotherapy and TDM 19
1.6.2 Polar cytostatics 20
1.6.3 Case study: Bleomycin — analytical and pharmacological challenges associated with a polar cytostatic 21
1.6.3.1 Pharmacological challenges related to Bleomycin 21
1.6.3.2 Analytical methods for bleomycin quantification 21
1.6.3.3 Extending the case study: parallels with other hydrophilic drugs 23

2 Aims and Hypotheses **25**

3 Publications **29**
3.1 Development and Application of an Integrated HILIC-RP NT Workflow for Comprehensive Polarity Coverage in Exposure Science 29
3.1.1 Nontargeted urinary profiling strategy for endocrine-disrupting chemicals in women with ovarian malignancies 29

3.1.2 Comparative assessment of suspect / non-target screening workflows for characterizing occupational human internal chemical exposure: results of a European interlaboratory study from the EU-PARC project 42
3.1.3 Comparing non-targeted screening workflows for perinatal chemical exposome analysis: a European interlaboratory study from the PARC EU project 84
3.2 Application of HILIC in Non-Targeted Metabolomics for Extended Coverage of Polar Metabolites 108
3.2.1 Integrated non-targeted exposomics and metabolomics reveal elevated endocrine-disrupting chemical burden and altered steroid metabolism in women with PCOS 108
3.2 The Use of HILIC-based Workflows for Metabolite Profiling in Other Biological Matrices 140
3.2.1 Foliar application of protein hydrolysates promotes growth and affects leaf ionome in olive 140
3.3 HILIC in Targeted Compound Monitoring for Pharmacotherapy and TDM ... 161
3.3.1 An effective validation of analytical method for determination of a polar complexing agent: the illustrative case of cytotoxic bleomycin 161
3.3.2 Quantitative analysis of trace-level bleomycin in complex matrices: application to in vitro electrochemotherapy 174
3.3.3 Support to TDM in clinical study attempting to reduce the dosage of API and thus reduce adverse effects: bleomycin concentration in patients' plasma and tumors after electrochemotherapy. A study from InspECT group 184

4 Conclusions and Future Perspectives **197**

References **201**

Bibliography **213**

Biography **217**

List of Figures

Figure 1.: Chemical space divided into unknown, detectable and identifiable space, adapted from Black et al.....2
Figure 2.: Distribution of monoisotopic mass and XLogP values of substances from the NORMAN Substance Database with reported ChemSpider XLogP values. 14
Figure 3.: Structures of bleomycin-copper complexes for A2, B2 and A5 congeners, illustrating the functional domains 23

Abbreviations

ADME	...	absorption, distribution, metabolism, and excretion
ANP	...	aqueous normal phase
API	...	active pharmaceutical ingredient
AUC	...	area under the curve
BEH	...	bridged ethylene hybrid
BLM	...	bleomycin
BLMH	...	bleomycin hydrolase
BoE	...	biomarker of exposure
CAS	...	Chemical Abstracts Service
CE	...	capillary electrophoresis
ChEBI	...	Chemical Entities of Biological Interest
CHMS	...	Canadian Health Measures Survey
CRM	...	certified reference material
CRS	...	Chemical Reference Substance (Ph. Eur.)
Cu–BLM	...	copper–bleomycin complex
DDA	...	data-dependent acquisition
DIA	...	data-independent acquisition
DMSO	...	dimethyl sulfoxide
DNA	...	deoxyribonucleic acid
ECT	...	electrochemotherapy
ELSD	...	evaporative light scattering detection
EMA	...	European Medicines Agency
ESI	...	electrospray ionization
FAIR	...	findable, accessible, interoperable, reusable
GC	...	gas chromatography
GC-MS	...	gas chromatography–mass spectrometry
GDB	...	generated database
GDPR	...	General Data Protection Regulation
GNPS	...	Global Natural Products Social Molecular Networking
HBM4EU	...	Human Biomonitoring for Europe
HILIC	...	hydrophilic interaction liquid chromatography
HMDB	...	Human Metabolome Database
HPLC	...	high-performance liquid chromatography
HRMS	...	high-resolution mass spectrometry
IARC	...	International Agency for Research on Cancer
InChI	...	International Chemical Identifier

IS	...	internal standard
KEGG	...	Kyoto Encyclopedia of Genes and Genomes
LC–MS	...	liquid chromatography–mass spectrometry
LC×LC	...	two-dimensional liquid chromatography
LLOQ	...	lower limit of quantification
MoNA	...	MassBank of North America
MRM	...	multiple reaction monitoring
MS1	...	full-scan mass spectrometry
MS2	...	tandem mass spectrometry
NT	...	non-targeted
PARC	...	Partnership for the Assessment of Risks from Chemicals
Ph. Eur.	...	European Pharmacopoeia
PubChem	...	PubChem chemical database
QA/QC	...	quality assurance and quality control
QC	...	quality control
RP	...	reversed-phase
RPLC	...	reversed-phase liquid chromatography
RNA	...	ribonucleic acid
RT	...	retention time
S/N	...	signal-to-noise ratio
SPE	...	solid-phase extraction
SS	...	suspect screening
SMILES	...	Simplified Molecular-Input Line-Entry System
TDM	...	therapeutic drug monitoring
TIC	...	total ion current
UHPLC	...	ultra-high-performance liquid chromatography
XLogP	...	predicted logP value (octanol–water partition coefficient)

Chapter 1

Introduction

1.1 Bioanalytics and Polar Compounds

1.1.1 Chemical space as a concept

The number of distinct organic molecules in existence is extraordinarily large and continues to grow. One of the naturally occurring questions in analytical chemistry is therefore: What is the actual number? This is followed by a more important question: How many of those are we actually able to detect and identify with current analytical tools? The totality, so all existing chemicals, has been defined as the ‘chemical space’, a concept that first appeared in the field of drug discovery to describe the enormous diversity of molecular structures that could, in principle, be designed or synthesized as potential bioactive compounds.

All chemical structures which are theoretically possible according to the laws of organic chemistry have been systematically enumerated, generating extremely large databases. GDB-17 (Generated Database 17) is one example of such computational/theoretical databases. It includes approximately 166.4 billion molecules (up to 17 atoms comprising C, N, O, S, and halogens), representing one of the largest compilations of small organic molecules generated to date [1]. It is important to note that these structures are not experimentally observed; they exist only as theoretical connectivity graphs defined by identifiers such as Simplified Molecular-Input Line-Entry System (SMILES) or International Chemical Identifier (InChI). Experimental databases, in contrast, are much smaller. PubChem describes only roughly 123 million unique chemical structures (as of January 2026) and CAS Registry about 275 million (as of January 2026). This means that current public collections represent only a minute fraction (well below 0.001%) of the conceivable chemical universe. These entries are considerably more extensive and include, in addition to structural identifiers, also experimental metadata such as various spectra (mass, UV, NMR etc.), physicochemical properties, biological activity, and bibliographic information [2]

Current efforts continue to expand both theoretical and experimental databases. Cheminformatics expands theoretical databases through additional molecular enumeration, improving coverage of the possible structure space. Experimental databases on the other hand expand through the addition of newly synthesized, isolated, or detected compounds, each accompanied by experimental annotations. For analytical sciences, particularly non-targeted LC-MS-based analyses, this expansion is essential: theoretical databases supply structural candidates for in-silico matching, while experimental databases provide the annotated spectra and metadata needed to evaluate and confirm real signals.

1.1.2 Chemical space coverage

The whole chemical space can be divided into individual subsets, most importantly measurable and identifiable space, which are much more informative for analytical sciences. These subsets can be defined for individual analytical methods or for the combined capabilities of current technology and expertise, representing what can realistically be achieved today. The so-called "detectable space" can be visualized as a relatively small subset of compounds within the whole chemical universe, while the "identifiable space" forms an even smaller subset within the detectable one, comprising compounds that can be identified, e.g. fully characterized (Fig. 1)

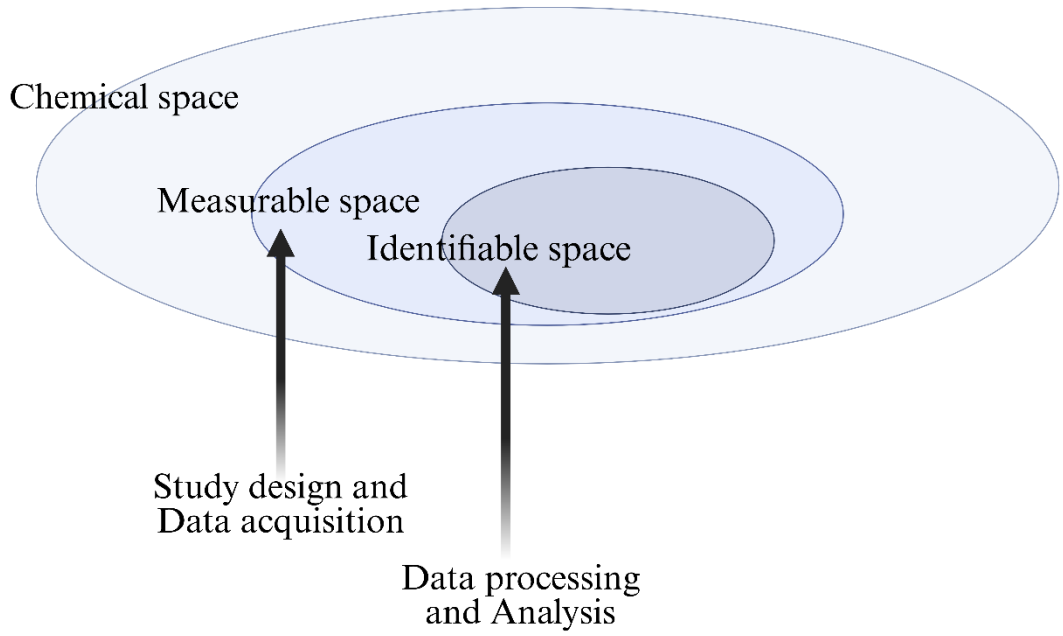


Figure 1: Chemical space divided into unknown, detectable and identifiable space, adapted from Black et al.

Defining the **measurable chemical space** serves as an assessment of the appropriateness of the selected analytical method for its intended application and can be either tested or calculated using existing models such as Chemspace [3]. Its size depends on study design and method's data acquisition strategy and is essentially an intersection of:

a) **Sampleable space** (compounds present in the chosen biological or environmental matrix);

b) **Extractable space** (defined by sample preparation protocols, including solvent choice, pH, extraction/cleanup media, and elution conditions);

c) **Separable space** (defined by chromatographic separation and instrumental platform);

d) **Detectable space** (instrumentation- and ionization-dependent, influenced by sensitivity and ionization efficiency) [3].

Finally, the **identifiable space** – the smallest subset within the measurable space – comprises only features to which a structure can be annotated with sufficient confidence. Its size is dependent on the availability, coverage, and quality of spectral libraries, reference standards, and auxiliary annotation tools, discussed later in the thesis. Because these resources remain incomplete, particularly for highly polar and environmentally relevant compounds, the identifiable space is typically only a small fraction of the total chemical space accessible to the method [3].

It is important to note that poor coverage of the relevant chemical space is not always the case. In drug discovery, for example, the measurable chemical space is often far larger than the pharmacologically relevant space. The opposite tends to be true in some other contexts, such as metabolomics, where the space of relevant small molecules and environmental exposures vastly exceeds what is currently measurable. Expanding the coverage of the measurable chemical space is therefore a priority in such fields and is being actively pursued through both technological and methodological innovation.

1.1.3 Polarity coverage and small polar compounds in liquid chromatography coupled to mass spectrometry (LC-MS)

When discussing chemical space coverage, compounds' polarity is one important factor that needs to be considered as it is directly linked to the separable chemical space. Most routinely used chromatographic workflows, especially in non-targeted screening, are optimized for compounds of intermediate polarity, whereas the extremes (both highly hydrophobic and hydrophilic analytes) remain insufficiently addressed.

This thesis focuses on these issues from the perspective of LC–MS, the dominant platform for small-molecule analysis across biomedical, pharmaceutical, and environmental sciences. Its broad dynamic range, sensitivity, and possibility of high-resolution detection make it indispensable for both targeted and untargeted applications [4, 5]. LC-MS-based analytical workflows most commonly apply reversed-phase (RP) chromatography, which uses hydrophobic stationary phases and decreasing-polarity gradients and retain non-polar to moderately polar compounds. Polar analytes in these conditions usually express either very poor retention or no retention at all, eluting in the void volume, which results in analytical blind spots [6].

As a consequence, the part of the relevant chemical space containing highly polar compounds remains underrepresented in analytical studies. Many polar compounds are however of high relevance to the research areas addressed in this thesis. Several endogenous metabolites (e.g., amino acids, nucleotides, central energy intermediates), environmental exposures and their metabolites (e.g. biomarkers of exposure), and active pharmaceutical ingredients (APIs) used in pharmacotherapy fall into this category [2, 7]. Their accurate measurement is critical for advancing metabolomics, exposomics, and therapeutic drug monitoring. Each of these areas will be discussed in detail in Chapters 1.3 -1.5.

Approaches, specifically designed for polar analytes, most notably hydrophilic interaction liquid chromatography (HILIC), extend separation into the hydrophilic range and have already demonstrated clear benefits in metabolomics and pharmacotherapy applications [8, 9, 10]. Expanding coverage towards the polar domain is therefore both an analytical challenge and a central motivation for the implementation of HILIC, which remains underexplored despite many recent advances.

The overall aim of this thesis is to explore and demonstrate the analytical versatility of HILIC in detecting the polar domain of chemical space. Through three case areas– metabolomics, exposure science, and pharmacotherapy–it examines how HILIC-based LC-MS workflows expand analytical coverage for compounds that are inaccessible to the

classical reversed-phase methods. Addressing its use in targeted and non-targeted approaches, dealing with multiple analyte and matrix types, the work highlights the capacity of HILIC to address diverse analytical needs across environmental, health and clinical contexts.

1.2 Fundamentals of HILIC

1.2.1 HILIC: retention mechanisms, stationary and mobile phases

The chromatographic mode first intended for the separation of polar metabolites was normal-phase chromatography, initially developed using silica as the stationary phase and non-polar solvents as the mobile phase. However, due to several limitations, such as incompatibility with mass spectrometry, poor peak shapes and limited robustness, this approach is now rarely used [11]. Nevertheless, it served as the foundation for the development of:
-**Reversed-phase chromatography (RP)**, currently the most widely used LC-MS technique for semi- to non-polar compounds;
-**Aqueous Normal Phase (ANP)** and **Hydrophilic Interaction Liquid Chromatography (HILIC)** as MS-compatible approaches for polar analytes.

ANP and HILIC, though the names are sometimes used interchangeably, as they both operate with gradients from high-organic to more aqueous conditions and retain polar compounds, differ in their stationary phases and retention mechanisms. The main difference, distinguishing the two is the formation of a stable water-enriched layer at the stationary phase surface, which is the main driver for retention in HILIC but does not appear in ANP [12, 13]. Retention in ANP is instead dominated by adsorption mechanisms, making ANP mechanistically closer to classical normal-phase chromatography but with MS-compatible mobile phases (most commonly acetonitrile with small amounts of water or alcohols). It employs low-silanol type-C silica with silicon-hydride groups and minimal residual silanol content (<5%). This reduces unwanted secondary interactions and yields improved peak shapes compared to traditional silica [14]. Two further distinctions are often noted: Firstly, HILIC stationary phases are generally more polar than ANP phases, so moderately polar compounds sometimes show stronger retention in ANP. Secondly, the absence of a water layer in ANP enables the use of very rapid gradients and shorter equilibration time, which is in HILIC crucial for aqueous layer stabilization [15].

HILIC itself was first introduced by Alpert in 1990 [12]. Despite its potential, adoption was initially slow due to challenges in method development and robustness. Interest grew substantially in the late 2000s, following influential reviews such as Hemström and Irgum [16] and by the early 2010s HILIC had become widely implemented. Its applications have since expanded far beyond initial metabolite studies, encompassing biomarkers, nucleosides, nucleotides, amino acids, peptides, saccharides, glycosides, oligosaccharides, hydrophilic drugs, alkaloids, and many other small polar or ionizable compounds [11, 13]. Today, HILIC is after reversed-phase the second most widely used chromatographic mode in LC-MS [17].

Retention mechanisms differ from RP chromatography significantly. The main retention mechanism in RP is partitioning of analytes between the aqueous mobile phase and the hydrophobic stationary phase with additional contributions arising from surface adsorption and electrostatic interactions [18, 19]. In HILIC, however, it is predominantly hydrophilic partitioning between an aqueous-organic mobile phase and a water-rich liquid layer immobilized on the stationary phase. Apart from this, multiple other mechanisms are present in HILIC and include:

-**hydrogen-bonding** between analytes and stationary phase or bound water,
-**dipole-dipole interactions**,
-**electrostatic interactions**, both attractive and repulsive, depending on surface charge and analyte properties;
-**molecular shape selectivity**, particularly with sterically demanding stationary phases
-**hydrophobic effect,** whereby nonpolar moieties of analytes preferentially associate with less polar regions of the stationary phase, contributing marginally to retention [20, 21]

The predominant mechanism for a compound in a certain stationary phase however varies and is difficult to define or quantify. Still, models have been developed for the quantitative assessment of retention mechanisms [22].

Stationary phases. Due to the recent surge in the popularity of HILIC, a wide range of stationary phases is now available. These include silica-based phases (bare silica or silica modified with polar functional groups), organic polymers, and alternative inorganic supports such as biosilica [23, 24]. Even bare silica exists in different variants which can be classified as:

-**Type A**, obtained by precipitation of silicates from solutions, with relatively high acidity;
-**Type B**, formed by aggregation of silica sols in air, more stable at high pH;
-**Type C**, featuring hydrosilated surfaces with reduced silanol activity.

More commonly, however, HILIC employs surface-modified silica phases. The development began with first-generation amino-silica phases (introduced in 1975), followed by second-generation phases such as diol- and amide-modified silica, and has since advanced to various mixed-mode and multiple-interaction stationary phases designed to broaden selectivity and enhance robustness [14, 25].

Many commercially available chromatographic columns are on the market today, some of the most commonly used include unbonded silica (Accucore HILIC, CORTECS HILIC), diol (Kromasil Diol, Luna HILIC), cyano (Kromasil Cyano, HSS Cyano), amino (TSKgel NH2), amide (TSKgel Amide 80, XBridge BEH Amide, Accucore Amide, Acquity UPLC BEH Amide), zwitterionic (ZIC-HILIC, ZIC-cHILIC) and others. In addition to these, numerous non-commercial phases have been developed in academic settings, often based on polymer-coated or functionalized silica. Such custom materials aim to address specific analytical challenges by offering tailored selectivity, improved stability, and reduced stationary phase bleeding–features particularly useful for the analysis of complex and highly polar analytes [24].

Mobile phases in HILIC typically consist of a water-miscible polar organic solvents or aprotic solvents combined with a small amount of water or volatile buffer. This composition enables the formation of a semi-immobilized aqueous layer on the stationary phase, which is essential for hydrophilic partitioning [12]. Acetonitrile is by far the most common organic component. It is polar and aprotic, highly miscible with water, and exhibits high volatility and relatively low viscosity. Its low hydrogen bond donor capability facilitates solvatation of salts, which are often used in the mobile phase. These properties make it ideal for HILIC [16]. A minimum of ~2% water is required in the mobile phase to establish the partially immobilized water layer. The gradient in metabolomic application does not reach over 40% of aqueous phase since higher percentages can also disrupt this layer and with that the whole mechanism, leading to longer equilibration times needed for its reestablishment [26].

Volatile salts and buffers can be added to control ionic strength and pH, provided they remain soluble in high-organic eluents. The most commonly employed buffers are ammonium acetate (effective buffering range pH 3.8-5.8) and ammonium formate (buffering range pH 2.7-4.7) [14] Buffer concentration influences the thickness and polarity of the water layer, thereby modulating both partitioning and retention. Higher ionic strength generally increases water layer thickness, but also shields electrostatic interactions: for example, higher salt concentrations can reduce anion retention on cationic phases, while increasing retention on anionic phases [11]. At higher buffer concentrations, it is vital that the mobile phase contains a sufficient percentage of water to ensure solvation [26].

Mobile phase composition, particularly pH and buffer concentration, strongly affect retention time reproducibility in HILIC. Alternative additives are sometimes employed in place of buffers, including formic or acetic acid and, less frequently, trifluoroacetic acid, methanesulfonic acid, or phosphate salts [16]. Choice of additive depends on analyte chemistry and the balance between chromatographic performance and MS compatibility.

1.2.2 Advantages and challenges of using HILIC in LC-MS analyses

Using HILIC in LC–MS offers a few clear benefits that come directly from how this technique works. The high percentage of organic mobile phase means lower viscosity of the mobile phase in comparison to RPLC and consequently lower back pressure. This enables the application of higher flow rates than with RP columns, use of smaller particles or longer columns [16]. High organic portion of the mobile phase also increases its volatility, leading to better detection sensitivity when using evaporative light scattering detection (ELSD) and electrospray ionization (ESI) detection techniques [26]. Another key advantage is HILIC' s orthogonality to RPLC, which makes it well suited for two-dimensional LC (2D-LC) workflows, either in online or offline formats [14], which significantly extends chemical space coverage when combined with RP.

Despite these advantages, HILIC also presents some practical limitations, the most frequently mentioned are the following:

-**Longer equilibration times** are often required due to the dynamics of re-establishing the stationary water layer;
-**Retention-time reproducibility** can be strongly affected by small variations in water or buffer content;
-**Method development is less standardized**, with retention mechanisms varying between stationary phases and analyte classes

These challenges were the reason for the slow start of HILIC applications despite its clear benefits in polarity coverage. However, much has changed with the recent developments, including the commercialization of HILIC columns, improved particle chemistry and morphology (smaller particles, core-shell technology), better understanding of retention, and development of guidelines.

There are other factors that require more attention, although they are not limitations per se:

Retention time prediction. Due to the complex retention mechanisms in HILIC, which significantly differs from RPLC, predicting retention times is for HILIC-based analyses less straightforward. Multiple factors, including partitioning, adsorption, electrostatic effects, and buffer composition, can all contribute to varying degrees depending on analyte and stationary phase. As a result, predictive models for HILIC

retention currently remain less mature and less accurate than those established for RP [27]. This complexity affects the downstream use of retention time as an important parameter in compound annotation.

Injection solvent and volume. Injection solvent compatibility is more critical in HILIC than in RP applications. Large deviations from the starting mobile phase composition, particularly higher percentages of water, act as a strong eluent, distorting peak shape and width. This presents a challenge for highly polar compounds with limited solubility in acetonitrile, the preferred solvent in HILIC. Substituting acetonitrile for different organic solvents can introduce additional issues. Polar protic solvents such as methanol or ethanol form strong hydrogen bonds, destabilizing the stationary water layer and resulting in poor peak shapes. Alternatives such as isopropanol (IPA), which is less disruptive, have been tested but do not consistently yield satisfactory performance [28]. Dimethyl sulfoxide (DMSO) is unsuitable as a full replacement for acetonitrile, but mixtures such as 70:30 acetonitrile-DMSO have been reported to provide acceptable peak shapes [28].

1.2.3 Current applications of HILIC-based methods

The need to cover the analysis of the polar chemical space exists in various fields where HILIC-based (or ANP-based) methods have been adopted (in some to a higher, in some to a lower degree). HILIC has found broader utility in several other areas of modern analytical chemistry. These include pharmaceutical analysis, where it is used both in drug discovery and in therapeutic drug monitoring; biochemistry, where it supports the characterization of highly polar biomolecules in various omics disciplines; as well as the food safety and environmental and health studies, where it enables the analysis of sugars, vitamins, additives, and, importantly, organic contaminants and exposure biomarkers in environmental and biological samples. Its application in **metabolomics**, **exposure science**, and **pharmacology** will be discussed in the following chapters.

1.3 Metabolomics: Analysis of Polar Metabolites

1.3.1 Basics of metabolomics: role, scope, biomarkers

Metabolomics, or the study of the metabolome, has developed over more than two decades into a well-established branch of the omics sciences. It is now recognized as a central tool in systems biology, with applications in plant, microbial, and mammalian research [29, 30]. As the name implies, the main task of metabolomics is assessing the metabolome - the complete set of small-molecule metabolites, produced or modified by a biological system [31]. These include products of gene expression and regulation, in itself studied by genomics, transcriptomics and proteomics, as well as compounds that reflect interactions with the external environment, together providing a comprehensive biochemical profile of cellular and organismal function [7].

Molecular changes within the metabolome can often be linked to clinical outcomes, helping to uncover disease mechanisms and identify potential biomarkers. In biomedical and environmental contexts, biomarkers are defined as measurable indicators of biological processes, disease states, or exposures [32, 33]. Because metabolites respond quickly to physiological and environmental disturbances, they provide sensitive and early signals of change, reflecting both the causes and consequences of altered metabolism. This gives metabolomics strong diagnostic and prognostic potential, making it an indispensable tool across biomedical research, toxicology, nutrition, pharmacology, and environmental health.

The metabolome comes from both endogenous (internally produced) and exogenous (externally introduced) sources. The dual origin makes metabolomics relevant not only in disease biomarker discovery but also in assessing environmental exposures and biological responses to them. For instance, exposomics, a related subdiscipline, focuses specifically on the external component of the metabolome and has gained prominence in environmental health research [34]. Exposomics will be further discussed in Chapter 1.4. Other branches include lipidomics [35], metallomics [36], and metabonomics [29], each focusing on a defined dimension of the metabolome.

Applications span both in vivo and in vitro systems, studying clinical cohorts as well as controlled experimental models [7]. The selection and handling of biological matrices strongly influence the obtained metabolomic profile, as metabolite composition, abundance, and stability differ significantly across sample types. Moreover, biological variability, depending on factors such as age, sex, diet, microbiome composition, circadian rhythm, and health status, further affects the metabolome and should be carefully accounted for in study design, normalization, and data interpretation.

1.3.2 Analytical needs and challenges in metabolomics

Analytical platforms supporting metabolomics are predominantly mass spectrometry (MS)-based. The main separation-detection combination is liquid chromatography-mass spectrometry (LC-MS), followed by gas chromatography-mass spectrometry (GC-MS). Nuclear magnetic resonance (NMR) spectroscopy remains an important complementary approach, as well as capillary electrophoresis-MS (CE-MS) [37]. Despite the important advances made in metabolomics studies, a comprehensive analysis of metabolism on one single analytical platform is, due to the nature of metabolome, far from possible. Combining multiple orthogonal methods is therefore currently considered the best option as it provides largest coverage of the relevant chemical space [38].

Samples. Metabolomics studies are performed on diverse biological matrices. Biofluids such as urine, serum, plasma, and saliva are most commonly used for biomarker discovery, as they are accessible, non- or minimally invasive, and reflective of systemic metabolism. For studying mechanistic pathways and localized pathophysiological processes however, cellular and tissue samples are more often employed. The samples are collected in a manner that protects sample integrity as much as possible. This includes immediately stopping all enzymatic activity, which is typically performed via rapid freezing using liquid nitrogen, dry ice or freeze-clamping, sometimes combined with organic solvent addition [39, 40, 41].

Sample preparation procedures vary depending on the sample type and analytical techniques, with the main objective of removing salts, bulk proteins and other matrix constituents while preserving the metabolome to the highest possible degree. The procedure is ideally simple, fast, reproducible, and unbiased, and is crucial for the accuracy of profiled metabolome and the resulting biochemical findings [38, 42]. Biofluids can be analyzed with minimal to no preparation. Urine is often analyzed directly without any extraction, and is usually just diluted. Minimal tampering results in minimal analyte losses but keeps all the matrix (in context of urine, this mostly involves salts), which cause ionization suppression and altered adduct formation. Blood-derived samples are usually subjected to organic-solvent-based protein precipitation or liquid-liquid extraction to remove bulk proteins and salts while retaining a broad range of metabolites [43, 44]. Solid-phase extraction and microextraction are used less frequently but offer higher selectivity and can improve dynamic range when matrix effects are critical. [45] In some workflows, biphasic or fractionated extraction is applied, separating polar and non-polar metabolites for subsequent analysis by complementary chromatographic modes. This was first used in the field of multi-omics to extract pure lipids from the rest of the metabolites [46, 47, 48].

Preparation of tissue and cell samples is somewhat more complex, requiring additional steps (such as lyophilization, homogenization, etc.) before extraction. Homogenization physically disrupts the tissue using a homogenizer and is widely employed, though relatively impractical for small sample amounts [49]. Alternatively, lyophilization or freeze-drying can be used and has proven suitable especially for wet tissues. By removing water, the results can be reported as quantities per dry sample weight, which is better for comparative analysis than reporting values relative to the original wet weight, where water content can differ between samples [50]. Sample preparation protocols are currently still not standardized, as procedures are typically adapted to the matrix, platform, and study objectives. However, greater harmonization of workflows would substantially improve interlaboratory comparability and data reproducibility [51]

Data acquisition. The two different approaches for profiling metabolites are targeted and non-targeted analyses. Targeted workflows quantify small predefined sets of metabolites, linked to specific pathways or hypotheses. The methods are optimized for a specific set of compounds, with every step of the workflow, from sample preparation to data processing, optimized and validated to ensure optimal performance and accurate quantification. As a result, they typically offer superior sensitivity, selectivity, and quantitative reliability compared to non-targeted methods.

Non-targeted approaches, on the other hand, aim for comprehensive profiling, acquiring data on as many features as possible in an unbiased manner, ideally covering all the small molecules present in a sample. Within the non-targeted domain, suspect screening (SS) targets compounds from predefined candidate lists, whereas non-targeted screening (NTS) remains open-ended. Both rely on high-resolution mass spectrometry (HRMS), typically operated in one of three acquisition modes: full-scan (MS1-only), data-dependent acquisition (DDA), and data-independent acquisition (DIA). Full-scan acquisition records accurate m/z values and signal intensities for all ions present in the samples, providing high sensitivity and the largest number of MS1 features among the three modes. MS2 spectra, important for compound annotation, are acquired either by DDA or DIA. DDA selectively fragments a limited number of the most intense precursor ions per scan, producing spectra of high quality but lower coverage compared to DIA, where all ions within defined m/z windows are fragmented, resulting in a substantially higher number of MS2 spectra, though with more complex data and lower spectral specificity [52].

Following data acquisition, data treatment represents the most complex and time-consuming stage of non-targeted LC-MS metabolomics. Its objective is to transform raw data into structured, interpretable profiles suitable for statistical analysis. Preprocessing typically includes the following steps: denoising and baseline correction, retention-time alignment across samples, peak detection, peak merging, and the generation of a data matrix summarizing all detected features. These steps can be performed using vendor-specific or open-source software tools. Subsequent processing involves handling missing or zero values, removing outliers, and applying normalization, centering, and scaling to ensure comparability across samples [53].

Metabolite annotation remains one of the most critical and challenging steps in untargeted metabolomics. Only a small fraction of detected signals can be confidently assigned to known compounds, as spectral databases cover only a limited part of the chemical space. Identification generally relies on matching experimental data to reference libraries or in silico predictions. This is explained in more detail in Chapter 1.5.

While metabolomics has become central to biomedical and environmental sciences, its analytical implementation faces persistent obstacles. These stem from the immense chemical diversity of metabolites, their broad concentration ranges, the complexity of biological matrices, and incomplete reference resources. The main analytical challenges are described below.

Chemical diversity and structural heterogeneity of the metabolome. The metabolome encompasses chemically diverse molecules ranging from highly lipophilic steroids to hydrophilic nucleotides. Functional group diversity, isomerism, and the presence of conjugated metabolites further complicate separation and detection. No single platform can provide full coverage, hence the need for complementary approaches such as LC-MS, GC-MS, CE-MS, and NMR [2].

Concentration range and dynamic range limitations. Metabolite concentrations vary across more than nine orders of magnitude – from millimolar levels of central energy metabolites to picomolar signaling molecules [54]. LC-MS-based analyses offer a limited dynamic range, forcing a compromise between measuring high-abundance metabolites without saturation and retaining enough sensitivity to detect those present at trace levels [55].

Matrix effects and ion suppression. Complex biological matrices can interfere with ionization, causing ion suppression or enhancement, particularly in electrospray ionization. Endogenous salts, proteins, and phospholipids compete with analytes during ionization, lowering sensitivity and reproducibility. Sample preparation strategies such as protein precipitation, solid-phase extraction, and phospholipid removal mitigate but do not eliminate these issues [56].

Lack of reference standards, quantification. Absolute quantification is hindered by the limited availability of isotopically labelled internal standards and certified reference materials. While targeted assays can reach clinical-grade reliability, untargeted workflows typically remain semi-quantitative, reporting relative intensities rather than absolute concentrations, which reduces comparability across studies [57]. Recent advances show that computational models of ionization efficiency (IE) can predict how strongly unknown metabolites will ionize under electrospray conditions, allowing estimation of absolute concentrations even when no authentic standard is available [58]. IE models are further discussed in Chapter 1.5.

Polarity coverage. Among all analytical challenges, the insufficient coverage of highly polar analytes represents one of the persistent and consequential blind spots in metabolomics. Conventional reversed-phase LC, which is mostly used in workflows, offers poor or no retention of hydrophilic metabolites, as discussed in Chapter 1.3.3. The elution in the void volume results in poor peak shapes and reproducibility, making them especially susceptible to matrix effects and co-elution [2].

Other analytical issues, such as data acquisition strategies, annotation bottlenecks, and limited spectral libraries, are not specific to metabolomics but shared with exposure analysis. These cross-domain aspects are therefore discussed collectively in Chapter 1.5. Overall, while metabolomics has established itself as an indispensable tool for investigating biochemical pathways and phenotypic states, its analytical implementation remains constrained by incomplete chemical coverage and the lack of standardized workflows. Among these limitations, this thesis focuses on the underrepresentation of highly polar metabolites. The next section therefore briefly describes the polar metabolome and the role of HILIC as a key complementary chromatographic approach for its characterization.

1.3.3 Polar metabolome and HILIC in metabolomics

A large portion of endogenous metabolome consists of hydrophilic metabolites, which is why HILIC is of such importance. These include the following groups:
-**small organic acids**,
-**amino acids** and other **amine-containing metabolites**, common biomarkers for human physiological processes,

-**nucleosides** and **nucleotides**, RNA metabolites, elevated in many metabolic diseases and tumors; many cancers involve also damaged DNA and its metabolites,
-**sulfur-containing compounds**,
-a subset of **lipid** classes, mostly phospho- and sphingolipids,
-other relevant compounds (acetyl, palmitoylcarnitines, allantoin, choline-derived compounds).

1.3.4 RP/HILIC complementarity and benefits

As stated above, HILIC has become an indispensable complement to reversed-phase LC in metabolomics by enabling the retention of highly polar metabolites, but also offering other practical advantages, including improved ionization efficiency due to high-organic conditions and the ability to operate at higher flow rates, thereby increasing throughput. When combined with RPLC, the two techniques together achieve far broader metabolome coverage than either could alone. This complementarity has been demonstrated repeatedly, both through parallel HILIC-RP analyses and in two-dimensional LC×LC setups designed to maximize chemical-space coverage [17, 59, 60, 61, 62, 63] Importantly, their orthogonality goes beyond polarity: HILIC and RPLC differ in separation mechanisms, matrix interferences, and ionization behavior, each highlighting distinct subsets of the metabolome. An example comes from lipidomics, where HILIC separates lipid classes by their polar headgroups while RPLC resolves them according to hydrophobic chain length and unsaturation [64]. Together, they therefore offer a more complete and reliable picture of biochemical composition, making their combined use the current standard for comprehensive LC-MS-based metabolomics.

The scope of metabolomics has over time extended beyond endogenous metabolism to include exogenous chemicals, entering the body from the food and environment. This perspective gave rise to exposomics, which builds on the same analytical approaches but focuses on tracing external exposures and understanding how they affect human biology.

1.4 Exposure Science and Exposomics: Analysis of Polar Biomarkers of Exposure

1.4.1 Human exposure to chemicals

People are constantly exposed to chemicals which are found everywhere in the environment and whose quantities are enormous due to their pervasive use in modern everyday. According to Eurostat reports, EU alone produced 218 million and consumed 227 million tons of industrial chemicals in the year 2023. Although these numbers represent a 13% decrease in production and 14% decrease in consumption compared with 2022, the quantities remain immense. Of the total production, the majority of the chemicals (167 million tons) is considered hazardous to health [65].

The exposures typically occur at low concentrations and originate from various sources, including the environment, diet, and personal care products, and enter the body through different pathways including inhalation, ingestion, and dermal contact. The exposure pathways are important in determining the subsequent distribution, metabolism, and bioactivity of chemicals within the body, influencing the biologically effective dose and associated health risks, and with that, the broader impact on public health. Studies namely show that the majority of chronic and noncommunicable diseases are attributable also to environmental and lifestyle factors, rather than solely to inherited genetic predispositions [34, 66]. Because exposures are numerous, variable over time, and intertwined with endogenous processes, they should be studied from a very broad, integrative perspective.

Traditional monitoring of single chemicals or exposure routes cannot capture this complexity or account for combined effects. This is where the concept of the exposome comes in. The term refers to the totality of environmental exposures an individual experiences from conception onward, considering both chemical and non-chemical factors. It was first introduced by Christopher P. Wild in 2005 and was initially conceptualized to complement genomic approaches in understanding disease etiology. Wild identified three domains of the exposome: the general external environment (including urbanization, climate, and social determinants), the specific external environment (such as diet, physical activity, tobacco use, and occupational exposures), and the internal environment (endogenous processes including metabolism, oxidative stress, inflammation, and the gut microbiome). Building upon this foundation, Miller and Jones proposed an expanded view of the exposome that integrates not only external exposures and internal biological responses but also behavioral risk factors and the dynamic biochemical processes that transform xenobiotics within the human body [67].

Within this framework, exposomics has developed as the systematic study of the exposome using high-resolution analytical platforms and computational methods. It aims to characterize the body's internal chemical environment and link external exposures to biological effects. These relationships are interpreted through three biomarker classes: biomarkers of exposure (exogenous chemicals or their metabolites present in the body), biomarkers of effect (early biological responses to an exposure), and biomarkers of susceptibility (inherent or acquired characteristics that modulate an individual's response). This classification is fundamental in interpreting exposomics data and linking environmental exposures to potential health outcomes [68].

In response to growing concerns, initiatives like the Human Biomonitoring for Europe (HBM4EU) have been established to monitor BoEs in selected human matrices (urine, blood, breast milk, and even placenta and follicular fluid) within specific populations. These screenings for known BoEs serve as the foundation for risk assessment and policy making [69, 70]. Building on HBM4EU, the European Partnership for the Assessment of Risks from Chemicals (PARC) was launched to further advance chemical risk assessment across Europe. It connects research institutions, regulatory agencies, and public health bodies to develop next-generation approaches that integrate human biomonitoring, environment, and innovative testing methodologies. The overarching aim is to create a more coherent and health-protective system for assessing chemical safety [71]. Beyond Europe, similar programs have been initiated by countries globally, including the U.S. National Health and Nutrition Examination Survey (NHANES) providing biomonitoring for general U.S. population, as well as the Canadian Health Measures Survey (CHMS) and Japan's Environment and Children's Study (JECS).

Collectively, these initiatives point to a global shift toward large-scale biomonitoring and exposomics. The emphasis is increasingly on prioritizing chemical exposures for further evaluation, as systematic chemical characterization alone does not inform risk unless it is followed by hazard and risk assessment, including for complex mixtures.

1.4.2 Analytical needs and challenges in metabolomics and exposure science

Exposure science in the framework of exposomics represents the domain concerned with the external and internal chemical exposures that can be measured directly in biological matrices. It focuses on the analytical characterization of exogenous compounds and their metabolites in humans [72]. These studies are mainly supported GC-MS and LC-MS for organic contaminants, while metals and metalloids are typically analyzed using inductively

coupled plasma-mass spectrometry (ICP-MS) [73, 74]. The following discussion will focus on LC-MS-based analyses.

As in human biomonitoring schemes, exposure science still largely relies on targeted methods for identifying and quantifying BoEs in biological samples. Yet, the rapid introduction of new chemicals into the market has revealed the limits of such predefined approaches, which cannot account for the diversity of emerging contaminants [4]. This has prompted a growing need for complementary analytical strategies capable of addressing the broader and evolving chemical landscape. In this context, non-targeted approaches, requiring no a priori knowledge of analytes, have become increasingly important. By extending the analytical reach toward unknown or unexpected compounds, they complement targeted analyses and together enable a more comprehensive view of the chemical exposome [2, 75].

Sample types and preparation. The choice of sample in exposure science depends on what aspect of exposure is being studied, as well as on how easily the sample can be collected. Similarly to metabolomics, biofluids are most frequently used. In exposure studies however, the preferred matrix for BoEs is urine as it allows non-invasive, repeated sampling and reflects accumulated exposure to xenobiotics and their metabolites excreted over time. When available, analyzing target tissues can offer more direct insight into bioaccumulation, persistence, or tissue-specific metabolism [76, 77]. Despite their informative value, tissue samples are less common in human exposure studies due to ethical and practical limitations.

Sample preparation for LC-MS analysis of BoEs generally involves an extraction step and is usually more extensive than in metabolomics. While metabolomics aims to preserve the native sample composition, exposure studies focus on clean-up and concentration, as contaminants are often present at trace levels. Removing endogenous interferences therefore takes precedence over maintaining sample integrity. Protein precipitation and liquid-liquid extraction are sometimes used, but solid-phase extraction (SPE) is preferred for its ability to efficiently purify and concentrate analytes, often using polymeric or HLB sorbents suitable for a wide polarity range of analytes [78, 79].

Data acquisition. Data acquisition approaches combine both targeted and untargeted LC-HRMS workflows and are largely similar to those used in metabolomics, which were discussed in Chapter 1.3. Targeted methods provide accurate and reliable quantitative determination of BoEs and are therefore crucial for regulatory monitoring and risk assessment needs. Yet, the chemical space of BoEs is enormous, and for many compounds, reference spectra are still unavailable. At the same time, new chemicals are constantly being introduced into the environment. These realities make suspect and non-target screening particularly important within the field. Still, compound identification remains one of the biggest challenges: even state-of-the-art LC-HRMS workflows usually manage to identify only a small fraction of detected features—often less than 5 % of those relevant to environmental and human exposure [2] .

Despite many technological advances, challenges appear in such types of analyses and are discussed below:

Low analyte concentrations. Complex biological matrices such as blood, plasma, urine, hair, and saliva contain numerous endogenous metabolites spanning a wide concentration range. The main analytical challenge in exogenous contaminants analyses is that these are usually present at much lower concentrations (often trace or ultra-trace levels, e.g., ng/L-pg/L in urine) than the abundant endogenous compounds, causing strong matrix effects in electrospray ionization. This makes sample preparation an essential step for both matrix reduction and analyte preconcentration. Excessive processing leads to

analyte loss, so a compromise between clean-up efficiency and sample integrity is required. Achieving sufficient sensitivity however depends not only on optimized pre-treatment and possible evaporative concentration, but also on high-performance instrumentation and advanced acquisition strategies. Despite the advances, reliable detection and quantification of such low concentrations remain a major bottleneck in exposure science.

Chemical space coverage. Relevant exposures span also many compounds that are highly polar, ionic, or otherwise poorly retained in conventional RP-LC, which has historically dominated biomonitoring workflows and are a subject for the application of HILIC, which is discussed in the next chapter [2, 80].

Furthermore, exposomics increasingly demands longitudinal coverage and mixture-level assessment, driving the adoption of NTS workflows in large cohort studies (e.g., HELIX, HBM4EU). Harmonization efforts, including resources such as NORMAN SusDat, CompTox, and Exposome-Explorer, provide essential support but cover only a fraction of the relevant chemical space.

1.4.3 Polar BoEs and HILIC in exposure science

Among organic contaminants, a substantial proportion are polar. The plot in Figure 2 illustrates the physicochemical diversity of substances included in the NORMAN Substance Database, where many compounds cluster in the low-mass, low-logP region. This distribution reflects the prevalence of polar and moderately hydrophilic chemicals that are analytically difficult to retain by RPLC. In addition, many phase I/II metabolites of xenobiotics (e.g., glucuronides and sulfates) are highly polar—even when derived from less polar parent compounds—and therefore remain among the most challenging biomarkers of exposure to measure reliably, despite their toxicological importance. HILIC extends LC–MS coverage into this polar domain and therefore complements reversed-phase separation, however, its use in exposure-science workflows targeting polar BoEs remains limited.

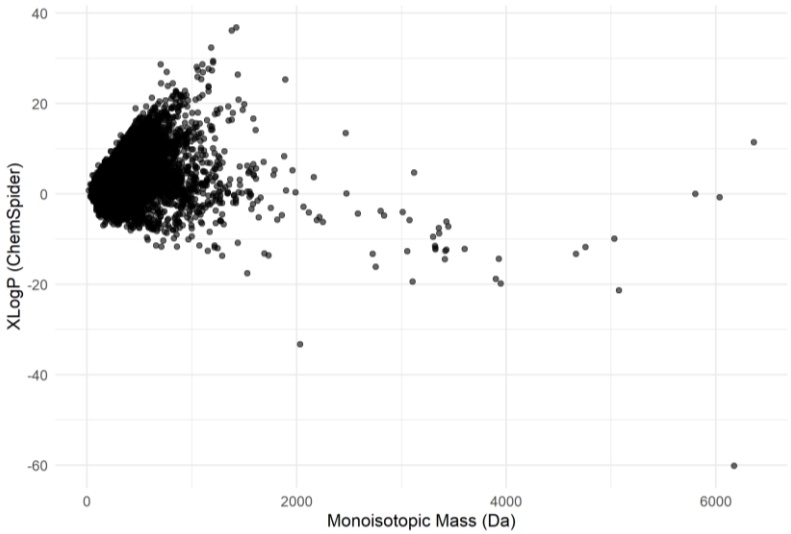


Figure 2: Distribution of monoisotopic mass and XLogP values of substances from the NORMAN Substance Database with reported ChemSpider XLogP values.

In exposure science, HILIC has primarily been used in targeted applications, rather than as a standalone platform for comprehensive chemical space coverage [81, 82]. There has been some preliminary work combining HILIC and RP, but such dual-mode setups are still predominantly applied in metabolomics rather than exposure science. For instance, Flasch

et al. integrated both chromatography modes in an exposomics-metabolomics workflow, enabling the detection of polar biomarkers of exposure alongside metabolic response markers in human samples. Jagani et al. similarly reported that dual RP–HILIC setups improve multiclass quantification of environmental chemicals by expanding coverage across a wider polarity range [17, 83]. While these studies illustrate the potential of dual-mode approaches to expand accessible chemical space, comprehensive exposure science workflows explicitly integrating HILIC and RP monitoring of exogenous compounds is yet to be explored.

1.5 Data Processing, Quality Assurance and Quality Control (QA/QC) in Non-Targeted Studies

Data processing challenges, common to non-targeted approaches appear in both exposure science as well as in metabolomics studies. While the biological context differs (biomarkers of exposure versus endogenous metabolites) the noteworthy data processing and interpretation considerations described here concern the non-targeted analytical approach itself and are largely similar across both fields. The minor differences are pointed out and discussed in the text.

Preprocessing. HRMS datasets often contain tens of thousands of detected signals—each defined by at least mass-to-charge ratio, intensity, and retention time—that must be aligned and grouped across samples before any statistical or identification steps can be performed.

This step is most often performed by using one of the dedicated software platforms, which comprise open-source tools (MZmine, MS-Dial, XCMS, OpenMS) and vendor-specific or commercial software (Compound Discoverer, MassHunter, Progenesis QI) [56, 84, 85, 86]. Despite their widespread use, these platforms require user-defined parameterization, which strongly influences preprocessing outcomes. Parameters for centroiding (e.g., smoothing algorithms), peak picking (m/z tolerance, estimated peak width, signal thresholds), retention-time correction (alignment penalties), and feature grouping (m/z and retention time (RT) tolerances, minimum detections) are particularly critical. Small parameter changes can importantly alter feature lists, leading to poor reproducibility between studies and even between runs processed with different settings. Feature detection may become either overly restrictive, missing low-abundance yet valid signals, or overly permissive, producing artificial peak splitting or merging of co-eluting species. The overlap of detected features between preprocessing tools is reported to be strikingly low, highlighting how parameter choice directly shapes analytical outcomes and thus the comparability of non-targeted screening results [87, 88, 89].

Feature annotation. Following data preprocessing, the next essential step is feature annotation, where tentative structures are assigned to the detected signals. Matching experimental spectra to molecular structures remains one of the most challenging and error-prone steps in non-targeted LC-HRMS analysis. The process relies primarily on matching experimental spectra against reference databases, using either empirical (in-house or online) spectral libraries or in silico approaches that predict MS2 fragmentation patterns. More recently, data-driven algorithms and generative models have been developed to predict plausible molecular structures directly from MS^2 spectra [90]. Among all the strategies, spectral library matching remains the most reliable route to confident annotation [91]. However, even the largest publicly available spectral databases (e.g., MassBank of North America, MassBank EU, GNPS, mzCloud) cover only a small fraction of the chemical space relevant to exposomics and metabolomics [90, 92]

Despite ongoing expansion of libraries and advances in in silico fragmentation and retention-time prediction, only a minor proportion of detected features can be annotated with high confidence. The vast remainder constitutes what has been termed the dark metabolome or dark exposome [93]. Importantly, this concept primarily reflects limitations in available reference data and annotation resources, rather than implying that all unannotated features should, or even could, be structurally resolved. In practice, annotation of the majority of detected features is rarely pursued, as it is neither feasible nor scientifically justified. Instead, the selection of features subjected to annotation depends strongly on the application field. In **metabolomics**, annotation efforts are typically limited to features that show statistically significant differences between experimental groups, following prior statistical data processing [94]. In **exposure science**, feature prioritization usually follows a different logic. Exogenous compounds are rarely ubiquitously present across samples and instead occur sporadically and often in only a subset of individuals, which complicates standard statistical approaches and limits their usefulness as a primary filtering step. In addition, biomarkers of exposure are generally present at substantially lower concentrations than endogenous metabolites, which often results in missing or low-quality MS2, negatively affecting annotation confidence. Consequently, annotation in exposure science is commonly led by suspect lists, which are applied either during data acquisition or in the early data-processing stage to prioritize features corresponding to chemicals of known or suspected relevance.

Annotation confidence. Inconsistent reporting practices create another issue related to results comparability. The Schymanski framework for communicating annotation confidence levels remains the de facto standard, yet interlaboratory comparisons continue to reveal substantial variability in how these levels are assigned and interpreted [5, 95]. Several newer frameworks, integrating in silico evidence, isotope patterns, and orthogonal validation such as retention-time or ion-mobility matching, have been proposed to improve transparency [96, 97, 98], but widespread adoption across laboratories is still limited [98].

Quantification, semi-quantification. Comprehensive quantification in non-targeted LC-HRMS studies is fundamentally limited by the absence of authentic standards for the vast majority of detected compounds. Although accurate mass measurements and MS2 spectra enable detection and tentative annotation, the lack of reference materials prevents reliable calibration and, consequently, absolute quantification. As a result, non-targeted workflows are typically qualitative, or at best semi-quantitative, providing only approximate comparisons of signal intensities across samples [99]. Recent work has sought to bridge this gap by developing quantification-without-standards strategies, most notably through ionization-efficiency modelling. These approaches use molecular descriptors and physicochemical parameters of compounds to predict their electrospray response factors and thereby estimate concentrations without the need for calibration standards. Multi-laboratory evaluations show that such models can reproduce experimental responses within roughly one order of magnitude for compounds of similar chemical properties and on the same instrument type, but with large variability across compound classes and instruments [100]. Despite these advances, the quantitative interpretation of non-targeted data remains uncertain and should generally be regarded as semi-quantitative.

Quality assurance and quality control (QA/QC) are vital components of non-targeted LC–HRMS workflows, as they provide the basis for evaluating analytical performance and defining the limits within which the resulting data can be meaningfully interpreted [101]. QA/QC strategies typically comprise a combination of measures implemented throughout the analytical sequence, encompassing both method characterization and continuous performance monitoring. These commonly include solvent and procedural blanks, quality-control (QC) samples, system suitability checks, and the addition and monitoring of internal standards. Each of these elements addresses a specific

aspect of analytical reliability. Blanks are used to identify background contamination, laboratory artefacts, and features originating from solvents, consumables, or instrumentation. System suitability mixtures serve to verify instrument readiness and stability before and after analytical batches. QC samples provide control of repeatability and help identify drift during analysis. Internal standards provide information on extraction efficiency, chromatographic performance, and ionization behavior for selected regions of chemical space and are in some cases used for signal intensity normalization [102]. Importantly, none of these elements alone can guarantee analytical reliability across the full feature space inherent to non-targeted datasets, which needs to be considered in the interpretation.

The general principles of QA/QC implementation in metabolomics and exposure science are largely similar. However, there are some important differences. In metabolomics, QC samples are most commonly prepared as pooled biological samples that are representative of the majority of detected endogenous metabolites. These pooled QCs are well suited for monitoring analytical stability, enabling drift correction and feature filtering. In exposure science, the same exact strategy would be much less rational for two reasons: many biomarkers of exposure are normally present at low concentrations and only in a subset of samples. Pooling of the samples would therefore lead to substantial dilution or complete absence of these compounds in QC material. QC samples in exposure-focused studies are therefore frequently prepared by spiking with a mixture of reference compounds. These do not represent all expected analytes but are instead selected to span the expected chemical space the method is supposed to cover. While common elements and reporting principles can be defined, strict standardization of QC composition, acceptance thresholds, or correction strategies is neither feasible nor desirable across different study types and analytical aims. Recent consensus frameworks therefore emphasize transparency, traceability, and explicit reporting of QA/QC design choices and criteria, rather than prescribing uniform workflows [51, 103].

From a data-processing perspective, QA/QC decisions directly influence results based on QC variability, removing blank-associated signals, or applying batch correction. These are not merely technical steps but define which parts of the dataset are considered analytically reliable. QA/QC should therefore not be regarded as a separate procedural stage, but as a foundational component of non-targeted data processing.

Corrections of analytical variability (inter-batch, sample-to-sample). Analytical variability remains one of the largest sources of uncertainty in untargeted LC-MS studies, even after appropriate QA/QC measures have been implemented [104]. Systematic variation arises from gradual signal drift, retention-time shifts, and intensity fluctuations caused by factors such as column ageing, source contamination, and changing instrumental conditions [101]. While QA/QC procedures allow such effects to be detected and characterized, correction steps are often required prior to statistical analysis.

Normalization and drift-correction strategies aim to reduce systematic variability while preserving biologically meaningful variations. Correction based on internal standards can partially mitigate analytical variability; however, in non-targeted workflows its effectiveness is inherently constrained. No finite set of internal standards can represent the analytical behavior of thousands of chemically diverse features, and even structure-informed assignment of features to similar standards improves correction only within narrow physicochemical domains. The role of internal standards therefore differs between metabolomics, where they are primarily used to verify analytical stability, and exposure science, where they are more frequently incorporated into correction of signal intensities as interpretation often focuses on defined compound classes or suspect lists.

Another correction strategy involves QC-sample-based methods, which are widely used to model and adjust signal drift within analytical sequences. These approaches rely on the

assumption that QC samples adequately reflect the analytical behavior of the retained feature space and that observed trends are predominantly technical rather than biological [46]. Their applicability therefore depends directly on QC design and feature filtering decisions established during QA/QC.

Inter-batch correction. Inter-batch variability is another major source of systematic error in large-scale untargeted LC–MS studies, arising from long-term drift, changing analytical conditions, and platform-specific artifacts. Before correction, QC samples typically cluster by batch, demonstrating substantial between-batch divergence. Batch-correction methods aim to reduce these systematic differences by aligning batch centroids while preserving biological differences. They are essential for reliable data interpretation. Despite such progress, reproducibility across laboratories remains limited, as correction performance depends heavily on platform characteristics, data-processing tools, and QC design.

Data integration and multiblock fusion. Often data on one sample set is collected with multiple analytical methods (different ionization polarity modes, complementary chromatographic modes or even orthogonal omics platforms) and needs to be combined for interpretation. This is especially relevant in the multi-omics approach. Data integration typically relies on multiblock or ensemble methods, such as multiblock PCA, O2-PLS, DIABLO, or other frameworks that analyze each dataset separately while modelling their shared structure [105, 106, 107]. These strategies enable more comprehensive biological insight than any single analytical platform alone.

Statistics considerations. The high dimensionality of non-targeted data introduces a substantial risk of overfitting and false discovery so statistical analysis should be performed and interpreted very carefully [108]. Different normalization, scaling, or imputation strategies can profoundly alter statistical outcomes and even reverse observed trends [109]. Consequently, statistical significance alone does not necessarily mean biological or toxicological relevance. Validation in independent cohorts, inclusion of appropriate negative controls, and the integration of orthogonal analytical or biological evidence remain essential for robust interpretation [56].

In summary, data processing remains one of the most influential and most sensitive steps in non-targeted LC–HRMS. Decisions made during preprocessing, annotation, and statistical analysis can substantially shape the detected features and the biological conclusions drawn from them. Despite methodological advances, non-targeted workflows still face strong dependence on software and parameter choices. Careful optimization, transparent reporting, and validation with orthogonal or independent evidence therefore remain essential to ensure robust and meaningful interpretation.

Data stewardship, FAIR principles, and reusability of non-targeted datasets. Non-targeted LC–HRMS studies generate large, information-rich datasets whose value extends beyond the original research question. To ensure that these data remain usable for future reprocessing with improved computational tools or for addressing new scientific questions, data stewardship should follow FAIR principles (Findable, Accessible, Interoperable, Reusable) [110]. In practical terms, this includes preservation of raw vendor files, open-format exports where possible (e.g., mzML), complete analytical metadata (sample identifiers, acquisition parameters, chromatographic conditions, calibration details), and the computational provenance of the processing workflow (software versions, parameter sets, and intermediate outputs). This is particularly important in non-targeted work because processing choices strongly affect the resulting feature table and without transparent recording of all parameters and software versions, reprocessing with improved tools is often impossible or yields non-comparable outputs. Public deposition of raw data and accompanying metadata in established repositories additionally supports reanalysis and enables the community to apply emerging algorithms (e.g., improved deconvolution,

MS/MS interpretation, and machine-learning–based annotation) to legacy datasets without repeated sample analysis.

Ethical considerations. For studies involving human-derived matrices, data processing and sharing are constrained by ethical requirements and data-protection regulations. Although HRMS files do not typically contain direct personal identifiers, they are derived from biological material and may carry indirect re-identification risk when linked with clinical metadata, dates, locations, or rare phenotypes. Consequently, datasets should be handled under appropriate ethics approvals, with clear governance on what metadata can be shared, under which access conditions, and with what degree of de-identification. In the EU, these considerations fall under the General Data Protection Regulation (GDPR) framework, which governs processing of personal data and special-category data such as health-related information [111]. In practice, compliant data stewardship in exposure science/metabolomics requires separation of identifiers from analytical files, minimization of shared metadata to what is scientifically required, and, where full open release is not appropriate, use of controlled-access repositories and data-use agreements.

Harmonization, transparency, traceability of data-processing workflows. Given the strong dependence of non-targeted results on software and parameter settings, harmonization efforts increasingly focus on improving transparency and traceability rather than enforcing identical workflows across laboratories. Key segments where harmonization is both feasible and impactful include: (i) minimum reporting of acquisition and preprocessing parameters; (ii) consistent use and reporting of QA/QC elements (pooled QC design, blanks, system suitability, acceptance limits); (iii) structured reporting of annotation confidence; and (iv) version-controlled documentation of computational workflows. Community reporting frameworks and checklists for non-targeted studies have been proposed to standardize what is reported and to improve comparability across laboratories (e.g., the NTA Study Reporting Tool) [103]. From a practical perspective, traceability should also include the full computational workflow, meaning that the feature table can be reconstructed from raw files using the reported software versions and processing parameters. This level of documentation is important because it determines whether results can later be independently verified, compared across studies, or reprocessed as analytical tools improve.

1.6 Pharmacotherapy and Therapeutic Drug Monitoring (TDM)

1.6.1 Analytical roles of LC-MS in support to pharmacotherapy and TDM

The expansion of the chemical space, covered by LC-MS-based analyses, described in the contexts of metabolomics and exposure science, is also a relevant topic in pharmacotherapy. Similar analytical challenges, observed when analyzing polar metabolites or exposure biomarkers also arise with therapeutic agents. As the quantification of hydrophilic drugs is critical for clinical safety and efficacy, any existing gaps should therefore be addressed.

LC-MS analyses play an important role in the development, optimization, and ensuring of safe clinical use of pharmaceuticals. They support toxicology, pharmacokinetics and pharmacodynamics (PK/PD), bioequivalence and bioavailability studies, as well as therapeutic drug monitoring (TDM). Pharmacokinetic (PK) studies measure how much of a certain drug is present in various body compartments over time, describing its absorption, distribution, metabolism, and excretion profile (ADME) after release from the

pharmaceutical formulation, whereas pharmacodynamic (PD) studies focus on drug's physiological and behavioral effects. Together, PK and PD link the effects of a drug to its concentration. In clinical settings, these principles form the basis of TDM; the monitoring of active pharmaceutical ingredients' concentration in patients over time for the purpose of individualizing the dosing regimens. This is especially relevant for pharmaceuticals with narrow therapeutic windows, unpredictable dose-response relationships, nonlinear PK, and high inter-patient variability [112]. TDM is well established in areas such as antimicrobial and antiepileptic therapy [113, 114]. However, it is still less developed in oncology, although it has gained recognition in recent years [112, 115]. Many cytostatics namely exhibit pronounced interindividual variability in plasma concentrations due to differences in metabolism, protein binding, and transport, and they are often administered at or near the maximal tolerated dose–conditions that provide a strong rationale for TDM. In addition, cytostatics are inherently associated with severe adverse effects, which are unacceptable in the treatment of non-malignant diseases. When administered to patients already burdened by the primary disease, the need for TDM is even more pronounced [116].

Ultimately, the usefulness of PK/PD data and TDM depends on our ability to measure drugs and their metabolites reliably in real biological samples. The following chapters focus more closely on polar cytostatics, outlining both the clinical motivation for TDM and the analytical obstacles that continue to limit its broader application in oncology.

1.6.2 Polar cytostatics

Conventional cytostatics are, despite advances in targeted and immune-based therapies, still widely used to this day. Many of these compounds are non-selective towards tumor cells, leading to serious side effects and narrow therapeutic windows. Mechanistically, classical cytostatics act on nucleic acids or nuclear enzymes, which are located intracellularly, making cell entry obligatory. The transition through phospholipid cell membrane is however for many polar agents a principal bottleneck. It rarely proceeds by passive diffusion, often relying on endocytosis or transmembrane carriers. This is the case for agents such as bleomycin, methotrexate, 5-fluorouracil, cisplatin etc. [117, 118, 119, 120].

Inefficient entry and thus limited access to the site of action means that higher systemic doses are required to achieve effective intracellular levels, leading to more toxicity. TDM has in these cases a very important role and should be used to adjust dosing. Efforts are also being made to improve delivery of such compounds by enhancing tumor selectivity to consequently reduce systemic exposure. Approaches being investigated include nanocarrier systems, liposomal formulations, conjugation with targeting moieties, and electrochemotherapy (ECT).

Taken together, polar cytostatics form a group where TDM would be clinically meaningful due to narrow therapeutic windows, variable intracellular disposition, and frequent toxicity. Yet TDM is not always implemented, partly because the physicochemical properties of these compounds often make reliable quantification difficult. These analytical limitations, discussed in the following chapters, contribute to knowledge gaps in basic pharmacokinetics (for example, incomplete understanding of intracellular exposure or enzyme-mediated inactivation) and slow the evaluation of novel delivery strategies. Improving analytical methods is therefore essential both for enabling TDM and for advancing pharmacotherapy research on this class of drugs.

1.6.3 Case study: Bleomycin – analytical and pharmacological challenges associated with a polar cytostatic

1.6.3.1 Pharmacological challenges related to Bleomycin

Bleomycin (BLM) is an example of a very polar cytostatic antibiotic, used in clinical practice to treat various neoplasms, particularly squamous carcinoma, lymphoma, and testicular carcinoma, despite its severe unwanted side effects [121]. Pharmacological challenges, limiting the safety and efficacy of BLM therapy are discussed below: only a small percentage of molecules actually pass through the phospholipid membrane into the cell where it causes single- and double-strand breaks of the DNA by creating reactive oxygen species [122]. This is largely a consequence of the molecule's high polarity (logP=-7.5) and size (around 1500 Da), impairing transition through the membranes. In this case, significantly increasing the dose to reach higher intracellular concentrations is not a viable solution, as it would aggravate the unwanted side effects, which are already severe and frequent. Tendency of BLM to accumulate in lung tissue leads to pulmonary toxicity in the form of pulmonary fibrosis and inflammation, which are major concerns in BLM therapy [123]. Avoiding this, delivery strategies such as electrochemotherapy (ECT) are being explored. Combining application of a drug with application of short electric pulses (e.g., electroporation), temporarily permeabilizing the membranes, it facilitates the transition of the drug into the cells. ECT with BLM has been used in clinical practice since 2006, though protocols are still being optimized [124]. The currently used regimen proves effective but comes with severe nerve stimulation, muscle contractions, and pain experienced in patients, which motivates further research. Currently, efficiency of shorter pulse durations, promising less adverse side effects, is being investigated [125].

The pharmacokinetics of bleomycin, particularly in solid tissues, has not yet been well researched, due to many analytical limitations. Current evidence suggests that tumor penetration is both low and inconsistent. The mechanisms contributing to this are still insufficiently characterized and include at least poor membrane transit, heterogeneous tissue architecture, and enzymatic inactivation of BLM. The latter is governed by bleomycin hydrolase (BLMH), a cytoplasmic enzyme catalyzing deamination and hence deactivation of BLM, and whose expression varies markedly between tissues and tumor types, contributing to variable biological response. Tissues with higher BLMH activity exhibit faster inactivation and therefore lower effective intracellular drug levels, while tumors with low BLMH activity may be more susceptible to BLM [126]. The analytical constraints, likely having contributed to the knowledge gaps here, are discussed in detail in the following chapter.

1.6.3.2 Analytical methods for bleomycin quantification

The need for sensitive, selective BLM assays in the clinic (e.g., TDM) as well as in research (e.g., ECT protocol optimization) has been highlighted. The apparent scarcity of published methods likely stems from the molecule's complex chemistry and how that impacts LC-MS-based analyses. In addition to being highly polar and hence demanding chromatography approaches alternative to the well-established RPLC, other noteworthy analytical challenges specific to BLM include its heterogeneity (a mixture of closely related congeners), strong metal-chelating properties, and tendency to form multiply charged ions in electrospray ionization (ESI) sources. These characteristics together make BLM an illustrative example of a complex analyte—one that simultaneously exposes the majority of difficulties inherent to targeted LC-MS analysis of polar biopharmaceuticals. Addressing such issues—from matrix effects and metal complexation control to metrological traceability in the absence of certified reference materials—requires a combination of

carefully designed sample preparation, instrumental method, and rigorous QA/QC. For that reason, the methodological strategies developed for BLM quantification are not only relevant to its own application but also serve as a practical case study of how analytical challenges in complex polar compounds should be systematically approached, validated, and controlled over time. Most important considerations are discussed below.

Heterogeneous mixture (congeners). BLM is produced by the bacterium Streptomyces verticillus and is actually a mixture of very closely related glycopeptides, or so-called fractions, rather than one single molecule. These fractions (BLM-A1–A6; BLM-B1–B5) vary only slightly in the structure, as illustrated on Figure 3. Clinically used BLM primarily contains A2 and B2 fractions. Pharmacopoeial and product specifications specify the content for BLM-A2 to be 55–70% and for BLM-B2 25–32%, while also setting limits on minor congeners—so analytical methods must either chromatographically separate and quantify A2/B2 or define and validate what "total BLM" means (including how minor fractions are handled) [127].

Metal complexation (speciation). BLM forms stable 1:1 complexes with redox-active metals, primarily with copper ions, which is relevant in this context as biological matrices are never metal-free [121]. Complexes vary from apo-BLM in mass, so the analytical measurand needs to be defined with caution. LC–MS workflows for human samples either preserve the complexes, formed in-matrix, or control the complex formation by adding excess metal ions to standardize response; in both cases, the reported result should state the targeted species and the conditions under which it was obtained.

Multiply charged ions in ESI. The macrochelate produces multiple charge states and closely spaced isotope clusters. This, in addition to the presence of both complexes and apo-forms can complicate the multiple reaction monitoring (MRM) selection. The abundance of signals in the MS calls for high-resolution MS (or very carefully chosen transitions) [8].

Photosensitivity. BLM and its complexes are photolabile; light protection is required throughout all handling [128].

Beyond analyte-specific chemistry, BLM assays face several general issues, including:

Very low concentrations (especially for *in vitro* ECT studies). ECT purposefully seeks strong local effect at low systemic doses; working towards the lowest possible lethal dose for tumor cells, which is determined to be at a few hundred BLM molecules per cell [129, 130]. This requires ultrasensitive quantitation methods and loss-minimizing sample preparation.

Matrix effects & recovery losses. Complex matrices (plasma, tumor tissue, cell lysates) demand more extensive extraction and clean-up, which increases the risk of analyte loss (e.g., adsorption/carryover) and should be controlled. The same complexity also makes ionization suppression/enhancement in ESI-MS more likely, so matrix effects should be assessed and accounted for.

Internal standard (IS) limitations. No isotopically labeled BLM is commercially available; so most studies rely on structural analogs or external standardization, which can under-correct matrix effects. Compensation with rigorous QCs and matrix-matched curves is essential.

Traceability & uncertainty. In the absence of a certified reference material (CRM) and isotopically labelled BLM, establishing traceability should be done differently, at least by using pharmacopoeial reference standards (e.g., Ph. Eur. Bleomycin sulfate CRS) and documenting the metrological chain, and reporting measurement uncertainty from validation/QC data.

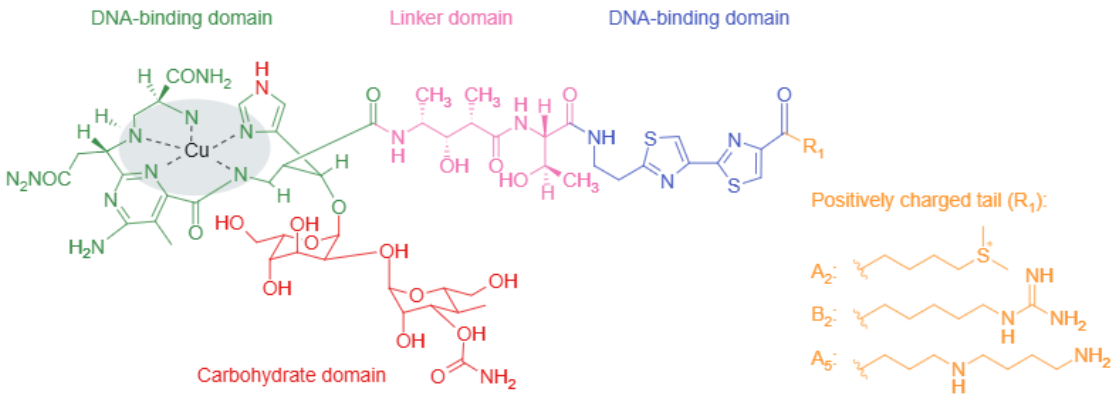


Figure 3: Structures of bleomycin-copper complexes for A2, B2 and A5 congeners, illustrating the functional domains (adapted from Plešnik et al., *An effective validation of analytical method for determination of a polar complexing agent: the illustrative case of cytotoxic bleomycin, Analytical and Bioanalytical Chemistry*, 2023).

1.6.3.3 Extending the case study: parallels with other hydrophilic drugs

The same analytical and pharmacological issues recur across other polar cytostatics as well as some other pharmaceuticals, which implies that the proposed solutions could be extended beyond the BLM analysis. **Membrane transit** is a limitation, often appearing with hydrophilic agents such as cisplatin and antifolates/antimetabolites (e.g. methotrexate, 5-FU), from which follows low intracellular exposure [131, 132, 133]. **Reference materials** are frequently lacking, with no CRMs available for several agents, thereby limiting analytical traceability. This can be additionally complicated by the absence of isotopically labelled internal standards and consequent matrix effect correction difficulties. **Metal complexation** is a frequent phenomenon, appearing in therapeutic agents with donor functional groups that can coordinate transition metals. Trace metal ions from biological matrices or laboratory material can form stable complexes even in the absence of deliberately added metals. Examples include bleomycin, tetracyclines, fluoroquinolones, methotrexate, etc. [134, 135, 136]. Presence of both metal-bound and free forms complicates quantification; where analytical control can be achieved either by ensuring complete absence of metals in both sample as well as the system (through passivation, e.g. chelator pre-treatment) or by defining a controlled complexation state through addition of a known metal excess, as demonstrated in this work for Cu–bleomycin. **Concentrations** in human matrices are often at or near the lower limits of quantification of existing analytical methods and, sometimes approaching the practical limits of what can realistically be achieved even with optimized LC–MS methods. This is especially true with compounds where efforts are made to lower the doses as much as possible, while complex matrices increase extraction losses and suppress ionization. Although these issues are presented here through the lens of bleomycin, they reflect general challenges shared across a wide spectrum of polar anticancer agents and other hydrophilic therapeutics. Accordingly, the practical solutions, developed on this complex analyte can be used to guide protocol optimizations for other compounds.

Chapter 2

Aims and Hypotheses

Literature reports **significant gaps in analytical methodologies** used for the detection and quantification of polar compounds, which are important contributors in biological, environmental, and therapeutic contexts. HILIC has shown great promise in analyzing these highly polar compounds, offering a necessary complement to traditional RP methods. However, despite several successful applications, the full potential of HILIC across pharmacotherapy, environmental health, and metabolomics remains underexplored. The aim of this dissertation is to **systematically address these gaps** by **optimizing and validating analytical methods** using HILIC and by evaluating its applicability across three analytically distinct but conceptually related fields. Within pharmacotherapy, this thesis includes the development and validation of HILIC-based analytical methods for bleomycin, a highly polar cytotoxic compound for which analytically robust methods remain limited despite clinical and research relevance. In environmental health and metabolomics, it explores the implementation of HILIC-based analytical methods as a complementary approach to traditional RP chromatography for comprehensive NTS. The following hypotheses will be addressed:

H1: Implementing a robust QA/QC protocol for long-term method monitoring improves accuracy and precision in the determination of complex polar analytes in the absence of CRM.

Brief justification of the hypothesis:
The analysis of highly polar and complex compounds is often challenging, and for many such analytes only a small number of validated methods is available. This might partially be the reason for the lack of CRMs for these compounds, but at the same time this lack stalls their development as objective assessment of new methods in terms of accuracy and precision becomes difficult. This creates a circular constraint in which limited methodological maturity and the absence of reference materials mutually restrict progress.

This hypothesis places quality assurance and quality control at the center of the analytical strategy. Using bleomycin as an example of a complex polar analyte, this work will propose and apply practical approaches for assessing and maintaining analytical reliability in the absence of CRMs. The aim is not to develop a bleomycin-specific solution, but to establish a transferable framework for evaluating accuracy and precision when reference materials are unavailable, particularly in long-term studies of complex polar compounds.

H2: An LC-MS-based method for quantification of intracellular bleomycin is sufficiently sensitive to support electrochemotherapy research that generates samples with ultra-trace levels of bleomycin.

Brief justification of the hypothesis:
The primary objective of electrochemotherapy, and of methodological developments in this field, is to improve the delivery of bleomycin to its intracellular site of action and thereby achieve the desired therapeutic effect at the lowest possible dose. It is accepted that only a few hundred bleomycin molecules per cell are sufficient to induce its death, implying that the relevant intracellular target concentrations are extremely low and analytically challenging to access. To date, and to our knowledge, there are no suitable LC–MS methods available for the quantification of intracellular bleomycin in the context of in vitro electrochemotherapy experiments. As a result, treatment efficacy is typically assessed exclusively through biological endpoints, without direct analytical confirmation of intracellular drug levels. The absence of such methods is not unexpected. In addition to the inherent analytical complexity of bleomycin as an analyte, the concentrations of interest are far below the lower limits of quantification reported for existing LC–MS methods, which are typically developed for extracellular or blood-derived matrices. Furthermore, the analysis of intracellular bleomycin necessitates extensive sample pretreatment, including cell lysis and multi-step clean-up, which directly affects the attainable lower limits of quantification through cumulative analyte losses. Complete removal of matrix components is not feasible, resulting in residual matrix effects that further limit method sensitivity and robustness.

Within the framework of this hypothesis, it is proposed that a suitable analytical workflow be developed and optimized to enable reliable quantification of intracellular bleomycin in in vitro electrochemotherapy studies. This will require systematic optimization of both sample preparation and instrumental parameters, as well as the use of state-of-the-art LC–MS instrumentation to approach the lowest practically achievable limits of quantification for this application.

H3: A non-targeted screening method utilizing HILIC in combination with HRMS provides a broader and more comprehensive chemical space coverage for polar exogenous biomarkers than current RP-based NTS workflows.

Brief justification of the hypothesis:
The objective of non-targeted analysis in exposure science is to detect as broad a range of biomarkers of exposure as possible within given samples. RP chromatography is currently the standard separation technique used in the screening workflows, as it enables coverage of a wide range of analytes with moderate to low polarity. HILIC is particularly well suited for their analysis, yet in the context of biomarkers of exposure its use has so far remained largely limited to targeted approaches. By contrast, in metabolomics HILIC is already routinely integrated into non-targeted workflows. This indicates that the potential of HILIC for non-targeted exposure science has not yet been fully explored.

Based on this, it is hypothesized that adding HILIC to RP-based non-targeted exposure science workflows would lead to a broader and more comprehensive coverage of the relevant chemical space, particularly for polar exogenous biomarkers. Within the framework of this hypothesis, a combined RP–HILIC non-targeted screening workflow will be developed. The objective is to systematically assess the extent to which chemical space coverage is expanded and to determine whether HILIC contributes a substantial number of biomarkers of exposure that would not be detected using RP-based analysis alone.

H4: HILIC-based NTS of urine samples reveals biomarkers of exposure that can be associated with reproductive diseases in women.

Brief justification of the hypothesis:
This hypothesis builds directly on the analytical framework established in the preceding parts of the thesis, stating that HILIC significantly extends polarity coverage and should therefore be implemented into non-targeted LC–HRMS workflows. Having already demonstrated the analytical feasibility of integrating HILIC with RP separations, the present hypothesis examines whether this broader polarity coverage improves detection of exposure biomarkers associated with reproductive and gynecological conditions in women. This will first be evaluated through a urinary exposure-oriented study in women with ovarian malignancies, where complementary RP and HILIC analysis will be applied to assess whether broader polarity coverage improves detection of biomarkers associated with disease status. The analytical concept will then be further examined in a polycystic ovary syndrome (PCOS) cohort, where non-targeted LC–HRMS will be applied across complementary matrices to assess both exposure-related and metabolic differences between healthy and diseased groups. Both cohorts are considered suitable in this context, as ovarian malignancies and PCOS have both been discussed in relation to endocrine-disrupting and other environmentally relevant exposures. The primary objective will be to evaluate how orthogonal chromatographic selectivity contributes complementary information in clinically relevant non-targeted studies addressing both exposure-related and metabolic differences between healthy and diseased groups.

The specific goals of the thesis are:
- To optimize and validate a high-throughput analytical method for the determination of bleomycin
- To establish a QA/QC protocol for this analysis as an illustrative case of how to perform QA/QC for analytes with no existing CRM or possible interlaboratory comparisons
- To investigate stability of bleomycin in relevant matrices
- To optimize HILIC-LC-MS/MS techniques for the targeted analysis of intracellular bleomycin at ultra-trace concentrations and apply this protocol by analyzing cells from electroporation studies
- To develop and validate a HILIC-LC-HRMS workflow for non-target screening of highly polar compounds in human urine and serum
-To apply the NTS workflow for performing analysis of urine samples of women (healthy and with ovarian cancer)
-To perform HILIC-based metabolomic profiling and NTS of serum samples from of individuals with polycystic ovary syndrome

The anticipated contributions of this research include enhanced analytical methods for polar compounds, improved understanding of the human exposome, and advancements in the targeted analysis of complex cytostatic agents like bleomycin. These contributions will not only expand the use of HILIC-based separations, but also provide valuable insights into environmental exposures and their impact on human health.

Chapter 3

Publications

3.1 Development and Application of an Integrated HILIC-RP NT Workflow for Comprehensive Polarity Coverage in Exposure Science

3.1.1 Nontargeted urinary profiling strategy for endocrine-disrupting chemicals in women with ovarian malignancies

Publised: Plešnik, H., Rekar, Ž., Stevanović, S., Virant-Klun, I., Imamović Kumalić, S., Sladič, M., Mazej, D., Snoj Tratnik, J., Horvat, M., Kosjek, T., Environmental Science & Technology, 2025

This paper represents the central exposure science case study of the thesis. It directly addresses and confirms Hypothesis H3, stating that a non-targeted screening method utilizing HILIC in combination with HRMS provides broader and more comprehensive chemical space coverage for polar exogenous biomarkers than current RP-based NTS workflows, while also providing direct analytical support for Hypothesis H4 through its application in a gynecological disease cohort. The work is framed around the development, evaluation, and application of a complete non-targeted urinary screening workflow designed to overcome the polarity limitations of conventional RP-based approaches.

The core methodological contribution lies in the combining of RP and HILIC separations within a single analytical workflow, supported by a SPE-based sample preparation that yields two complementary fractions from the same urine sample. This design supports systematic exploration of both semipolar and highly polar regions of chemical space, with HILIC explicitly targeting compound classes that are poorly retained or entirely missed under RP conditions. The performance of the workflow was evaluated both by using reference standards and by application to real biological samples, which provided empirical assessment of polarity-dependent increases in detected and annotated features.

When applied to urine samples from women with ovarian malignancies and matched controls, the combined RP/HILIC approach resulted in a measurable expansion of detected chemical space (28% increase in overall chemical space coverage), with HILIC contributing a substantial fraction of annotated biomarkers of exposure that were not observable in RP data alone. This directly confirms Hypothesis H3 in a real-world setting. Importantly, one of the additionally detected compounds showed statistically significant differences between case and control groups, demonstrating that the expanded chemical space is not merely analytical in nature but also clinically informative.

Within the broader structure of the dissertation, this work establishes a practical and validated template for integrating HILIC into non-targeted exposure science workflows. It serves as a methodological bridge between the theoretical discussion of polarity coverage and later applications to other biological matrices, illustrating how chromatographic complementarity translates into increased discovery potential in complex human studies.

Environmental Science & Technology

pubs.acs.org/est

Open Access

This article is licensed under CC-BY 4.0

Article

Nontargeted Urinary Profiling Strategy for Endocrine-Disrupting Chemicals in Women with Ovarian Malignancies

Published as part of Environmental Science & Technology special issue "Non-Targeted Analysis of the Environment".

Helena Plešnik, Žan Rekar, Stefanela Stevanović, Irma Virant-Klun, Senka Imamović Kumalić, Mateja Sladič, Darja Mazej, Janja Snoj Tratnik, Milena Horvat, and Tina Kosjek*

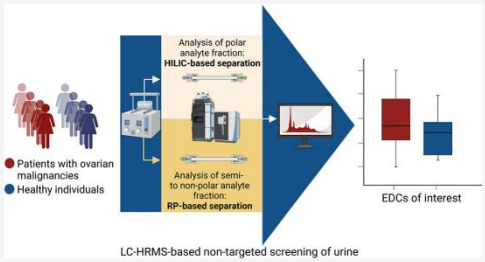
Cite This: Environ. Sci. Technol. 2025, 59, 8380−8390

Read Online

ACCESS | Metrics & More | Article Recommendations | Supporting Information

Downloaded via INST JOZEF STEFAN on January 29, 2026 at 15:50:50 (UTC).
See https://pubs.acs.org/sharingguidelines for options on how to legitimately share published articles.

ABSTRACT: Endocrine-disrupting chemicals (EDCs), including known and unknown parent compounds, their metabolites, and transformation products, are pervasive in daily life, posing increasing risks to human health and the environment. This study employed a high-resolution mass spectrometry-based nontargeted screening approach, integrating polar (HILIC) and reversed-phase separations to expand the chemical space coverage and, supported by open-science tools and resources, evaluated urinary chemical profiles to assess internal EDC exposure. Among 106 annotated biomarkers of exposure, six exhibited significantly higher normalized intensities in patients with ovarian malignancies compared to healthy controls ($p < 0.05$). This suggests their greater exposure to phthalates (diethylhexyl phthalate and diethyl phthalate), pesticides (metolachlor metabolite and 4-nitrophenol), a UV filter (benzophenone-1), and an industrial byproduct (4-methyl-2-nitrophenol). These compounds may interfere with hormonal regulation, potentially contributing to cancer development. While these findings highlight potential differences in internal EDC exposure, the study primarily demonstrates the applicability of nontargeted urinary profiling for chemical exposure assessment. By providing new insights into EDCs burden and its pathological implications, this work contributes to advancing next-generation chemical risk assessment within the European Partnership for the Assessment of Risks from Chemicals initiative and supports the development of preventive strategies to mitigate environmental cancer risks.



KEYWORDS: *ovarian cancer, biomarkers, exposure, nontargeted screening, high-resolution mass spectrometry, analytical coverage, reversed-phase, HILIC*

INTRODUCTION

Ovarian cancer (OC) remains one of the most lethal gynecological malignancies worldwide. Despite advances in diagnostic technologies and treatments, the 5-year survival rate for advanced-stage OC remains around 50%.[1] Risk factors for OC include genetic predispositions, reproductive history, hormonal imbalances, and lifestyle behaviors.[2] Environmental exposures, including endocrine-disrupting chemicals (EDCs), have gained significant attention as potential contributors to hormone-sensitive cancers, such as OC, with an estimated 90% of cancers attributed to environmental factors.[3] EDCs, a heterogeneous group of compounds, interfere with hormonal systems by mimicking, blocking, or altering hormone function. Although research has extensively examined the effects of EDCs on breast, prostate, and testicular cancers, their role in OC remains underexplored.[4] Emerging evidence links exposure to compounds such as phthalates,[5] bisphenols,[6,7] triclosan,[8] and chlorotriazines[9] with increased OC risk. Additionally, in vitro studies suggest that also benzophenones, such as benzophenone-1 (BP-1), may stimulate OC cell proliferation,[10] likely through mechanisms involving oxidative stress, chronic inflammation, and disruption of hormonal homeostasis. These findings underscore the need for a deeper understanding of EDCs' role in OC etiology, particularly in the context of cumulative and lifelong exposures. Borderline ovarian tumors (BOT), which are less aggressive and carry a better prognosis than OC, share some overlapping risk factors.

Received: November 28, 2024
Revised: April 10, 2025
Accepted: April 11, 2025
Published: April 22, 2025



ACS Publications

© 2025 The Authors. Published by American Chemical Society

https://doi.org/10.1021/acs.est.4c13290
Environ. Sci. Technol. 2025, 59, 8380−8390

However, their association with environmental exposures, including EDCs, remains poorly understood.[11] Investigating both OC and BOT within the exposome framework — encompassing the entirety of an individual's environmental exposures from conception onward[12] — provides a comprehensive approach to elucidate the role of environmental factors in gynecological cancers. In this sense, the exposome concept offers a more holistic understanding of environmental contributions to cancer risk, and along with the technological progress and innovation, new methodological approaches have emerged that enable us to expand our knowledge about environmental and human chemical exposure.[13]

Urinary biomonitoring has emerged as a powerful method for assessing environmental exposures due to its non-invasive nature and ability to reflect both endogenous and exogenous compounds. Despite these advantages, current methodologies face significant challenges in detecting low-abundance contaminants, particularly in nontargeted and suspect screening (NTS/SS) approaches. Limitations include incomplete chemical coverage, particularly of highly polar biomarkers of exposure (BoEs),[14] and the complexity of identifying low-concentration analytes against a backdrop of endogenous compounds.

This study explores chemical exposure profiles in women with ovarian malignancies (OM), focusing on EDCs and their potential role in OC. Advanced NTS/SS methodologies integrated with human biomonitoring aim to address critical gaps in exposure science. A novel urine sample preparation method was developed for dual-column ultrahigh-performance liquid chromatography (UHPLC), combining hydrophilic interaction liquid chromatography (HILIC) and reversed-phase (RP) separations with HRMS. This approach enhances compound detection across a wide polarity range, improving the detection and identification of urinary BoEs. Applied to samples from OM patients and healthy controls (HC), the approach identifies exposure differences and their potential links to cancer risk. The study advances analytical methods while providing insights into environmental contributions to cancer. Findings support regulatory frameworks for chemical safety and align with the goals of the Partnership for the Assessment of Risks from Chemicals (PARC) initiative.[15] Particularly, it focuses on early warning tools for chemicals of emerging concern.

■ MATERIALS AND METHODS

Materials and Chemicals are listed in S1 (Chapter 1) and reference standards are listed in Table S2-A1.

Samples. First-morning urine samples involved those of 25 healthy pregnant women (healthy controls, HC, average age 33.6 ± 2.8) with a singleton pregnancy between 37 and 41 weeks of gestation and without chronic diseases, and 25 women diagnosed with OM (average age 46.4 ± 16.1), of which 10 with BOT (average age 40.3 ± 16.1) and 15 with OC (average age 50.5 ± 14.7), all of whom provided informed consent. The diagnosis of BOT and OC was based on the histopathological examination. All participants provided first-morning urine samples after fasting.

Urine samples were collected in polypropylene containers prewashed with 10% nitric acid, aliquoted, and immediately stored at −80 °C to preserve sample integrity. Shortly prior to analysis, samples were thawed at room temperature. The study was conducted in accordance with the Declaration of Helsinki and was approved by the Slovenian National Commission for Medical Ethics (license no.: 0120-158/2022/9).

For method development, validation, and column conditioning throughout the study, pooled urine samples from 5 healthy donors were used. Procedural bank samples used LC-MS grade water as the matrix.

Sample Preparation. The protocol was adopted from our previous studies.[16,17] To 1 mL of thawed urine, 430 μL of LC-MS grade water, 50 μL of 3 M sodium acetate buffer (pH 5.2), and 20 μL of β-glucuronidase/arylsulfatase solution (*Helix pomatia*, type H-2) were added to achieve the final enzyme concentration of 135 U/mL. The mixture was incubated at 37 °C for 16 h on an orbital thermo-shaker to facilitate deconjugation. For solid-phase extraction (SPE), we conditioned a 60 mg sorbent packed in an Oasis-HLB 96-well plate with 1 mL of ethyl acetate (EtOAc), 1 mL of methanol (MeOH), and equilibrated it with 1 mL of LC-MS grade water. After loading the sample, we eluted the analytes from the sorbent with 1.5 mL of 30% (v/v) MeOH in water (the "wash fraction") and collected it separately from the subsequent 1.5 mL of 10% (v/v) EtOAc in acetonitrile (ACN) ("elution fraction"). We added isotopically labeled internal standards (IS) (listed in Table S2-A1) to both fractions at final concentrations of 500 μg/L in the wash fraction and 100 μg/L in the elution fraction. These concentrations were optimized based on the different instrumental methods used and were necessary due to differences in the sensitivity and ionization efficiency of the methods. 10 μL of DMSO were added exclusively to the elution fraction to serve as a keeper, with the volume chosen to effectively minimize analyte loss while preventing interference with LC analysis. Both fractions (wash and elution) were then dried under a gentle nitrogen stream while being heated to 40 °C in heat blocks to speed up the evaporation. Prior to the instrumental analysis, we reconstituted the wash and elution fractions with 250 μL of 80% (v/v) ACN in water and 250 μL of 10% (v/v) ACN in water, respectively, and filtered samples using 0.2 μm syringe filters with regenerated cellulose membrane. Procedural blank samples, calibrators, and all quality control (QC) standards, except for system suitability controls, were prepared following the same procedure.

Instrumental Analysis. Instrumental analyses were performed using a Thermo Fisher Vanquish UHPLC system coupled to a Thermo Fisher Orbitrap Exploris 240 mass spectrometer (Thermo Fisher Scientific Inc., Waltham, MA, USA), which was calibrated accordingly with the manufacturer's instructions. Scan-to-scan mass correction was applied during acquisition to ensure the highest mass accuracy throughout the analysis. HILIC and RP-based acquisitions were applied to the wash and elution fractions, respectively. In the HILIC-based acquisition, we achieved the separation using a Waters BEH amide (2.1 × 100 mm, 1.7 μm) column with (A) ACN and (B) 20 mM ammonium formate with 0.1% formic acid (pH 3.5) as mobile phases. The elution gradient was as follows: 5% B (0−2 min), 5−45% B (2−15 min), 45% B (15−16 min) 45−5% B (16−16.5 min), 5% B (16.5−30 min). The flow rate was 0.4 mL/min, the column temperature was 35 °C and the injection volume was 5 μL. Heated electrospray ionization (HESI) was used as the ionization source with the following settings: capillary voltage, 3.5 and −2.5 kV for positive and negative mode, respectively; sheath gas, 50 AU; auxiliary gas, 10 AU; sweep gas, 1 AU; ion transfer tube temperature, 325 °C; vaporizer temperature, 350 °C. The

https://doi.org/10.1021/acs.est.4c13290
Environ. Sci. Technol. 2025, 59, 8380−8390

Table 1. Outline of the Validation Plan for the Analytical Method, Including Specified Acceptance Limits for Mass Accuracy, RT Variability, Method Repeatability, Trueness, Linearity, LOD, and Carry-Over[a]

parameter	definition	criteria
mass accuracy	difference between measured and theoretical m/z	mass error < 5 ppm
RT variability	RT of QC standards compared to the defined RT	RP: RT error < 0.10 min HILIC: RT error < 0.25 min
method repeatability	% CV of peak heights, normalized with IS (3 QC standards, spiked with 100 μg/L)	< 30% CV
trueness	% difference between spiked and experimentally determined concentration, expressed as % Bias (3 QC standards, spiked with 100 μg/L)	< ±35% bias
linearity	pooled urine samples, spiked with reference standards at 1, 5, 25, 50, 100, and 150 μg/L injected to establish linearity of response and detection range.	evaluated, but not used as exclusion criteria
LOD	lowest calibrator with a signal/noise ratio ≥ 3	evaluated, but not used as exclusion criteria
carry-over	solvent blanks injected after the highest calibrator	< 20% of the LOD peak height for spiked reference standard

[a]CV: coefficient of variation; HILIC: hydrophilic interaction liquid chromatography; IS: internal standard; LOD: limit of detection; ppm: parts per million; QC: quality control; RP: reversed-phase; RT: retention time.

full scan mass acquisition scanned the mass range of 80−1000 m/z at the resolution of 90,000 fwhm, while the MS2 data was acquired at the resolution of 30,000. The centroiding was performed directly, without postacquisition conversion. The data-dependent acquisition (DDA) involved intensity threshold for the MS/MS events set to 1.0×10^3, with the top 8 most intense ions selected for fragmentation. Dynamic exclusion with a 9 s time window and 5 ppm mass tolerance was applied. A 20% apex window was used for DDA, with an isolation window of 1.5 m/z for precursor ions. Higher-energy collisional dissociation (HCD) was applied with normalized stepped collision energies of 30, 50, and 150% to ensure comprehensive fragmentation.

In the RP-based acquisition, we used a Waters Acquity HSS-T3 (2.1 × 100 mm, 1.8 μm) column with (A) ACN with 0.1% formic acid and (B) water containing 0.1% formic acid (pH 2.6) as the mobile phases. The elution gradient was as follows: 95−75% B (0−3 min), 75−60% B (3−7 min), 60−40% B (7−15 min), 40−30% B (15−18 min), 30−0% (18−24.5 min), 0% B (24.5−26.5 min), 0−95% B (26.5−27.5 min), 95% B (27.5−33 min). The flow rate was 0.3 mL/min, the column temperature was 35 °C and the injection volume was 5 μL. The HESI settings involved capillary voltage of 4.5 kV for positive and −3.0 kV for negative ionization mode; sheath gas, 40 AU; auxiliary gas, 15 AU; sweep gas, 2 AU; ion transfer tube temperature, 350 °C; vaporizer temperature, 400 °C. The full scan mass acquisition covered the mass range of 100−900 m/z and was acquired with a resolution of 90,000 while MS2 data was acquired with a resolution of 30,000. The centroiding was performed directly, without postacquisition conversion. The DDA intensity threshold for the MS/MS events was set to 1.0×10^4, and the top 7 most intense ions were selected for fragmentation. Dynamic exclusion with a 9 s time window and 5 ppm mass tolerance was applied. A 20% apex window was used for DDA, with an isolation window of 1.5 m/z for precursor ions. HCD was applied with normalized stepped collision energies of 30, 50, and 150% to ensure comprehensive fragmentation.

Validation, Quality Assurance, and Quality Control. Validation followed a modified protocol from Grijseels et al.,[18] assessing mass accuracy, retention time (RT) variability, method repeatability, trueness, linearity, and limit of detection (LOD) of the reference standards listed in S2-A1.[18] Validation parameters and the set criteria are shown in Table 1.

We prepared two separate batches, one for validation and one for sample analysis. The latter was randomized to ensure unbiased distribution and robust results. We started each batch with a reconstitution solvent as a system blank. System control standards were solvents spiked with reference standards at 150 and 300 μg/L, which we injected at the beginning and end of each batch to ensure consistent system performance, evaluate mass accuracy (mass error < 5 ppm) and RT variation (±0.25 min (HILIC) and ± 0.10 min (RP)) of the spiked reference standards. Three quality control (QC) standards were prepared from pooled urine spiked with reference standards at 100 μg/L pre-extraction. Each QC was injected twice per batch, resulting in a total of 6 QC injections total, performed every 10 samples to monitor system stability. The IS signals were monitored in all samples and QCs to confirm proper injection and identify any anomalies. The reference standard and IS lists are provided in Table S2-A1, and monitored system control reference standards are listed in Table S2-A2. The QC charts were established to control for any variations across the batches and are presented in S1 (Figures S1-1−4).

Data Analysis. Raw data were processed using mzmine 4.3.0,[19] with processing parameters detailed in S1-2.1 and S1-2.2. Features present in the procedural blanks (ratio between samples to procedural blanks < 3), those without MS2 data, and features eluted in the void were excluded. Feature heights were normalized using the closest eluting IS (normalized intensities). Heights were preferred over peak areas to minimize inaccuracies in baseline estimation, particularly for low abundance analytes, a common challenge in NTS data preprocessing.

BoEs annotation followed two approaches as illustrated in Figure 1 and was based on a modified version of the Schymanski scale.[20] *Nontargeted screening* involved matching MS2 spectra to libraries. Matches to the in-house library (positive.mgf and negative.mgf), which was built using our reference standards, complying with our established criteria (mass error of the parent ion < 5 ppm, three matched MS2 signals (mass error < 10 ppm), and RT variation ± 0.25 min (HILIC) and ± 0.10 min (RP)), were assigned level 1 ID confidence. Matches to the MoNA (Mass Bank of North America) experimental MS2 library,[21] applying the same mass accuracy criteria as level 1, along with cosine similarity > 0.8, were reported as level 2 ID confidence. In silico fragmentation and identification were performed by uploading MS2 spectra

https://doi.org/10.1021/acs.est.4c13290
Environ. Sci. Technol. 2025, 59, 8380−8390

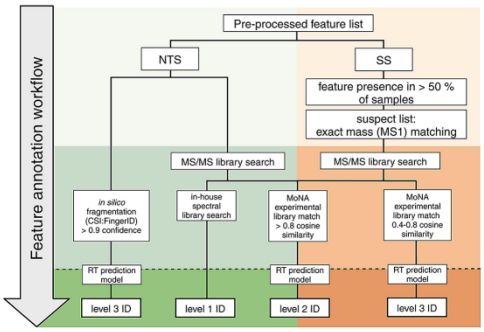


Figure 1. Feature annotation workflow.

to SIRIUS+CSI:FingerID,[22] and then generating possible structural candidates from selected libraries (KEGG,[23] ChEBI,[24] HMDB,[25] and GNPS[26]). The candidates with match confidence > 0.9 and with all matching substructures were reported at the level 3 ID confidence. Urine endogenous and food-derived biomarkers were filtered out at this stage using information from HMDB.[25]

Suspect screening annotation approach was applied to features present in more than 50% of samples. It involved matching MS1 data to an in-house suspect list with a mass tolerance of 5 ppm, followed by MS2 data matching to the MoNA experimental library. The suspect list included 801 entries with name, monoisotopic mass, m/z values, IUPAC name, InChI, and canonical SMILES for molecular ions of xenobiotic compounds compiled from Exposome Explorer,[27] T3DB,[28] and HBM4 EU CECscreen.[29] The inclusion list contained entries of various classes of contaminants, including pesticides, plasticizers, plastic-related chemicals, personal care products, and persistent organic pollutants. Matches with similarity scores above 0.8, were reported as level 2 ID annotations, and matches with similarity scores from 0.4 to 0.8, considering only the best match, were reported as level 3 ID annotations.

Finally, RT prediction models, developed for each method using the Retip package,[30] were applied to exclude tentatively annotated compounds whose RT deviated by more than three times the mean absolute error of the corresponding model.

For statistical analysis focusing on BoEs, pharmaceutical residues, and caffeine were excluded, as their presence primarily reflects voluntary use or lifestyle choices rather than background exposure. The analysis was conducted based on the annotated BoEs to assess differences between (a) HC and OM, and (b) HC, BOT, and OC groups separately. Urine dilution was corrected using specific gravity adjustment prior to analysis. A detailed description of the procedure and calculation is provided in S1 (Chapter 5).

a) Normality of the data was assessed using the Shapiro-Wilk test, and homoscedasticity across the groups was evaluated using Levene's test. Based on the results, a nonparametric Mann−Whitney U-test was selected to compare the normalized intensities of BoEs between the two independent groups ($p < 0.05$).
b) Variations in distribution among the three groups (HC, BOT, and OC), as well as trends in median values across the health spectrum were assessed solely for the BoEs exhibiting significant differences ($p < 0.05$) in step (a), with the objective to link higher median normalized intensities with the condition severity. For those BoEs identified in step (a), a Kruskal−Wallis test was applied to the three groups, followed by pairwise Mann−Whitney U-tests for each group pair (HC vs BOT, HC vs OC, and BOT vs OC) to allow comparisons of distributions among the specific group combinations. For the pairwise comparisons, the Bonferroni correction was applied to adjust for multiple testing, ensuring that the significance level was maintained across all group combinations. Therefore, a threshold of $p < 0.017$ was set as the criterion for statistical significance.

To ensure thorough reporting of the research, the NTA Study Reporting Tool (SRT)[31,32] was used in the preparation of this manuscript.

RESULTS AND DISCUSSION

Analytical Method Development. The analytical method was optimized to maximize compound coverage while minimizing sample volume and simplifying preparation to reduce processing time and contamination risk. A sequential wash and elution protocol was used, where the wash fraction with highly polar compounds was analyzed with HILIC-based approach and the elution fraction, containing semipolar compounds, was analyzed with RP-based approach. The selection of analyte sets was purpose-driven, with 57 compounds for method development, 90 for detection rate assessment, and 32 for QA/QC monitoring, ensuring a balance between comprehensive evaluation and practicality (Table S2-A1).

To determine the optimal solvent composition, 57 representative reference standards spanning diverse BoEs and a broad XLogP3 range (−7.5 to 7.4) were evaluated (Table S2-A1 and Figure S1-5). Testing various solvent compositions revealed an optimal balance between the two complementary fractions, maximizing compound abundance and coverage across positive and negative ionization modes in both HILIC and RP approaches.

Following scaling the reference standards' normalized intensities from 0 to 1, the outcomes are illustrated as heatmaps for HILIC (Figure S1-6) and RP (Figure S1-7). Notably, the wash fraction demonstrated a higher abundance of polar compounds, with some (e.g., malathion dicarboxylic acid, bleomycin) being exclusively present there (Figure S1-6). Conversely, the elution fraction exhibited the highest presence of less polar compounds, as evident from the predominant red color in the top left corner in Figure S1-7, particularly when using the stronger elution solvent, E2 (30% EtOAc in ACN).

To quantify the overall efficiency of different solvent combinations, scaled normalized efficiencies were summed as presented in Figure S1-8. While differences were minor, the optimal combination was identified as 30% MeOH in water as the wash solvent and 10% EtOAc in ACN as the elution solvent.

Analytical Method Performance Assessment. We evaluated the analytical method's performance by assessing mass accuracy, RT variability, method repeatability, trueness, linearity, and LOD on a selected subset of reference standards for positive and negative acquisition modes in HILIC and RP-based instrumental approaches. The summarized results are presented in Table S2-A3 and confirm linear responses within the tested concentration ranges, with most R^2 values exceeding

https://doi.org/10.1021/acs.est.4c13290
Environ. Sci. Technol. 2025, 59, 8380−8390

0.900. While a few exceptions showed slightly lower linearity, the lowest R^2 observed was 0.818 in the case of 5-fluorouracil, which is still within a reasonable range. The demonstrated LODs for many compounds are substantially low, especially with the RP-based approach, enabling robust detection at trace levels, which strengthens the analytical framework for sensitive biomonitoring. This can be attributed, at least in part, to the fractionation-based sample preparation, which yields cleaner samples by reducing potential interferences. It is also important to note that, due to the lack of a true blank urine matrix, LODs could not be determined for compounds that exhibited signals in blanks, indicating their presence in the matrix. Also, the repeatability and trueness were below the set criteria (<30% CV and <35% Bias). Normalized intensities of selected reference standards were tracked in QCs across each batch and plotted in QC charts (Figures S1-1−4), showing low deviations and confirming satisfactory method stability, though variations were somewhat higher in the HILIC approach.

A comprehensive set of 90 reference standards, spanning a broad polarity range, was utilized to assess the overall method performance and validate the dual-column approach. The true positive detection rate (TPR) was calculated as proposed by Fisher et al.,[33] yielding a score of 0.90, respectively, with 81 out of 90 spiked test standards successfully detected. This high TPR demonstrates the method's efficacy in accurately detecting known test standards across different polarities. Specifically, 48 test standards were identified as RP-specific, 5 as HILIC-specific, and 28 were detected by both instrumental approaches. Nine reference standards were however not detected, likely due to low ionization efficiency, mobile phase incompatibility, weak fragmentation, or high polarity/poor retention (e.g., tris(2-ethylhexyl) trimellitate, bisphenol A, ibuprofen, glyphosate).

Nontargeted and Suspect Screening Results of the Real Samples. Out of 106 annotated BoEs we classified 32 of them under level 1, 50 under level 2, and 24 under level 3, following the criteria given in Figure 1. The annotated BoEs are listed in Table S2-A4 and encompass a diverse range of compound classes, predominantly pharmaceuticals, plasticizers, and pesticides. The addition of the HILIC approach to the RP-based analysis resulted in the detection of 23 additional BoEs, representing a 28% increase in coverage. Additionally, 9 BoEs were detected by both approaches, indicating an overlap. The Venn diagram (Figure 2) illustrates the advantages of the dual-column strategy, highlighting unique and overlapping annotations across individual acquisition modes in HILIC and RP-based instrumental approaches. This demonstrates the broader chemical space achieved by combining both approaches. Moreover, the expansion of chemical space coverage is depicted in Figure 3, which plots the XLogP3 values against the number of BoEs detected using individual HILIC and RP-based approaches. The results strongly support the presented strategy, showing significantly wider coverage across different polarities compared to the traditional RP-based approach alone. This enhanced coverage is essential for comprehensive urinary profiling, particularly when aiming to detect low-abundance exogenous biomarkers that may have biological relevance to disease states such as OC.

Notably, the detection of 10 residual glucuronides between the detected BoEs (Table S2-A4) likely results from incomplete hydrolysis, as deconjugation efficiency depends on enzyme specificity, substrate complexity, and reaction conditions (pH, temperature, incubation time).[34]

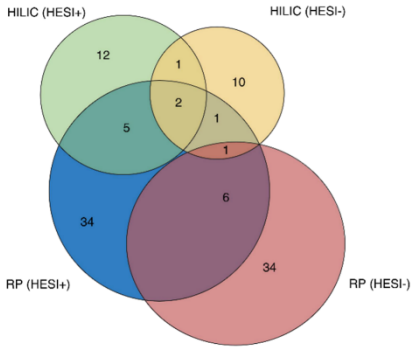


Figure 2. Venn diagram showing the number and overlap between BoEs detected with each instrumental method and annotated according to the criteria following Figure 1.

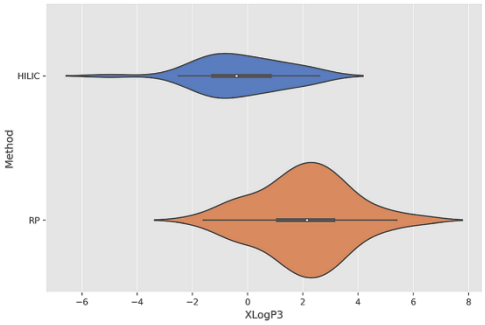


Figure 3. Polarity chemical space coverage: XLogP3 of BoEs, detected with HILIC and RP-based approaches.

A large share of the annotated biomarkers reflects lifestyle choices, such as consumption of caffeine and tobacco products, or the use of pharmaceuticals to treat or prevent symptoms or diseases. In contrast, industrial chemicals, pesticides, and other compounds primarily indicate involuntary exposure.[35] Using the Mann−Whitney test ($p < 0.05$) we compared the differences in exposure to these chemicals and found significant differences in the normalized intensities of eight BoEs between the HC and OM individuals. The results are detailed in Table S2-A5 and are visualized in Figure 4. The results reveal significantly higher normalized intensities of mono(2-ethyl-5-carboxypentyl) phthalate (cx-MEPP), mono-ethyl phthalate (MEP), metolachlor TP NOA 413173, BP-1, 4-methyl-2-nitrophenol, and 4-nitrophenol (4-NP) in the OM group. Notably, these BoEs belong to phthalates, pesticides, and UV filters, many of which are known or suspected EDCs, potentially linking them to hormone cancers, such as OC.[36] On the contrary, mono-(4-methyl-7-hydroxyoctyl) phthalate (OH-MINP), and 2-(4-(diethylamino)-2-hydroxybenzoyl)-benzoic acid were higher in HC.

By further statistical analysis of the discriminatory BoEs, we aimed to find any potential differences related to cancer malignancy by comparing HC, BOT, and OC ($p < 0.017$). The results are visualized in Figure 5 with the corresponding data

https://doi.org/10.1021/acs.est.4c13290
Environ. Sci. Technol. 2025, 59, 8380−8390

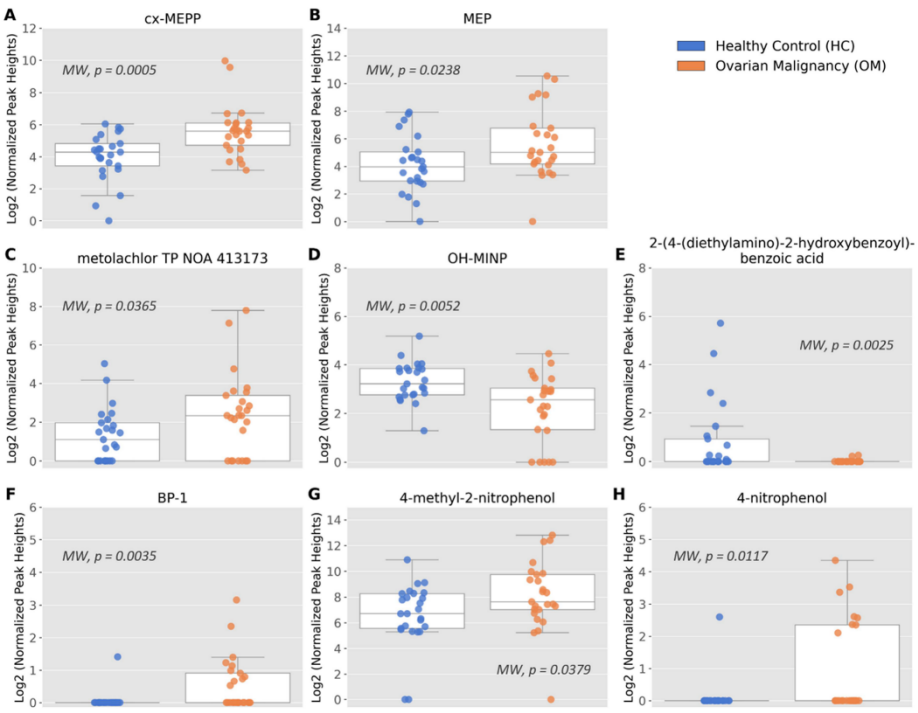


Figure 4. Box-Whisker plots (A–H) of Log2 normalized intensities for BoEs identified as having statistically significant differences with the Mann–Whitney test ($p < 0.05$) between OM ($n = 25$, orange) and HC ($n = 25$, blue).

presented in Table S2-A6. Briefly, in women with OC, the normalized intensities of cx-MEPP, BP-1, and 4-NP in the urine were statistically significantly higher than in HC, indicating a higher exposure. Additionally, the normalized intensities of cx-MEPP were significantly elevated in OC compared to the BOT group. Also, in women with BOT, the normalized intensities of BP-1 in urine were statistically significantly higher than in HC. On the other hand, the normalized intensities of OH-MINP and 2-(4-(diethylamino)-2-hydroxybenzoyl)benzoic acid were statistically significantly lower in the urine of OC than in HC (Figure 5).

Below, we discuss the substances detected with statistically significant differences between women with OM and HC, along with their implications.

Phthalates and Their Metabolites. Phthalates (PHs) are extensively used in plastics, cosmetics, and pharmaceuticals,[37,38] leading to pervasive food and environmental contamination. PHs and their metabolites have been detected in various human tissues and biological fluids.[39] They are metabolized and excreted mainly through urine,[40,41] with exposure linked to reproductive toxicity, endocrine disruption, and ovarian dysfunction.[42,43] Diethylhexyl phthalate (DEHP) and its metabolite mono ethylhexyl phthalate (MEHP) are particularly well studied, with evidence of impaired ovarian function and increased metastasis risk in OC models.[5,44,45] DEHP, dibutyl phthalate (DBP), di-isobutyl phthalate (DIBP), and benzyl butyl phthalate (BBP) are classified as toxic to reproduction, largely based on animal evidence (1B).[46] In the present study, we observed that normalized intensities of cx-MEPP, a secondary metabolite of DEHP, were significantly elevated in OM patients as compared to HC ($p < 0.05$), suggesting higher exposure and potentially differing lifestyle habits. Additionally, cx-MEPP intensities were particularly elevated in the OC group, exhibiting a trend of OC > BOT > HC. This pattern indicates a possible association between DEHP exposure and OC development. However, further research is needed to confirm causality, taking into account also genetic susceptibility to phthalate exposure as a contributing factor.[47] Likewise, the normalized intensities of MEP, the primary metabolite of diethyl phthalate (DEP), were elevated in OM patients, though its toxicity and OC relevance remain unclear.[48] Conversely, OH-MINP, a secondary metabolite of diisononyl phthalate (DINP), was significantly lower in OM and OC patients compared to HC. While DINP exposure has been linked to ovarian dysfunction,[49] direct evidence linking DINP exposure to OC is lacking.

Our results highlight significant differences in the normalized intensities of PHs metabolites, which serve as reliable indicators of PHs exposure. While these metabolites primarily reflect short-term exposure due to the rapid metabolism and excretion of PHs, their detection may also suggest chronic exposure. This could be attributed to lifestyle factors, indicating prolonged or even lifelong exposure to PHs.

https://doi.org/10.1021/acs.est.4c13290
Environ. Sci. Technol. 2025, 59, 8380−8390

Environmental Science & Technology pubs.acs.org/est Article

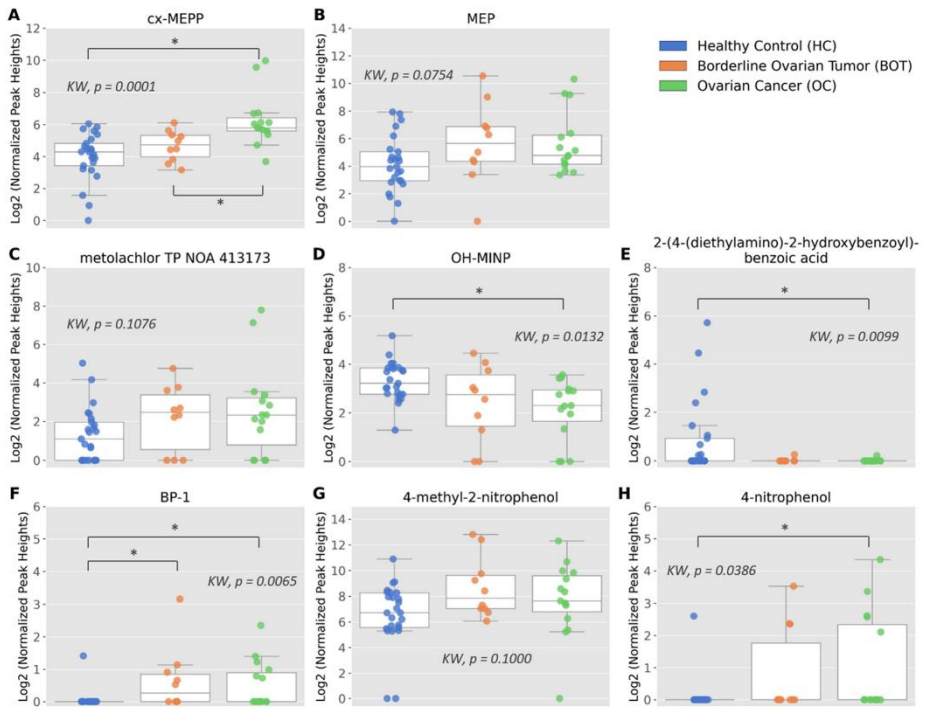


Figure 5. Box-and-whisker plots (A–H) of Log2 normalized intensities for the eight discriminatory BoEs in cancer subtypes (BOT, n = 10, orange; OC, n = 15, green) and HC (n = 25, blue). Statistically significant differences were tested using Kruskal–Wallis (KW) among three groups and the Mann–Whitney test between each two groups. Statistically significant differences (MW, $p < 0.017$) are indicated with an asterisk (*).

Phytosanitary. Metolachlor TP NOA 413173, a metabolite of the chloroacetanilide herbicide metolachlor, and specifically its S stereoisomer (S-metolachlor) is currently classified as a suspected carcinogen by the European Chemicals Agency.[50] Studies have linked metolachlor exposure to an increased risk of lymphoid malignancies[51] and endocrine disruption.[52,53] In our study, we observed substantially elevated normalized intensities of metolachlor TP NOA 413173 in the overall OM population, suggesting a possible link between metolachlor exposure and OC.

Similarly, 4-NP, a common intermediate in the synthesis of various chemicals and metabolite of now-banned organophosphate insecticides, showed elevated normalized intensities in the OM group, predominantly in OC patients. Though 4-NP exhibits estrogenic and antiandrogenic properties, its relevance to OC remains unclear.[54,55]

UV Filters. A large group of benzophenone derivatives are commonly found in sunscreens and other cosmetic products, leading to ubiquitous human exposure.[56] They have been associated with endocrine disruption, particularly affecting thyroid and sex hormones, and potential carcinogenicity.[10,57] Both BOT and OC subgroups exhibited elevated normalized intensities of BP-1 as compared to HC, which may reflect increased exposure, altered metabolism, or accumulation in tumor tissues.

Further, 2-(4-(diethylamino)-2-hydroxybenzoyl)benzoic acid is likely the metabolite of a UV filter, 2-(4-(diethylamino)-2-hydroxybenzoyl)benzoate (DHHB), another discriminatory BoE found in OM and HC samples.[58] Although no studies have directly associated DHHB with endocrine-disrupting properties, similar compounds within the same chemical class exhibit such effects, suggesting the need for further investigation. Our results show significantly higher normalized intensities of 2-(4-(diethylamino)-2-hydroxybenzoyl)benzoic acid in the HC samples as compared to the OM group. Additionally, normalized intensities were significantly lower in the OC subgroup compared to the HC group. This can be explained by the lower exposure to the parent compound, but also by possible metabolic alterations associated with OC, leading to possible altered metabolism and/or excretion.

Other BoEs. 4-methyl-2-nitrophenol is an industrial intermediate with limited toxicity data, which was elevated in OM patients. Its structural similarity to known hazardous nitrophenols suggests a need for further investigation.

Interpreting Biomarker Variations. The observed differences in normalized BoEs intensities between OM and HC suggest complex interactions between environmental exposures and cancer onset. Elevated normalized intensities of certain BoEs in cancer patients may not necessarily indicate a causal relationship but could also reflect lifestyle changes, altered

https://doi.org/10.1021/acs.est.4c13290
Environ. Sci. Technol. 2025, 59, 8380–8390

metabolism, or tumor-related processes, which were not specifically assessed in this study. This consideration is crucial, as severe malignancies such as OC are often accompanied by significant lifestyle changes, leading to altered exposure profiles. A similar dynamic applies to comparisons between patients with BOT and OC. A notable limitation in the study design is the composition of the HC cohort, which included pregnant women. Pregnancy involves substantial physiological changes, including altered metabolism and kidney function, which differ from the general population. However, unlike women with OM, these individuals had healthy ovaries with normal function, enabling successful pregnancy. The relatively small sample size in each group presents another limitation, though patient recruitment was carefully controlled to ensure group validity. Overall, while findings suggest possible links between specific exposures and OC, they do not establish causality.

This study successfully utilized a fractionation-based sample preparation and combined HILIC and RP-UHPLC-HRMS to profile the urinary exposome of women with OM, uncovering significant differences in specific EDCs compared to HC.

Elevated normalized intensities of cx-MEPP, MEP, metolachlor TP NOA 413173, and BP-1 reinforce concerns about the potential role of these ubiquitous BoEs in hormone-related cancers. Notably, cx-MEPP normalized intensities correlated with malignancy severity, suggesting a possible link between DEHP exposure and cancer development. Additionally, the use of open-source software for data processing enhances accessibility and reproducibility, promoting their broader adoption.

With minor adaptations, this approach could be applied to various biological, environmental, and food matrices, further supporting PARC's mission to establish robust tools for chemical monitoring and early warning systems for compounds of emerging concern. While these findings offer valuable insights, further research with larger, more diverse cohorts and longitudinal analyses is needed to confirm these findings, refining our understanding of the relationship between environmental exposures and OC development.

■ ASSOCIATED CONTENT

Supporting Information

The Supporting Information is available free of charge at https://pubs.acs.org/doi/10.1021/acs.est.4c13290.

Materials and chemicals, data processing parameters, quality control charts, standard class and XLogP3 distribution chart, SPE optimization results charts, and specific gravity adjustment (PDF)

Table of reference standards, table of system control reference standards and validation results, table of identified BoEs, and statistical analysis results tables (XLSX)

Mass spectral library: positive.mgf (PDF)

negative.mgf (PDF)

■ AUTHOR INFORMATION

Corresponding Author

Tina Kosjek − *Department of Environmental Sciences, Jožef Stefan Institute, 1000 Ljubljana, Slovenia; Jožef Stefan International Postgraduate School, 1000 Ljubljana, Slovenia;* orcid.org/0000-0002-6421-0344; Email: tina.kosjek@ijs.si

Authors

Helena Plešnik − *Department of Environmental Sciences, Jožef Stefan Institute, 1000 Ljubljana, Slovenia; Jožef Stefan International Postgraduate School, 1000 Ljubljana, Slovenia*

Žan Rekar − *Department of Environmental Sciences, Jožef Stefan Institute, 1000 Ljubljana, Slovenia; Jožef Stefan International Postgraduate School, 1000 Ljubljana, Slovenia*

Stefanela Stevanović − *Faculty of Computer and Information Science, University of Ljubljana, 1000 Ljubljana, Slovenia*

Irma Virant-Klun − *Clinical Research Centre, University Medical Centre Ljubljana, 1000 Ljubljana, Slovenia; Faculty of Medicine, University of Ljubljana, 1000 Ljubljana, Slovenia*

Senka Imamović Kumalić − *Faculty of Medicine, University of Ljubljana, 1000 Ljubljana, Slovenia; Division of Obstetrics and Gynecology, University Medical Centre Ljubljana, 1000 Ljubljana, Slovenia*

Mateja Sladič − *Faculty of Medicine, University of Ljubljana, 1000 Ljubljana, Slovenia; Division of Obstetrics and Gynecology, University Medical Centre Ljubljana, 1000 Ljubljana, Slovenia*

Darja Mazej − *Department of Environmental Sciences, Jožef Stefan Institute, 1000 Ljubljana, Slovenia*

Janja Snoj Tratnik − *Department of Environmental Sciences, Jožef Stefan Institute, 1000 Ljubljana, Slovenia*

Milena Horvat − *Department of Environmental Sciences, Jožef Stefan Institute, 1000 Ljubljana, Slovenia; Jožef Stefan International Postgraduate School, 1000 Ljubljana, Slovenia*

Complete contact information is available at: https://pubs.acs.org/10.1021/acs.est.4c13290

Author Contributions

H.P. and Ž.R. contributed equally and share the first authorship. Conceptualization: H.P., Ž.R., T.K.; Methodology: H.P., Ž.R., S.S., T.K.; Software: H.P., Ž.R., S.S.; Validation: H.P., Ž.R.; Formal analysis: H.P., Ž.R., S.S.; Investigation: H.P., Ž.R., I.V.K., M.S., S.I.K.; Resources: T.K., I.V.K., M.H.; Writing−original draft: H.P., Ž.R., T.K.; Writing−review and editing: all; Visualization: H.P., Ž.R., S.S., T.K.; Supervision: T.K., M.H.; Project administration: T.K., I.V.K., M.H.; Funding acquisition: M.H., T.K., I.V.K.

Notes

The authors declare no competing financial interest.

■ ACKNOWLEDGMENTS

This work was supported by the project Partnership for the Assessment of Risks from Chemicals (PARC) funded by the European Union research and innovation program Horizon Europe (grant agreement 101057014). The funding by the Slovenian Research and Innovation Agency − ARIS through the program group P-0134, and research projects J3-2530 and J7-50230 is acknowledged. Ž.R. acknowledges ARIS for the Young Researcher grant. We would like to thank Tome Eftimov (Department of Computer Systems Department, Jožef Stefan Institute) and Tomo Testen (Faculty of Computer and Information Science, University of Ljubljana) for all the valuable work they contributed to this research.

■ ABBREVIATIONS

ACN	acetonitrile
AU	arbitrary unit
BOT	borderline ovarian tumors

https://doi.org/10.1021/acs.est.4c13290
Environ. Sci. Technol. 2025, 59, 8380−8390

CV	coefficient of variation
DMSO	dimethyl sulfoxide
EDCs	endocrine-disrupting compounds
EtOAc	ethyl acetate
HC	healthy controls
HCD	higher-energy collisional dissociation
HESI	heated electrospray ionization
HILIC	hydrophilic interaction liquid chromatography
HRMS	high-resolution mass spectrometry
IS	internal standard
LOD	lower limit of detection
MeOH	methanol
MS/MS	tandem mass spectrometry
NTS	nontargeted screening
OC	ovarian cancer
OM	ovarian malignancies
QC	quality control
RP	reversed-phase
SPE	solid-phase extraction
SS	suspect screening
TPR	true positive detection rate
UHPLC	ultrahigh-performance liquid chromatography

REFERENCES

(1) *Cancer of the Ovary - Cancer Stat Facts*; SEER. https://seer.cancer.gov/statfacts/html/ovary.html (accessed Sep 16, 2024).

(2) Stewart, S. L. Ovarian Cancer Incidence: Current and Comprehensive Statistics. In *Ovarian Cancer - Clinical and Therapeutic Perspectives*; Farghaly, S. A., Ed.; InTech: 2012.

(3) Anand, P.; Kunnumakara, A. B.; Sundaram, C.; Harikumar, K. B.; Tharakan, S. T.; Lai, O. S.; Sung, B.; Aggarwal, B. B. Cancer Is a Preventable Disease That Requires Major Lifestyle Changes. *Pharm. Res.* **2008**, *25* (9), 2097−2116.

(4) García-Pérez, J.; Lope, V.; López-Abente, G.; González-Sánchez, M.; Fernández-Navarro, P. Ovarian Cancer Mortality and Industrial Pollution. *Environ. Pollut.* **2015**, *205*, 103−110.

(5) Leng, J.; Li, H.; Niu, Y.; Chen, K.; Yuan, X.; Chen, H.; Fu, Z.; Zhang, L.; Wang, F.; Chen, C.; Héroux, P.; Yang, J.; Zhu, X.; Lu, W.; Xia, D.; Wu, Y. Low-Dose Mono(2-Ethylhexyl) Phthalate Promotes Ovarian Cancer Development through PPARα-Dependent PI3K/Akt/NF-κB Pathway. *Sci. Total Environ.* **2021**, *790*, No. 147990.

(6) Hafezi, S. A.; Abdel-Rahman, W. M. The Endocrine Disruptor Bisphenol A (BPA) Exerts a Wide Range of Effects in Carcinogenesis and Response to Therapy. *Curr. Mol. Pharmacol* **2019**, *12* (3), 230−238.

(7) Pivonello, C.; Muscogiuri, G.; Nardone, A.; Garifalos, F.; Provvisiero, D. P.; Verde, N.; de Angelis, C.; Conforti, A.; Piscopo, M.; Auriemma, R. S.; Colao, A.; Pivonello, R. Bisphenol A: An Emerging Threat to Female Fertility. *Reprod Biol. Endocrinol* **2020**, *18* (1), 22.

(8) Kim, J.-Y.; Yi, B.-R.; Go, R.-E.; Hwang, K.-A.; Nam, K.-H.; Choi, K.-C. Methoxychlor and Triclosan Stimulates Ovarian Cancer Growth by Regulating Cell Cycle- and Apoptosis-Related Genes via an Estrogen Receptor-Dependent Pathway. *Environ. Toxicol Pharmacol* **2014**, *37* (3), 1264−1274.

(9) Young, H. A.; Mills, P. K.; Riordan, D. G.; Cress, R. D. Triazine Herbicides and Epithelial Ovarian Cancer Risk in Central California. *J. Occup Environ. Med.* **2005**, *47* (11), 1148−1156.

(10) Park, M.-A.; Hwang, K.-A.; Lee, H.-R.; Yi, B.-R.; Jeung, E.-B.; Choi, K.-C. Benzophenone-1 Stimulated the Growth of BG-1 Ovarian Cancer Cells by Cell Cycle Regulation *via* an Estrogen Receptor Alpha-Mediated Signaling Pathway in Cellular and Xenograft Mouse Models. *Toxicology* **2013**, *305*, 41−48.

(11) Seidman, J. D.; Ronnett, B. M.; Kurman, R. J. Pathology of Borderline (Low Malignant Potential) Ovarian Tumours. *Best Practice & Research Clinical Obstetrics & Gynaecology* **2002**, *16* (4), 499−512.

(12) adttsihe. *The exposome*; IHEN. https://humanexposome.net/the-exposome/ (accessed 2024-11-05).

(13) Vermeulen, R.; Schymanski, E. L.; Barabási, A.-L.; Miller, G. W. The Exposome and Health: Where Chemistry Meets Biology. *Science* **2020**, *367* (6476), 392−396.

(14) Hulleman, T.; Turkina, V.; O'Brien, J. W.; Chojnacka, A.; Thomas, K. V.; Samanipour, S. Critical Assessment of the Chemical Space Covered by LC−HRMS Non-Targeted Analysis. *Environ. Sci. Technol.* **2023**, *57* (38), 14101−14112.

(15) Marx-Stoelting, P.; Rivière, G.; Luijten, M.; Aiello-Holden, K.; Bandow, N.; Baken, K.; Cañas, A.; Castano, A.; Denys, S.; Fillol, C.; Herzler, M.; Iavicoli, I.; Karakitsios, S.; Klanova, J.; Kolossa-Gehring, M.; Koutsodimou, A.; Vicente, J. L.; Lynch, I.; Namorado, S.; Norager, S.; Pittman, A.; Rotter, S.; Sarigiannis, D.; Silva, M. J.; Theunis, J.; Tralau, T.; Uhl, M.; van Klaveren, J.; Wendt-Rasch, L.; Westerholm, E.; Rousselle, C.; Sanders, P. A Walk in the PARC: Developing and Implementing 21st Century Chemical Risk Assessment in Europe. *Arch. Toxicol.* **2023**, *97* (3), 893−908.

(16) Tkalec, Ž.; Codling, G.; Klánová, J.; Horvat, M.; Kosjek, T. LC-HRMS Based Method for Suspect/Non-Targeted Screening for Biomarkers of Chemical Exposure in Human Urine. *Chemosphere* **2022**, *300*, No. 134550.

(17) Tkalec, Ž.; Codling, G.; Tratnik, J. S.; Mazej, D.; Klánová, J.; Horvat, M.; Kosjek, T. Suspect and Non-Targeted Screening-Based Human Biomonitoring Identified 74 Biomarkers of Exposure in Urine of Slovenian Children. *Environ. Pollut.* **2022**, *313*, No. 120091.

(18) Grijseels, S.; Vasskog, T.; Heinsvig, P. J.; Myhre, T. N.; Hansen, T.; Mardal, M. Validation of Two LCHRMS Methods for Large-Scale Untargeted Metabolomics of Serum Samples: Strategy to Establish Method Fitness-for-Purpose. *Journal of Chromatography A* **2024**, *1732*, No. 465230.

(19) Schmid, R.; Heuckeroth, S.; Korf, A.; Smirnov, A.; Myers, O.; Dyrlund, T. S.; Bushuiev, R.; Murray, K. J.; Hoffmann, N.; Lu, M.; Sarvepalli, A.; Zhang, Z.; Fleischauer, M.; Dührkop, K.; Wesner, M.; Hoogstra, S. J.; Rudt, E.; Mokshyna, O.; Brungs, C.; Ponomarov, K.; Mutabdžija, L.; Damiani, T.; Pudney, C. J.; Earll, M.; Helmer, P. O.; Fallon, T. R.; Schulze, T.; Rivas-Ubach, A.; Bilbao, A.; Richter, H.; Nothias, L.-F.; Wang, M.; Orešič, M.; Weng, J.-K.; Böcker, S.; Jeibmann, A.; Hayen, H.; Karst, U.; Dorrestein, P. C.; Petras, D.; Du, X.; Pluskal, T. Integrative Analysis of Multimodal Mass Spectrometry Data in MZmine 3. *Nat. Biotechnol.* **2023**, *41* (4), 447−449.

(20) Schymanski, E.; Jeon, J.; Gulde, R.; Fenner, K.; Ruff, M.; Singer, H.; Hollender, J. Identifying Small Molecules via High Resolution Mass Spectrometry: Communicating Confidence. *Environ. Sci. Technol.* **2014**, *48*. 2097.

(21) *MassBank of North America*. https://mona.fiehnlab.ucdavis.edu/ (accessed 2024-11-07).

(22) Dührkop, K.; Fleischauer, M.; Ludwig, M.; Aksenov, A. A.; Melnik, A. V.; Meusel, M.; Dorrestein, P. C.; Rousu, J.; Böcker, S. SIRIUS 4: A Rapid Tool for Turning Tandem Mass Spectra into Metabolite Structure Information. *Nat. Methods* **2019**, *16* (4), 299−302.

(23) Kanehisa, M.; Goto, S. KEGG: Kyoto Encyclopedia of Genes and Genomes. *Nucleic Acids Res.* **2000**, *28* (1), 27−30.

(24) Hastings, J.; Owen, G.; Dekker, A.; Ennis, M.; Kale, N.; Muthukrishnan, V.; Turner, S.; Swainston, N.; Mendes, P.; Steinbeck, C. ChEBI in 2016: Improved Services and an Expanding Collection of Metabolites. *Nucleic Acids Res.* **2016**, *44* (D1), D1214−D1219.

(25) Wishart, D. S.; Guo, A.; Oler, E.; Wang, F.; Anjum, A.; Peters, H.; Dizon, R.; Sayeeda, Z.; Tian, S.; Lee, B. L.; Berjanskii, M.; Mah, R.; Yamamoto, M.; Jovel, J.; Torres-Calzada, C.; Hiebert-Giesbrecht, M.; Lui, V. W.; Varshavi, D.; Varshavi, D.; Allen, D.; Arndt, D.; Khetarpal, N.; Sivakumaran, A.; Harford, K.; Sanford, S.; Yee, K.; Cao, X.; Budinski, Z.; Liigand, J.; Zhang, L.; Zheng, J.; Mandal, R.; Karu, N.; Dambrova, M.; Schiöth, H. B.; Greiner, R.; Gautam, V. HMDB 5.0: The Human Metabolome Database for 2022. *Nucleic Acids Res.* **2022**, *50* (D1), D622−D631.

(26) Wang, M.; Carver, J. J.; Phelan, V. V.; Sanchez, L. M.; Garg, N.; Peng, Y.; Nguyen, D. D.; Watrous, J.; Kapono, C. A.; Luzzatto-Knaan,

https://doi.org/10.1021/acs.est.4c13290
Environ. Sci. Technol. 2025, 59, 8380−8390

T.; Porto, C.; Bouslimani, A.; Melnik, A. V.; Meehan, M. J.; Liu, W.-T.; Crüsemann, M.; Boudreau, P. D.; Esquenazi, E.; Sandoval-Calderón, M.; Kersten, R. D.; Pace, L. A.; Quinn, R. A.; Duncan, K. R.; Hsu, C.-C.; Floros, D. J.; Gavilan, R. G.; Kleigrewe, K.; Northen, T.; Dutton, R. J.; Parrot, D.; Carlson, E. E.; Aigle, B.; Michelsen, C. F.; Jelsbak, L.; Sohlenkamp, C.; Pevzner, P.; Edlund, A.; McLean, J.; Piel, J.; Murphy, B. T.; Gerwick, L.; Liaw, C.-C.; Yang, Y.-L.; Humpf, H.-U.; Maansson, M.; Keyzers, R. A.; Sims, A. C.; Johnson, A. R.; Sidebottom, A. M.; Sedio, B. E.; Klitgaard, A.; Larson, C. B.; Boya, P.; A, C.; Torres-Mendoza, D.; Gonzalez, D. J.; Silva, D. B.; Marques, L. M.; Demarque, D. P.; Pociute, E.; O'Neill, E. C.; Briand, E.; Helfrich, E. J. N.; Granatosky, E. A.; Glukhov, E.; Ryffel, F.; Houson, H.; Mohimani, H.; Kharbush, J. J.; Zeng, Y.; Vorholt, J. A.; Kurita, K. L.; Charusanti, P.; McPhail, K. L.; Nielsen, K. F.; Vuong, L.; Elfeki, M.; Traxler, M. F.; Engene, N.; Koyama, N.; Vining, O. B.; Baric, R.; Silva, R. R.; Mascuch, S. J.; Tomasi, S.; Jenkins, S.; Macherla, V.; Hoffman, T.; Agarwal, V.; Williams, P. G.; Dai, J.; Neupane, R.; Gurr, J.; Rodríguez, A. M. C.; Lamsa, A.; Zhang, C.; Dorrestein, K.; Duggan, B. M.; Almaliti, J.; Allard, P.-M.; Phapale, P.; Nothias, L.-F.; Alexandrov, T.; Litaudon, M.; Wolfender, J.-L.; Kyle, J. E.; Metz, T. O.; Peryea, T.; Nguyen, D.-T.; VanLeer, D.; Shinn, P.; Jadhav, A.; Müller, R.; Waters, K. M.; Shi, W.; Liu, X.; Zhang, L.; Knight, R.; Jensen, P. R.; Palsson, B. Ø.; Pogliano, K.; Linington, R. G.; Gutiérrez, M.; Lopes, N. P.; Gerwick, W. H.; Moore, B. S.; Dorrestein, P. C.; Bandeira, N. Sharing and Community Curation of Mass Spectrometry Data with Global Natural Products Social Molecular Networking. *Nat. Biotechnol.* **2016**, *34* (8), 828−837.

(27) Neveu, V.; Nicolas, G.; Salek, R. M.; Wishart, D. S.; Scalbert, A. Exposome-Explorer 2.0: An Update Incorporating Candidate Dietary Biomarkers and Dietary Associations with Cancer Risk. *Nucleic Acids Res.* **2019**, *48* (D1), D908−D912.

(28) Wishart, D.; Arndt, D.; Pon, A.; Sajed, T.; Guo, A. C.; Djoumbou, Y.; Knox, C.; Wilson, M.; Liang, Y.; Grant, J.; Liu, Y.; Goldansaz, S. A.; Rappaport, S. M. T3DB: The Toxic Exposome Database. *Nucleic Acids Res.* **2015**, *43* (Database issue), D928−D934.

(29) Meijer, J.; Lamoree, M.; Hamers, T.; Antingac, J.-P.; Hutinet, S.; Debrauwer, L.; Covaci, A.; Huber, C.; Krauss, M.; Walker, D. I.; Schymanski, E.; Vermeulen, R.; Vlaanderen, J. *S71 | CECSCREEN | HBM4 EU CECscreen: Screening List for Chemicals of Emerging Concern Plus Metadata and Predicted Phase 1 Metabolites*; Zenodo: 2022.

(30) Bonini, P.; Kind, T.; Tsugawa, H.; Barupal, D. K.; Fiehn, O. Retip: Retention Time Prediction for Compound Annotation in Untargeted Metabolomics. *Anal. Chem.* **2020**, *92* (11), 7515−7522.

(31) Peter, K. T.; Phillips, A. L.; Knolhoff, A. M.; Gardinali, P. R.; Manzano, C. A.; Miller, K. E.; Pristner, M.; Sabourin, L.; Sumarah, M. W.; Warth, B.; Sobus, J. R. Nontargeted Analysis Study Reporting Tool: A Framework to Improve Research Transparency and Reproducibility. *Anal. Chem.* **2021**, *93* (41), 13870−13879.

(32) *NTA Study Reporting Tool (Excel)*. figshare. .

(33) Fisher, C. M.; Peter, K. T.; Newton, S. R.; Schaub, A. J.; Sobus, J. R. Approaches for Assessing Performance of High-Resolution Mass Spectrometry-Based Non-Targeted Analysis Methods. *Anal Bioanal Chem.* **2022**, *414* (22), 6455−6471.

(34) Fareed, Y.; Braun, D.; Flasch, M.; Globisch, D.; Warth, B. A Broad, Exposome-Type Evaluation of Xenobiotic Phase II Biotransformation in Human Biofluids by LC-MS/MS. *Exposome* **2022**, *2* (1), No. osac008.

(35) Vámos, C.; Scheider, S.; Sonnenschein, T.; Vermeulen, R. Ontology of Active and Passive Environmental Exposure. *Semantic Web* **2024**, *15* (5), 1733−1761.

(36) Samtani, R.; Sharma, N.; Garg, D. Effects of Endocrine-Disrupting Chemicals and Epigenetic Modifications in Ovarian Cancer: A Review. *Reprod. Sci.* **2018**, *25* (1), 7−18.

(37) Gkrillas, A.; Dirven, H.; Papadopoulou, E.; Andreassen, M.; Hjertholm, H.; Husøy, T. Exposure Estimates of Phthalates and DINCH from Foods and Personal Care Products in Comparison with Biomonitoring Data in 24-h Urine from the Norwegian EuroMix Biomonitoring Study. *Environ. Int.* **2021**, *155*, No. 106598.

(38) Gao, C.-J.; Kannan, K. Phthalates, Bisphenols, Parabens, and Triclocarban in Feminine Hygiene Products from the United States and Their Implications for Human Exposure. *Environ. Int.* **2020**, *136*, No. 105465.

(39) Frederiksen, H.; Skakkebaek, N. E.; Andersson, A.-M. Metabolism of Phthalates in Humans. *Molecular Nutrition & Food Research* **2007**, *51* (7), 899−911.

(40) Katsikantami, I.; Sifakis, S.; Tzatzarakis, M. N.; Vakonaki, E.; Kalantzi, O.-I.; Tsatsakis, A. M.; Rizos, A. K. A Global Assessment of Phthalates Burden and Related Links to Health Effects. *Environ. Int.* **2016**, *97*, 212−236.

(41) Panagiotou, E. M.; Ojasalo, V.; Damdimopoulou, P. Phthalates, Ovarian Function and Fertility in Adulthood. *Best Practice & Research Clinical Endocrinology & Metabolism* **2021**, *35* (5), No. 101552.

(42) Wang, Y.-X.; Zeng, Q.; Sun, Y.; Yang, P.; Wang, P.; Li, J.; Huang, Z.; You, L.; Huang, Y.-H.; Wang, C.; Li, Y.-F.; Lu, W.-Q. Semen Phthalate Metabolites, Semen Quality Parameters and Serum Reproductive Hormones: A Cross-Sectional Study in China. *Environ. Pollut.* **2016**, *211*, 173−182.

(43) Axelsson, J.; Rylander, L.; Rignell-Hydbom, A.; Jönsson, B. A. G.; Lindh, C. H.; Giwercman, A. Phthalate Exposure and Reproductive Parameters in Young Men from the General Swedish Population. *Environ. Int.* **2015**, *85*, 54−60.

(44) Hlisníková, H.; Petrovičová, I.; Kolena, B.; Šidlovská, M.; Sirotkin, A. Effects and Mechanisms of Phthalates' Action on Reproductive Processes and Reproductive Health: A Literature Review. *International Journal of Environmental Research and Public Health* **2020**, *17* (18), 6811.

(45) Panagiotou, E. M.; Damdimopoulos, A.; Li, T.; Moussaud-Lamodière, E.; Pedersen, M.; Lebre, F.; Pettersson, K.; Arnelo, C.; Papaikonomou, K.; Alfaro-Moreno, E.; Lindskog, C.; Svingen, T.; Damdimopoulou, P. Exposure to the Phthalate Metabolite MEHP Impacts Survival and Growth of Human Ovarian Follicles *in Vitro*. *Toxicology* **2024**, *505*, No. 153815.

(46) *Ftalati - ECHA*. https://echa.europa.eu/sl/hot-topics/phthalates (accessed Oct 26, 2024).

(47) Stajnko, A.; Runkel, A. A.; Kosjek, T.; Snoj Tratnik, J.; Mazej, D.; Falnoga, I.; Horvat, M. Assessment of Susceptibility to Phthalate and DINCH Exposure through CYP and UGT Single Nucleotide Polymorphisms. *Environ. Int.* **2022**, *159*, No. 107046.

(48) Weaver, J. A.; Beverly, B. E.; Keshava, N.; Mudipalli, A.; Arzuaga, X.; Cai, C.; Hotchkiss, A. K.; Makris, S. L.; Yost, E. E. Hazards of Diethyl Phthalate (DEP) Exposure: A Systematic Review of Animal Toxicology Studies. *Environ. Int.* **2020**, *145*, No. 105848.

(49) Chen, J.; Yang, S.; Ma, B.; Wang, J.; Chen, J. Di-Isononyl Phthalate Induces Apoptosis and Autophagy of Mouse Ovarian Granulosa Cells via Oxidative Stress. *Ecotoxicology and Environmental Safety* **2022**, *242*, No. 113898.

(50) *Substance Information - ECHA*. https://echa.europa.eu/sl/substance-information/-/substanceinfo/100.133.472 (accessed Oct 26, 2024).

(51) Busson, A.; Boulanger, M.; Meryet-Figuière, M.; Perrier, S.; Monnereau, A.; Baldi, I.; Tual, S.; Lebailly, P. O-406 Exposure to Chloroacetamide Herbicides in Agriculture and Lymphoid Malignancies, Overall and by Subtypes, in the AGRIculture and CANcer (AGRICAN) Cohort. In *Oral Presentations*; BMJ Publishing Group Ltd: 2021; p A37.2.

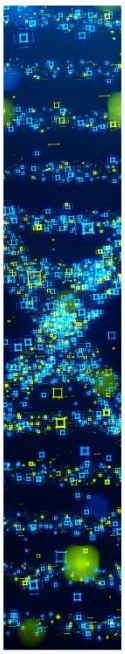
(52) Laville, N.; Balaguer, P.; Brion, F.; Hinfray, N.; Casellas, C.; Porcher, J.-M.; Aït-Aïssa, S. Modulation of Aromatase Activity and mRNA by Various Selected Pesticides in the Human Choriocarcinoma JEG-3 Cell Line. *Toxicology* **2006**, *228* (1), 98−108.

(53) Mathias, F. T.; Romano, R. M.; Sleiman, H. K.; de Oliveira, C. A.; Romano, M. A. Herbicide Metolachlor Causes Changes in Reproductive Endocrinology of Male Wistar Rats. *ISRN Toxicol.* **2012**, *2012*, No. 130846.

(54) Ren, S.; Li, Y.; Li, C. Effects of P-Nitrophenol Exposure on the Testicular Development and Semen Quality of Roosters. *Gen. Comp. Endocrinol.* **2021**, *301*, No. 113656.

https://doi.org/10.1021/acs.est.4c13290
Environ. Sci. Technol. 2025, 59, 8380−8390

(55) Wu, D.; Tao, X.; Chen, Z.-P.; Han, J.-T.; Jia, W.-J.; Zhu, N.; Li, X.; Wang, Z.; He, Y.-X. The Environmental Endocrine Disruptor *p*-Nitrophenol Interacts with FKBP51, a Positive Regulator of Androgen Receptor and Inhibits Androgen Receptor Signaling in Human Cells. *Journal of Hazardous Materials* **2016**, *307*, 193−201.
(56) Zhang, Y.; Shah, P.; Wu, F.; Liu, P.; You, J.; Goss, G. Potentiation of Lethal and Sub-Lethal Effects of Benzophenone and Oxybenzone by UV Light in Zebrafish Embryos. *Aquat Toxicol* **2021**, *235*, No. 105835.
(57) In, S.-J.; Kim, S.-H.; Go, R.-E.; Hwang, K.-A.; Choi, K.-C. Benzophenone-1 and Nonylphenol Stimulated MCF-7 Breast Cancer Growth by Regulating Cell Cycle and Metastasis-Related Genes Via an Estrogen Receptor α-Dependent Pathway. *Journal of Toxicology and Environmental Health, Part A* **2015**, *78* (8), 492−505.
(58) Santos, A. J. M.; da Silva, J. C. G. E. Degradation Studies of UV Filter Hexyl 2-[4-(Diethylamino)-2-Hydroxybenzoyl]-Benzoate (DHHB) in Aqueous Solution. *J. Contam Hydrol* **2021**, *236*, No. 103740.


CAS BIOFINDER DISCOVERY PLATFORM™
STOP DIGGING THROUGH DATA —START MAKING DISCOVERIES
CAS BioFinder helps you find the right biological insights in seconds
Start your search
CAS
A division of the American Chemical Society

https://doi.org/10.1021/acs.est.4c13290
Environ. Sci. Technol. 2025, 59, 8380−8390

3.1.2 Comparative assessment of suspect / non-target screening workflows for characterizing occupational human internal chemical exposure: results of a European interlaboratory study from the EU-PARC project

Submitted: Habchi, B., Martin Remy, A., Belova, L., Covaci, A., Damont, A., Kosjek, T., Huber, C., Grova, N., Antoine, G., Moufawad, T., Baira, E., Baudry, C., Chalet, C., Dervilly, G., Duca, R.C., Fenaille, F., Fernández, M.F., Gabriel, C., Huet, C., Jadé, G., Kajtazi, A., Kärkkäinen, O., Kasiotis, K.M., Kevrekidou, A., Koudelka, Š., Kozlowska, L., Lamoree, M., Lamiceli, A.L., Laurentie, M., Le Bizec, B., Nieuwenhuyse, A., Nijssen, R., Oberacher, H., Plešnik, H., Price, E.J., Rekar, Ž., Rodriguez-Carrillo, A., Santo, R., Sarigiannis, D., Savignac, J.-M., Stelmasiak, M., Sunnarborg, K., Termentzi, A., Vuillaume, R., Schymanski, E.L., Rutledge, D.N., Antignac, J.-P., Ndaw, S., 2026

This paper contributes to the exposomics and methodological sections of the thesis by addressing chemical-space coverage and method complementarity in large-scale non-targeted screening, specifically in an interlaboratory context. Conducted within the PARC framework, the study evaluates how different SS/NTS workflows based on LC-HRMS and GC-HRMS perform across multiple laboratories when applied to shared urine and plasma samples spiked with a common QA/QC compound set. Rather than proposing a single optimized method, the work examines how analytical diversity combined with minimal harmonization can achieve broad and reproducible chemical coverage.

Within the thesis narrative, the paper provides empirical support for Hypothesis 3, showing that complementary chromatographic approaches, particularly inclusion of HILIC alongside RP, extend accessible chemical space in non-targeted workflows. The interlaboratory design demonstrates that polarity-driven differences in detectability are reproducible across independent laboratories and platforms rather than method-specific artifacts. The results confirm that no single analytical setup is sufficient to cover the full range of occupationally relevant compounds, and that combining RP, HILIC, and GC approaches leads to broader detection across matrices.

My contribution was the implementation and execution of the HILIC-based LC-HRMS analysis as the JSI partner. The HILIC data supported comparative evaluation of chromatographic selectivity and showed that certain compounds were consistently detected only, or more reliably, by HILIC methods across laboratories. In the context of the thesis, this confirms that HILIC materially expands non-targeted chemical coverage in real exposure studies.

More broadly, the paper places analytical concepts developed in earlier thesis chapters within a regulatory and operational framework. It shows how polarity-aware method selection and QA/QC design influence detection performance at scale, reinforcing the central thesis argument that comprehensive exposure characterization requires coordinated multi-modal analytical strategies rather than reliance on a single chromatographic platform.

Comparative Assessment of Screening Workflows for characterizing occupational exposure to chemicals in humans: An EU-PARC interlaboratory study

Baninia Habchi[1*], Aurélie Martin Remy[1], Lidia Belova[2], Adrian Covaci[2], Annelaure Damont[3], Tina Kosjek[4,5], Carolin Huber[6], Nathalie Grova[1], Guillaume Antoine[1], Tarek Moufawad[7], Eirini Baira[8], Christian Baudry[9], Clément Chalet[3], Riccardo De Santo[10], Gaud Dervilly[7], Radu Corneliu Duca[11,12,13], François Fenaille[3], Mariana F. Fernández[14,15], Catherine Gabriel[16,17], Corentin Huet[7], Gaëlle Jadé[9], Anna Laura Iamiceli[18], Ardiana Kajtazi[2], Olli Kärkkäinen[19], Konstantinos M. Kasiotis[8], Alkistis Kevrekidou[16,17], Štěpán Koudelka[20,21], Lucyna Kozlowska[22], Marja Lamoree[23], Michel Laurentie[24], Bruno Le Bizec[7], Rosalie Nijssen[25], Herbert Oberacher[26], Elliott J. Price[20,21], Helena Plešnik[4,5], Žan Rekar[4,5], Andrea Rodriguez-Carrillo[14,15], Dimosthenis Sarigiannis[16,17], Jean-Marie Savignac[27], Marta Stelmasiak[22], Katriina Sunnarborg[19,28], Aikaterini Termentzi[8], An Van Nieuwenhuyse[11,12], Romain Vuillaume[27], Emma L. Schymanski[29], Douglas N. Rutledge[30,31,32], Jean-Philippe Antignac[7], Sophie Ndaw[1]

[1]INRS (French National Research and Safety Institute for the Prevention of Occupational Accidents and Diseases), Department of Toxicology and Biomonitoring, France
[2]Toxicological Centre, University of Antwerp, Antwerp, Belgium
[3]Université Paris-Saclay, CEA, INRAE, Département Médicaments et Technologies pour la Santé (DMTS), MetaboHUB, F-91191 Gif sur Yvette, France
[4]Jožef Stefan Institute, Ljubljana, Slovenia
[5]Jožef Stefan International Postgraduate School, Ljubljana, Slovenia
[6]Department of Exposure Science, Helmholtz Centre for Environmental Research – UFZ, Permoserstr. 15, Leipzig, German
[7]Oniris, INRAE, LABERCA, Nantes, France
[8]Laboratory of Pesticides' Toxicology, Scientific Directorate of Pesticides Control and Phytopharmacy, Benaki Phytopathological Institute, 145 61 Kifissia, Greece
[9]Ploufragan-Plouzané-Niort Laboratory, Ruminant Diseases and Welfare Unit, French Agency for Food, Environmental and Occupational Health & Safety, 60 Rue Pied de Fond, 28440, 79024 Niort, CS, France
[10]Department of Chemistry, Sapienza University, Piazzale Aldo Moro 5, 00185 Rome, Italy
[11]Laboratoire national de santé, Department Health Protection, Dudelange, Luxembourg
[12]Environment and Health, Department of Public Health and Primary Care, KU Leuven, Leuven, Belgium
[13]Department of Health Protection, Health Directorate, Ministry of Health and Social Security, Strassen, Luxembourg
[14]Instituto de Investigación Biosanitaria de Granada (ibs.GRANADA), 18016 Granada, Spain. & Spanish Consortium for Research on Epidemiology and Public Health (CIBERESP), Madrid, Spain
[15]Biomedical Research Center (CIBM), Department Radiology and Physical Medicine, School of Medicine, University of Granada, 18016 Granada, Spain
[16]Aristotle University of Thessaloniki, Department of Chemical Engineering, Environmental Engineering Laboratory, University Campus, Thessaloniki 54124, Greece
[17]HERACLES Research Center on the Exposome and Health, Center for Interdisciplinary Research and Innovation, Balkan Center, Bldg. B, 10th km Thessaloniki – Thermi Road, 57001, Greece
[18]Department of Environment and Health, Italian National Institute for Health (ISS), Rome, Italy
[19]School of Pharmacy, University of Eastern Finland, Kuopio, Finland
[20]RECETOX, Faculty of Science, Masaryk University, Kotlarska 2, Brno, Czech Republic
[21]Czech node of the European Infrastructure for Human Exposome Research (EIRENE-CZ)
[22]Warsaw University of Life Sciences, Institute of Human Nutrition Science, Nowoursynowska 166, 02-787 Warsaw, Poland
[23]Vrije Universiteit Amsterdam, Amsterdam Institute for Life and Environment (A-LIFE), Section Chemistry for Environment and Health, De Boelelaan 1085, 1081 HV Amsterdam, the Netherlands
[24]Statistical Analysis Platform, French Agency for Food, Environmental and Occupational Health & Safety, 10 Bis Rue Claude Bourgelat, 35306 Fougères Laboratory, Fougères, France
[25]Wageningen Food Safety Research, part of Wageningen University and Research, Wageningen, The Netherlands
[26]Medical University of Innsbruck, Institute of Legal Medicine and Core Facility Metabolomics, Austria
[27]Univ Toulouse, EI-Purpan, ENVT, INRAE, Toxalim, Toulouse, France
[28]Finnish Institute of Occupational Health, Oulu, Finland
[29]Luxembourg Centre for Systems Biomedicine (LCSB), University of Luxembourg, 6 avenue du Swing, 4367, Belvaux, Luxembourg
[30]Muséum national d'Histoire naturelle, France
[31]Charles Sturt University, Australia
[32]Université Paris-Saclay, Faculté de Pharmacie, France

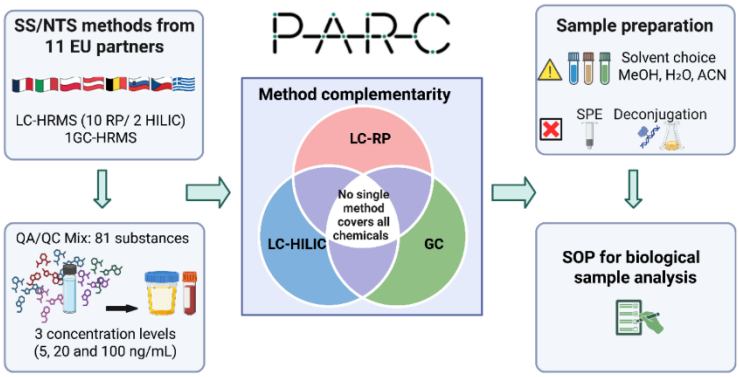
*Corresponding author: Dr. Baninia Habchi, INRS, Department of Toxicology and Biomonitoring, Vandoeuvre-Lès-Nancy, France. E-mail address: baninia.habchi@inrs.fr

Abstract

Biomonitoring of occupational exposure to mixtures of chemicals remains a major challenge, as conventional targeted approaches can only cover a limited number of compounds. Suspect and non-target screening (SS/NTS) using high-resolution mass spectrometry offers a more comprehensive approach, however wider implementation requires robust and comparable analytical strategies with broad chemical coverage. An interlaboratory study was conducted within the European Partnership for the Assessment of Risks from Chemicals (PARC) to evaluate the comparability and complementarity of SS/NTS approaches and to support the development of a standard operating procedure (SOP) for occupational biomonitoring. Urine and plasma samples fortified with 81 occupationally-relevant exposure markers at three concentration levels were distributed to eleven European laboratories from eight Member States and measured via their respective in-house Liquid Chromatography- and Gas Chromatography-High Resolution Mass Spectrometry (LC- and GC-HRMS) workflows. Thirteen different analytical methods were applied: nine to both matrices, three to urine only and one exclusively to plasma samples. Eleven methods enabled detection of more than half of the fortified exposure markers (>40 compounds) in the standard mixture, whilst eight and seven methods achieved the same for urine and plasma samples, respectively. Despite substantial methodological differences, numerous compounds were shared across Reversed-Phase (RP) and Hydrophilic Interaction Liquid Chromatography (HILIC) methods (57 in urine and 34 in plasma), with RP providing higher overall detection rates (eleven and 29 compounds detected exclusively by RP in urine and plasma, respectively). In addition, four compounds were detected exclusively by GC-HRMS in the biological matrices, demonstrating that combining SS/NTS workflows broadens chemical space coverage. The solvent selected for extraction appears to have an influence on the detection performance, with solvents providing broader polarity coverage, such as mixtures of methanol or acetonitrile with water, generally associated with optimal results, across the different sample preparation techniques employed. Solid phase extraction and deconjugation did not show an improvement in performance in these large-scale SS applications. Based on this interlaboratory study, a minimal SOP is proposed to support SS/NTS implementation in future large-scale human biomonitoring studies, including characterization of occupational cohorts within PARC.

Keywords: Non-target Screening, Occupational exposure, Interlaboratory comparison, EU-PARC, SOP

Graphical abstract



1. Introduction

In occupational exposure, assessing multiple chemical exposure sources is essential for protecting workers' health and guiding regulations. Targeted methods, valued for providing quantitative data with high reproducibility, repeatability, and accuracy, are commonly used to monitor human exposure [1]. However, in a general framework of diverse occupational exposure profiles involving thousands of potentially hazardous compounds, the challenge lies in designing, selecting and/or combining the most suitable methods for selected analytes, which is generally a tedious, time-consuming and costly process. In addition, while parent compounds with available reference standards can generally be quantified, their metabolites remain less commonly investigated due to the absence of standards or a lack of knowledge about their metabolism. Furthermore, exposure to mixtures may result in more pronounced effects than exposure to a single compound; and even when biomarkers of exposure are undetectable, adverse effects may still occur [1, 2]. In this case, the identification and quantification of suitable biomarkers of effect becomes essential. Use of broader approaches such as suspect and non-targeted screening (SS/NTS) can solve these limitations [3-9].

The European (EU) PARC (Partnership for the Assessment of Risks from Chemicals) project previously published recommendations to advance the use of innovative SS/NTS methods for chemicals risk assessment [10]. Based on high-resolution mass spectrometry (HRMS), the advantages highlighted were that SS/NTS approaches (i) enable the simultaneous detection of numerous molecules, (ii) provide a broad chemical profile from each sample including biomarkers of both exposure and effect, and (iii) allow data to be archived for retrospective analysis as new knowledge becomes available [10-12].

Despite their advantages, these approaches face major limitations in terms of harmonization and the comparability of results across different screening methods or laboratories. Unlike targeted methods, for which criteria for result comparability and validity are well-established, a clear and consensual common basis for the assessment of SS/NTS method performance and comparison of results is lacking. Key challenges include (i) the need for a minimal harmonization of analytical procedures in terms of sample preparation, data acquisition and quality assurance/quality control (QA/QC) measures [12-16]; (ii) a better harmonization of data processing workflows with QA/QC provisions for comprehensive and robust MS and MS/MS data preprocessing in HRMS-based SS/NTS [17-19]; and (iii) compound annotation and related identification confidence level reporting across the research community, which, despite existing guidelines [20, 21], faces challenges due to methodological differences, residual subjectivity and limitations in automated workflows [10]. Interlaboratory studies are therefore needed to evaluate consistency and improve annotation practices [22]. In this study, we focus specifically on challenge (i), as it addresses upstream analytical variability. Challenges (ii) and (iii) are being investigated within other PARC activities based on shared inter-laboratory datasets and coordinated testing of data processing workflows [17].

To evaluate individual method performances and improve SS/NTS harmonization, several collaborative trials involving suspect screening have already been performed by different European institutes, particularly within the NORMAN network [23]. These studies have mainly focused on environmental matrices, such as water and dust specimens [24-29]. They pointed out the challenges mentioned above, including the need to harmonize the analytical processes at both the sample preparation and data acquisition stages.

For biological matrices, studies such as those conducted under the Human Biomonitoring for Europe (HBM4EU) initiative implemented harmonized sample preparation protocols, instrumentation, and analytical methods across five laboratories, supported by QA/QC procedures [30-32]. This approach improved interlaboratory comparability and enabled the consolidation of laboratory capacities, especially for the identification of pesticide metabolites in urine samples. These approaches offered several advantages and represented an important first step toward a more comprehensive assessment of mixtures and method comparability across EU partners. However, strict standardization potentially reduces the complementary value-added of diverse analytical methods. Clear definition of the minimum requirements that enable result comparability whilst preserving the complementarity of multiple method-specific analytical approaches (e.g., complementary workflows) continue to be needed.

Therefore, in this study we performed an interlaboratory comparison across eleven European partners within the EU-PARC program, to evaluate the comparability of in-house SS/NTS workflows and to assess the methodological harmonization through the development of a standard operating procedure (SOP). The presented study is part of the PARC project, which includes numerous activities across multiple research areas. We specifically focused on development of SS/NTS approaches to characterize complex chemical exposures in occupational exposure scenarios. In a second phase of our work, over 1,000 urine and 500 plasma samples per sector collected under other PARC activities will be analyzed across participating laboratories according to their capabilities. The presented study aims at establishing and informed strategy for these analyses. Targeted analyses of selected chemical families (e.g., flame retardants, phthalates, bisphenols, cytotoxic drugs) are being conducted within PARC complementary activities, while this study focuses on SS/NTS approaches to broaden chemical space coverage. SS/NTS is applied here as a semi-quantitative approach enabling group comparisons and the identification of new biomarkers of exposure and effect. Therefore, to ensure high quality data for the subsequent phase, this study focuses on the comparability and interoperability of SS results across laboratories. The results of this work are expected to identify the strengths and weaknesses of current approaches, establish minimum harmonization requirements and recommendations, while maintaining the advantages of the complementarity among the different in-house SS methods.

In NTS studies, unknown compounds are annotated without relying on suspect lists, which hampers the comparability of methods and results across partners. To facilitate reliable comparison of analytical performance, this study focused on a defined set of compounds. Therefore, this study should be considered as a SS investigation rather than a fully non-targeted approach. A QA/QC mix consisting of 81 chemical standards was prepared to evaluate the detection capabilities of SS approaches in different matrices. Three pooled urine samples with different specific gravities (low, medium, high), and one pooled plasma sample were prepared. Alongside non-fortified matrices, each urine and plasma pool were fortified at three concentration levels. A total of twelve urine and four plasma samples were distributed to partners with the QA/QC mix. In-house extraction and analysis methods based on liquid chromatography (LC) and gas chromatography (GC) coupled with HRMS instruments were applied in accordance with the partners' existing internal protocols. The comparison of results included detection capabilities, matrix effects via urines with different specific gravities and blank contamination assessment, and the impact of sample preparation protocols on compounds detection within the QA/QC mix.

2. Materials and methods

2.1. Sample preparation

2.1.1. QA/QC mix preparation

A QA/QC mix consisting of 81 standard compounds was prepared, as detailed in **Table S1**. The chemicals were selected to represent occupational exposure scenarios in two main sectors: healthcare and waste management. The selection is consistent with ongoing EU studies that will collect samples from these sectors for target and SS/NTS analysis. In the healthcare sector, the mixture included 25 compounds, of which fifteen are cytotoxic drugs commonly handled by medical staff (e.g., cyclophosphamide, ifosfamide, 5-fluorouracil, gemcitabine, methotrexate, vincristine, etoposide, paclitaxel, irinotecan). These compounds are considered to be hazardous drugs. In the waste management sector, 45 compounds were selected to reflect exposure associated with plastic and electronic waste. This includes industrial chemicals and additives such as bisphenols, phthalates, flame retardants, per- and polyfluoroalkyl compounds, as well as transformation products and degradation compounds released during waste processing activities. The mix also contained metabolites that are more likely to be detected in urine, such as glucuronide, sulfate, and mercapturate conjugates, enabling assessment of internal exposure through biomonitoring. In addition, two lifestyle-related compounds, associated with smoking consumption were added as well-established compounds to provide additional evaluation criteria for SS/NTS workflows. Ten non-polar compounds more amenable to GC were included as well. The mix was designed to cover a broad chemical space, including a wide spectrum of molecular masses and polarities. The set of 81 QA/QC standards was obtained from multiple commercial suppliers. The IUPAC and common name, commercial suppliers, SMILES, InChIKey, InChI, CAS, PubChem CID, molecular formula, and monoisotopic mass are given for each standard (**Table S1**). Each compound was initially dissolved at 1 mg/mL in the most suitable solvent. Based on this compatibility, the standards were grouped into five stock mixes: fourteen in water, 34 in ethanol (EtOH), seventeen in methanol (MeOH), seven in dimethyl sulfoxide (DMSO), and nine in cyclohexane as detailed in **Table S1**. From these, 1 µg/mL working solutions of each mix were prepared by dilution in the same solvents used for the initial stock preparation, and 1 mL aliquots were distributed to all participating laboratories. A unified QA/QC mixture containing all 81 standards at 10 µg/mL was prepared by evaporating the required volume of the cyclohexane stock solution, adding the required volumes of the remaining four stock solutions, and adjusting the final volume with methanol. This mix was used to fortify urine and plasma samples across the concentration range defined below.

Additional Mixes: additional mixes were prepared and provided based on the analytical techniques used by each partner. The *NORMAN mix* (30 compounds) [33] and the *Alkanes mix* (24 compounds) [34] designed to align and compare retention times (RT) across LC and GC methods, respectively, were supplied to all partners (1 mL/partner at 10 µg/mL). The complete list of compounds, along with relevant details is described in **Tables S2** and **S3** for *NORMAN* and *Alkanes* mixes, respectively. These reference mixtures were included as additional quality control materials, as they are commonly used for evaluating RT comparability and RT prediction between methods. However, this was not the primary objective of the present study. Instead, these mixes were analyzed alongside the biological matrices at the beginning and/or end of each sequence to monitor system performance by each partner and to ensure data availability for potential future RT benchmarking studies. In addition, two mixes containing four internal (to be added at the beginning of the extraction process) and four external (to be added directly in the reconstitution solvent before analysis) labeled markers were prepared and distributed (200 µL of each mixture per participant, in MeOH at a concentration of 1 µg/mL) to partners who had not individually added reference standards, in order to ensure a minimal and harmonized set of quality control markers across laboratories under reasonable cost and feasibility constraints. The details of the compounds included in these mixes are provided in **Table S4**. These mixes were used for data quality validation; as well as to assess extraction efficiency and sample preparation procedures by each partner prior to reporting results.

2.1.2. Urine and plasma sample preparation

Three urine samples (100 mL each) were prepared by pooling the surplus of individual urine samples collected as part of an ongoing study on occupational exposure in France (ethical permit number: 2022-A01643-40). The low specific gravity (LSG) sample was made up of 37 urine specimens with specific gravity (SG) values ranging from 1.0017 to 1.0099, resulting in a final SG of 1.0050. The medium specific gravity (MSG) sample was prepared by pooling 35 urine specimens with SG values between 1.0190 and 1.0210, resulting in a final SG of 1.0200. The high specific gravity (HSG) sample was produced by combining 33 urine specimens with SG values ranging from 1.0281 to 1.0401, resulting in a final SG of 1.0300. Additionally, a 36 mL pooled plasma sample was prepared by combining 16 mL from three donors (Slovenia, ethical permit number: 0120-323/2023/6) and 20 mL from 246 donors (Greece, ethical permit numbers: 86801/2021 and 136778/2023). All plasma donors were adults from the general population participating in the URBANOME project. All urine (LSG, MSG, and HSG) and plasma samples were prepared as non-fortified samples and fortified with the QA/QC mix at concentrations of 5, 20, and 100 ng/mL. Each partner received 1 mL of each urine sample and 500 µL of each plasma sample.

2.2. Sample analysis

Eleven partners from eight EU Member States participated in this interlaboratory study. In total, thirteen different analytical methods were used, with nine methods applied to both matrices, three to urine only and one to plasma samples only. Each partner followed their in-house SOPs for sample preparation and analysis. Each analytical method was assigned a unique code reflecting the chromatographic approach selected by the laboratory and the biological matrix analyzed. Reversed-phase (RP) liquid chromatography methods are designated as **RP-Mx**, hydrophilic interaction chromatography (HILIC) methods as **HL-Mx**, and gas chromatography methods as **GC-Mx**, where x corresponds to the method number. The suffix **-U** indicates urine, and **-P** plasma. For example, RP-M1-U and RP-M1-P represent the same RP liquid chromatography - mass spectrometry (LC-MS) method, differing only in the matrix-specific sample preparation performed. All sequences included procedural blanks (extraction solvent without the biological matrix processed like the samples to detect background contamination), QA/QC solvent mixes, NORMAN and/or Alkanes mixes, and the pooled biological samples to be analyzed. The main characteristics of the methods applied to urine and plasma are summarized in **Table 1** and **Table 2**, respectively. Further details on the sample preparation procedures for each matrix are provided in **Tables S5** and **S6**, information on data collection and instrumentation is listed in **Table S7**.

For urine samples, most laboratories applied LC-HRMS-based workflows (n=eleven), with one GC-HRMS method (GC-M1-U). Sample preparation approaches included dilute-and-shoot (n=four), solid phase extraction (SPE) (n= four), liquid-liquid extraction (LLE) (n= three) and solvent transfer (ST) (n=one), with one method including enzymatic hydrolysis (RP-M3-U). LC analyses mainly used RP chromatography, with two methods employing HILIC (HL-M1-U, HL-M2-U). Orbitrap mass spectrometers were the most commonly used (n= eight) followed by four methods using quadrupole time-of-flight (Q-TOF) systems. Analyses were conducted in both positive and negative electrospray ionization (ESI) modes for all LC methods using separate injections, while the GC method was run in full-scan positive electron ionization (EI+) mode only. LC acquisition strategies were divided between Data-Dependent Acquisition (DDA) and Data-Independent Acquisition/All Ion Fragmentation (DIA/AIF), with four methods adopting the latter. LC-mobile phases were generally composed of water with 0.1 % formic acid (v/v) as phase A and MeOH or acetonitrile (ACN) as phase B. Some methods additionally used ammonium-based modifiers, including ammonium acetate, ammonium formate, or ammonium fluoride, depending on the method (**Table 1**).

For plasma samples, LC-HRMS was again the predominant technique (n=nine), with one GC-HRMS method (GC-M1-P). Protein precipitation was the most common sample preparation, often followed by either LLE or direct reconstitution. SPE-based workflow using lipid filtration cartridges and

enzymatic hydrolysis were also reported in selected methods. Many workflows included evaporation of the sample extract to dryness and then reconstitution, typically using ACN or MeOH as solvents. LC separations were primarily performed using reversed-phase columns, with one HILIC-based method (HL-M1-P). Orbitrap instruments were most frequently used (n= eight), with Q-TOF systems applied in two methods. Ionization was performed in both positive and negative ionization modes for LC methods using separate injections, while GC was run in positive mode only. Data acquisition relied mainly on DDA, while a smaller number of DIA/AIF workflows. Mobile phases were generally water with 0.1 % (v/v) formic acid (phase A) and MeOH or ACN (phase B). Some methods additionally used ammonium-based modifiers, depending on the method (**Table 2**).

2.3. Data reporting

Data processing for peak detection and intensity reporting was performed by partners using their in-house procedures and software. **Table S8** summarizes the main data processing parameters and steps applied by partner for each method. Each partner validated the cleaned data and reported the results using a common template developed to standardize reporting across all partners, with an example provided in the supplementary information (**Table S9**). For each method, the template includes details such as laboratory name, experimental results, analytical approach (LC or GC), ionization polarity (positive or negative), and RT for each compound. It also includes the intensity values detected in the procedural blank and in each sample at the three concentration levels for each fortified compound. All standards used for data quality checks, whether internal and external labeled markers (provided by this study/inter-laboratory exercise), or in-house, are also reported in the template. Two supplementary sheets were created for reporting experimental results: one for the NORMAN mix for LC methods (**Table S10**), and another for the alkane mix for GC methods (**Table S11**).

Finally, to support structured reporting and method evaluation, the Study Reporting Tool (SRT, Peter et al., 2021; 10.6084/m9.figshare.19763482 [PDF]) for NTS was used in the preparation of this manuscript [35]. The completed template is provided in Supplementary Information (PDF document).

2.4. Data evaluation and comparison

2.4.1. Descriptive analysis

Descriptive analyses were performed using Stata 19.0 software (StataCorp. 2025. *Stata Statistical Software: Release 19.* College Station, TX: StataCorp LLC).

Background level and blank contamination assessment: Compounds detected in procedural blanks were first evaluated based on their detection. Then their signal intensities were compared to the signal intensities detected in non-fortified urine or plasma samples. This comparison makes it possible to

distinguish contaminants originating from the analytical method from compounds naturally present in the sample matrix, for the 81 reference standards. Contamination was assessed based on the number of standards detected in procedural blanks with their reported intensity, enabling cross-laboratory comparison and the identification of systematic contamination patterns.

Detectability of QA/QC mix compounds: For each compound, detection was defined as the presence of at least one reported non-zero signal intensity, regardless of intensity level, in any biological sample. The number of compounds detected by each method in the QA/QC mix, but not in the biological matrices was recorded, as this may indicate either a limit of sensitivity or matrix effects.

Impact of urine specific gravity on matrix effects and detection: A dedicated assessment was carried out to evaluate the impact of the SG on the matrix effect of urine on detection efficiency, since the considerable inter- and intra-individual variability in urine composition observed in large cohorts can impact ionization efficiencies differently. This SG-related variability represents one contributing component of the overall matrix effect, which is known to arise from multiple factors. This was addressed by including three pooled urine matrices covering three levels of SG, namely LSG, MSG and HSG. The number of detected compounds was calculated at each fortified concentration level and for each SG level. To assess the impact of SG on the matrix effects especially the ionization suppression, the number of detected compounds at a given fortified concentration level was compared across the different SG levels. In the absence of matrix effects, the number of compounds detected is expected to remain stable from LSG to HSG at a fixed fortification level. In contrast, matrix effects are evidenced by a progressive decrease in the number of compounds detected from LSG to HSG.

Concentration-response relationship: The ability of the NTS methods to capture concentration-response relationships was assessed by comparing the number of compounds detected across different fortification levels in each SG urine and plasma sample. Then, the concentration-response profile for each compound was evaluated based on the presence or absence of a concentration-dependent response. The concentration-response relationship was quantified using: (i) the Pearson correlation coefficient (ρ) between the concentration (0, 5, 20, and 100 ng/mL in urine/plasma) and the measured intensities; (ii) the coefficient of variation (CV), calculated from the mean and standard deviation of the intensities at the three fortified concentration. Based on these metrics, three categories were defined:

- If $\rho > 0.7$, the molecule is considered to exhibit a “concentration-response relationship”, meaning its intensity increases proportionally with the concentration.
- If $\rho < 0.7$ and CV < 30 %, the molecule’s intensity response is classified as “consistent”, indicating that the intensity shows little variation with changing concentrations.

- If $\rho < 0.7$ and CV > 30 %, the molecule's intensity response is classified as "variable", meaning the intensity fluctuates irregularly and does not reflect the increase of the spiking level.

A molecule classified as showing a "concentration-response relationship" can be considered less affected by matrix effects, even when such effects are present, as the concentration-response pattern ensures reliable measurement, for example in group comparisons. In contrast, a molecule classified as "consistent" suggests that the signal intensity remains relatively stable across conditions, which may reflect limited sensitivity to changes in spiked concentration, high baseline level in the non-fortified samples, or other sample- and analyte-specific factors in addition to matrix effects. Conversely, a molecule classified as "variable" suggests fluctuating signal responses, that may be influenced by matrix effects but can also arise from analytical variability, low signal intensity, or instability of the compound in the biological matrix.

Comparative evaluation of analytical methods using an S-score system: To evaluate the detection performance of each analytical method, we used the S-score system (Summary score for binary data) designed to assess binary qualitative results [36]. In this study, we specifically applied "method 3" of the S-score system, as it is based on predefined correct results (81 compounds) and is therefore most appropriate for an objective evaluation of the SS/NTS methods. Methods 1 and 2 are typically used for targeted results and assign a performance penalty (S-score ≥ 3) in case of incorrect results. Method 4 is used for expected results derived statistically from participant data; however, it was not applied in this work because the correct outcomes were not defined statistically but based on known reference information. For this study, only method 3 was retained to ensure a reference-based and objective performance assessment. All 81 exposure markers were considered as desirable but not mandatory, and all with equal priority. According to this "method 3", the non-detection of some markers could not produce an S-score ≥ 3. Instead, it leads to S-score values in the range 2 ≤ S-score < 3, where lower values indicate better analytical performance. As a result, all methods were expected to yield S-scores greater than 2, as achieving a value of 1 (corresponding to 100 % detection) was not considered realistic given the number of components evaluated and the high variability of chemical properties excluding a detection of all markers with a single instrumental platform (n = 81). In this context, any non-detection of a compound automatically leads to an S-score above 2, where lower decimal part indicates better method performance. The S-score was used as a global metric for comparing the methods; it was calculated for each method and each fortifying level, as well as for each SG in the case of urine samples.

2.4.2. Multivariate analysis

Following the descriptive analyses, a multivariate strategy was applied to integrate the data obtained from the various methods applied to the same set of samples. The goal was to perform an unsupervised multivariate analysis to explore inherent patterns in the data without prior assumptions or predefined hypotheses, with the aim of identifying shared trends and overall distributional similarities across the combined datasets from all participating laboratories. The analysis was performed using an extension of the Common Components and Specific Weights Analysis (ComDim) that integrates Independent Components Analysis (ICA) within ComDim [37]. This approach allows the extraction of common components (CC), which are like principal components in PCA, but instead of resulting from the analysis of just one dataset, they correspond to patterns that are shared across multiple data blocks, while preserving block-specific contributions, enabling comparison of analytical responses among participating laboratories. ComDim-ICA has previously demonstrated advantages for the interpretation of complex multi-block datasets, including non-target HRMS data [38], as it preserves the block structure, separates shared and block-specific variation, and enables the identification of discriminant features, in contrast to PCA, which relies on data concatenation and does not account for the contribution of individual data blocks. To apply ComDim-ICA, the data of each individual method was considered as a block. Each block for the urine dataset consisted of thirteen samples: one procedural blank and twelve urine samples. For the plasma data, each block consisted of five samples: one procedural blank and four plasma samples. In all blocks, the columns corresponded to the 81 compounds, with values reflecting their measured intensities. This block structure was identical across all analytical methods. The single GC method was excluded from this analysis because its results were not comparable to those generated by using the LC platforms. In total, eleven methods (eleven blocks) were available for urine and nine methods for plasma data. The non-detects were replaced with low-intensity random noise, followed by Pareto normalization of the data. Then ComDim-ICA was performed using four CCs for both the urine and plasma matrices using MATLAB® (R2023b, MathWorks, Natick, MA, USA) with an in-house script and functions. An S-plot was used to identify key compounds contributing to each CC across the data blocks. The S-plot combines covariance and correlation between the X matrix and the ComDim-ICA scores where covariance reflects contribution strength and correlation indicates reliability. Compounds with both high covariance and correlation were considered important. Discriminative features were selected if their covariance exceeded ± 2 standard deviations from the mean.

3. Results

3.1. Background level and blank contamination assessment

Procedural blanks (environmental and analytical contamination): In procedural blanks, the number of compounds detected in urine methods ranged from zero to nine, with the exception of two methods (HL-M1-U and RP-M6-U), which showed higher numbers of detected compounds (25 and 36, respectively, **Figure S1**). Similarly, for plasma methods, detections ranged from zero to fifteen compounds, except for RP-M6-P, which detected 35 compounds (**Figure S2**). While a relatively high number of compounds were reported in procedural blanks for HL-M1-U and RP-M6-U, comparison of analyte-to-blank signal intensities shows that the ratios were sufficiently high, indicating a negligible impact of these blank signals on the reported results. Signal intensity ratios (mean spiked urine *vs.* procedural blank) were markedly higher for the vast majority of compounds, with mean ratios of 2379 and 1340 for HL-M1-U and RP-M6-U, respectively. Similarly, in plasma, a mean ratio of 2267 was observed. Overall, these results confirm that signals detected in procedural blanks have a negligible contribution compared to true sample signals. In addition, only a small number of compounds were detected in procedural blanks by more than four methods, indicating a limited level of background contamination that was generally method- and/or lab-specific. Overall, contamination from the analytical workflow does not appear to be a major issue for most laboratories.

Non-fortified biological matrix (background exposure markers): In contrast, non-fortified urine samples showed detection ranges from two to 22 compounds, again with the exception of RP-M6-U, which detected 35 compounds. For non-fortified plasma samples, detections ranged from 4 to 25 compounds, with RP-M6-U again reporting the highest number (45 compounds). For both matrices, most methods detected a higher number of QA/QC markers in non-fortified biological samples than in procedural blanks (**Figures S1** and **S2**). Higher signal intensities were observed for compounds detected in non-fortified biological matrices than in procedural blanks, with at least 60 % of compounds exhibiting intensities ≥ 10-fold higher compared to procedural blanks. In non-fortified urine samples, compounds such as acetaminophen (and its conjugated forms), lidocaine, cotinine, and hydroxycotinine were each detected by more than seven of the twelve methods, reflecting a background exposure rather than analytical contamination. Methods that did not detect these compounds were either outside their analytical scope (e.g., the GC method GC-M1-U and the method with deconjugation step RP-M3-U for conjugated forms) or had limited coverage for specific compounds (e.g., RP-M5-U, RP-M6-U, and RP-M9-U). The detection of more compounds in non-fortified urine and plasma samples than in procedural blanks is expected since these compounds originate from exposure to these compounds by the individuals providing the biological samples. The

consistent detection of these exposure markers across multiple laboratories demonstrates good comparability of the results.

Based on these results, procedural blanks are strongly recommended and should be systematically included and analyzed in SS/NTS workflows with biological samples to identify and account for any contamination from the analytical process. In addition, careful data processing and consistent reporting are essential to ensure accurate interpretation of results and to maintain data quality.

3.2. Detectability of QA/QC mix compounds

The number of compounds detected in the QA/QC mix reflects both the instrumental coverage of the applied methods and the capability of the SS approach to detect a broad range of compounds. When all methods were combined, detection rates reached 79 out of 81 compounds in the QA/QC mix, 76 in urine, and 75 in plasma samples (**Figure 1 and Table 3**). In addition, eleven of the thirteen methods applied detected more than 40 compounds (i.e., more than 50 %) in the QA/QC mixture, compared with eight of the twelve methods in urine and seven of the ten methods in plasma. The differences in detection rates between the solvent-only QA/QC sample and the matrix samples can be explained by matrix effects and/or analytical sensitivity. The partners could inject the QA/QC mix at higher concentrations to create their in-house library from the reference standards. **Table S12** summarizes the reported detection polarity and RT for the 81 compounds in the QA/QC mixture using the applied analytical methods. The two LC ionization modes provided complementary coverage, with 38 compounds detected in both modes with differing sensitivities, sixteen compounds detected only in negative mode and 24 only in positive mode.

The detection frequency varied among the LC methods, with RP-M1-U/P and RP-M4-U/P detecting up to 71 compounds in the QA/QC mix. In biological matrices, RP-M6-U/P performed best, identifying 66 compounds in urine and 65 in plasma samples (**Figure 1**, **Table 3**).

When comparing RP and HILIC methods, RP generally detected a larger number of compounds than HILIC. Although LC-RP detected all other compounds that were also detected by HILIC, some polar compounds showed better detectability by HILIC. Paraquat and 2,4-dichlorophenol were detected at the lowest spiking level (5 ng/mL) in MSG and HSG samples only by HILIC methods. 2,3,4,5-Tetrabromophenol was detected only by the HL-M2-U method and was observed only in the QA/QC mix (**Figure S3**). The detection of 2,3,4,5-tetrabromophenol and 2,4-dichlorophenol by HILIC methods, may be related to less effective ionization under the LC-RP conditions. Specifically, the presence of acetic and formic acid in LC-RP mobile phases can suppress deprotonation of phenolic compounds, which ionize most efficiently in negative electrospray ionization mode under conditions with minimal or no acidic modifiers. The type of organic modifier and/or mobile phase additive can influence the

detection of certain compounds, as reported by Malm et al (2026) [39]. Although this effect was not specifically evaluated in the present interlaboratory study, these findings underline the importance of mobile phase composition for the detection of certain analytes. Overall, these results indicate that LC-RP methods provide broader compound coverage, with HILIC methods offering higher sensitivity for certain polar compounds. It should also be noted that this comparison could be influenced by the unequal number of methods evaluated (nine RP methods versus two HILIC methods). In addition, the QA/QC mixture contained a higher proportion of non-polar compounds (higher LogP values), which are more favorably detected by RP methods.

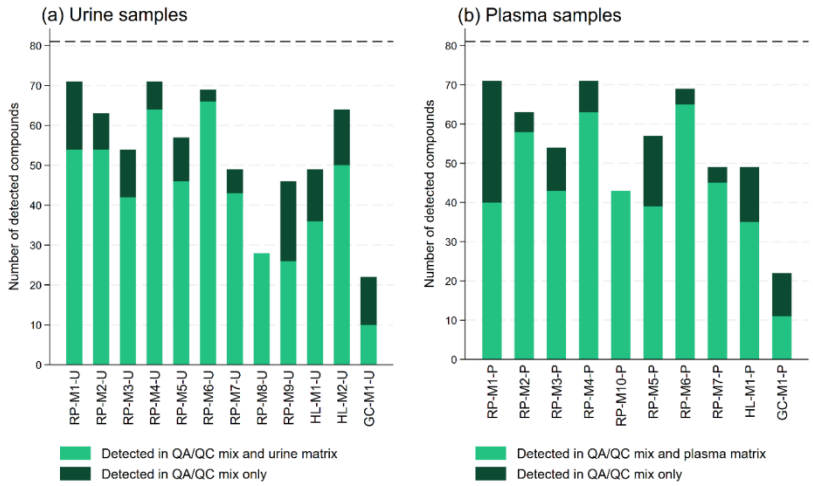


Figure 1: *Number of compounds detected by each method in* ***(a)*** *urine samples and* ***(b)*** *plasma samples. The dashed line represents the maximum number of compounds analyzed, corresponding to the 81 compounds in the QA/QC mix.*

Table 3: *Number of compounds detected by each method in the QA/QC mix and in at least one biological matrix (urine or plasma). The number of detected compounds was defined as the presence of at least one reported non-zero signal intensity, regardless of intensity level, in any biological sample.*

	Number of detected compounds per matrix among the 81 target compounds		
Sample	**QA/QC mix**	**Urine samples**	**Plasma samples**
All methods	79	76	75
RP-M1-U/P	71	54	40
RP-M2-U/P	63	54	58
RP-M3-U/P	54	42	43
RP-M4-U/P	71	64	63
RP-M5-U/P	57	46	39
RP-M6-U/P	69	66	65

RP-M7-U/P	49	43	45
RP-M8-U	28	28	n.a.
RP-M9-U	46	26	n.a.
RP-M10-P	43	n.a.	43
HL-M1-U/P	49	36	35
HL-M2-U	64	50	n.a.
GC-M1-U/P	22	10	11

n.a.: method not applied to this matrix

Ten compounds were detected by the GC method in urine samples. This is in line with the general expectation that the compounds investigated are more easily detected using LC-based techniques, since the analytical mix was primarily designed for LC rather than GC. Additionally, a single GC method was compared with eleven LC methods. The GC-based analysis showed unique advantages for specific compounds. In urine, three polycyclic aromatic hydrocarbons (PAHs, namely benz[a]anthracene, benzo[a]pyrene, and indeno[1,2,3-cd]pyrene) were detected only by the GC method (GC-M1-U). Moreover, 2,2',4,4',5,5'-hexachlorobiphenyl (PCB-153) was detected only by the GC method at the lowest spiking levels and in MSG and HSG urine samples. These four compounds were also detected exclusively by the GC method in plasma samples (**Table S13** and **S14**). These compounds are non-polar and do not ionize efficiently under ESI conditions, which explains their non-detection in LC-MS analyses [40]. GC-MS analyses were instead performed using EI in positive mode, a gas-phase ionization technique better suited for these non-polar compounds. These results show the importance of including complementary techniques, such as GC-MS methods and derivatization-based approaches, for improving the detectability and stability, especially for compounds that are not well-detected by LC-MS, depending on their physicochemical properties and the study objectives.

Analytical performance across LC methods and sample preparation effect: For urine samples, the comparison of analytical methods revealed variability in detection performance. Eight of the twelve methods applied were able to detect more than 50 % of the 81 compounds in the matrix (**Figure 1a**; **Table 3** and **S13**). The highest detection rates were achieved by RP-M6-U (66 compounds) and RP-M4-U (64 compounds), followed by RP-M1-U and RP-M2-U (54 compounds each) and HL-M2-U (50 compounds). The results indicate that neither instrument platform (Q-TOF *vs.* Orbitrap), nor column type/polarity had a clear or systematic effect on performance, since methods achieving both the highest and lowest detection rates used different combinations of those without any evident systematic trend (**Table 1**). A similar observation applies to sample preparation strategies, where methods achieving the highest detection rates were associated with different extraction approaches. For example, RP-M6-U, which achieved the highest detection rate, relied only on a solvent transfer; while RP-M4-U used SPE, and RP-M1-U used a dilute-and-shoot procedure. Conversely, RP-M8-U, which used a dilute-and-shoot strategy, showed one of the lowest detection rates. These results

suggest that differences may be more closely related to solvent composition upon sample preparation and reconstitution, although other methodological factors cannot be excluded based on the present data. Most laboratories used either water mixed with an organic solvent or an organic solvent alone (typically ACN or MeOH). In RP-M8-U, however, the samples were exclusively reconstituted in water with an initial H_2O/MeOH (95/5) gradient, while RP-M9-U used a solvent extraction mixture of tetrahydrofuran/1-hexanol, which is not commonly used for LC-HRMS workflows. Together, these observations suggest that the detection capacity may be partially influenced by solvent selection used for sample preparation; however, the available data do not allow a definitive attribution to this factor alone over the overall parameters in the extraction and analytical methods. Notably, the use of SPE did not systematically improve detection performance based on the present evaluation and in several cases, led to the loss of some analytes.

For plasma samples, seven of the ten methods detected more than 40 compounds of the QA/QC markers (**Figure 1b**; **Table 3** and **S14**). Similarly to urine samples, RP-M6-P and RP-M4-P achieved the highest coverage (65 and 63 compounds, respectively). The other LC methods showed detection counts ranging from 35 (HL-M1-P) to 58 compounds (RP-M2-P). As observed in urine, neither instrument platform (Q-TOF *vs.* Orbitrap) nor column type affected the performance significantly, whereas sample preparation strategies appeared to have a major impact. The methods using protein precipitation achieved better results than the method using an SPE lipid-filtration step. This was particularly evident when comparing RP-M1-P and RP-M2-P, which showed identical detection rates in urine (54 compounds), but diverged in plasma samples (40 *vs.* 58 compounds, respectively; **Table 3**) despite using the same instrumentation and chromatographic conditions, as in the case of urine samples. These results suggest that some analytes could be lost during the SPE extraction step, indicating that SPE does not necessarily improve detection rates in this context and that simpler sample preparation approaches may be sufficient for this type of analysis.

Systematic and method-specific detections: In urine samples, four compounds (ifosfamide, ipconazole, methotrexate, and ciprofloxacin) were systematically detected by all eleven LC-based methods applied mainly in positive ionization mode. Similarly, in plasma samples, ten compounds were detected by all the nine LC methods applied. These compounds include all perfluoroalkyl acids detected in negative ionization mode (perfluorohexanesulfonic acid (PFHxS), perfluorooctanesulfonic acid (PFOS), perfluorooctanoic acid (PFOA) and perfluorononanoic acid (PFNA)) except for the smaller pentafluoroethanesulfonic acid, which was detected by eight of nine LC methods. Chloroalkyl phosphate bis(1,3-dichloro-2-propyl) phosphate (BDCIPP) and fipronil sulfone were also detected in negative mode while N,N-diethyl-m-toluamide (DEET), ipconazole, lidocaine, and irinotecan were

detected in positive mode across all LC platforms. These results demonstrate the broad analytical detectability of these compounds across different LC platforms.

Some compounds were detected by only a single analytical method, showing the importance of methodological diversity. In urine, 5-azacytidine and sevoflurane were each detected by only one method (methods RP-M6-U and RP-M1-U, respectively). In plasma, aminomethylphosphonic acid (AMPA), paraquat, caffeic acid 3-O-sulfate, and ibuprofen were each detected by only one method, although the specific method differed among the compounds. Additionally, several compounds were detected by only two different methods. In urine, these included alpha-fluoro-beta-alanine, cytarabine, paraquat, and PCB-153; whereas in plasma, alpha-fluoro-beta-alanine, resorcinol, alpha-hexabromocyclododecane, and tris(2-ethylhexyl) trimellitate were detected (**Table S13** and **S14**). The method specific compound detection confirms the complementarity of the diverse analytical strategies used. Neither 1,3-dichloro-2-propanol (1,3-DCP) nor di-(2-ethylhexyl)-tetrabromophthalate (TBPH) were detected by any of the analytical method, even in the QA/QC mix solvent without matrix. This non-detection could be related to an extraction issue, especially for TBPH which should be detectable by GC methods. TBPH is poorly ionized in ESI conditions and its detection by LC-MS methods could be done using Atmospheric Pressure Chemical Ionization (APCI) [41, 42]. 1,3-DCP is a small and volatile compound, with a poor ionization efficiency under RP LC-MS conditions. Its detection would likely be improved using dedicated GC-based approaches, such as headspace GC or derivatization prior to GC-MS analysis, to enhance stability and detectability [43].

Note that the differences between urine and plasma results can be attributed in part to the fact that not all methods were applied to both matrices. Furthermore, matrix-specific factors, such as compound solubility and chemical stability may influence the compounds' detectability.

3.3. Impact of urine specific gravity on matrix-effects and detection

The results show a clear correlation in the number of detected compounds decreasing slightly as SG increased across all tested concentrations (5, 20, and 100 ng/mL in urine) for nine out of the twelve methods, as illustrated in **Figure S4**. This decrease was less marked at the highest fortifying level for some methods. RP-M3-U and RP-M8-U exhibited a variable number of detected compounds and did not follow the general trend observed for the other methods. The decrease in detected compounds seem to be related to matrix effects or dilution, depending on whether a normalization step was applied prior to sample preparation. Only two laboratories applied such normalization: RP-M8-U, based on osmolality and HL-M2-U, based on SG. RP-M8-U did not display a consistent trend with increasing SG, instead, the intensities fluctuated. HL-M2-U, despite normalization, still showed a decreasing trend similar to that observed in the other laboratories. In this case, the observed trend

may be linked to dilution effects introduced by the normalization procedure (as HSG samples become more diluted), whereas for the other methods, the trend is probably associated with matrix-induced effects related to the SG. Finally, the compounds contributing to the small differences in detection across SG levels were not consistent between methods or laboratories.

In addition, as matrix effects may also impact signal variability and analytical precision, the CVs of both internal and external labeled markers were further evaluated for all methods. CVs were calculated within the SG group (three urine samples per SG) and across all samples (twelve urine samples) (**Table S15**). Across all methods, 45 % of the reported standards showed a CV below 20 % when considering all urine samples. This proportion increased to 90 % for the LSG and MSG groups and 81 % for the HSG group. The results from individual methods showed fluctuations, without any evident trends that could be related to specific matrix-effect patterns. The comparison with the plasma samples, where 76 % of the CVs were below 20 % (**Table S16**), indicates higher precision than for the combined urine-samples (45 %). However, this was still lower than the performance observed within each urine SG group, where over 80 % of the CVs were below 20 %.

3.4. Concentration-response trends

The capacity of the SS approaches to detect "concentration-response relationship" was evaluated across fortified concentrations. For both urine and plasma samples, the total number of compounds detected increased as the spiking level increased from 5 to 100 ng/mL (**Figure S4** and **S5**, respectively). However, this increase in the number of compounds detected does not directly indicate whether the compounds display a reproducible "concentration -response trend".

To confirm this "concentration-response relationship", compounds were classified according to their concentration-response behavior as described in section 2.4.1. In brief, the Pearson correlation coefficient (ρ) and the CV across fortified concentrations were used to distinguish compounds with strong "concentration-response intensity" (green), "consistent intensity" (orange) and "variable intensity" (purple). The classification results show that, for all methods, the largest proportion of compounds exhibited clear "concentration-response intensity" (green), both in urine and plasma matrices (**Figure 2**). In urine samples, some compounds were classified as having a "consistent intensity" by almost all methods. These included compounds such as acetaminophen (and its conjugated metabolites) and hydroxycotinine, which were already present at significant levels in non-fortified urine samples (**Table 4**). In these cases, the presence of these compounds in the non-fortified urine masked any additional "concentration-response intensity". A very low number of compounds were classified as "variable" with limited repeatability in some in-house methods related to extraction or analytical procedures. The maximum number was four compounds by method in urine samples

(except RP-M8-U reaching eight compounds) and one compound in plasma samples (except RP-M1-P with five compounds). These findings demonstrate that SS approaches provide robust and reproducible detection of "concentration-response intensity" across most laboratories despite differences in sample preparation protocols, data acquisition, and instrumentation.

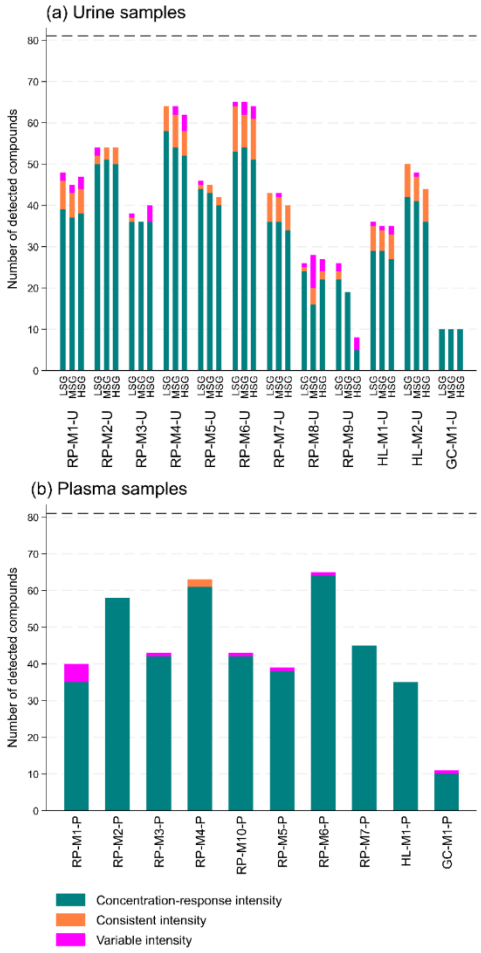


Figure 2: *Classification of compounds based on concentration-response relationship* in ***(a)*** *urine samples and* ***(b)*** *plasma samples. The number of compounds is calculated according to two metrics: the Pearson correlation coefficient (ρ) between the concentration level (0, 5, 20, and 100 ng/mL) and signal intensity, and the coefficient of variation (CV) calculated from intensities at all three fortified*

concentration levels. Compounds with ρ > 0.7 were classified as showing a "concentration-response intensity" (green), those with ρ < 0.7 and CV < 30 % as "consistent intensity" (orange), and those with ρ < 0.7 and CV > 30 % as "variable intensity" (purple). The dashed line represents the maximum number of compounds analyzed, corresponding to the 81 compounds in the QA/QC mix.

Table 4: *Summary of detection performance and* concentration-*response trends for acetaminophen, bisphenol A (BPA), and their conjugates across SS Workflows in urine and plasma samples.* ↑: "concentration-response intensity" ; ━: "consistent intensity"; ⩛ : "variable intensity" and U, urine; P, plasma; n.d., not detected; *, method applying deconjugation step.

Urine samples Compound Name	**SG**	**RP-M1-U**	**RP-M2-U**	**RP-M3-U***	**RP-M4-U**	**RP-M5-U**	**RP-M6-U**	**RP-M7-U**	**RP-M8-U**	**RP-M9-U**		**HL-M1-U**	**HL-M2-U**
Acetaminophen	LGS	↑	↑		↑	━	━	━	n.d.	↑		━	━
Acetaminophen sulfate	LSG	━	⩛	n.d.	━	n.d.	━	━	n.d.	━		━	━
Acetaminophen mercapturate	LSG	↑	↑	n.d.	━	n.d.	━	━	↑	↑		━	━
Acetaminophen glucuronide	LSG	━	⩛	n.d.	━	n.d.	━	━	━	n.d.		━	━
Acetaminophen	MSG	n.d.	↑	↑	↑	━	━	━	n.d.	↑		━	↑
Acetaminophen sulfate	MSG	━	━	n.d.	━	n.d.	━	━	n.d.	n.d.		⩛	━
Acetaminophen mercapturate	MSG	━	↑	↑	━	n.d.	↑	━	⩛	↑		↑	━
Acetaminophen glucuronide	MSG	━	━	n.d.	━	n.d.	━	━	━	n.d.		━	━
Acetaminophen	HSG	━	━	⩛	━	━	━	━	n.d.	n.d.		━	━
Acetaminophen sulfate	HSG	↑	━	↑	━	n.d.	━	━	n.d.			━	━
Acetaminophen mercapturate	HSG	━	↑	↑	━	n.d.	━	━	⩛	n.d.		━	━
Acetaminophen glucuronide	HSG	━	↑	⩛	━	n.d.	━	━	━	n.d.		━	━
Bisphenol A	LGS	━	n.d.	↑	n.d.	↑	↑	n.d.	↑	↑		n.d.	↑
Bisphenol A sulfate	LSG	↑	↑	n.d.	↑	↑	↑	↑	↑	n.d.		n.d.	↑
Bisphenol A b-D-Glucuronide	LSG	↑	↑	n.d.	↑	↑	↑	↑	↑	n.d.		↑	n.d.
Bisphenol A	MSG	↑	n.d.	n.d.	n.d.	↑	━	n.d.	↑	↑		n.d.	↑
Bisphenol A sulfate	MSG	↑	↑	n.d.	↑	↑	↑	↑	↑	n.d.		n.d.	↑
Bisphenol A b-D-Glucuronide	MSG	n.d.	↑	n.d.	↑	↑	↑	↑	↑	n.d.		↑	n.d.
Bisphenol A	HSG	━	n.d.	n.d.	n.d.	↑	━	n.d.	↑	⩛		n.d.	n.d.
Bisphenol A sulfate	HSG	↑	↑	n.d.	↑	↑	↑	↑	↑	n.d.		n.d.	↑
Bisphenol A b-D-Glucuronide	HSG	↑	↑	n.d.	↑	↑	↑	↑	↑	n.d.		↑	n.d.
Plasma samples Compound Name		**RP-M1-P**	**RP-M2-P**	**RP-M3-P***	**RP-M4-P**	**RP-M5-P**	**RP-M6-P**	**RP-M7-P**			**RP-M10-P**	**HL-M1-P**	
Acetaminophen		↑	↑	↑	↑	n.d.	↑	↑			↑	↑	
Acetaminophen sulfate		↑	↑	↑	↑	n.d.	↑	↑			↑	↑	
Acetaminophen mercapturate		n.d.	↑	n.d.	↑	n.d.	↑	↑			↑	↑	
Acetaminophen glucuronide		n.d.	↑	n.d.	↑	n.d.	↑	↑			⩛	↑	
Bisphenol A		⩛	n.d.	n.d.	n.d.	↑	↑	n.d.			n.d.	n.d.	
Bisphenol A sulfate		↑	↑	↑	↑	↑	↑	↑			n.d.	↑	
Bisphenol A b-D-Glucuronide		n.d.	↑	n.d.	↑	↑	↑	↑			↑	↑	

3.5. Conjugated metabolite profiling using SS

Acetaminophen and Bisphenol A (BPA), plus their glucuronide and sulfate conjugates, were assessed to evaluate the performance of SS workflows for the detection of both parent compounds and phase II metabolites in biological matrices.

In the urine samples, systematic detection of acetaminophen and its conjugates was observed in the workflows from RP-M4-U, RP-M6-U, RP-M7-U, HL-M1-U and HL-M2-U (**Table 4**). RP-M1-U and RP-M2-U reported similar detection frequencies, although their intensity trends were inconsistent, suggesting variability in sensitivity or matrix effects. RP-M3-U, which included a deconjugation step for urine samples, achieved full coverage of acetaminophen and its conjugates in QA/QC solvent samples and detected only the deconjugated form in LSG and MSG urine. This difference reflects, the absence of a biological matrix in solvent-based QA/QC samples, which generally results in improved detection performance compared to urine matrix. The conjugated forms were detected in HSG urine, which indicates potential variability in the deconjugation step due to higher matrix effects. RP-M5-U, did not apply a deconjugation step and showed a method coverage for all forms as detected in the QA/QC mix only, but detected only the parent acetaminophen. This result is probably related to a limited extraction efficiency for the conjugates due to the use of a methanol/hexane solvent mixture. RP-M8-U identified acetaminophen glucuronide and mercapturate in the QA/QC mix and urine samples. Nevertheless, RP-M8-U failed to detect the sulfate conjugate or parent compound even in QA/QC solvent, indicating possible method coverage limitations. RP-M9-U detected conjugates only in LSG urine and exhibited abnormal “concentration-response intensity” behavior, probably due to matrix effects or the use of tetrahydrofuran/1-hexanol as extraction solvents.

For BPA, conjugated forms were reliably detected by RP-M1-U, RP-M5-U, RP-M6-U and RP-M8-U, with RP-M5-U and RP-M8-U showing the most reproducible “concentration-response intensity” (**Table 4**). Methods RP-M2-U, RP-M4-U and RP-M7-U detected only conjugated BPA and not the parent compound, which aligns with their reported method coverage, as parent BPA was not detected even in QA/QC solvent. This detection could be related to the greater detectability of conjugated BPA metabolites compared with the parent compound in negative ESI ionization. RP-M9-U and the HILIC-based methods (HL-M1-U and HL-M2-U) exhibited reproducible intra-method results but did not achieve full coverage of all BPA forms, which is probably due to sensitivity or method coverage limitations. Method RP-M3-U did not detect BPA conjugates, since a deconjugation step was applied.

In plasma samples, the results were comparable to those obtained for urine, with acetaminophen exhibiting very reproducible “concentration-response intensity” (**Table 4**). This difference with the consistent signal intensity observed in urine is related to the difference between individuals providing

these two biological matrices. The non-fortified plasma was free of background levels, while urine contained high baseline levels of these analytes prior to fortifying.

3.6. Comparative evaluation of analytical methods using an S-score system

The S-scores calculated for each matrix, analytical method and fortifying level confirm the observations previously described. Calculation of the S-score and the detection frequency for each compound, provide a fast visualisation of compounds detected by multiple analytical methods (e.g., Ifosfamide, Ipconazole, Chlorfenvinphos), while others appeared more method-specific, highlighting the complementarity between analytical methods (**Table S17**). Methods with the highest detection rates pointed out the lowest method S-scores, particularly RP-M6, RP-M4 and RP-M2 (**Figure S6**). HILIC methods show scores relatively comparable to RP, supporting their complementarity to RP methods for exposure characterization. Although the GC method showed higher S-scores, for specific compounds more amenable to GC analysis, higher detection frequencies were observed (**Table S17**). A "concentration-response intensity" was illustrated by the lower S-score at higher fortifying levels. In urine, higher S-scores were obtained at HSG compared with MSG and LSG indicating stronger matrix effects at HSG.

3.7. Multivariate data analysis using ComDim-ICA

Urine samples: The application of ComDim-ICA with four CCs to the urine data captured most of the shared variance (99.6 %) across the different methods (**Figure 3a** and **b**). Each CC explains a major effect among those explored in the previous sections. However, the CCs were extracted directly from the data, without any prior assumptions. This approach enables the identification of compounds with "consistent intensity" across the urine matrices regardless of spiking level, as extracted by CC1 (65.3 % of the total variance). Saliences, which indicate how much each data block contributes to a given CC (CC1, **Figure 3b**), highlights the methods with the highest contribution as they detected the compounds with "consistent intensity" (acetaminophen and its conjugates, as well as hydroxycotinine) in each SG urine sample. The global score profiles indicate that the intensities of these compounds remain stable across the SG conditions (**Figure 3a-CC1**), with the highest intensity observed in HSG, followed by LSG and MSG urine samples. CC3 (12.9 % of the total variance) extracted the information directly aligned with the study's objectives. It captures the key variation related to both "concentration-response intensity" and matrix effects. The global scores (**Figure 3b-CC3**) show clear "concentration-response intensity" trends within each SG category (LSG, MSG, HSG), and most methods effectively distinguish the 100 ng/mL concentration samples from the lower concentration. **Figure 3a-CC3** displays the methods with the highest contribution to CC3, with RP-M3-U, RP-M9-U, RP-M5-U, and RP-M6-U (blocks three, nine, five and six, respectively) displaying the highest saliences. The relatively lower

salience contributions of the other methods, despite their local scores clearly showing "concentration-response intensity" trends, can be explained by the fact that those methods detected all compounds with "consistent intensity" contributed more strongly to CC1 (**Figure 3a-CC1**). Consequently, these methods show reduced contributions to CC3 (**Figure 3a-CC3**).

These multivariate results detected methods with similar behavior even without prior knowledge and demonstrate that SS methods can detect "concentration-response intensity" relationship. Despite some variation in local scores across methods, the "concentration-response intensity" trend remained evident, indicating that SG normalization preserved relative signal intensity or that matrix effects did not obscure the "concentration-response intensity" relationship. CC1 and CC3 demonstrate the complementarity between the analytical methods. CC1 primarily detects specific compounds related to acetaminophen and its conjugated forms, whereas CC3 is more associated with compounds showing "concentration-response intensity" relationship.

The most discriminative compounds were selected from the S-plot when their covariance values exceeded ± 2 standard deviations from the mean of the local loadings. This threshold identifies the most contributing compounds shared across platforms, even though more compounds showed "concentration-response intensity" relationships within individual methods. **Table S18** summarizes the key compounds contributing to the observed "concentration-response intensity" relationship across methods. In total, 26 out of the 50 selected compounds were selected in the local loadings of five or more blocks, indicating strong agreement across methods. An additional twelve compounds were selected by two to four methods, while twelve were selected by a single method, highlighting some complementarity between the analytical methods. Compounds selected by a single method should be interpreted with caution, particularly if these compounds have been identified by other methods but with "consistent intensity".

Plasma samples: For plasma samples, CC1 (**Figure 3**) explained 99.8 % of the total variance, with all methods contributing similarly (**Figure 3c-CC1**). These results indicate a unified signal related to the "concentration-response intensity" relationships observed across all analytical methods (**Figure 3d-CC1**). The most contributing compounds selected from each analytical method are summarized in **Table S19**. 25 of the 45 most discriminant compounds were selected from the loadings of five or more blocks, thus highlighting strong inter-method comparability. An additional seven compounds were selected by two to three methods, while thirteen were predominantly selected by a single method, reflecting the complementarity strengths of the various analytical methods applied. These results offer an additional unsupervised confirmation of the trends previously identified in the "concentration-response intensity" relationship section and demonstrate that SS approaches can detect

"concentration-response intensity" in a semi-quantitative manner, with reproducible results across all methods.

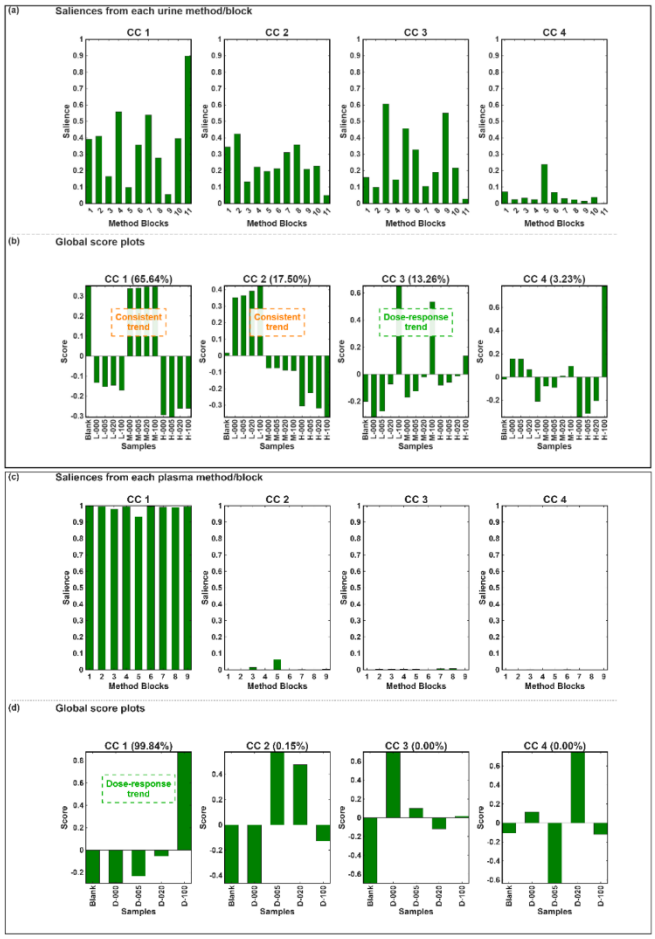


Figure 3: *ComDim-ICA analysis results of the LC-HRMS datasets from all methods for urine* ***(a-b)*** *and plasma* ***(c-d). (a)*** *Salience from each data block for the four common components (CC1–CC4) for the urine dataset. Blocks 1-11 correspond to RP-M1-U to RP-M9-U, followed by HL-M1-U and HL-M2-U.* ***(b)*** *Global score plots of the four CCs for urine samples. These components represent shared sources of variance across laboratories, highlighting consistent patterns among the three urine types (L, M, and H specific gravity) and the non-fortified (0 ng/mL) and the different fortifying concentration samples (5 to 100* ng/mL*). **(c)** Salience from each data block for the four common components (CC1–CC4) for plasma samples. Blocks 1-9 correspond to RP-M1-P to RP-M7-P, followed by RP-M10-P, and HL-M1-P.*

(d) *Global score plots for the four CCs for plasma samples. These components represent sources of variance shared across laboratories in the non-fortified (0 ng/mL) and the different fortifying concentration samples (5 to 100* ng/mL*).*

4. Discussion

This extensive interlaboratory study evaluated a set of SS methods applied to urine and plasma samples to assess method complementarity and support harmonization in the analysis of occupational samples collected under the EU-PARC project. Detection rates for the combined SS methods were high across sample types, 97.5 % in the QA/QC mix, 93.8 % in urine, and 92.6 % in plasma, demonstrating globally strong and robust performance. In addition, despite differences in in-house procedures, instrumentation, and samples preparation, eleven of thirteen, eight of twelve and seven of ten of the applied methods detected more than half of the QA/QC exposure markers in the standard solution, urine, and plasma, respectively. The compounds not detected by any methods (1,3-DCP and TBPH) were outside the applicability domain of LC-ESI-HRMS. While both compounds are, in principle, more amenable to GC-based analysis, they were not detected by the GC method applied in this interlaboratory study. This highlights an important limitation of NTS methods, where compounds with extreme chemical properties may fall outside the chemical space coverage of specific methods and may require tailored methods. The use of only one GC method in our study restricted the detection of these two compounds. Alternative GC approaches, such as headspace sampling or methods employing APCI ionization, could improve detection. These results underline the complementarity between different analytical methods and the importance of their combination to expand chemical space coverage. Finally, the clear concentration-response trends in signal intensities indicate the suitability of SS for large-scale human biomonitoring, as they support its use as a semi-quantitative approach for group comparisons in occupational cohorts.

Sample preparation

Optimization of solvent and extraction techniques: In this study, SPE did not provide a systematic advantage and, in several cases, led to the loss of some analytes. This finding aligns with previous reports comparing sample preparation strategies for NTS approaches. For example, Gutierrez-Martin et al. (2023) systematically evaluated five extraction protocols across diverse chemical classes, including pharmaceuticals, plastic additives, personal care products, and pesticides [44]. By examining extraction recovery, linearity, matrix effects, sensitivity, and reproducibility, the authors demonstrated that SPE-based preconcentration and clean-up impact sensitivity, mainly due to incomplete removal of matrix components and residual matrix effects associated with complex sample matrices. On the other hand, previous studies highlighting the importance of carefully selecting sample preparation

methods have demonstrated the advantages of SPE for specific exposomics applications, depending on the analytical objective [45-47]. Musatadi et al. (2024) compared eleven sample preparation procedures to screen persistent, mobile, and toxic compounds in human urine, including their phase II metabolites. They reported that SPE provided better results for synthetic or fortified samples, where analytes were at low concentrations, whereas the dilute-and-shoot approach offered the widest coverage of the suspect list for real urine samples, outperforming both SPE and LLE in that context. [45]. Finally, Lepoittevin et al. (2023) reported reduced reproducibility in comparative analyses of plasma and serum extraction strategies when SPE was applied, emphasizing the need for careful optimization and critical evaluation of the true benefit of broader chemical coverage [48]. Other studies demonstrated the importance of solvent selection to reduce incomplete metabolite extraction and matrix effects, which can introduce substantial bias in metabolomics studies [46, 49]. These studies, consistent with our results, highlight the importance of solvents with broader polarity coverage, such as mixtures of MeOH or ACN with water, which may improve analyte recovery while minimizing methodological biases. These results demonstrate the importance of strategically streamlining sample preparation steps in combination with careful selection of an appropriate solvent. This approach improves data quality while providing significant benefits in terms of analysis time, personnel requirements, and costs, without compromising analytical performance.

Deconjugation step: In this interlaboratory assay, RP-M3-U/P was the only method that applied deconjugation and therefore, in principle, should not detect conjugated forms. Interestingly, deconjugation did not work systematically in all urine samples. This was especially evident for MSG and for HSG urine samples, which have higher background concentrations of acetaminophen and its conjugated forms, as well as a stronger matrix effect. Under these conditions, some conjugates (acetaminophen mercapturate and acetaminophen sulfate) were still detected, indicating that deconjugation was not complete in these samples.

Across all methods without a deconjugation step, the findings point out that SS workflows were generally effective in detecting parent compounds and conjugates but that no single method reliably detected all acetaminophen and BPA forms across all samples with reproducible trends. The contrasting performances between BPA and acetaminophen within the same analytical platforms, such as RP-M5-U, highlight that compound-specific limitations arise from physicochemical differences and extraction compatibility. Methods using extraction solvents, such as mixtures of MeOH or ACN with water, allowed for more reliable detection of conjugated metabolites, likely due to improved recovery. The detection of conjugated metabolites can be advantageous. For example, conjugated metabolites were among the most discriminant compounds differentiating between pesticide-exposed and control groups [50], and unhydrolyzed urine showed higher discriminatory power than

urine with hydrolysis step for distinguishing disease states based on steroid conjugates [51]. Therefore, based on these results, we have recommended performing SS/NTS analyses of biological samples in the next phase of the project without a deconjugation step.

Method complementarity

A first level of complementarity is explained by the detection polarity, as compound-specific ionization preferences resulted in differential detection between positive and negative modes. Secondly, although RP approaches generally exhibited superior overall detection performance in our study, some compounds were more reproducibly detected by the HILIC method, like 2,3,4,5-tetrabromophenol, paraquat, and 2,4-dichlorophenol. Even within RP methods, differences in the extraction procedure as well as variations in stationary phases or gradient conditions allowed the detection of molecules that may be missed by other RP setups. GC, in turn, provides unique advantages for classes of compounds that are poorly ionized with LC coupling, such as the four compounds, benz[a]anthracene, benzo[a]pyrene, indeno[1,2,3-cd]pyrene and PCB-153 exclusively detected by the GC method (**Figure S3**). These findings are consistent with previous studies emphasizing the importance of methodological complementarity [5]. Achieving the most comprehensive coverage of diverse chemical exposures, while addressing the reproducibility issues of a single-method, requires an integrated strategy that leverages complementarity at multiple levels [52-58]. In addition, the complementarity of SS/NTS approaches is particularly important for improving targeted methods by including biomarkers discovered through non-target strategies. For example, Grova et al. used an SS/NTS approach to identify and quantify new tetrahydroxylated PAH metabolites, and expand the coverage of biomarkers to include more toxic PAHs [59]. Therefore, the combination of different analytical techniques provides broader chemical space coverage and is essential for comprehensive metabolite profiling, as well as for the discovery of novel effect-related biomarkers.

Data quality and QA/QC importance

To ensure reliable and comparable data in SS/NTS studies, it is essential to implement minimal necessary harmonized QC measures, including the use of common QA/QC standard mixes across batches and laboratories. Each batch should include at least one high-dose fortified QC, ideally complemented by a lower-dose QC, with clearly defined acceptance criteria, such as CV thresholds to monitor performance and detect deviations. Harmonized QC practices and systematic outlier handling further support early identification of method-specific issues and improve cross method comparability [12, 15, 32]. Transparent and detailed reporting of extraction conditions, solvent systems, and QA/QC performance is critical, as recommended by the Benchmarking and Publications for Non-Targeted Analysis Working Group (BP4NTA) - SRT, because it facilitates evaluation of the data quality, and

improves the interpretation of data across different analytical methods [35]. Therefore, with additional interlaboratory exercises conducted under WP4/Task 4.3 on similar and other biological matrices within EU-PARC, the findings will be used to inform the development of dedicated LC-based and GC-based QA/QC mixes for SS/NTS analysis. These mixes will be made available to participating laboratories in a subsequent phase to further support methodological harmonization and will be applied during the analysis of biological samples.

Innovative data processing methods

The data processing procedure and the implementation of data analysis strategies are indispensable for extracting reliable and reproducible insights from complex experimental datasets, especially when obtained by multiple platforms/methods. The application of ComDim-ICA in this study enabled the global evaluation of sample preparation limitations, methodological differences, "concentration-response intensity" relationships, matrix effects, and method comparability. These strategies are not restricted to interlaboratory contexts and they could be applied to real-world sample cohorts, allowing the integration of heterogenous data across laboratories and methods. These approaches identify shared patterns without requiring prior assumptions and improve the interpretability of data across diverse methods and biomarker discovery.

Towards a minimal standard operating procedure (SOP)

The results provide guidance for the next phase of this project under EU-PARC, which involves analyzing biological samples from a large cohort across different countries. The "PARC-H02 – SOP for real sample analysis" and injection sequence (**Table S20**) are presented in the supporting information files. A summary of key SOP requirements is provided in Box 1. The sample analysis should prioritize the inclusion of both LC- RP- and HILIC- phases and GC-based platforms to broaden the analytical coverage and the adoption of a shared QA/QC framework with occupationally relevant compounds to monitor comparability and repeatability across laboratories. Such an approach balances flexibility with standardization and ensures that SS/NTS workflows remain both comprehensive and reliable for biomonitoring applications.

Box 1. Key SOP requirements for biological sample analysis

- **Common QC samples:** NORMAN mix; LC- and GC-MS QA/QC mixes; high-level fortified reference matrices; internal and external labeled markers; field blanks (if available).
- **Sample preparation:** Procedural and field blanks prepared as specified; internal and external labeled markers added to all samples; QC pools prepared and fortified at low and high levels with the LC or GC mix.
- **Restricted procedures:** Use broad-polarity solvents only (e.g., methanol, water, acetonitrile); no deconjugation step; SPE allowed only with clear justification.
- **Instrumental analysis:** Predefined injection sequence followed by all partners (**Table S20**).
- **Data handling:** Standardized file naming (*YYYYMMDD_XXX_SAMPLE_IonMode_Instrument_Lab*, where XXX = injection order) and unified reporting template should be used.
- **Partner responsibility:** Each laboratory completed the full workflow, including analysis, data pre-processing, and initial statistical evaluation.

Strengths and limitations of the study

This interlaboratory study establishes a structured framework for evaluating SS methods by introducing a defined QA/QC mix for occupational exposure assessment in the workplace. Our study enables systematic comparison of method performance across diverse platforms. Analyses were performed on urine and plasma, both representing matrices commonly used for human biomonitoring. Urine samples were tested covering varying specific gravities and multiple fortifying levels of the QA/QC mix, which allowed robust assessment of method sensitivity. We incorporate different in-house screening workflows to provide insight into inter-laboratory variability and identify the strengths, the limitations, and the complementarity of these methods. The experimental parameters of the different methods used by all partners were provided. This can serve as a reference point for new laboratories interested in beginning to implement the SS/NTS approach in their own laboratory. We developed an SOP for biological sample analysis with the requirements regarding sample preparation and analysis steps to reduce costs and improve data comparability. Finally, robust and harmonized reference materials for urine and plasma, supporting biological sample analyses collected from workers in waste management and healthcare sectors will be implemented in the next phase of the project.

Our study faces several limitations. First, the QA/QC mix provided to partners consisted of 81 pre-selected target chemicals and therefore represents only a small fraction of the chemical space relevant to occupational exposures. In addition, participating laboratories were not blinded to the provided chemical list, which may have influenced data acquisition and data processing strategies. Consequently, the comparison largely reflected suspect or target screening data analysis workflows rather than true NTS, limiting its relevance for identifying truly unknown compounds, where authentic standards are unavailable. In addition, the concentration range of the analytes investigated in this study may not fully reflect the variability encountered in real biological samples, where some

compounds can occur at significantly lower or higher levels, potentially affecting detection performance. Second, the analytical approaches varied substantially between laboratories, including differences in instrumentation, data acquisition methods and processing workflows. This methodological heterogeneity introduces variability that complicates direct comparison of individual performance metrics and limits the ability to attribute differences to any single parameter with certainty. Moreover, the evaluation was based on pooled samples rather than biological samples from the EU-PARC occupational cohort which may introduce additional variability due to matrix effects and unknown interferences. Finally, participating laboratories applied only two HILIC methods and one GC method limiting the coverage of these techniques in comparison to the more developed RP methods. Since all LC-based analyses used ESI ionization, it was not possible to assess the incorporation of additional ionization techniques, such as APCI, which could expand the analytical coverage further.

5. Conclusions

This interlaboratory study evaluated analytical SS methods across eleven European partners, focusing on the detection performance and data comparability for characterizing occupational exposure using model compounds. HRMS-based SS/NTS enabled broad detection of occupationally relevant compounds and produced reproducible results across laboratories, including "concentration--response intensity" trends.

This study further indicates that solvent selection may contribute strongly to variability in detection performance, whereas the choice of extraction technique had a relatively minor impact in the present dataset. Extraction solvents with broader polarity coverage were associated with improved analytical performance, while SPE did not systematically improve detection. Similarly, deconjugation procedures, which represent a substantial investment of time and resources in large cohort SS/NTS studies, did not show systematic advantages in this interlaboratory study. Therefore, routine inclusion of deconjugation or SPE should be carefully evaluated and justified by clear analytical benefit.

A key strength of the evaluated in-house methods lies in their complementarity. Maintaining diverse GC- and LC-based analytical strategies is essential for maximizing chemical space coverage, as no single workflow can fully capture the chemical complexity of biological matrices. Efforts should prioritize coordination instead of strict standardization, ensuring interlaboratory comparability without constraining analytical diversity. However, as analyzing samples across a large number of laboratories is often impractical, the use of at least two complementary analytical methods and both ionization polarities represents a feasible minimum to ensure adequate chemical space coverage. This collaborative work relies on the systematic implementation of shared QA/QC compound mixes to enable robust performance assessment and data comparability across different workflows. Finally, this

work provides a solid methodological foundation for the analysis of real biological samples and has led to the development of a minimal, fit-for-purpose PARC-H02 SOP, considered as project-specific operational guidance. This SOP will serve as a blueprint for the next phase of the project under EU-PARC, in which more than 1,000 urine and 500 plasma samples collected from both waste management and healthcare sectors will be analyzed by participating laboratories, with methodological adjustments supported by the findings of this interlaboratory study. By balancing essential harmonization with analytical flexibility, the proposed methodology enables high-quality, large-scale exposure assessment and represents an important step toward harmonized occupational biomonitoring in Europe and beyond.

List of abbreviations and definitions

1,3-DCP	1,3-dichloro-2-propanol
1-HexOH	1-hexanol
ACN	Acetonitrile
AcOH	Acetic acid
AIF	All ion fragmentation
AMPA	Aminomethylphosphonic acid
APCI	Atmospheric pressure chemical ionization
BDCIPP	Bis(1,3-dichloro-2-propyl) phosphate
BP4NTA	Benchmarking and Publications for Non-Targeted Analysis Working Group
BPA	Bisphenol A
CAS	Chemical abstracts service
CC	Common component
ComDim	Common components and specific weights analysis
CV	Coefficient of variation
D	Dilute-and-shoot
DDA	Data-dependent acquisition
DEET	N,N-diethyl-m-toluamide
DIA	Data-independent acquisition
DMSO	Dimethyl sulfoxide
EI	Electron ionization
ESI	Electrospray ionization
EtOH	Ethanol
EU	European
GC	Gas chromatography
GC-HRMS	Gas chromatography-high resolution mass spectrometry
GC-M	Gas chromatography-method
H2O	Water
HBM4EU	Human biomonitoring for Europe
HCOOH	Formic acid
Hex	Hexane
HILIC	Hydrophilic interaction liquid chromatography
HL-M	Hydrophilic interaction chromatography method
HRMS	High resolution mass spectrometry
HSG	High specific gravity
ICA	Independent components analysis
InChI	International chemical identifier
InChIKey	International chemical identifier key
IUPAC	International union of pure and applied chemistry
LC	Liquid chromatography
LC-HRMS	Liquid chromatography - high resolution mass spectrometry
LLE	Liquid-liquid extraction
LSG	Low specific gravity
MeOH	Methanol
MS	Mass spectrometry
MS/MS	Tandem mass spectrometry

MSG	Medium specific gravity
n.a.	Not applied
n.d.	Not detected
NH4F	Ammonium fluoride
NH4HCO2	Ammonium formate
NH4OAc	Ammonium acetate
NH4OH	Ammonium hydroxide
NORMAN	Network of reference laboratories, research centres and related organisations for monitoring of emerging environmental substances
-P	Plasma
PAHs	Polycyclic aromatic hydrocarbons
PARC	Partnership for assessment of risks from chemicals
PB	Phosphate buffer
PCB-153	2,2',4,4',5,5'-Hexachlorobiphenyl
PFHxS	Perfluorohexanesulfonic acid
PFNA	Perfluorononanoic acid
PFOA	Perfluorooctanoic acid
PFOS	Perfluorooctanesulfonic acid
PubChem CID	PubChem compound identification number
QA/QC	Quality assurance/quality control
Q-TOF	Quadrupole time-of-flight
RP	Reversed-phase
RP-M	Reversed-phase liquid chromatography methods
RT	Retention time
SG	Specific gravity
SMILES	Simplified molecular input line entry system
SOP	Standard operating procedure
SPE	Solid-phase extraction
SRT	Study Reporting Tool
SS/NTS	Suspect/non-target screening
S-score	Summary score for binary data
ST	Solvent transfer
TBPH	Di-(2-ethylhexyl)-tetrabromophthalate
THF	Tetrahydrofuran
-U	Urine
ρ	Pearson correlation coefficient

Supplementary Information

Supplementary Information file 1: Additional data processing results and a detailed SOP for sample analysis (.docx)

Supplementary Information file 2: Nineteen tables including details regarding the reference standards used, samples preparation and data acquisition procedures as well as additional results (.xlsx).

Declarations

Ethics approval and consent to participate:

Not applicable as pooled urine and plasma samples were used only.

Consent for publication

Not applicable.

Availability of data and materials

The raw datasets generated and analyzed during the current study are not publicly available but are available from the corresponding author on reasonable request.

Disclosure of the use of AI-assisted technology in the writing process

The authors used the professional version of Chat-GPT during the preparation of this work to improve the language quality and phrasing of selected sentences originally written by the authors themselves. The revised text was carefully reviewed and further edited by all contributing authors, including native English speakers to ensure accuracy and consistency of the intended meaning. The authors take full responsibility for the content of the publication.

Competing interests

The authors declare that they have no competing interests.

Funding

This work received funding from the European Union research and innovation program Horizon Europe under Grant Agreement No 101057014T.

Authors' contributions

Conceptualization: B.H., JP.A., S.N.; **Data curation**: B.H., A.M.R., L.B., A.D., T.K., G.A., T.M., E.B., C.C., R.D.S., Co.H., A.L.I., A.Ka., K.M.K., S.K., L.K., H.O., H.P., Z.R., M.S., A.T., R.V.; **Formal Analysis**: B.H., L.B., A.D., T.K., G.A., T.M., E.B., C.C., R.D.S., Co.H., A.L.I., A.Ka., K.M.K., S.K., L.K., R.N., H.O., H.P., D.N.R., Z.R., M.S., A.T., R.V., **Funding acquisition**: S.N.; **Investigation**: B.H., A.M.R., L.B., A.C., A.D., T.K., Ca.H., N.G., G.A., T.M., E.B., C.C., R.D.S., Co.H., A.L.I., K.M.K., S.K., L.K., H.O., H.P., E.J.P., Z.R., M.S., A.T., R.V.; **Methodology**: B.H., A.M.R., T.M., JP.A., S.N.; **Project administration**: B.H., S.N.; **Resources**: E.J.P., JP.A., S.N.; **Software**: B.H., A.M.R., B.C., G.J., M.Lau., D.N.R; **Supervision**: SN; **Validation**: BH, SN; **Visualization**: B.H., A.M.R.; **Writing – original draft**: B.H., L.B.; **Writing – review and editing**: B.H., A.M.R., L.B., A.C., A.D., T.K., Ca.H., N.G., G.A., T.M., E.B., B.C., C.C., G.D., R.C.D., F.F., M.F.F., C.G., R.D.S., Co.H., G.J., A.L.I., A.Ka., O.K., K.M.K., A.Ke., S.K., L.K., M.L., M.Lau., B.LB., A.N., R.N., H.O., H.P., E.J.P., Z.R., A.R.C., D.S., JM.S., M.S., K.S., A.T., R.V., E.L.S., D.N.R., JP.A., S.N..

Acknowledgements

This work was supported by the EU-PARC project and has received funding from the European Union research and innovation program Horizon Europe under Grant Agreement No 101057014T. The authors gratefully acknowledge AUTH, JSI and INRS partners for providing the pooled biological matrices used in this study. LB, AK, and AC are supported by the Exposome Centre of Excellence of the University of Antwerp (BOF grants, Antigoon database 41222 and 50211). EJP & SK acknowledge the support from the European Union's Horizon 2020 research and innovation program under grant agreement No 857560 (CETOCOEN Excellence), the CETOCOEN EXCELLENCE project (CZ.02.1.01/0.0/0.0/17_043/0009632), and the RECETOX RI (No LM2023069) financed by the Czech MEYS.

Views and opinions expressed are those of the author(s) only and do not necessarily reflect those of the European Union or the granting authority, European Health and Digital Executive Agency (HADEA). Neither the European Union nor the granting authority can be held responsible for any use that may be made of the information it contains.

References

1. Vorkamp, K., et al., *Biomarkers, matrices and analytical methods targeting human exposure to chemicals selected for a European human biomonitoring initiative.* Environ Int, 2021. **146**: p. 106082.
2. Vandenberg, L.N., et al., *Addressing systemic problems with exposure assessments to protect the public's health.* Environ Health, 2023. **21**(Suppl 1): p. 121.
3. Grashow, R., et al., *Integrating Exposure Knowledge and Serum Suspect Screening as a New Approach to Biomonitoring: An Application in Firefighters and Office Workers.* Environ Sci Technol, 2020. **54**(7): p. 4344-4355.
4. Pourchet, M., et al., *Suspect and non-targeted screening of chemicals of emerging concern for human biomonitoring, environmental health studies and support to risk assessment: From promises to challenges and harmonisation issues.* Environ Int, 2020. **139**: p. 105545.
5. Manz, K.E., et al., *Non-targeted analysis (NTA) and suspect screening analysis (SSA): a review of examining the chemical exposome.* J Expo Sci Environ Epidemiol, 2023. **33**(4): p. 524-536.
6. Lu, P., et al., *Urinary metabolic alterations associated with occupational exposure to metals and polycyclic aromatic hydrocarbons based on non-target metabolomics.* J Hazard Mater, 2025. **487**: p. 137158.
7. Oresic, M., et al., *Metabolome informs about the chemical exposome and links to brain health.* Environ Int, 2025. **203**: p. 109741.
8. Roggeman, M., et al., *Comprehensive suspect screening for the identification of contaminants of emerging concern in urine of Flemish adolescents by liquid chromatography high-resolution mass spectrometry.* Environ Res, 2022. **214**(Pt 3): p. 114105.
9. Newmeyer, M.N., et al., *Implementing a suspect screening method to assess occupational chemical exposures among US-based hairdressers serving an ethnically diverse clientele: a pilot study.* J Expo Sci Environ Epidemiol, 2023. **33**(4): p. 566-574.
10. Tkalec, Z., et al., *Innovative analytical methodologies for characterizing chemical exposure with a view to next-generation risk assessment.* Environ Int, 2024. **186**: p. 108585.
11. Hollender, J., et al., *High resolution mass spectrometry-based non-target screening can support regulatory environmental monitoring and chemicals management.* Environmental Sciences Europe, 2019. **31**(1).

12. Hollender, J., et al., *NORMAN guidance on suspect and non-target screening in environmental monitoring.* Environmental Sciences Europe, 2023. **35**(1).
13. Mosley, J.D., et al., *Establishing a framework for best practices for quality assurance and quality control in untargeted metabolomics.* Metabolomics, 2024. **20**(2): p. 20.
14. Kirwan, J.A., et al., *Quality assurance and quality control reporting in untargeted metabolic phenotyping: mQACC recommendations for analytical quality management.* Metabolomics, 2022. **18**(9): p. 70.
15. Caballero-Casero, N., et al., *Towards harmonised criteria in quality assurance and quality control of suspect and non-target LC-HRMS analytical workflows for screening of emerging contaminants in human biomonitoring.* TrAC Trends in Analytical Chemistry, 2021. **136**.
16. Broeckling, C.D., et al., *Current Practices in LC-MS Untargeted Metabolomics: A Scoping Review on the Use of Pooled Quality Control Samples.* Anal Chem, 2023. **95**(51): p. 18645-18654.
17. Lennon, S., et al., *Harmonized quality assurance/quality control provisions to assess completeness and robustness of MS1 data preprocessing for LC-HRMS-based suspect screening and non-targeted analysis.* TrAC Trends in Analytical Chemistry, 2024. **174**.
18. Oberacher, H., et al., *A European proposal for quality control and quality assurance of tandem mass spectral libraries.* Environmental Sciences Europe, 2020. **32**(1).
19. Bader, T., et al., *General strategies to increase the repeatability in non-target screening by liquid chromatography-high resolution mass spectrometry.* Anal Chim Acta, 2016. **935**: p. 173-86.
20. Schymanski, E.L., et al., *Identifying small molecules via high resolution mass spectrometry: communicating confidence.* Environ Sci Technol, 2014. **48**(4): p. 2097-8.
21. Alygizakis, N., et al., *Towards a harmonized identification scoring system in LC-HRMS/MS based non-target screening (NTS) of emerging contaminants.* TrAC Trends in Analytical Chemistry, 2023. **159**.
22. Houriet, J., et al., *Multilaboratory Untargeted Mass Spectrometry Metabolomics Collaboration to Identify Bottlenecks and Comprehensively Annotate A Single Dataset.* Anal Chem, 2025. **97**(30): p. 16110-16122.
23. Dulio, V., et al., *The NORMAN Association and the European Partnership for Chemicals Risk Assessment (PARC): let's cooperate!* Environmental Sciences Europe, 2020. **32**(1).
24. Schymanski, E.L., et al., *Non-target screening with high-resolution mass spectrometry: critical review using a collaborative trial on water analysis.* Anal Bioanal Chem, 2015. **407**(21): p. 6237-55.
25. Rostkowski, P., et al., *The strength in numbers: comprehensive characterization of house dust using complementary mass spectrometric techniques.* Anal Bioanal Chem, 2019. **411**(10): p. 1957-1977.
26. Schulze, B., et al., *Inter-laboratory mass spectrometry dataset based on passive sampling of drinking water for non-target analysis.* Sci Data, 2021. **8**(1): p. 223.
27. NORMAN Network. *NORMAN Interlaboratory Studies Website*. 2025 [cited 2025 22 Ocober]; Available from: https://www.norman-network.net/?q=interlab-studies.
28. Malm, L., et al., *Quantification Approaches in Non-Target LC/ESI/HRMS Analysis: An Interlaboratory Comparison.* Anal Chem, 2024. **96**(41): p. 16215-16226.
29. Haglund, P., et al., *Comprehensive characterization of European house dust contaminants: Concentrations and profiles, geographical variability, and implications for chemical regulation and health risk.* Sci Total Environ, 2024. **957**: p. 177639.
30. Ottenbros, I., et al., *Assessment of exposure to pesticide mixtures in five European countries by a harmonized urinary suspect screening approach.* Int J Hyg Environ Health, 2023. **248**: p. 114105.
31. Huber, C., et al., *A large scale multi-laboratory suspect screening of pesticide metabolites in human biomonitoring: From tentative annotations to verified occurrences.* Environ Int, 2022. **168**: p. 107452.

32. Vitale, C.M., et al., *Harmonized Quality Assurance/Quality Control Provisions for Nontargeted Measurement of Urinary Pesticide Biomarkers in the HBM4EU Multisite SPECIMEn Study.* Anal Chem, 2022. **94**(22): p. 7833-7843.
33. Aalizadeh, R., et al., *Development and Application of Liquid Chromatographic Retention Time Indices in HRMS-Based Suspect and Nontarget Screening.* Anal Chem, 2021. **93**(33): p. 11601-11611.
34. Van Den Dool, H. and P.D. Kratz, *A generalization of the retention index system including linear temperature programmed gas–liquid partition chromatography.* Journal of Chromatography, 1963. **11**: p. 463–471.
35. Peter, K.T., et al., *Nontargeted Analysis Study Reporting Tool: A Framework to Improve Research Transparency and Reproducibility.* Anal Chem, 2021. **93**(41): p. 13870-13879.
36. Baudry, C., et al., *S-score: a new score for binary qualitative proficiency testing schemes interpretable as the z-score.* Accreditation and Quality Assurance, 2024. **29**(2): p. 103-113.
37. Jouan-Rimbaud Bouveresse, D. and D.N. Rutledge, *A synthetic review of some recent extensions of ComDim.* Journal of Chemometrics, 2022. **38**(5).
38. Baqueta, M.R., et al., *Enhancing mass spectrometry interpretability by ComDim-ICA multi-block analysis: Geographical and varietal traceability of Brazilian Coffea canephora.* Talanta, 2025. **281**: p. 126927.
39. Malm, L., et al., *In-Depth Analysis of the Data from an Interlaboratory Study of Quantitative Non-Target Screening—How Do the Instrumental Methods Compare?* Molecules 2026. **31**(5): p. 875.
40. Tian, Y., Y. Meng, and R.N. Zare, *Simultaneous Detection of Polar and Nonpolar Molecules by Nano-ESI MS with Plasma Ignited by an Ozone Generator Power Supply.* Molecules, 2025. **30**(12).
41. Zhou, S.N., et al., *Development of liquid chromatography atmospheric pressure chemical ionization tandem mass spectrometry for analysis of halogenated flame retardants in wastewater.* Anal Bioanal Chem, 2010. **396**(3): p. 1311-20.
42. Wang, Q., et al., *Temporal Trends and Suspect Screening of Halogenated Flame Retardants and Their Metabolites in Blubbers of Cetaceans Stranded in Hong Kong Waters during 2013-2020.* Environ Sci Technol, 2023. **57**(25): p. 9298-9308.
43. Crews, C., G. LeBrun, and P. Brereton, *Determination of 1,3-dichloropropanol in soy sauces by automated headspace gas chromatography-mass spectrometry.* Food Additives and Contaminants, 2002. **19**(4): p. 343-349.
44. Gutierrez-Martin, D., et al., *Comprehensive profiling and semi-quantification of exogenous chemicals in human urine using HRMS-based strategies.* Anal Bioanal Chem, 2023. **415**(29-30): p. 7297-7313.
45. Musatadi, M., et al., *Sample preparation for suspect screening of persistent, mobile and toxic substances and their phase II metabolites in human urine by mixed-mode liquid chromatography.* Talanta, 2024. **271**: p. 125698.
46. Hajeb, P., et al., *Sample preparation techniques for suspect and non-target screening of emerging contaminants.* Chemosphere, 2022. **287**(Pt 3): p. 132306.
47. Gu, Y., M.L. Feuerstein, and B. Warth, *High-Throughput Solid Phase Extraction for Targeted and Nontargeted Exposomics.* Anal Chem, 2025. **97**(11): p. 6075-6082.
48. Lepoittevin, M., et al., *Comparison between 5 extractions methods in either plasma or serum to determine the optimal extraction and matrix combination for human metabolomics.* Cell Mol Biol Lett, 2023. **28**(1): p. 43.
49. Liao, H.W., et al., *Bias caused by incomplete metabolite extraction and matrix effect: Evaluation of critical factors for plasma sample preparation prior to metabolomics.* J Pharm Biomed Anal, 2022. **219**: p. 114930.
50. Jamin, E.L., et al., *Untargeted profiling of pesticide metabolites by LC-HRMS: an exposomics tool for human exposure evaluation.* Anal Bioanal Chem, 2014. **406**(4): p. 1149-61.

51. Vogg, N., et al., *An untargeted metabolomics approach to evaluate enzymatically deconjugated steroids and intact steroid conjugates in urine as diagnostic biomarkers for adrenal tumors.* Clinical Chemistry and Laboratory Medicine (CCLM), 2025. **63**(5): p. 1004-1015.
52. Jeppesen, M.J. and R. Powers, *Multiplatform untargeted metabolomics.* Magn Reson Chem, 2023. **61**(12): p. 628-653.
53. Tang, D.Q., et al., *HILIC-MS for metabolomics: An attractive and complementary approach to RPLC-MS.* Mass Spectrom Rev, 2016. **35**(5): p. 574-600.
54. Gonzalez-Dominguez, A., et al., *An Overview on the Importance of Combining Complementary Analytical Platforms in Metabolomic Research.* Curr Top Med Chem, 2017. **17**(30): p. 3289-3295.
55. Cannavacciuolo, C., et al., *LC-MS and GC-MS Data Fusion Metabolomics Profiling Coupled with Multivariate Analysis for the Discrimination of Different Parts of Faustrime Fruit and Evaluation of Their Antioxidant Activity.* Antioxidants (Basel), 2023. **12**(3).
56. Haggarty, J., et al., *Serially coupling hydrophobic interaction and reversed-phase chromatography with simultaneous gradients provides greater coverage of the metabolome.* Metabolomics, 2015. **11**(5): p. 1465-1470.
57. Lv, W., et al., *Alternate reversed-phase and hydrophilic interaction liquid chromatography coupled with mass spectrometry for broad coverage in metabolomics analysis.* J Chromatogr B Analyt Technol Biomed Life Sci, 2020. **1152**: p. 122266.
58. Zeki, O.C., et al., *Integration of GC-MS and LC-MS for untargeted metabolomics profiling.* J Pharm Biomed Anal, 2020. **190**: p. 113509.
59. Grova, N., et al., *Identification of new tetrahydroxylated metabolites of Polycyclic Aromatic Hydrocarbons in hair as biomarkers of exposure and signature of DNA adduct levels.* Analytica Chimica Acta, 2017. **995**: p. 65-76.

1 ***Table 1:*** *Summary of analytical protocols used by participating laboratories for sample preparation and data acquisition applied to urine samples.*

Methods	RP-M1-U	RP-M2-U	RP-M3-U	RP-M4-U[a]	RP-M5-U[b]	RP-M6-U	RP-M7-U	RP-M8-U	RP-M9-U	HL-M1-U[a]	HL-M2-U	GC-M1-U[b]
Normalization	No	No	No	No	No	No	No	Osmolality	No	No	SG	No
Phase II hydrolysis	No	No	Yes	No	No	No	No	No	No	No	No	No
Preparation technique	D	SPE	SPE	SPE	LLE	ST[c]	D	D	LLE	SPE	D	LLE
Solvent for dilution/extraction	n.a.	H_2O	PB	H_2O	MeOH/Hex	MeOH	n.a.	n.a.	THF/1-Hexanol	H_2O	n.a.	MeOH/Hex
Evaporated to dryness	No	Yes	Yes	Yes	No	Yes	No	No	Yes	Yes	No	No
Solvent for dilution/ reconstitution	MeOH/H_2O	MeOH/H_2O	MeOH/H_2O	ACN/H_2O	MeOH	MeOH/H_2O	MeOH	H_2O	MeOH	ACN/H_2O	ACN/H_2O	Hex
Sample volume change factor	0.25	0.5	6.67	5	4	1	0.33	0.25	5	5	0.1	4
Mass analyzer	Q-TOF	Orbitrap	Q-TOF	Orbitrap	Orbitrap	Orbitrap	Orbitrap	Orbitrap	Q-TOF	Orbitrap	Q-TOF	Orbitrap
Acquisition mode and polarity	Fast DDA ESI +/-	DDA ESI +/-	DDA ESI +/-	DDA ESI +/-	DDA ESI +/-	AIF ESI +/-	DDA ESI +/-	DDA ESI +/-	DIA ESI +/-	DDA ESI +/-	AIF ESI +/-	Full Scan EI + (70eV)
Chromatographic column	Waters Acquity HSS-T3	Kinetex Biphenyl	InfinityLab Poroshell 120 EC-C18	Waters Acquity HSS-T3	Waters Acquity Premier HSS-T3	COSMOSIL COSMOCORE 2.6PBr	Thermo Hypersil C18 Gold	Thermo Hypersyl C18	Waters BEH C18	Waters BEH amide	Merck SeQuant® ZIC®-pHILIC	Agilent DB-5MS Ultra Inert
Mobile phase or carrier Gas	(A) H_2O + 0.1 % (V/V) HCOOH (B) ACN	(A) H_2O + 0.1 % (V/V) HCOOH (B) MeOH + 0.1 % (V/V) HCOOH	ESI +: (A) H_2O + 0.1 % (V/V) HCOOH (B) MeOH + 0.1 % (V/V) HCOOH ESI -: (A) H_2O + 5 mM NH_4OAc (B) MeOH + 5 mM NH_4OAc	(A) ACN + 0.1% HCOOH (B) H_2O + 0.1% (V/V) HCOOH	(A) H_2O + 0.3mM NH_4F (B) ACN	(A) H_2O + 0.1% (V/V) HCOOH (B) MeOH + 0.1% (V/V) HCOOH	(A) H_2O + 0.1 % (V/V) HCOOH (B) ACN + 0.1 % (V/V) HCOOH	(A) H_2O/MeOH (95/5) + 0.1% (V/V) AcOH (B) MeOH + 0.1% (V/V) AcOH	(A) H_2O + 0.1% (V/V) HCOOH (B) ACN + 0.1% (V/V) HCOOH	(A) ACN (B)H_2O + 20 mM NH_4HCO_2+ 0.1% (V/V) HCOOH	(A) H_2O + 5 mM NH_4OAc + 0.04% (V/V) NH_4OH (B) ACN	Carrier Gas: Helium

2 ***RP-M****, reversed-phase liquid chromatography method;* ***HL-M****, hydrophilic interaction chromatography method;* ***GC-M****, gas chromatography method; suffix* ***-U****, urine;* ***SG****,*
3 Specific gravity; ***SPE****, solid-phase extraction;* ***LLE****, liquid-liquid extraction;* ***D****, Dilute-and-shoot;* ***ST****, Solvent transfer;* ***DIA****, data-independent acquisition;* ***AIF****, All ion*
4 *fragmentation;* ***DDA****, data-dependent acquisition;* ***EI****, Electron ionization;* ***ESI****, electrospray ionization;* ***H_2O****, water;* ***MeOH****, methanol;* ***ACN****, acetonitrile;* ***HCOOH****, formic acid;*
5 ***AcOH****, acetic acid;* ***NH_4OAc****, ammonium acetate;* ***NH_4F****, ammonium fluoride;* ***NH_4HCO2****, ammonium formate;* ***NH_4OH****, ammonium hydroxide;* ***THF****, tetrahydrofuran;* ***PB****,*
6 *phosphate buffer;* ***Hex****, Hexane;* ***n.a.****, not applied;* [a] *and* [b], method applied by the same partner; [c], ST *refers to protein precipitation followed by solvent evaporation and*

7 *reconstitution, rather than LLE. Urine was mixed with methanol to precipitate proteins, centrifuged, and the supernatant was evaporated and reconstituted in 66% methanol*
8 *prior to analysis. No immiscible phase separation is involved.*

Table 2: *Summary of analytical protocols used by participating laboratories for sample preparation and data acquisition applied to plasma samples.*

Methods	RP-M1-P	RP-M2-P	RP-M3-P	RP-M4-P[a]	RP-M5-P[b]	RP-M6-P	RP-M7-P	RP-M10-P	HL-M1-P[a]	GC-M1-P[b]
Phase II hydrolysis	No	No	Yes	No	No	No	No	No	No	No
Preparation technique	Lipid filtration (SPE)	Protein precipitation	Lipid filtration (SPE)	Protein precipitation	Protein precipitation (LLE)	Protein precipitation	Protein precipitation	Protein precipitation (LLE)	Protein precipitation	Protein precipitation (LLE)
Solvent for dilution/extraction	H_2O/MeOH	ACN	ACN	ACN	MeOH	MeOH	MeOH	MeOH	ACN	MeOH
Evaporated to dryness	Yes	Yes	Yes	Yes	No	No	Yes	No	Yes	No
Solvent for dilution/ reconstitution	ACN	MeOH/H_2O	MeOH	ACN/H_2O	MeOH	MeOH	MeOH/ ACN/H_2O	MeOH	ACN/H_2O	Hex
Sample volume change factor	0.66	3	5	0.75	4	0.33	0.33	0.25	0.75	4
Mass analyzer	Q-TOF	Orbitrap	Q-TOF	Orbitrap	Orbitrap	Orbitrap	Orbitrap	Orbitrap	Orbitrap	Orbitrap
Acquisition mode and polarity	Fast DDA ESI +/-	DDA ESI +/-	DDA ESI +/-	DDA ESI +/-	DDA ESI +/-	AIF ESI +/-	DDA ESI +/-	DDA ESI +/-	DDA ESI +/-	Full Scan EI + (70eV)
Chromatographic column	Waters Acquity HSS-T3	Kinetex Biphenyl	InfinityLab Poroshell 120 EC-C18	Waters Acquity HSS-T3	Waters Acquity Premier HSS-T3	COSMOSIL COSMOCORE 2.6PBr	Thermo Hypersil C18 Gold	Fortis SpeedCore C18	Waters BEH amide	Agilent DB-5MS Ultra Inert
Mobile phase or carrier Gas	(A) H_2O + 0.1 % (V/V) HCOOH (B) ACN	(A) H_2O + 0.1 % (V/V) HCOOH (B) MeOH + 0.1 % (V/V) HCOOH	ESI +: (A) H_2O + 0.1 % (V/V) HCOOH (B) MeOH + 0.1 (V/V) % HCOOH ESI -: (A) H_2O + 5 mM NH_4OAc (B) MeOH + 5 mM NH_4OAc	(A) ACN + 0.1% (V/V) HCOOH (B) H_2O + 0.1% (V/V) HCOOH	(A) H_2O + 0.3mM NH_4F (B) ACN	(A) H_2O + 0.1% (V/V) HCOOH (B) MeOH + 0.1% (V/V) HCOOH	(A) H_2O; + 0.1 % (V/V) HCOOH (B) ACN + 0.1 % (V/V) HCOOH	ESI +: (A) H_2O + 5 Mm NH_4HCO_2 (B) MeOH ESI -:(A) H_2O + 0.1% (V/V) HCOOH (B) MeOH	(A) ACN (B)H_2O + 20 mM NH_4HCO2 + 0.1% (V/V) HCOOH	Carrier Gas: Helium

RP-M*, reversed-phase liquid chromatography method;* ***HL-M****, hydrophilic interaction chromatography method;* ***GC-M****, gas chromatography method; suffix -****P****, plasma;* ***SPE****, solid-phase extraction;* ***LLE****, liquid-liquid extraction;* ***DIA,*** *data-independent acquisition;* ***AIF,*** *All ion fragmentation;* ***DDA,*** *data-dependent acquisition;* ***EI,*** *Electron ionization;* ***ESI,*** *electrospray ionization;* ***H_2O****, water;* ***MeOH****, methanol;* ***ACN****, acetonitrile;* ***HCOOH****, formic acid;* ***NH_4OAc****, ammonium acetate;* ***NH_4F****, ammonium fluoride;* ***NH_4HCO_2,*** *ammonium formate;* ***Hex****, Hexane;* [a] *and* [b], method applied by the same partner.

3.1.3 Comparing non-targeted screening workflows for perinatal chemical exposome analysis: a European interlaboratory study from the PARC EU project

Submitted: Moufawad, T., Ayeni, K., Baira, E., Baudry, C., Belova, L., Chaker, J., Chalet, C., Covaci, A., Damont, A., David, A., Fernandez, M.F., Habchi, B., Huber, C., Jadé, G., Kosjek, T., Krauss, M., Laurentie, M., Ndaw, S., Nijssen, R., Oberacher, H., Plešnik, H., Rekar, Ž., Rizzo, S., Salamanca-Fernandez, E., Termentzi, A., Vorkamp, K., Warth, B., Zhu, L., Kasiotis, K.M., Le Bizec, B., Lamoree, M., Antignac, J.-P., 2026

This paper contributes primarily to the QA/QC-oriented parts of the thesis by examining how established SS/NTS workflows perform across laboratories when applied to shared human biomonitoring samples from a perinatal exposure study. Conducted within the PARC framework, it involved 11 European laboratories applying in-house LC-HRMS and/or GC-HRMS workflows to common urine, serum, and maternal milk samples spiked with 50 compounds spanning a broad polarity range.

In contrast to the preceding interlaboratory paper, which focused mainly on chemical-space complementarity across platforms, this study addresses how methodological variability influences detection performance once such complementarity is acknowledged. A shared QA/QC concept was implemented through common spiking levels, standardized reporting, and S-score benchmarking, enabling structured comparison while preserving analytical diversity.

Within the thesis framework, the paper supports Hypothesis 3 from a different perspective: chromatographic selectivity defines accessible chemical space, but detection performance within that space is strongly influenced by sample preparation. For urine and serum, statistical analysis showed that extraction strategy, sample volume, and precipitation conditions affected detection rates more strongly than mass spectrometric platform alone. Procedural blank evaluation further demonstrated that background contamination can substantially affect apparent concentration–response behavior, emphasizing the importance of systematic blank control in comparative SS/NTS studies.

My contribution was the implementation of the HILIC-based LC-HRMS workflow at the JSI. In the context of the thesis, the paper shows that while HILIC remains necessary for highly polar compounds, broad chemical coverage alone is insufficient without transparent QA/QC design and control of interlaboratory variability.

Comparing Non-Targeted Screening Workflows for Perinatal Chemical Exposome Analysis: A European Interlaboratory Study from the PARC EU Project

Tarek Moufawad[1], Kolawole Ayeni[2], Eirini Baira[3], Christian Baudry[4], Lidia Belova[5], Jade Chaker[6], Clement Chalet[7], Adrian Covaci[5], Annelaure Damont[7], Arthur David[6], Mariana F. Fernandez[8,9], Baninia Habchi[10], Carolin Huber[11], Gaëlle Jadé[4], Tina Kosjek[12], Martin Krauss[11], Michel Laurentie[13], Sophie Ndaw[10], Rosalie Nijssen[14], Herbert Oberacher[15], Helena Plesnik[12], Zan Rekar[12], Serena Rizzo[14], Elena Salamanca-Fernandez[8,9], Aikaterini Termentzi[3], Katrin Vorkamp[16], Benedikt Warth[2,17], Linyan Zhu[16], Konstantinos M. Kasiotis[3], Bruno Le Bizec[1], Marja Lamoree[18], Jean-Philippe Antignac[1*]

[1,] Oniris, INRAE, LABERCA, Nantes, 44300, France

[2,] Department of Food Chemistry and Toxicology, Faculty of Chemistry, University of Vienna, Austria

[3,] Laboratory of Pesticides' Toxicology, Scientific Directorate of Pesticides' Control & Phytopharmacy, Benaki Phytopathological Institute, 145 61 Kifissia, Attica, Greece

[4,] Ploufragan-Plouzané-Niort Laboratory, Ruminant Diseases and Welfare Unit, French Agency for Food, Environmental and Occupational Health & Safety, 60 Rue Pied de Fond, 28440, 79024 Niort, CS, France

[5,] Toxicological Centre, University of Antwerp, Antwerp, Belgium

[6,] Univ Rennes, Inserm, EHESP, Irset (Institut de Recherche en Santé, Environnement et Travail), Rennes, NA, France

[7,] Université Paris-Saclay, CEA, INRAE, Département Médicaments et Technologies pour la Santé (DMTS), MetaboHUB, F-, France

[8,] Instituto de Investigación Biosanitaria de Granada (ibs.GRANADA), Granada, Spain

[9], CIBER de Epidemiología y Salud Pública (CIBERESP), Madrid, Spain.

[10,] Institut National de Recherche et de Sécurité (INRS), Vandoeuvre-lès-Nancy, France

[11,] Department Exposure Science, Helmholtz Centre for Environmental Research-UFZ, 04318 Leipzig, Germany

[12,] Jožef Stefan Institute, Department of Environmental Sciences, Jamova cesta 39, Ljubljana 1000, Slovenia

[13,] Statistical Analysis Platform, French Agency for Food, Environmental and Occupational Health & Safety, 10 Bis Rue Claude Bourgelat, 35306 Fougères LaboratoryFougères, France

[14,] Wageningen Food Safety Research (WFSR), Wageningen University & Research, Akkermaalsbos 2, 6708 WB, Wageningen, the Netherlands

[15,] Institute of Legal Medicine and Core Facility Metabolomics, Medical University of Innsbruck, 6020 Innsbruck, Austria

[16,] Department of Environmental Science, Aarhus University, Frederiksborgvej 399, 4000 Roskilde, Denmark

[17,] Exposome Austria, National Research Infrastructure and EIRENE-AT Node, Austria

[18,] Amsterdam Institute for Life and Environment (A-LIFE), Vrije Universiteit Amsterdam, De Boelelaan 1108, 1081 HZ Amsterdam, the Netherlands

Corresponding author:
jean-philippe.antignac@oniris-nantes.fr

Abstract
Early-life chemical exposures may contribute to adverse health outcomes later in life. However, conventional chemical analyses typically cover only a limited subset of the chemical exposome. Suspect and non-target screening (SS/NTS) using high-resolution mass spectrometry (HRMS) workflows provide a powerful framework for comprehensive assessments of exposure, with the potential to detect a broad range of environmental contaminants and emerging chemicals. An interlaboratory assay involving 12 laboratories was performed to evaluate SS/NTS approaches for maternal urine, serum, and milk, based on reversed phase (RPLC), hydrophilic interaction liquid chromatography (HILIC) and gas chromatography (GC) with HRMS. Participants used in-house methods to detect 50 compounds of varying polarity spiked at three concentrations. Detection rates ranged from 4% to 72%, with RPLC-HRMS for compounds with logP 0-6, while HILIC-HRMS and GC-HRMS extended coverage. Univariate and multivariable analyses of RPLC-HRMS results for serum and urine identified sample preparation steps as key factors influencing the detection rates. Workflow performances were additionally benchmarked using the S-score. These findings demonstrate the complementarity of SS/NTS platforms for extending chemical-space coverage for most comprehensive exposure characterisation. Therefore, efforts should be made for harmonized QA/QC provisions while conserving the added value of different workflows for exposure data for risk assessment.

Keywords: Chemical profiling, Exposure, Human biomonitoring, Human milk, Serum, Urine, PARC, High-resolution mass spectrometry

1. Introduction:

Human biomonitoring (HBM) programs face the challenge of thousands of chemicals that humans might be exposed to from a multitude of sources and typically exceeding the number of substances covered by conventional targeted analyses[1]. In recent years, suspect and non-targeted screening (SS/NTS) approaches, based on high-resolution mass spectrometry (HRMS), have emerged with the potential to expand the scope of HBM and to achieve a more comprehensive exploration of the human chemical exposome. These methodologies enable the detection, tentative identification, and relative quantification of a broad array of chemical exposure markers including not only known, but also previously unmonitored and unknown compounds as well as biotransformation products. Thus, SS/NTS results can contribute to the prioritization of chemicals for further target analysis, exposure assessment, toxicological evaluation and regulatory action, also in the context of early warning systems[2,3]. As such, SS/NTS provides a powerful complementary technique to established targeted analysis.

However, unlike target analysis for which harmonization has been achieved through decades of method development and rigorous quality assurance and control measures, in their current state of development in the HBM field, SS/NTS studies still suffer from a lack of comparability. Among other factors, this is related to attempts to extend the captured chemical space, resulting in several technical options regarding the sample preparation, data acquisition and data processing components [4–8]. Thus, different laboratories have developed in-house SS/NTS workflows that differ in sample preparation, instrument settings for data acquisition, and data processing. This lack of harmonization hampers the acceptance of SS/NTS results for risk assessments and regulatory purposes. Indeed, there are still no widely adopted guidelines for SS/NTS analysis, despite various initiatives and proposals in this field in the past decade[9–11]. While the regulatory need for high-quality, unambiguous and reproducible datasets is recognized, it can also be argued that methodological diversity enhances complementarity and broadens the coverage of the chemical space [1,5].

On one hand, there is a recognized regulatory need to obtain more comparable high-quality chemical exposure data from SS/NTS, which has prompted calls for more harmonized and QA/QC consolidated guidelines and analytical workflows. In response to regulatory needs for better comparability of SS/NTS results, the scientific community worldwide and European networks in particular[12,13], have initiated common protocols, guidelines and benchmarks for HRMS-based SS/NTS analyses, although more recently in the HBM field[9,13,14] than in the environmental field[15]. These harmonization initiatives, through the assessment of the analytical performances will likely reduce the variability across laboratories thanks to similar protocols for sample preparation, data acquisition and data processing[16–18]. However, standardization developments based on fixed technical parameters may also lead to restrictions in the accessible chemical space that a variety of analytical workflows would cover. Moreover, standardized approaches may impair the beneficial exploratory potential and technical development of SS/NTS in the context of this front-of-science area where new instrumental and data analysis options rapidly become available.

On the other hand, progressing towards harmonized procedures for assessing and transparently documenting the performance of individual SS/NTS methods certainly appears as an urgent need, as a basis for data interpretation and comparability. In that respect, interlaboratory trials and proficiency tests remain the gold standard to evaluate how different SS/NTS workflows affect results for identical samples. Such collaborative trials have already been executed in the environmental field[18,19], but still remain underdeveloped in the HBM field[1]. These limitations likely reflect both less structured collaborative networks and the inherent complexity of human biological matrices, including low

biomarker concentrations, limited sample volumes, differences in the distribution of parent compounds and metabolites across compartments, and lack of certified reference materials. A recent laboratory intercomparison under the auspices of the NORMAN network showed limited comparability for SS/NTS of fish samples, besides a relatively high risk of false negatives, i.e. no detection of compounds spiked to the samples[20].

The Horizon Europe Partnership for the Assessment of Risks from Chemicals (PARC) has brought together a large group of laboratories and research institutes in the fields of human biomonitoring, environmental and food monitoring. The objective of this study was to conduct an interlaboratory trial in the group of laboratories familiar with SS/NTS to assess the performance of various individual SS/NTS workflows applied to human matrices collected in the frame of a perinatal chemical exposure study. Twelve participant laboratories across Europe participated, each applying their in-house methods from sample preparation, LC-HRMS and/or GC-HRMS measurements to data analysis. The study focused on three matrices commonly used in HBM, urine, serum, and maternal milk. Specifically, the study aims were (i) based on identical samples, to assess and compare the analytical performances of diverse SS/NTS workflows applied by the participating laboratories, (ii) to explain the chemical space captured by each method as a basis for discussing data comparability, iii) to identify the most critical analytical parameters in the overall workflow that influence compound detection and annotation and (iv) to implement and discuss the newly introduce S-score.

2. Materials and Methods

2.1. Samples and experimental design

The biological samples supporting the present study were collected at the Hospital Universitario San Cecilio (HUSC) in Granada (Spain), between June and July 2023, when women came to the hospital to give birth. A total of 30 mother-newborn pairs were included. The inclusion criteria were: 1) women ≥18 years of age; 2) single full-term pregnancy (≥37 weeks), and 3) absence of relevant obstetric complications during both pregnancy and delivery. The study protocol was reviewed and approved by the Granada Research Ethics Committee (April 18, 2023, #0494-N-23), and all participants signed written informed consent prior to sample collection. Each woman provided a urine and blood (serum) sample prior to delivery, and maternal milk was collected at postpartum (several days after delivery when breastmilk was established). Biological samples were collected following a standardized protocol, processed, and aliquoted immediately after collection. All samples were irreversibly anonymized after completion of collection. Samples were then shipped to the coordinating laboratory (LABERCA, ONIRIS-INRAE, France) where individual samples of each type (urine, serum, and maternal milk) were pooled.

Each of these pools was then fortified with a mixture of 50 known selected chemicals at three concentration levels, with final concentrations in the matrix of 5, 20, and 100 $ng \cdot mL^{-1}$. These spiked samples served as positive controls, while non-fortified samples were used as negative controls. The 50 compounds represented a wide range of substance classes and physicochemical properties, including logP values from -4.47 to 10.18 and molecular weights from 111 to 702 $g \cdot mol^{-1}$. Consequently, their determination would likely require complementary analytical techniques, such as gas chromatography (GC), reversed phase liquid chromatography (RPLC) and hydrophilic interaction liquid chromatography (HILIC), combined with HRMS. These 50 exposure markers covered various substances classes and associated usages including phytosanitary products, cosmetics, plasticizers, etc. A detailed list of these markers, including identifiers and physicochemical properties, is provided in Table SI.1-a.

All participants received a solution of this mixture for reference. In addition, they received an aliquot of the NORMAN RTI Mix[20] (Table SI.2), and a mixture of *n*-Alkane compounds (C7–C30) (Table SI.3) to be used for retention time alignment and/or retention time index (RTI) calculations for LC- and GC-data, respectively. Two sets of labelled standards to be used as internal and external markers, respectively, to support quality assurance and data comparability were also provided to the participants (Table SI.1-b).

2.2. Participating laboratories and analytical platforms

A total of 12 laboratories (coded A-L) from 8 different European countries participated in the study (Fig. 1a). All participating laboratories had prior experience with SS/NTS approaches and were free to select which sample type(s) to analyse and to apply in-house methods and associated analytical platform for these analyses. The in-house methods included both sample preparation steps and data analytical workflows. An overview of the analyses performed by the different participants (sample type and instrumental platform) is shown in Figure 1b.

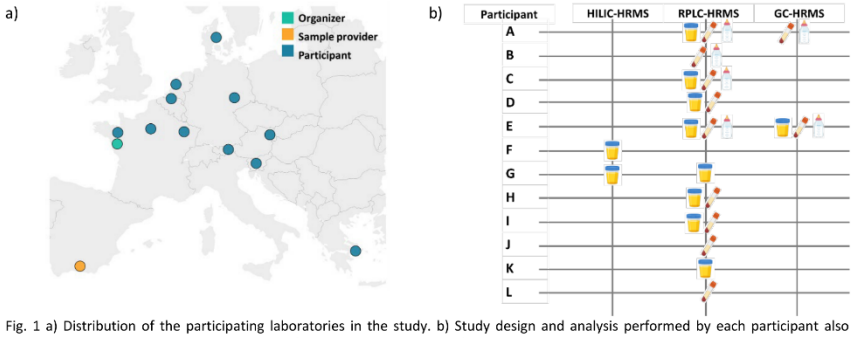


Fig. 1 a) Distribution of the participating laboratories in the study. b) Study design and analysis performed by each participant also indicating which type of matrix was analysed (urine, serum, human milk). HILIC: Hydrophilic interaction liquid chromatography. RPLC: Reserved phase liquid chromatography. GC: Gas chromatography. HRMS: High-resolution mass spectrometry.

2.3. Data reporting

Participants were requested to report their results using a template (Table SI.4) designed by the organisers to ensure harmonized reporting, and to facilitate data compilation and comparison. Reporting requirements included compound identifiers (Chemical Abstract Services (CAS) numbers, simplified molecular input line entry systems (SMILES), international chemical identifiers (InChIKey), retention times, *m/z* ratios and signal intensities at different spiking concentration levels, presence in procedural blanks, and identification confidence levels according to the scale of Schymanski et al.[21]. Experimental retention times observed for the reference NORMAN and *n*-Alkane mixtures were also reported. Moreover, detailed information on the individual methods for both sample preparation and data acquisition were collected from all participants (Table SI.5-SI.10).

2.4. Data assessment

To assess method performance and comparability across laboratories, detection rates for the different exposure markers detected with different analytical workflows were analysed. The chemical space coverage of the applied workflows (from sample preparation to data processing) was evaluated with regard to the logP and molecular weight values of the detected compounds. Furthermore, the detection of various chemical classes was compared between methods.

Statistical analysis included a combination of Chi-square tests and univariate and multivariate approaches with a significance level of 0.05. The tests used logistic regression models on experimental descriptors with the binary response variable corresponding to the detection of each compound (1 = detected, 0 = not detected) across all participants. Analyses were performed using R (version 4.5.0) and associated packages FactoMineR, broom, ggsignif, and rstatix.

2.5. S-score implementation

The S-score was developed for the evaluation of qualitative and binary detection outcomes[22]. For the application in this study, the 50 markers of the spiking mix were categorized as proficiency testing item class 3 (PTI3), i.e. considering of these markers as desirable, but not mandatory for detection. This strategy was adopted in line with the overall design of this study that considered complementarity of different analytical SS/NTS workflows and thus assumed that certain markers would remain undetected if only one method was applied. This case (a non-detection of a marker, or a subset of markers) would not lead to a "non-acceptable" or unsatisfactory result. Consequently, the S-scores will all indicate "acceptable" results but provide a ranking of results reflecting the capacity of each method to capture chemicals among the entire 50 markers list. The S-score was calculated for each participant, for each instrumental platform-matrix pair, and for each spiking level. A global S-score combining the results obtained for all spiking levels was also calculated for each participant.

3. Results and Discussion

3.1. Detection rates and chemical space coverages

The detection rates for the 50 spiked compounds in each matrix by each participant and by analytical platform are shown in Fig 2. The overall detection rates of the 50 markers ranged from 4% to 72% (mean 44%, median 46%). Across all matrices, the detection rate ranged between 4% to 36%, 32% to 72% and 14% to 56% for GC-HRMS, RPLC-HRMS and HILIC-HRMS based analyses, respectively. On average, laboratories reached about 50% detection with RPLC-HRMS platforms (Fig. 2), which is consistent with the high versatility of RPLC, as this platform is the most developed and widely applied one for SS/NTS[17]. The detection rates for HILIC- and GC- based systems were lower, reaching an average detection rate of about 35% for HILIC and 20% for GC. It is noteworthy that the majority of the 50 used markers is known to be amenable by RPLC. One participant (F) developed a high performance HILIC-HRMS approach on urine allowing the detection of 56% of the spiked compounds (Fig. 2a). Most of the compounds detected with this method had a retention time of 1-2 min, although this retention time window did not impair their identification.

The number of detected compounds slightly increased with the increasing spiking levels for both HILIC-HRMS, GC-HRMS and some RPLC-HRMS analyses. However, this effect was not observed consistently. It was most clearly observed for RPLC-HRMS analysis on serum (Fig. 2b), where the detection rates increased with higher spike concentrations for same participants, for example from 38 to 46 and 48 % for participant A. On the other hand, some participants (E, I and J) showed a consistently high detection rate independent of the fortification level, indicating high sensitivity and a broad chemical space even at a low spiking level (5 ng·mL^{-1}). The influence of the fortification level on the identification confidence of the detected compounds (ID) was found also generally low (Fig. SI1), although several compounds shifted to less certain IDs at the lowest concentration. For instance, participant C detected two compounds (acetaminophen, 2-hydroxyatrazine in urine) with an ID level of 1 at HL, that decreased to 2 at ML (20 ng·mL^{-1}). and LL (5 ng·mL^{-1}). This trend was observed across all matrices.

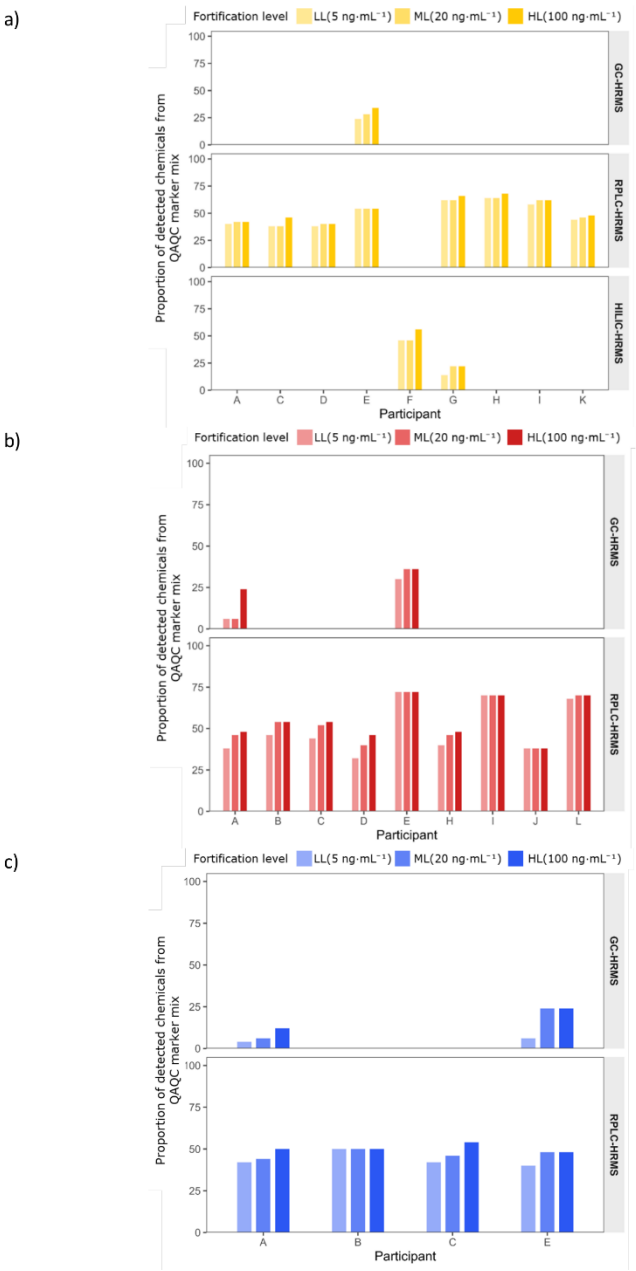


Fig. 2 Proportion of the 50 spiked compounds detected by the participants (A-L) in a) urine, b) serum and c) maternal milk. GC: Gas chromatography. RPLC: Reserved phase liquid chromatography. HILIC: Hydrophilic interaction liquid chromatography. HRMS: High-resolution mass spectrometry. LL: Low level. ML: Medium level. HL: High level.

The chemical space coverage represented by the 50 marker compounds shows that most laboratories achieved broad and consistent detection for compounds with intermediate lipophilicity (i.e., logP between 0 and 6), primarily through RPLC-HRMS workflows (Fig. 3; blue dots). This is in line with the well-established application range of RPLC-HRMS providing appropriate retention and ionization for polar to moderately hydrophobic small molecules, which makes it the default discovery platform in exposomics and metabolomics[23,24]. Consistent with its orthogonal selectivity, HILIC-HRMS (green dots) extends coverage towards more polar, low-logP analytes that are weakly retained or even unretained in RPLC. The combination of hydrophilic partitioning and surface adsorption in HILIC with common RPLC increases the number of detectable features compared with RPLC alone[25].

Interestingly, participant G conducted both RPLC-HRMS and HILIC-HRMS analysis on urine (Fig. 2a) and detected 11 compounds out of the 50 with HILIC-HRMS (22 %), while 33 compounds (66 %) were detected with RPLC-HRMS. Only 3 compounds were detected uniquely by HILIC-HRMS (malathion dicarboxylic acid, bisphenol S Bis-b-d-glucuronide and chlormequat chloride). These results highlight the importance of HILIC-HRMS for the detection of polar metabolites in HBM, as exogenous chemicals are frequently biotransformed to more polar molecules than the parent compounds[7,26].

At the opposite end of the lipophilicity range, GC-HRMS (pink dots) expanded the window toward more hydrophobic and volatile species, complementing LC-based methods which are less efficient for compounds with high logP. For example, participant E detected 27 compounds (54 %) and 17 compounds (34 %) in urine with RPLC- and GC-HRMS, respectively. Ten compounds (20 %) were detected only by GC-HRMS (hexachlorobiphenyl, benz(a)anthracene, benzo[a]pyrene, di(2-ethylhexyl) phthalate, dibutyl decanedioate, indeno[1,2,3-cd]pyrene,…), with seven (14 %) of the compounds detected by both ensuring a good overlap.

Recent reviews of human exposomics and multi-platform strategies consistently recommended pairing LC-HRMS with GC-HRMS to maximize chemical coverage [7,23,27]. The pattern across participants and matrices shows that multi-platform usage is complementary and expands the chemical space for detection: While RPLC-HRMS can provide a core of detections is in the mid-polarity region, HILIC-HRMS and GC-HRMS contribute with additional low and high logP markers, respectively. Furthermore, highly polar metabolites might require HILIC approaches, while omnipresent and hardly transformed persistent organic pollutants are best detected with GC techniques. This aligns with current best practice in exposomics, where complementary chromatographic modes are intentionally combined to broaden the accessible chemical space[7,23,27].

3.2. Comparison of detection performances

A chi-square test was applied to assess interlaboratory variability in detection performances. The analyses focused on RPLC-HRMS results, which had the highest statistical power because of the largest number of participating laboratories. Detection rates were not significantly influenced by the three fortification levels, as also indicated in Fig. 2. A global chi-square test was then performed to evaluate differences in detection rates between the workflows When significant differences were observed ($p < 0.05$), pairwise chi-square goodness-of-fit comparisons were conducted to identify specific pairs of participants exhibiting distinct detection profiles. As shown in Fig. SI.2, significant differences between participants were observed for RPLC-HRMS analysis of urine and serum (χ^2, $p < 0.05$). In contrast, no significant differences were observed for maternal milk, where the smallest p-value was 0.457.

In light of the statistical significance in the detection rates of the participants analysing urine and serum, associations between sample preparation, analytical method variables and the probability of

detection were investigated using univariate and multivariate analyses. In these analyses, macroscopic descriptors were assigned to each experimental and instrumental step. A summary of the applied analytical workflows for urine, serum, and maternal milk according to this categorized description is provided in Table SI.5-SI.10.

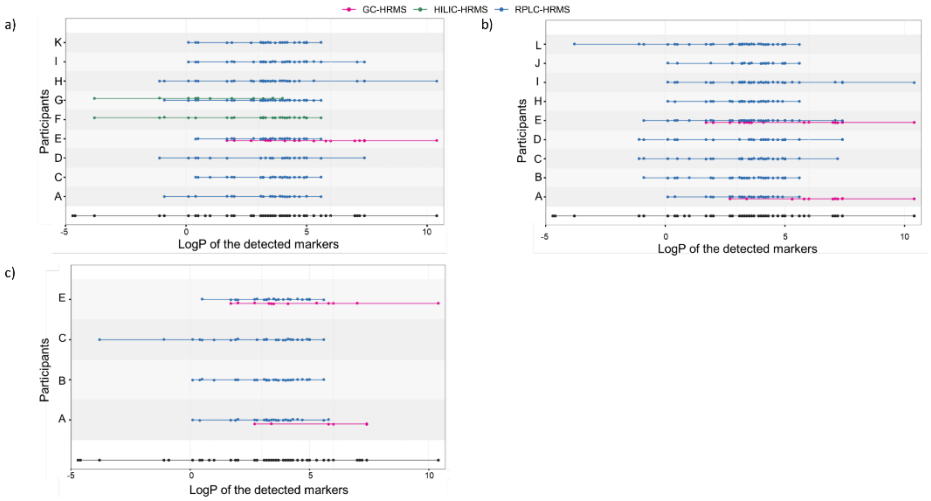


Fig. 3 Chemical coverage plot, expressed as logP (partitioning coefficient between octanol and water) of the spiked compounds detected in a) urine; b) serum and c) maternal milk by the participant (A-L) . GC: Gas chromatography. RPLC: Reserved phase liquid chromatography. HILIC: Hydrophilic interaction liquid chromatography. HRMS: High-resolution mass spectrometry. The black dots represent the 50 spiked compounds.

Serum analysis

Univariate logistic models were fitted for each macroscopic analytical descriptor with detection as the binary outcome and a randomly chosen reference level per descriptor, given the absence of a universal reference workflow. The results are summarized in Table SI.11 and Fig. 4. No effect of the fortification level was observed on the detection rate. The signal intensity and confidence level were not taken into consideration for these statistical analyses, only the overall number of the detected markers The result of no fortification effect is consistent with the previously performed Chi-square test.

Several parameters related to sample preparation steps were statistically associated with the detection rate. Notably, a sample volume of 150 or 500 µL was negatively associated with the detection rate compared to a 100 µL volume (β = -0.5579, p-value = 0.0041 and β = -0.3490, p-value = 0.0185 for 150 and 500 µl, respectively), whereas a sample volume of 200 and 240 µL showed a significant positive probability (β = 0.8155, p-value = 8.4×10^{-5} and β = 0.6766, p-value = 0.00084). Using acetonitrile rather than an acetonitrile/methanol mixture for protein precipitation improved detection (β = 0.8350, p-value = 1.2×10^{-5}), while methanol alone was not found to have significant effects compared to the acetonitrile/methanol mixture. Filtration of the final extract prior to the injection was associated with a modest increase in detection (β = 0.1860, p-value = 0.0342).

Among instrumental parameters, Time-of-Flight (TOF) analyser exhibited lower odds of detection than Orbitrap instruments (β = -0.8111, p-value = 6.6×10^{-12}). Within column types, Poroshell 120 was associated with a reduced detection relative to Acquity BEH (β = -0.5101, p-value = 0.0152), and Kinetex Biphenyl with a positive effect (β = -0.5160, p-value = 0.0190), while other columns did not differ significantly in terms of captured chemicals. No differences in the detection rates were associated with the type of organic solvent used in the mobile phase. However, the use of mobile phase additives, either acid/salt or salt alone, increased the detection compared with acid only (β = 0.3440 and 0.3780, both p-value = 0.027, respectively). These results indicate that choices in sample volume, protein precipitation solvent, filtration, MS technology, column chemistry, and modifier composition can influence the probability of detection when considered separately.

Subsequently, a multivariable logistic regression model was fitted regrouping the experimental descriptors shown to significantly influence detection in the univariate logistic models (i.e. sample volume, protein precipitation solvent, filtration, MS technology, column type, and mobile phase modifier). In this aggregated model, a 500 µL sample volume was confirmed to be associated with reduced odds of detection relative to the other sample volume (β = -0.708, p-value = 0.043) whereas acetonitrile as the protein precipitation solvent was confirmed with increased detection odds relative to the reference mixture of acetonitrile/methanol (β = 0.827, p-value = 0.0180). Filtration, MS technology, column type and modifier composition were not statistically significant in these analyses. It is important to note that some parameter combinations did not present estimable coefficients due to insufficient statistical power (Table SI.12).

Fig. 5 shows a heat map in which participants are clustered according to their detection profile, without considering the experimental workflow applied. Three clusters can be observed of participants A and H, E-I and L, as well as C and D with highly similar detection profiles. More precisely, participants A and H display identical detection patterns sharing several analytical parameters including the same sample volume (500 µL), the same protein precipitation solvent (acetonitrile), and the same MS technology (Orbitrap), while differing only in the type of HPLC column. A similar concordance is observed for E, I and L, which share the same protein precipitation solvent and MS technology and used comparable sample volumes. Participants C and D also cluster together; both used a sample volume of 100 µL and methanol as protein precipitation solvent, while differing in MS technology and column. The

participant J was the only participant using a mixture of solvents for protein precipitation, not leading to clusters with any other participant. Taken together, these unsupervised groupings are consistent with the univariate and multivariable results, which identified sample volume and precipitation solvent as key determinants of detection outcomes. Based on these results, central steps in the sample preparation thus have a larger influence on compound detection in serum samples than the instrumental parameters.

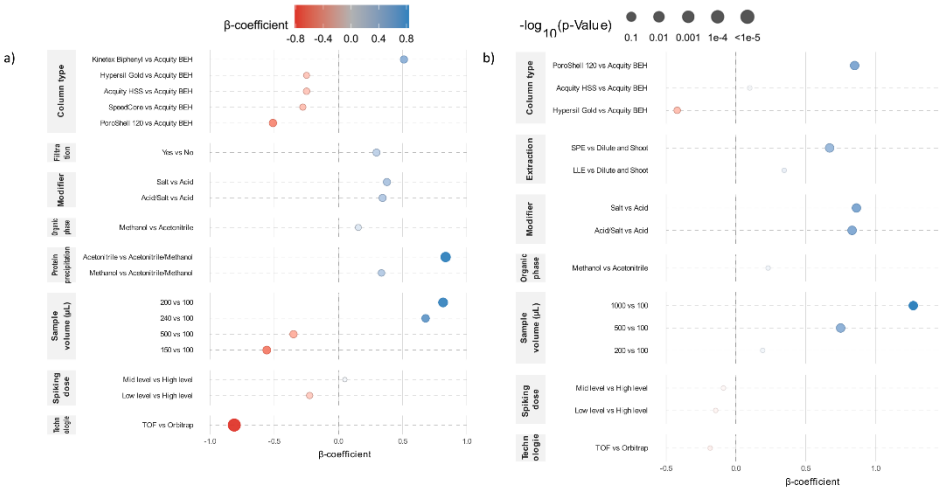


Fig. 4 Logistic univariate regression parameters linking the detection rate with individual analytical method descriptors. The figure shows the associated β-coefficient and p-values, for a) serum and b) urine analysis using RPLC-HRMS. RPLC: Reserved phase liquid chromatography. HRMS: High-resolution mass spectrometry

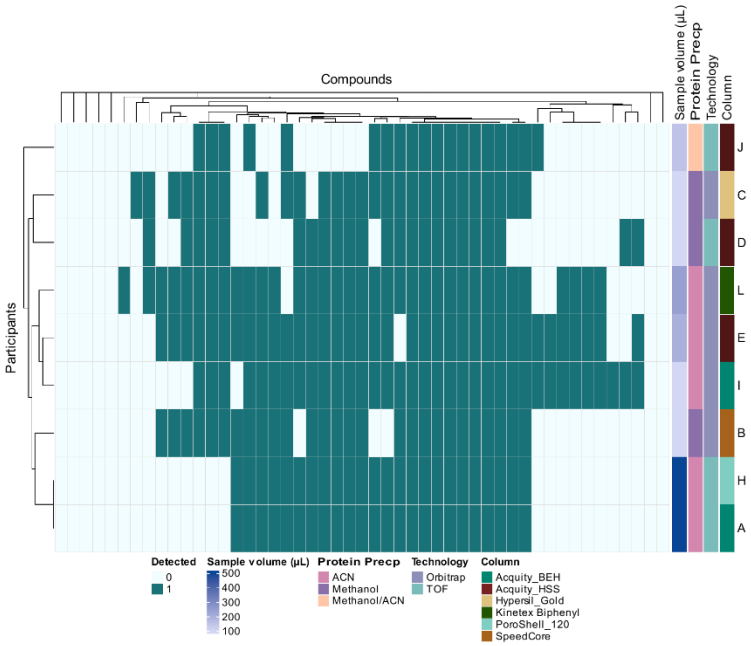


Fig. 5 Heatmap clustering of the detected compounds among the 50 markers mix (0, not detected; 1, detected) in serum via RPLC-HRMS by all the participants (A-L) and the associated analytical method descriptors. ACN: Acetonitrile. TOF: Time-of-Flight. RPLC: Reserved phase liquid chromatography. HRMS: High-resolution mass spectrometry

Urine analysis

Regarding the urine sample preparation steps, larger (500 or 1000 µL) sample volumes appeared to improve detection rates ($\beta = 0.7500$, p-value = 0.0002 and $\beta = 1.2700$, p-value = 8.2×10^{-7} for 500 and 1000 µL, respectively), whereas 200 µL did not show significantly different results from 100 µL (p-value = 0.3462) (Table SI.13 and Fig. 4). Compared with dilute and shoot approaches, solid phase extraction (SPE) was associated with a significant increase in detection rates ($\beta = 0.6710$, p-value = 0.00048), while liquid-liquid extraction (LLE) showed no significant effect (p-value = 0.1053).

Regarding data acquisition, neither of the employed MS technologies showed a significant effect on the detection (p-value = 0.1440). Within column types, Hypersil Gold and PoroShell 120 were associated with a lower and higher detection rate, respectively, relative to Acquity BEH ($\beta = -0.4203$, p-value = 0.0370 and $\beta = 0.8502$, p-value = 6.6×10^{-5} for Hypersil Gold and PoroShell 120, respectively), whereas Acquity HSS did not differ significantly. The mobile phase solvent was not found clearly significant (p-value = 0.059). In contrast, the use of salt or both acid as modifiers in the RPLC mobile phase appeared to increase detection compared with acid only, ($\beta = 0.8630$ and 0.8320, p-values = 8.2×10^{-8} and 7.0×10^{-9}, respectively).

Overall, these results indicate that larger samples volumes, SPE, specific column characteristics, and the addition of salt in the mobile phase are associated with improved detection of the 50 markers in urine when each factor is considered independently. In a multivariable logistic regression with only these statistically significant descriptors (sample volume, type of extraction, column and modifier

type), the use of salt in the mobile phase did not show a statistically significant effect on the detection rate, while the high sample volume, the LLE and the Acquity HSS column were associated with a higher detection rate. Thus, the multivariate analysis modified some of the conclusions from univariate analyses (Table SI.14). Compared with the serum analyses, sample volume was confirmed as an influential parameter, while instrumental parameters, in terms of column type, were only significant for the urine analyses.

In the heat map clustering similar detection profiles between the participants (Fig. 6), two main clusters appeared, including participants I, G and K, and participants A, C and E, respectively. Within the first cluster, the participants shared the same sample volume, extraction process and MS technology. Within the second cluster, participants used similar sample volumes (100 and 200 µL) and applied either dilute-and-shoot injection or LLE. Although the three participants in this second block used different instrument types and columns, these factors did not appear to drive the clustering. Participant D, despite using a sample volume comparable to the second group, applied SPE clean-up which may account for the distinct detection profile. Participant H shows a profile close to the first group, sharing the same extraction approach, but it was the only laboratory using a sample volume of 1000 µL, a descriptor that showed strong statistical significance. Overall, this aggregated clustering is consistent with the statical findings, indicating that sample volume and extraction strategy are the primary drivers of similarity in urine detection profiles, whereas instrument technology and column selection played a minor role.

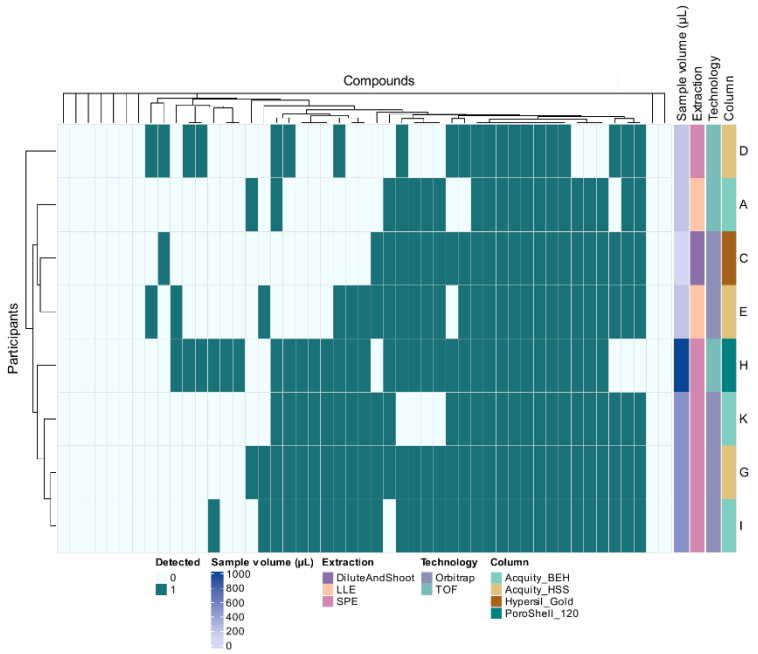


Fig. 6 Heatmap clustering of detected compounds among the 50 markers mix (0, not detected; 1, detected) in urine via RPLC-HRMS by all the participants (A-K) and the associated analytical method descriptors. LLE: Liquid-liquid extraction. SPE: Solid phase extraction. TOF: Time-of-Flight. RPLC: Reserved phase liquid chromatography. HRMS: High-resolution mass spectrometry

Overall, the main factors influencing the detection rates of the 50 markers in both serum and urine was sample preparation, whereas chromatographic conditions, instrument type and mobile phase solvent had comparatively minor influence. Importantly, the statistical analysis focused on RPLC results and did not include detections from GC or HILIC-HRMS platforms. However, sample preparation steps are typically determined by the sample matrix and the intended chromatographical platform (GC or LC). For example, participants A and E applied sample preparation protocols leading to two separate extracts to be analysed by RPLC and GC-HRMS analysis, and participant G prepared urine for both HILIC and RPLC-HRMS (Fig. 1b). These optimized steps might include salt and electrolyte reduction benefit HILIC-HRMS[28], and lipid removal prior to GC-HRMS analyses[29,30]. This treatment could result in a lower detection rate in RPLC, while yielding to a more robust results for HILIC[31] and GC-HRMS[32]. When each platform is evaluated independently, this may appear as a decrease in detection rate, however aggregating the datasets from the different platforms may result in an overall increase of chemical-space coverage and higher detection rate [33].

3.3. External contaminations and negative control samples (blank) management issues

Inclusion, analysis and management of procedural and field blank samples are pivotal in both targeted and SS/NTS workflows. The extent of the chemical space potentially captured by SS/NTS however make this issue even more prominent. Several studies have reported a high number of detected peaks in blanks[34,35], and recently, Krauss *et al.* investigated the origin of background contamination arising from medical grade sample tubes, as well as the impact of cleaning procedures on both the number and signal intensities of background contaminants[36]. In the present study, the participants were invited to also report results of procedural blanks. A systematic contamination was observed by almost for some phthalates (mono-2-ethylhexyl phthalate, di(2-ethylhexyl) phthalate, and bis(2-ethylhexyl) terephthalate), parabens (butylparaben), and pesticides (N,N-Diethyl-meta-toluamide (DEET) and fipronil). A procedural blank contamination for the four perfluoroalkyl substances (PFAS) included in the set of markers (perfluorononanoic acid, perfluorohexanesulfonic acid, perfluorooctanesulfonic acid and perfluorooctanoic acid) was reported by four participants across the three matrices.

Beside the risk of false positive results, blank contamination can also impair semi-quantitative interpretation of the results by affecting the spike concentration and peak intensity relationship for the corresponding detected signal. Table 1 illustrates this issue for the two markers butylparaben and acetaminophen detected across the different matrices and in the procedural blanks. For butylparaben in urine, participants D, G, H and I showed high coefficients of determination between the three fortification levels, although H reported blank contamination. However, for participant C, no dose-signal intensity correlation ($R^2 = 0.18$) was observed due to a significant contamination observed in the procedural blanks. Likewise, participant D found no dose-signal intensity relationship for acetaminophen in urine as the marker was also present in the procedural blank ($R^2 = 0.09$), but a strong dose-signal intensity in serum when no blank contamination was observed ($R^2 = 0.99$). This issue of contamination and its heterogeneity across matrices and compounds underscores the need for rigorous blank characterisation that could have a significant impact on results especially when using them in a semi-quantitative approach. Similar observations were made by Hernandes *et al.* where background contamination resulted in high variability in concentrations of the detected compounds in dried blood spots, leading to a low confidence in the quantification of the compounds found in the background contamination [37].

Table 1. Detection of butylparaben and acetaminophen in procedural blanks analysed together with the samples of this study and coefficients of determination for the resulting dose-signal intensity relationship (R^2). LL: Low level. ML: Medium level. HL: High level. These terms reflect the different spike concentrations.

Matrix	Marker	Participant	Detection in procedural blank	R^2 of the dose-signal intensity curve (LL, ML, HL)
Urine	Butylparaben	C	Yes	0.18
		D	No	0.99
		I	No	0.99
		H	Yes	0.99
		G	No	0.99
	Acetaminophen	K	No	0.99
		D	Yes	0.09
		I	No	0.99
Serum	Butylparaben	D	No	0.99
		E	No	0.99
		C	Yes	0.73
	Acetaminophen	B	No	0.99
		D	No	0.99
		E	Yes	0.97
Maternal Milk	Butylparaben	C	Yes	0.80
		B	No	0.94
		E	No	0.95
	Acetaminophen	B	No	0.96
		E	No	0.97

3.4. Global performance assessment using S-scores

Fig. 7 summarizes the calculated S-scores by matrix, analytical platform, and fortification level. Based on this scoring approach, participants using RPLC-HRMS exhibited the strongest overall performance, with most S-scores remaining below 2.7 across matrices and fortification levels, indicating a satisfying basis of detection even in complex human matrices and at low fortification level. The values of the S-score are regrouped in the Table SI15. Notably, participant F, who applied a HILIC workflow optimized for urine samples obtained S-scores comparable to those of RPLC users. A dose to detection rate effect on the detection rate was observed in most cases, with median S-scores decreasing from low to high spiking levels, reflecting improved detection at higher concentration for some participants (Fig. 2). Nevertheless, several participants exhibited little or no dose effect on the detection rate, indicating high sensitivity and stable performance of RPLC analyses even at the lowest spiking level. The S-score flexibility and adaptability to case-specific study requirements represents additional strengths for SS/NTS studies with binary detect/non-detect outcomes supporting its implementation in both research and regulatory settings.

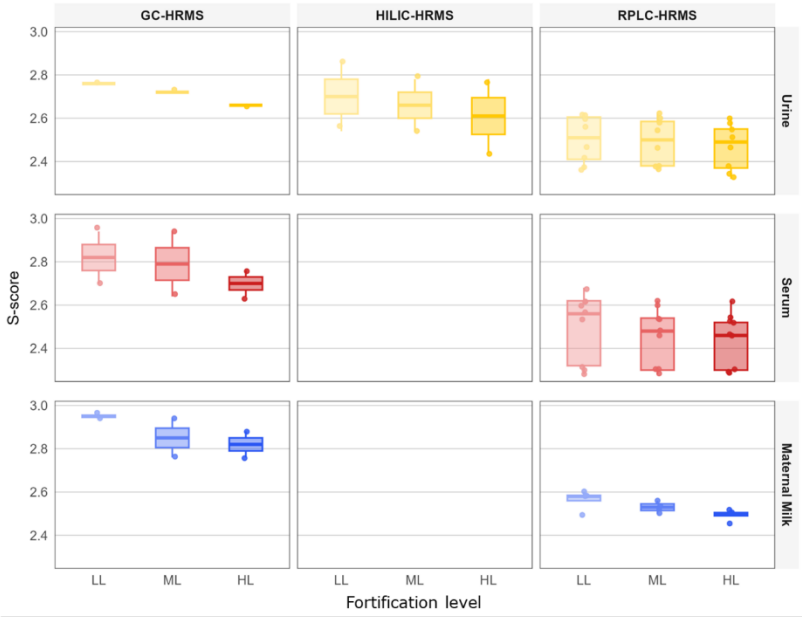


Fig. 7 S-Scores calculated for the different participants at the three fortification levels in the three matrices. GC: Gas chromatography. RPLC: Reserved phase liquid chromatography. HILIC: Hydrophilic interaction liquid chromatography. HRMS: High-resolution mass spectrometry. LL: Low level. ML: Medium level. HL: High level. Serum and maternal milk were not analysed with HILIC-HRMS.

Conclusions

An interlaboratory assay was conducted to assess and compare the results of various SS/NTS methods applied by 12 European participants to maternal human urine, blood and milk samples. The assay included 50 exposure markers embracing a range of substance classes and physicochemical properties to be detected at three concentration levels (5, 20, and 100 $ng \cdot mL^{-1}$).

Overall, the results demonstrated that RPLC-HRMS based workflows capture the core set of the tested exposures markers (32% to 72% %) across biological matrices, primarily covering compounds with logP values between 0 and 6. HILIC-HRMS and GC-HRMS extended the detectable chemical space toward the lower and higher logP regions, respectively. Univariate and multivariate statistical analyses, together with global clustering of participant detection profiles, were subsequently applied and enabled the identification of key workflow parameters influencing compound detection by RPLC-HRMS. Procedural blank analyses revealed a shared environmental background across participants, particularly for selected phthalates and parabens, with implications for the linearity of the dose–signal intensity relationship. Finally, the S-score framework was implemented to benchmark the performance of the applied SS/NTS workflows in a rapid, harmonized, and comparable manner. Taken together, the results of this study support a complementary multi-platform strategy as best practice for suspect and non-targeted screening analyses with the objective of expanding characterisation of the chemical exposome.

This work provides a proof-of-concept illustrating how collaborative initiatives can advance insights into the applicability of SS/NTS for human internal exposure assessment with strong potential for application in HBM programs. Conducted within the PARC-EU project[38], the study addresses a pressing

need in regulatory science for robust, comparable data on human chemical exposure, while using the advantages of comprehensive SS/NTS approaches. The insights gained into critical steps and inter-laboratory variability can support the development of protocols optimized for different matrices and analytical platforms. Ultimately, establishing, harmonized high-quality insurance and inter-comparable SS/NTS results will support the generation of comparable and complimentary exposure data across countries and the integration of SS/NTS techniques into chemical risk assessment and management.

4. Abbreviations

Acetonitrile	ACN
Chemical Abstract Services	CAS
Gas Chromatography	GC
High Level	HL
High-Resolution Mass Spectrometry	HRMS
Human Biomonitoring	HBM
Hydrophilic Interaction Liquid Chromatography	HILIC
International Chemical Identifiers	InChIKey
Liquid-Liquid Extraction	LLE
Low Level	LL
Medium Level	ML
N,N-Diethyl-Meta-Toluamide	DEET
Partnership For The Assessment Of Risks From Chemicals	PARC
Perfluoroalkyl Substances	PFAS
Proficiency Testing Item Class 3	PTI3
Retention Time Index	RTI
Reversed Phase Liquid Chromatography	RPLC
Simplified Molecular Input Line Entry Systems	SMILES
Solid Phase Extraction	SPE
Suspect And Non-Target Screening	SS/NTS
Time-Of-Flight	TOF

5. Acknowledgments

This work was carried out in the framework of the European Partnership for the Assessment of Risks from Chemicals (PARC) and has received funding from the European Union's Horizon Europe research and innovation programme under Grant Agreement No 101057014. Views and opinions expressed are, however, those of the author(s) only and do not necessarily reflect those of the European Union or the Health and Digital Executive Agency. Neither the European Union nor the granting authority can be held responsible for them. The authors gratefully acknowledge UGR partners for providing the biological matrices used in this study.

6. References

(1) Pourchet, M.; Debrauwer, L.; Klanova, J.; Price, E. J.; Covaci, A.; Caballero-Casero, N.; Oberacher, H.; Lamoree, M.; Damont, A.; Fenaille, F.; Vlaanderen, J.; Meijer, J.; Krauss, M.; Sarigiannis, D.; Barouki, R.; Le Bizec, B.; Antignac, J.-P. Suspect and Non-Targeted Screening of

Chemicals of Emerging Concern for Human Biomonitoring, Environmental Health Studies and Support to Risk Assessment: From Promises to Challenges and Harmonisation Issues. *Environ. Int.* **2020**, *139*, 105545. https://doi.org/10.1016/j.envint.2020.105545.

(2) Meijer, J.; Lamoree, M.; Hamers, T.; Antignac, J.-P.; Hutinet, S.; Debrauwer, L.; Covaci, A.; Huber, C.; Krauss, M.; Walker, D. I.; Schymanski, E. L.; Vermeulen, R.; Vlaanderen, J. An Annotation Database for Chemicals of Emerging Concern in Exposome Research. *Environ. Int.* **2021**, *152*, 106511. https://doi.org/10.1016/j.envint.2021.106511.

(3) Vermeulen, R.; Schymanski, E. L.; Barabási, A.-L.; Miller, G. W. The Exposome and Health: Where Chemistry Meets Biology. *Science* **2020**, *367* (6476), 392–396. https://doi.org/10.1126/science.aay3164.

(4) Chaker, J.; Kristensen, D. M.; Halldorsson, T. I.; Olsen, S. F.; Monfort, C.; Chevrier, C.; Jégou, B.; David, A. Comprehensive Evaluation of Blood Plasma and Serum Sample Preparations for HRMS-Based Chemical Exposomics: Overlaps and Specificities. *Anal. Chem.* **2022**, *94* (2), 866–874. https://doi.org/10.1021/acs.analchem.1c03638.

(5) Chaker, J.; Gorrochategui Matas, E.; Chevrier, C.; Campone, M.; Frenel, J.-S.; Bigot, F.; Bessonneau, V.; David, A. Blood Sample Preparation for Human Chemical Exposomics: Insights from Large-Scale Applications. *Environ. Sci. Technol.* **2025**, *59* (40), 21421–21430. https://doi.org/10.1021/acs.est.5c01686.

(6) Gu, Y.; Peach, J. T.; Warth, B. Sample Preparation Strategies for Mass Spectrometry Analysis in Human Exposome Research: Current Status and Future Perspectives. *TrAC Trends Anal. Chem.* **2023**, *166*, 117151. https://doi.org/10.1016/j.trac.2023.117151.

(7) Vitale, C. M.; Price, E. J.; Miller, G. W.; David, A.; Antignac, J.-P.; Barouki, R.; Klánová, J. Analytical Strategies for Chemical Exposomics: Exploring Limits and Feasibility. *Exposome* **2021**, osab003. https://doi.org/10.1093/exposome/osab003.

(8) Gu, Y.; Feuerstein, M. L.; Warth, B. High-Throughput Solid Phase Extraction for Targeted and Nontargeted Exposomics. *Anal. Chem.* **2025**, *97* (11), 6075–6082. https://doi.org/10.1021/acs.analchem.4c06177.

(9) Caballero-Casero, N.; Belova, L.; Vervliet, P.; Antignac, J.-P.; Castaño, A.; Debrauwer, L.; López, M. E.; Huber, C.; Klanova, J.; Krauss, M.; Lommen, A.; Mol, H. G. J.; Oberacher, H.; Pardo, O.; Price, E. J.; Reinstadler, V.; Vitale, C. M.; van Nuijs, A. L. N.; Covaci, A. Towards Harmonised Criteria in Quality Assurance and Quality Control of Suspect and Non-Target LC-HRMS Analytical Workflows for Screening of Emerging Contaminants in Human Biomonitoring. *TrAC Trends Anal. Chem.* **2021**, *136*, 116201. https://doi.org/10.1016/j.trac.2021.116201.

(10) Place, B. J.; Ulrich, E. M.; Challis, J. K.; Chao, A.; Du, B.; Favela, K.; Feng, Y.-L.; Fisher, C. M.; Gardinali, P.; Hood, A.; Knolhoff, A. M.; McEachran, A. D.; Nason, S. L.; Newton, S. R.; Ng, B.; Nuñez, J.; Peter, K. T.; Phillips, A. L.; Quinete, N.; Renslow, R.; Sobus, J. R.; Sussman, E. M.; Warth, B.; Wickramasekara, S.; Williams, A. J. An Introduction to the Benchmarking and Publications for Non-Targeted Analysis Working Group. *Anal. Chem.* **2021**, *93* (49), 16289–16296. https://doi.org/10.1021/acs.analchem.1c02660.

(11) Peter, K. T.; Phillips, A. L.; Knolhoff, A. M.; Gardinali, P. R.; Manzano, C. A.; Miller, K. E.; Pristner, M.; Sabourin, L.; Sumarah, M. W.; Warth, B.; Sobus, J. R. Nontargeted Analysis Study Reporting Tool: A Framework to Improve Research Transparency and Reproducibility. *Anal. Chem.* **2021**, *93* (41), 13870–13879. https://doi.org/10.1021/acs.analchem.1c02621.

(12) Hollender, J.; van Bavel, B.; Dulio, V.; Farmen, E.; Furtmann, K.; Koschorreck, J.; Kunkel, U.; Krauss, M.; Munthe, J.; Schlabach, M.; Slobodnik, J.; Stroomberg, G.; Ternes, T.; Thomaidis, N. S.; Togola, A.; Tornero, V. High Resolution Mass Spectrometry-Based Non-Target Screening Can Support Regulatory Environmental Monitoring and Chemicals Management. *Environ. Sci. Eur.* **2019**, *31* (1), 42. https://doi.org/10.1186/s12302-019-0225-x.

(13) Oberacher, H.; Sasse, M.; Antignac, J.-P.; Guitton, Y.; Debrauwer, L.; Jamin, E. L.; Schulze, T.; Krauss, M.; Covaci, A.; Caballero-Casero, N.; Rousseau, K.; Damont, A.; Fenaille, F.; Lamoree, M.; Schymanski, E. L. A European Proposal for Quality Control and Quality Assurance of Tandem

Mass Spectral Libraries. *Environ. Sci. Eur.* **2020**, *32* (1), 43. https://doi.org/10.1186/s12302-020-00314-9.

(14) Vitale, C. M.; Lommen, A.; Huber, C.; Wagner, K.; Garlito Molina, B.; Nijssen, R.; Price, E. J.; Blokland, M.; Van Tricht, F.; Mol, H. G. J.; Krauss, M.; Debrauwer, L.; Pardo, O.; Leon, N.; Klanova, J.; Antignac, J.-P. Harmonized Quality Assurance/Quality Control Provisions for Nontargeted Measurement of Urinary Pesticide Biomarkers in the HBM4EU Multisite SPECIMEn Study. *Anal. Chem.* **2022**, *94* (22), 7833–7843. https://doi.org/10.1021/acs.analchem.2c00061.

(15) Hollender, J.; Schymanski, E. L.; Ahrens, L.; Alygizakis, N.; Béen, F.; Bijlsma, L.; Brunner, A. M.; Celma, A.; Fildier, A.; Fu, Q.; Gago-Ferrero, P.; Gil-Solsona, R.; Haglund, P.; Hansen, M.; Kaserzon, S.; Kruve, A.; Lamoree, M.; Margoum, C.; Meijer, J.; Merel, S.; Rauert, C.; Rostkowski, P.; Samanipour, S.; Schulze, B.; Schulze, T.; Singh, R. R.; Slobodnik, J.; Steininger-Mairinger, T.; Thomaidis, N. S.; Togola, A.; Vorkamp, K.; Vulliet, E.; Zhu, L.; Krauss, M. NORMAN Guidance on Suspect and Non-Target Screening in Environmental Monitoring. *Environ. Sci. Eur.* **2023**, *35* (1), 75. https://doi.org/10.1186/s12302-023-00779-4.

(16) Haglund, P.; Alygizakis, N. A.; Covaci, A.; Melymuk, L.; Nizzetto, P. B.; Rostkowski, P.; Albinet, A.; Alirai, S.; Aurich, D.; Bieber, S.; Ballesteros-Gómez, A.; Brennan, A. A.; Budzinski, H.; Castro, G.; den Ouden, F.; Dévier, M.-H.; Dulio, V.; Feng, Y.-L.; Gabriel, M.; Gallampois, C.; García-Vara, M.; Giovanoulis, G.; Harrad, S.; Jacobs, G.; Jobst, K. J.; Kaserzon, S.; Kumirska, J.; Lestremau, F.; Lambropoulou, D.; Letzel, T.; de Alda, M. L.; Nipen, M.; Oswald, P.; Poma, G.; Přibylová, P.; Price, E. J.; Raffy, G.; Schulze, B.; Schymanski, E. L.; Šenk, P.; Wei, S.; Slobodnik, J.; Andújar, B. T.; Täubel, M.; Thomaidis, N. S.; Wang, T.; Wang, X. Comprehensive Characterization of European House Dust Contaminants: Concentrations and Profiles, Geographical Variability, and Implications for Chemical Regulation and Health Risk. *Sci. Total Environ.* **2024**, *957*, 177639. https://doi.org/10.1016/j.scitotenv.2024.177639.

(17) Malm, L.; Liigand, J.; Aalizadeh, R.; Alygizakis, N.; Ng, K.; Frokjær, E. E.; Nanusha, M. Y.; Hansen, M.; Plassmann, M.; Bieber, S.; Letzel, T.; Balest, L.; Abis, P. P.; Mazzetti, M.; Kasprzyk-Hordern, B.; Ceolotto, N.; Kumari, S.; Hann, S.; Kochmann, S.; Steininger-Mairinger, T.; Soulier, C.; Mascolo, G.; Murgolo, S.; Garcia-Vara, M.; López De Alda, M.; Hollender, J.; Arturi, K.; Coppola, G.; Peruzzo, M.; Joerss, H.; Van Der Neut-Marchand, C.; Pieke, E. N.; Gago-Ferrero, P.; Gil-Solsona, R.; Licul-Kucera, V.; Roscioli, C.; Valsecchi, S.; Luckute, A.; Christensen, J. H.; Tisler, S.; Vughs, D.; Meekel, N.; Talavera Andújar, B.; Aurich, D.; Schymanski, E. L.; Frigerio, G.; Macherius, A.; Kunkel, U.; Bader, T.; Rostkowski, P.; Gundersen, H.; Valdecanas, B.; Davis, W. C.; Schulze, B.; Kaserzon, S.; Pijnappels, M.; Esperanza, M.; Fildier, A.; Vulliet, E.; Wiest, L.; Covaci, A.; Macan Schönleben, A.; Belova, L.; Celma, A.; Bijlsma, L.; Caupos, E.; Mebold, E.; Le Roux, J.; Troia, E.; De Rijke, E.; Helmus, R.; Leroy, G.; Haelewyck, N.; Chrastina, D.; Verwoert, M.; Thomaidis, N. S.; Kruve, A. Quantification Approaches in Non-Target LC/ESI/HRMS Analysis: An Interlaboratory Comparison. *Anal. Chem.* **2024**, *96* (41), 16215–16226. https://doi.org/10.1021/acs.analchem.4c02902.

(18) Dürig, W.; Lindblad, S.; Golovko, O.; Gkotsis, G.; Aalizadeh, R.; Nika, M.-C.; Thomaidis, N.; Alygizakis, N. A.; Plassmann, M.; Haglund, P.; Fu, Q.; Hollender, J.; Chaker, J.; David, A.; Kunkel, U.; Macherius, A.; Belova, L.; Poma, G.; Preud'Homme, H.; Munschy, C.; Aminot, Y.; Jaeger, C.; Lisec, J.; Hansen, M.; Vorkamp, K.; Zhu, L.; Cappelli, F.; Roscioli, C.; Valsecchi, S.; Bagnati, R.; González, B.; Prieto, A.; Zuloaga, O.; Gil-Solsona, R.; Gago-Ferrero, P.; Rodriguez-Mozaz, S.; Budzinski, H.; Devier, M.-H.; Dierkes, G.; Boulard, L.; Jacobs, G.; Voorspoels, S.; Rüdel, H.; Ahrens, L. What Is in the Fish? Collaborative Trial in Suspect and Non-Target Screening of Organic Micropollutants Using LC- and GC-HRMS. *Environ. Int.* **2023**, *181*, 108288. https://doi.org/10.1016/j.envint.2023.108288.

(19) Schymanski, E. L.; Singer, H. P.; Slobodnik, J.; Ipolyi, I. M.; Oswald, P.; Krauss, M.; Schulze, T.; Haglund, P.; Letzel, T.; Grosse, S.; Thomaidis, N. S.; Bletsou, A.; Zwiener, C.; Ibáñez, M.; Portolés, T.; de Boer, R.; Reid, M. J.; Onghena, M.; Kunkel, U.; Schulz, W.; Guillon, A.; Noyon, N.; Leroy, G.; Bados, P.; Bogialli, S.; Stipaničev, D.; Rostkowski, P.; Hollender, J. Non-Target Screening with High-Resolution Mass Spectrometry: Critical Review Using a Collaborative Trial on Water

Analysis. *Anal. Bioanal. Chem.* **2015**, *407* (21), 6237–6255. https://doi.org/10.1007/s00216-015-8681-7.

(20) Aalizadeh, R.; Alygizakis, N. A.; Schymanski, E. L.; Krauss, M.; Schulze, T.; Ibáñez, M.; McEachran, A. D.; Chao, A.; Williams, A. J.; Gago-Ferrero, P.; Covaci, A.; Moschet, C.; Young, T. M.; Hollender, J.; Slobodnik, J.; Thomaidis, N. S. Development and Application of Liquid Chromatographic Retention Time Indices in HRMS-Based Suspect and Nontarget Screening. *Anal. Chem.* **2021**, *93* (33), 11601–11611. https://doi.org/10.1021/acs.analchem.1c02348.

(21) Schymanski, E. L.; Jeon, J.; Gulde, R.; Fenner, K.; Ruff, M.; Singer, H. P.; Hollender, J. Identifying Small Molecules via High Resolution Mass Spectrometry: Communicating Confidence. *Environ. Sci. Technol.* **2014**, *48* (4), 2097–2098. https://doi.org/10.1021/es5002105.

(22) Baudry, C.; Jadé, G.; Rayneau, P.; Lombard, B.; Feinberg, M.; Laurentie, M. S-Score: A New Score for Binary Qualitative Proficiency Testing Schemes Interpretable as the z-Score. *Accreditation Qual. Assur.* **2024**, *29* (2), 103–113. https://doi.org/10.1007/s00769-023-01561-y.

(23) Lai, Y.; Koelmel, J. P.; Walker, D. I.; Price, E. J.; Papazian, S.; Manz, K. E.; Castilla-Fernández, D.; Bowden, J. A.; Nikiforov, V.; David, A.; Bessonneau, V.; Amer, B.; Seethapathy, S.; Hu, X.; Lin, E. Z.; Jbebli, A.; McNeil, B. R.; Barupal, D.; Cerasa, M.; Xie, H.; Kalia, V.; Nandakumar, R.; Singh, R.; Tian, Z.; Gao, P.; Zhao, Y.; Froment, J.; Rostkowski, P.; Dubey, S.; Coufalíková, K.; Seličová, H.; Hecht, H.; Liu, S.; Udhani, H. H.; Restituito, S.; Tchou-Wong, K.-M.; Lu, K.; Martin, J. W.; Warth, B.; Godri Pollitt, K. J.; Klánová, J.; Fiehn, O.; Metz, T. O.; Pennell, K. D.; Jones, D. P.; Miller, G. W. High-Resolution Mass Spectrometry for Human Exposomics: Expanding Chemical Space Coverage. *Environ. Sci. Technol.* **2024**, *58* (29), 12784–12822. https://doi.org/10.1021/acs.est.4c01156.

(24) Soares, J. X.; Santos, Á.; Fernandes, C.; Pinto, M. M. M. Liquid Chromatography on the Different Methods for the Determination of Lipophilicity: An Essential Analytical Tool in Medicinal Chemistry. *Chemosensors* **2022**, *10* (8). https://doi.org/10.3390/chemosensors10080340.

(25) Contrepois, K.; Jiang, L.; Snyder, M. Optimized Analytical Procedures for the Untargeted Metabolomic Profiling of Human Urine and Plasma by Combining Hydrophilic Interaction (HILIC) and Reverse-Phase Liquid Chromatography (RPLC)–Mass Spectrometry*. *Mol. Cell. Proteomics* **2015**, *14* (6), 1684–1695. https://doi.org/10.1074/mcp.M114.046508.

(26) Flasch, M.; Fitz, V.; Rampler, E.; Ezekiel, C. N.; Koellensperger, G.; Warth, B. Integrated Exposomics/Metabolomics for Rapid Exposure and Effect Analyses. *JACS Au* **2022**, *2* (11), 2548–2560. https://doi.org/10.1021/jacsau.2c00433.

(27) Talavera Andújar, B.; Schymanski, E. L. High Resolution Mass Spectrometry to Investigate the Human Exposome: Where Are We? *Exposome* **2026**, *6* (1), osaf017. https://doi.org/10.1093/exposome/osaf017.

(28) Periat, A.; Kohler, I.; Thomas, A.; Nicoli, R.; Boccard, J.; Veuthey, J.-L.; Schappler, J.; Guillarme, D. Systematic Evaluation of Matrix Effects in Hydrophilic Interaction Chromatography *versus* Reversed Phase Liquid Chromatography Coupled to Mass Spectrometry. *J. Chromatogr. A* **2016**, *1439*, 42–53. https://doi.org/10.1016/j.chroma.2015.09.035.

(29) David, F.; Devos, C.; Dumont, E.; Yang, Z.; Sandra, P.; Huertas-Pérez, J. F. Determination of Pesticides in Fatty Matrices Using Gel Permeation Clean-up Followed by GC-MS/MS and LC-MS/MS Analysis: A Comparison of Low- and High-Pressure Gel Permeation Columns. *Talanta* **2017**, *165*, 201–210. https://doi.org/10.1016/j.talanta.2016.12.032.

(30) Xie, H.; Sdougkou, K.; Bonnefille, B.; Papazian, S.; Bergdahl, I. A.; Rantakokko, P.; Martin, J. W. Chemical Exposomics in Human Plasma by Lipid Removal and Large-Volume Injection Gas Chromatography–High-Resolution Mass Spectrometry. *Environ. Sci. Technol.* **2024**, *58* (40), 17592–17605. https://doi.org/10.1021/acs.est.4c05942.

(31) Ivanisevic, J.; Zhu, Z.-J.; Plate, L.; Tautenhahn, R.; Chen, S.; O'Brien, P. J.; Johnson, C. H.; Marletta, M. A.; Patti, G. J.; Siuzdak, G. Toward 'Omic Scale Metabolite Profiling: A Dual Separation–Mass Spectrometry Approach for Coverage of Lipid and Central Carbon Metabolism. *Anal. Chem.* **2013**, *85* (14), 6876–6884. https://doi.org/10.1021/ac401140h.

(32) Motteau, S.; Dervilly, G.; Cariou, R.; Margalef, M.; Lamoree, M.; Hamers, T.; König, M.; Escher, B. I.; Vinggaard, A. M.; Rørbye, C.; Le Bizec, B.; Antignac, J.-P. Determination of Chemical Mixtures in Environmental, Food, and Human Samples Using High-Resolution Mass Spectrometry-Based Suspect Screening Approaches. *Environ. Sci. Technol.* **2025**, *59* (39), 21265–21277. https://doi.org/10.1021/acs.est.4c12608.

(33) Manz, K. E.; Feerick, A.; Braun, J. M.; Feng, Y.-L.; Hall, A.; Koelmel, J.; Manzano, C.; Newton, S. R.; Pennell, K. D.; Place, B. J.; Godri Pollitt, K. J.; Prasse, C.; Young, J. A. Non-Targeted Analysis (NTA) and Suspect Screening Analysis (SSA): A Review of Examining the Chemical Exposome. *J. Expo. Sci. Environ. Epidemiol.* **2023**, *33* (4), 524–536. https://doi.org/10.1038/s41370-023-00574-6.

(34) Schymanski, E. L.; Singer, H. P.; Longrée, P.; Loos, M.; Ruff, M.; Stravs, M. A.; Ripollés Vidal, C.; Hollender, J. Strategies to Characterize Polar Organic Contamination in Wastewater: Exploring the Capability of High Resolution Mass Spectrometry. *Environ. Sci. Technol.* **2014**, *48* (3), 1811–1818. https://doi.org/10.1021/es4044374.

(35) Beckers, L.-M.; Brack, W.; Dann, J. P.; Krauss, M.; Müller, E.; Schulze, T. Unraveling Longitudinal Pollution Patterns of Organic Micropollutants in a River by Non-Target Screening and Cluster Analysis. *Sci. Total Environ.* **2020**, *727*, 138388. https://doi.org/10.1016/j.scitotenv.2020.138388.

(36) Krauss, M.; Huber, C.; Schulze, T.; Bartel-Steinbach, M.; Weber, T.; Kolossa-Gehring, M.; Lermen, D. Assessing Background Contamination of Sample Tubes Used in Human Biomonitoring by Non-Targeted Liquid Chromatography–High Resolution Mass Spectrometry. *Environ. Int.* **2024**, *183*, 108426. https://doi.org/10.1016/j.envint.2024.108426.

(37) Hernandes, V. V.; Zeyda, M.; Wisgrill, L.; Warth, B. Dried Blood Spots Analysis for Targeted and Non-Targeted Exposomics. *Environ. Int.* **2025**, *205*, 109814. https://doi.org/10.1016/j.envint.2025.109814.

(38) Marx-Stoelting, P.; Rivière, G.; Luijten, M.; Aiello-Holden, K.; Bandow, N.; Baken, K.; Cañas, A.; Castano, A.; Denys, S.; Fillol, C.; Herzler, M.; Iavicoli, I.; Karakitsios, S.; Klanova, J.; Kolossa-Gehring, M.; Koutsodimou, A.; Vicente, J. L.; Lynch, I.; Namorado, S.; Norager, S.; Pittman, A.; Rotter, S.; Sarigiannis, D.; Silva, M. J.; Theunis, J.; Tralau, T.; Uhl, M.; van Klaveren, J.; Wendt-Rasch, L.; Westerholm, E.; Rousselle, C.; Sanders, P. A Walk in the PARC: Developing and Implementing 21st Century Chemical Risk Assessment in Europe. *Arch. Toxicol.* **2023**, *97* (3), 893–908. https://doi.org/10.1007/s00204-022-03435-7.

7. Supplementary Information

Supplementary Information file 1: Supplementary figures to show data in support of the manuscript (.docx)

Supplementary Information file 2: 15 tables including details regarding the reference standards used, samples preparation and data acquisition procedures as well as additional results (.xlsx)

3.2 Application of HILIC in Non-Targeted Metabolomics for Extended Coverage of Polar Metabolites

3.2.1 Integrated non-targeted exposomics and metabolomics reveal elevated endocrine-disrupting chemical burden and altered steroid metabolism in women with PCOS

In preparation: Rekar, Ž., Plesnik, H., Tkalec, Ž., Srnovršnik, T., Viranz Klun, I., Pinter, B., Mazej, D., Snoj Tratnik, J., Horvat, M., Kosjek, T.

This paper represents the principal metabolomics-oriented case study of the dissertation and primarily supports Hypothesis H4, which states that non-targeted analysis combining HILIC and RP separations can reveal biologically relevant endogenous and exogenous biomarkers associated with reproductive disorders. In contrast to the ovarian-malignancy study, which focused exclusively on exposure biomarkers, this work integrates exposure-oriented screening in urine and serum with complementary serum metabolomics, thereby addressing both environmental and metabolic dimensions of PCOS within the same cohort.

The central methodological contribution lies, once again, in the use of complementary HILIC and RP serum analysis, providing further experimental support for the broader thesis concept that HILIC extends non-targeted coverage toward highly polar metabolites beyond RP alone. The HILIC part constituted my primary analytical contribution, including the interpretation of HILIC-derived metabolomic signals. This was particularly important for metabolite classes such as amino-acid-related compounds and steroid conjugates, which contributed substantially to the final biological interpretation.

The acquired results showed that women with PCOS had a higher urinary burden of several endocrine-disrupting chemical biomarkers, while serum metabolomics identified significant differences in steroid metabolism, lipid composition, and amino-acid-related metabolites. The dataset included both metabolites consistently reported as altered in PCOS and compounds not previously described in this context. Several of these were detected primarily in the HILIC datasets, further demonstrating the analytical relevance of chromatographic complementarity.

Within the dissertation, this work demonstrates that HILIC contributes directly to biologically meaningful interpretation in clinical non-targeted metabolomics and strengthens the broader thesis argument that inclusion of HILIC substantially improves analytical access to the polar region of chemical space.

Integrated non-targeted exposomics and metabolomics reveal elevated endocrine-disrupting chemical burden and altered steroid metabolism in women with PCOS

Žan Rekar[1,2‡], Helena Plešnik[1,2‡], Žiga Tkalec[1], Tinkara Srnovršnik [3,4], Irma Virant Klun[5], Bojana Pinter [4,6], Darja Mazej[1], Milena Horvat[1,2], Tina Kosjek[1,2*]

[1] Department of Environmental Sciences, Jožef Stefan Institute, Ljubljana, Slovenia
[2] Jožef Stefan International Postgraduate School, Ljubljana, Slovenia
[3] Division for Women's Healthcare, Šiška Unit, Community Health Centre Ljubljana, Ljubljana, Slovenia
[4] Faculty of Medicine, University of Ljubljana, Ljubljana, Slovenia
[5] Clinical Research Centre, University Medical Centre Ljubljana, Ljubljana, Slovenia
[6] Division of Obstetrics and Gynecology, University Medical Centre Ljubljana, Ljubljana, Slovenia

‡ These two authors contributed equally to this work

* Corresponding author contact: tina.kosjek@ijs.si

Abstract

Polycystic ovary syndrome (PCOS) is a heterogeneous endocrine and metabolic disorder whose pathogenesis remains incompletely understood and is thought to involve both endogenous metabolic dysregulation and exogenous influences. To assess both dimensions within the same cohort, we applied an integrated non-targeted LC-HRMS workflow combining exposomics in urine and serum with complementary serum metabolomics using both hydrophilic interaction liquid chromatography (HILIC) and reversed-phase (RP) chromatography.

Women with PCOS showed a significantly higher urinary burden of several phthalate metabolites, together with elevated levels of butyl paraben and resorcinol. This was further reflected in significantly higher cumulative phthalate and overall endocrine-disrupting chemical burden scores, indicating a distinct urinary exposomics profile between women with PCOS and healthy controls. Although no individual serum biomarker of exposure differed significantly between groups, per- and polyfluoroalkyl substances showed strong positive intercorrelations, consistent with their frequent co-occurrence in human serum and long biological half-lives. Serum metabolomics revealed significant alterations across several biochemical classes. PCOS patients exhibited alteration in steroid metabolism compared to controls, with elevated androstenedione and downstream androgen conjugates, consistent with established increased steroid turnover and androgen excess in PCOS. In addition, glycerophospholipids such as lysophosphatidylcholines (LPC O-24:1, LPC 16:1, LPC 20:4, and LPC 22:5) and lysophosphatidylethanolamines (LPE P-18:0, LPE 20:4, and LPE 22:4), were consistently decreased in serum of PCOS patients, while amino acids and their metabolites, including lysine and pipecolic acid, as well as fatty acid-derived compounds such as dodecanedioic acid and 12,13-dihydroxy-9Z-octadecenoic acid (12,13-DiHOME), were increased.

Integrating exposomics and metabolomics profiling enabled thorough characterisation of exposure and metabolite profiles of PCOS patients, which sheds light on environmental influences and biology in PCOS.

Keywords
Polycystic ovary syndrome, non-targeted screening, high-resolution mass spectrometry, urine, serum, hyperandrogenism, biomarker of exposure

1. Introduction

Polycystic ovary syndrome (PCOS) is a complex endocrine and metabolic disorder characterised by hormonal imbalance and metabolic disturbances, with onset typically occurring during the reproductive years. It is one of the most common endocrine disorders in this population, with prevalence estimates between 5% and 20%, depending on the diagnostic criteria applied[1–3]. Clinically, PCOS presents a heterogeneous spectrum of manifestations, including menstrual irregularities reflecting ovulatory dysfunction (often chronic anovulation), clinical and/or biochemical hyperandrogenism (commonly presenting as hirsutism, acne, or androgenic alopecia), and distinct ovarian morphological features on ultrasound[4,5]. Beyond its reproductive manifestations, PCOS is associated with metabolic dysregulation, encompassing obesity, dyslipidemia, hyperinsulinemia, and insulin resistance, which likely underlie the elevated risk of cardiovascular sequelae, including ischemic heart disease, myocardial infarction, stroke, and potentially cardiovascular mortality[3,6]. Despite its high prevalence and clinical significance, PCOS remains substantially underdiagnosed, with estimates suggesting that up to 75% of affected women are never clinically diagnosed[7,8]. This diagnostic gap is attributable, in large part, to the inherently heterogeneous nature of the syndrome, wherein symptom presentation varies considerably across individuals, age groups, and ethnicities[7]. Several diagnostic criteria have been proposed over the decades, reflecting the lack of consensus in the field and underscoring the absence of a universally standardized diagnostic approach[4,5,9–11]. Of these, the Rotterdam criteria[4], established by the European Society of Human Reproduction and Embryology and the American Society for Reproductive Medicine (ESHRE/ASRM), remain the most widely adopted, permitting diagnosis when any two of three core features are present: oligo/anovulation, clinical and/or biochemical hyperandrogenism, and polycystic ovarian morphology (PCOM).

The pathogenesis of PCOS is multifactorial and remains incompletely elucidated. Current understanding implicates an interplay of genetic, epigenetic, microbiota, developmental, and environmental factors that collectively drive the prominent pathophysiological abnormalities of the syndrome, including impaired gonadotropin secretion, androgen excess, insulin resistance, low-grade systemic inflammation, and adipose tissue dysfunction[7,12–14].

This incomplete mechanistic understanding, together with the heterogeneity of the syndrome, has motivated extensive use of metabolomic approaches in PCOS research. Reported were recurrent differences in lipid and lipoprotein metabolism, steroid biosynthesis, carbohydrate/energy pathways, and amino-acid handling[15–18], indicating that PCOS is accompanied by systemic metabolic remodelling. However, results frequently vary, likely due to factors such as different phenotype definitions, analytical strategies applied, and underpowered studies with too few participants.

Lipidomics further highlights shifts in specific lipid species, particularly sphingolipids, with patterns that vary across insulin-resistant and obesity-related PCOS subgroups and may track metabolic severity[19]. Finally, elevations in branched-chain and aromatic amino acids and related intermediates

are frequently observed and tend to align with insulin resistance rather than PCOS diagnosis in isolation[20].

Beyond endogenous metabolic alterations, increasing attention has been directed toward the contribution of chemical exposure to PCOS. Emerging evidence suggests a link between certain endocrine-disrupting chemicals (EDCs) and the pathogenesis and exacerbation of PCOS[21], such as bisphenols, phthalates, parabens, polychlorinated biphenyls, organochlorine pesticides, per- and polyfluoroalkyl substances (PFAS), dioxins, and various industrial chemicals[22]. Among these, bisphenol A (BPA) is the most extensively investigated[23], owing to its environmental ubiquity; most studies report significantly elevated serum BPA levels in women with PCOS compared to controls and positive associations with hyperandrogenism and insulin resistance[23,24]. Increasing efforts have been directed toward the integration of multi-omics approaches in PCOS research to better understand the molecular mechanisms of its pathophysiology. Since studies show that endogenous processes as well as environmental factors may contribute to the onset of the disease, integrating metabolomics and exposomics data can provide holistic insight into its pathophysiology.

In this study, we applied an integrated non-targeted exposomics and metabolomics workflow to simultaneously characterise the environmental chemical burden and endogenous metabolic profile associated with the syndrome. By linking these complementary layers, we aimed to (i) compare the environmental chemical burden between women with PCOS and healthy controls (HC), (ii) identify endogenous metabolic alterations in women with PCOS, and (iii) explore potential associations between biomarkers of exposure (BoEs) and serum metabolomic profiles.

2. Materials and methods

Materials and Chemicals are listed in S1 (Chapter 1) and Table S2-A1. S1 Chapter 1 lists materials and chemicals used in sample preparation and software tools used in raw data processing and statistical analysis. Table S2-A1 lists all reference standards and isotopically labelled internal standards used for analyte confirmation, retention-time matching, signal normalization, and QA/QC assessment..

Study population. This retrospective case-control study was based on biological samples and clinical data collected between between October 2022 and July 2023 at the Division of Obstetrics and Gynecology, University Medical Centre Ljubljana. Informed written consent was obtained from all participants. The participants were able to withdraw from the study at any time. The study was conducted in accordance with the Declaration of Helsinki and approved by the Republic of Slovenia National Medical Ethics Committee. Participant recruitment and sample collection were approved under protocol 0120-530/2021/6 (18 February 2022), while the retrospective exposomics and metabolomics analyses were approved under amendment/protocol 0120-530-2021/2711-9 (14 April 2026).

The study included 29 women diagnosed with PCOS and 31 HC aged 20-39 years with a body mass index (BMI) between 18.5-29.9 kg/m². PCOS diagnosis was established according to the Rotterdam criteria[11], requiring the presence of at least two of the following three features: oligo- or anovulation, clinical and/or biochemical symptoms of hyperandrogenism, and/or polycystic ovary morphology (presence of ≥ 12 follicles 2-9 mm in diameter in at least one ovary) on ultrasound. Exclusion criteria for both groups included pregnancy, hormonal treatment within the preceding three months

(hormonal contraception, hormone replacement therapy, or progestogens), hyperprolactinaemia, thyroid dysfunction, premature ovarian insufficiency, primary amenorrhoea, endometriosis, and chronic conditions including diabetes mellitus, depression, Crohn's disease, coeliac disease, cardiovascular, hepatic, renal, pulmonary, musculoskeletal, neurological, or oncological diseases. Detailed anthropometric, ultrasonographic, and laboratory characteristics of the study cohort, including reproductive hormone profiles, have been published elsewhere[25].

Samples. First-morning urine and venous blood samples were collected after an overnight fast from 31 HC (mean age 28.4 ± 6.0 years, BMI 21.3 ± 1.9 kg/m²) and 29 women diagnosed with PCOS (mean age 28.8 ± 4.8 years, BMI 23.1 ± 2.7 kg/m²), between the second and the fifth day of the spontaneous menstrual cycle or anytime following ≥ 2 months of amenorrhea at the Institute of Clinical Chemistry and Biochemistry, University Medical Centre Ljubljana. Venous blood was drawn under sterile conditions into heparin tubes, from which serum was subsequently obtained. Urine samples were collected in polypropylene containers pre-washed with 10% nitric acid. All samples were immediately aliquoted into cryovials and stored at −80 °C until analysis. Samples were thawed at room temperature immediately before being prepared for analysis.

Sample preparation. Urine samples were used for exposomics analysis only, whereas serum samples were used for both exposomics and metabolomic analysis (Figure 1).

Serum. For the hydrophilic interaction liquid chromatography coupled to high-resolution mass spectrometry (HILIC-HRMS) analysis, 80 µL of thawed serum was added to 320 µL of ice-cold ACN spiked with internal standard (IS) at the final concentration of 400 µg/L. The mixture was centrifuged at 7,200 rpm and 4 °C for 15 min, after which 150 µL of supernatant was transferred to a vial with a fitted insert and analyzed. For the reversed-phase liquid chromatography high-resolution mass spectrometry (RPLC-HRMS), 150 µL of thawed serum was added to 600 µL of ice-cold ACN spiked with IS at a final concentration of 10 µg/L. The mixture was centrifuged at 7,200 rpm and 4 °C for 15 min, and 600 µL of supernatant was dried under a gentle stream of nitrogen at 35 °C. The residue was reconstituted in 60 µL of 10% (v/v) ACN in water prior to analysis and transferred to a 2 mL vial with fitted insert. Procedural blanks and quality control (QC) samples were prepared following the same procedure. System suitability controls, however, were prepared independently by diluting the standard mixture in reconstitution solvent (10% (v/v) ACN in water for RPLC-HRMS analysis and 20% (v/v) water in ACN for HILIC-HRMS analysis.

Urine. The sample preparation protocol was adapted from our previous studies[26,27]. Briefly, to 0.6 mL of thawed urine, 430 µL of LC-MS grade water, 50 µL of 3 M sodium acetate buffer (pH 5.2), and β-glucuronidase/arylsulfatase solution (*Helix pomatia*, type H-2) were added to achieve a final enzyme concentration of 600 U/mL. The mixture was incubated at 37 °C for 16 h on an orbital thermoshaker to facilitate enzymatic deconjugation. Solid-phase extraction (SPE) was performed using a 60 mg sorbent Oasis-HLB 96-well plate, conditioned sequentially with 1 mL ethyl acetate (EtOAc), 1 mL methanol (MeOH), and 1 mL water. After sample loading, the sorbent was washed with 0.5 mL of water, and analytes were eluted with 1.5 mL of 10% (v/v) MeOH in ACN. The eluate was dried under a gentle stream of nitrogen at 40 °C, and the residue was reconstituted in 120 µL of 10% (v/v) ACN in water prior to analysis with the RPLC-HRMS method. Procedural blanks and QC samples were prepared following the same procedure.

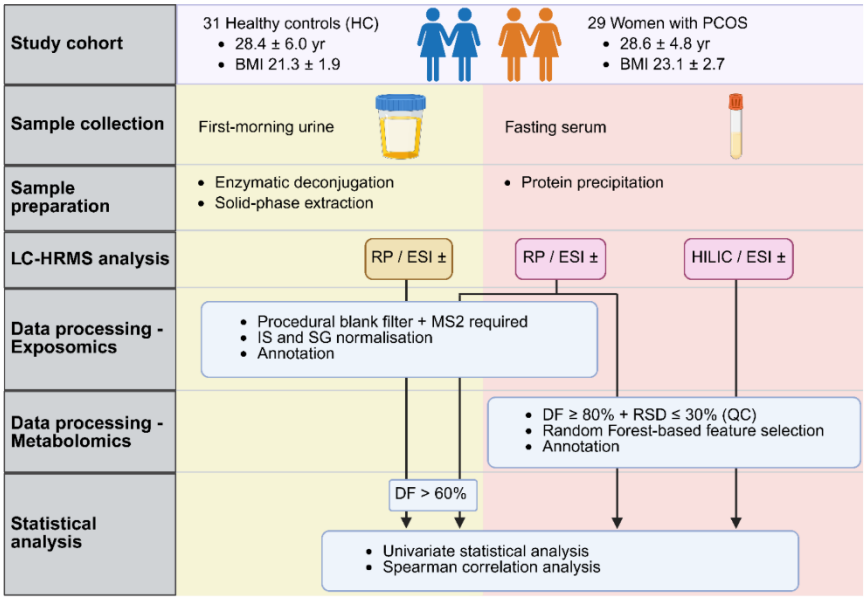


Figure 1. Schematic overview of the multi-omics study workflow for exposomics and metabolomics profiling in HC and women with PCOS.

Instrumental analysis. Instrumental analyses were performed using a Thermo Fisher Vanquish UHPLC system coupled to a Thermo Fisher Orbitrap Exploris 240 mass spectrometer (Thermo Fisher Scientific Inc., Waltham, MA, USA), which was calibrated according to the manufacturer's instructions. Scan-to-scan mass correction was applied during acquisition to ensure the highest mass accuracy throughout the analysis. In the HILIC-HRMS analysis, separation was achieved using a Waters BEH amide (2.1 × 100 mm, 1.7 µm) column with (A) ACN and (B) 20 mM ammonium formate with 0.1 % formic acid (pH 3.5) as mobile phases. The elution gradient was as follows: 10 % B (0-2 min), 10-45 % B (2-15 min), 45 % B (15-16 min), 45-10 % B (16-16.5 min), 5 % B (16.5-30 min). The flow rate was 0.4 mL/min, the column temperature was 35 °C, and the injection volume was 5 µL. Heated electrospray ionization (HESI) was used as the ionization source with the following settings: capillary voltage, 3.5 kV and -2.5 kV for positive and negative mode, respectively; sheath gas, 50 AU; auxiliary gas, 10 AU; sweep gas, 1 AU; ion transfer tube temperature, 325 °C; vaporizer temperature, 350 °C. The full scan mass acquisition scanned the mass range of 70-1000 *m/z* at the resolution of 120,000 FWHM, while the MS2 data were acquired at the resolution of 30,000. MS data was acquired in centroided mode. The data-dependent acquisition (DDA) involved an intensity threshold for the MS/MS events set to $1.0e^4$, with the top 8 most intense ions selected for fragmentation. Dynamic exclusion with a 9 s time window and 5 ppm mass tolerance was applied. Higher-energy collisional dissociation (HCD) was applied with normalised stepped collision energies of 30 %, 50 %, and 150 % to ensure comprehensive fragmentation.

In the RPLC-HRMS acquisition, separation was achieved using a Waters Acquity HSS-T3 (2.1 × 100 mm, 1.8 µm) column with (A) ACN with 0.1 % formic acid and (B) water containing 0.1 % formic acid (pH 2.6) as the mobile phases. The elution gradient was as follows: 95-75 % B (0-3 min), 75-60 % B (3-7

min), 60-40 % B (7-15 min), 40-30 % B (15-18 min), 30-0 % B (18-24.5 min), 0 % B (24.5-26.5 min), 0-95 % B (26.5-27.5 min), 95 % B (27.5-33 min). The flow rate was 0.3 mL/min, the column temperature was 35 °C, and the injection volume was 5 µL. The HESI settings involved a capillary voltage of 4.5 kV for positive and -3.0 kV for negative ionization mode; sheath gas, 40 AU; auxiliary gas, 15 AU; sweep gas, 2 AU; ion transfer tube temperature, 350 °C; vaporizer temperature, 400 °C. The full scan mass acquisition covered the mass range of 100-900 *m/z* and was acquired with a resolution of 120,000, while MS2 data were acquired with a resolution of 30,000. MS data was acquired in centroided mode. The DDA intensity threshold for the MS/MS events was set to $1.0e^4$, and the top 7 most intense ions were selected for fragmentation. Dynamic exclusion with a 9 s time window and 5 ppm mass tolerance was applied. A 20 % apex window was used for DDA, with an isolation window of 1.5 *m/z* for precursor ions. HCD was applied with normalised stepped collision energies of 30 %, 50 %, and 150 % to ensure comprehensive fragmentation.

Quality assurance and quality control. Samples were prepared and analysed in a randomized order. A reconstitution solvent (see Sample preparation) was injected as a system blank prior to each analytical batch. A system suitability control, consisting of reconstitution solvent spiked with reference standards at 200 µg/L, was injected at the beginning and end of each batch to assess system performance, including mass accuracy (mass error < 5 ppm) and retention-time stability (RPLC = ± 0.10 min; HILIC = ± 0.25 min)[26].

Pooled QC samples (pooled serum spiked with IS and pooled urine spiked with a mixture of representative BoE reference standards and IS) were injected every 10 samples to monitor instrumental stability (tR, mass accuracy, singnal intensity) and assess whole-method repeatability. Signal intensities of internal standards were monitored across all samples and pooled QCs to assess injection reproducibility, detect potential analytical anomalies, and evaluate variability within pooled QCs and across the analytical batch. Detailed QC results, including method repeatability for reference standards, variability in pooled QC for reference standards and IS, and within-batch IS variability, all expressed as their RSD, are reported in Table S2-A2. Peak heights were used in preference to peak areas to minimize inaccuracies in baseline estimation, particularly for low-abundance analytes, a common challenge in MS-based exposomics and metabolomics profiling.

Raw data processing and peak annotation. Raw data were processed using MzMine 4.8.3[28], with processing parameters detailed in S1 (Chapter 3). In metabolomic profiling, features with a detection frequency (DF) < 80% and a relative standard deviation (RSD) > 30% in pooled QCs (n = 7) were excluded from further data analysis. In exposomics profiling, features present in procedural blanks (sample-to-blank ratio < 3) and those lacking MS2 data were excluded. For urinary exposomics profiling, feature heights were normalised to the closest eluting IS, followed by specific gravity (SG) normalisation to account for urine dilution. A detailed description of the SG normalisation procedure and calculation is provided in S1 (Chapter 2).

Exposomics. Annotation of BoEs was based on a modified Schymanski scale[29]. Annotation involved matching MS2 spectra against spectral libraries. Matches to the in-house library, constructed from reference standards, were assigned level 1 identification (ID) confidence when meeting the following criteria: parent ion mass error < 5 ppm, at least three matched MS2 signals (mass error < 10 ppm), and RT within ± 0.10 min. Matches to the MoNA (Mass Bank of North America)[30], MassBank[31], HMDB[32], and GNPS[33] libraries, applying the same mass accuracy criteria as level 1 alongside a cosine similarity

> 0.80, were assigned level 2 ID confidence. Endogenous and food-derived biomarkers in urine and serum were subsequently excluded using the HMDB[32] database.

Metabolomics. Metabolite annotation followed the same library matching approach as described for exposomics profiling. Level 1 ID confidence criteria were identical to those applied in exposomics analysis, whereas level 2 ID confidence required a cosine similarity > 0.80 against the aforementioned MS2 libraries, with the same mass accuracy criteria applied. Additionally, *in silico* fragmentation and identification were performed by uploading MS2 spectra to SIRIUS+CSI:FingerID[34]. Structural candidates were generated from KEGG[35], ChEBI[36], HMDB[32], and GNPS[33] libraries, and those meeting a match confidence > 0.75 with all matching substructures confirmed were reported at level 3 ID confidence.

Modelling and statistical analysis.

Exposomics. Prior to statistical analysis, pharmaceutical residues, caffeine, nicotine, and nicotine metabolites were excluded from the BoEs dataset, as their presence primarily reflects voluntary use or lifestyle choices rather than background environmental, dietary, or consumer-product-related exposures. exposure. Only BoEs with a DF > 60% across all samples were included in the statistical analysis, to limit sparsity and reduce the influence of imputation. Missing values in this subset were imputed using a half-minimum approach, whereby undetected values were replaced with half the minimum positive value observed for each BoE. All intensity values were $\log_{10}$-transformed before statistical testing. Normality of the $\log_{10}$-transformed data was assessed independently for each group using the Shapiro-Wilk test. Where both groups satisfied the normality assumption ($p > 0.05$), a Welch t-test was applied; otherwise, a Mann-Whitney U-test was used. Differences were considered statistically significant at $p < 0.05$.

To assess cumulative exposure, composite burden scores were calculated for phthalates and a broader panel of EDCs in urine and PFAS in serum. For each analyte, a robust Z-score was calculated across all samples as $Z = (X_i - \text{median}) / \text{IQR}$, where X_i represents the $\log_{10}$-transformed normalized intensity of BoE in an individual sample, and the median and IQR were estimated across the full study population (n = 60). A composite burden score was then calculated as the mean robust Z-score across all contributing BoEs. Additionally, three phthalate-specific scores were derived: (i) an overall phthalate score incorporating all 13 phthalate metabolites, (ii) a di(2-ethylhexyl) phthalate (DEHP) subscore based on four DEHP-specific metabolites (MEHP, OH-MEHP, oxo-MEHP, cx-MEPP), and (iii) a diisononyl phthalate (DiNP) subscore based on three DiNP-specific metabolites (OH-MINP, oxo-MINP, cx-MINP). Further, a composite EDC burden score was computed across 17 selected BoEs, encompassing known and potential EDCs. A PFAS burden score was computed across four perfluoroalkyl substances in serum (PFNA, PFOA, PFOS, and PFHxS). Group differences in these composite scores were assessed using the same statistical framework as described above.

Metabolomics. Raw data was filtered to retain only features with DF ≥ 80% and RSD ≤ 30% in pooled QCs. Prior to modelling, data were $\log_2(x + 10^{-6})$-transformed and autoscaled. A Random Forest (RF) classification model was constructed for each analytical mode (HILIC positive, HILIC negative, RPLC positive, and RPLC negative) to discriminate between PCOS and HC. The RF model was used to highlight the discriminatory features between PCOS patients and HC. Model performance was evaluated using five-fold stratified cross-validation, ensuring that class proportions were preserved

across folds. Performance was assessed using the area under the receiver operating characteristic curve (ROC AUC), accuracy, precision, recall, and F1-score. The decision threshold was optimized on cross-validated prediction probabilities to improve the balance between precision, recall, and F1-score for each model (S1, Chapter 4). For each analytical mode, the 100 highest-ranked features based on mean decrease in impurity (MDI) were selected for downstream annotation, as described above.

Annotated metabolites were subsequently subjected to univariate statistical analysis following the same approach as for exposomics analysis: missing values were imputed using the half-minimum approach as described for exposomics analysis, followed by $\log_{10}$ transformation of peak heights. Normality was assessed using the Shapiro-Wilk test, and group differences between PCOS and HC were evaluated using either Welch's t-test or the Mann–Whitney U test, as appropriate. Statistical significance was set at $p < 0.05$.

Correlation analysis. Pairwise associations between $\log_{10}$-transformed intensities were assessed using Spearman's rank correlation. To account for multiple testing, Benjamini-Hochberg false discovery rate (BH-FDR) correction was applied across all tested correlations, and adjusted *q*-values < 0.05 were considered statistically significant.

3. Results

Quality assessment. To ensure accurate biological interpretation and the reliability of the generated datasets, analytical performance and data quality were evaluated prior to downstream statistical analyses. For the metabolomics workflow, internal standard responses were monitored in pooled QC samples and across the analytical batch, with RSDs not exceeding 27.9% and 27.8% for HILIC and RPLC analyses, respectively. For the exposomics workflow, the spiked BoE standard mixture in pooled QC samples exhibited RSDs below 25.1%. Overall, the observed analytical variability was considered acceptable for untargeted LC-HRMS analyses and supported the use of the datasets for downstream statistical analyses..

Exposomics. The class distribution of annotated BoE by biological matrix is shown in Figure S1-5. A total of 53 BoEs were annotated in urine samples, of which 32 were assigned level 1 and 21 level 2 ID confidence (Table S2-A3).

After exclusion of pharmaceuticals and their metabolites, caffeine, nicotine, and nicotine metabolites, and after applying the DF > 60% threshold, 21 urinary BoEs were retained for statistical analysis. Of these, five differed significantly between women with PCOS and HC (Table S2-A4): butyl paraben (BuP; MWU, $p = 0.009$), mono-benzyl phthalate (MBzP; Welch t-test, $p = 0.022$), mono-2-ethylhexyl phthalate (MEHP; MWU, $p = 0.031$), mono-isobutyl phthalate (MiBP; MWU, $p = 0.043$), and resorcinol (MWU, $p = 0.044$), all of which revealed higher normalized peak intensities in women with PCOS as compared to HC (Figure 2).

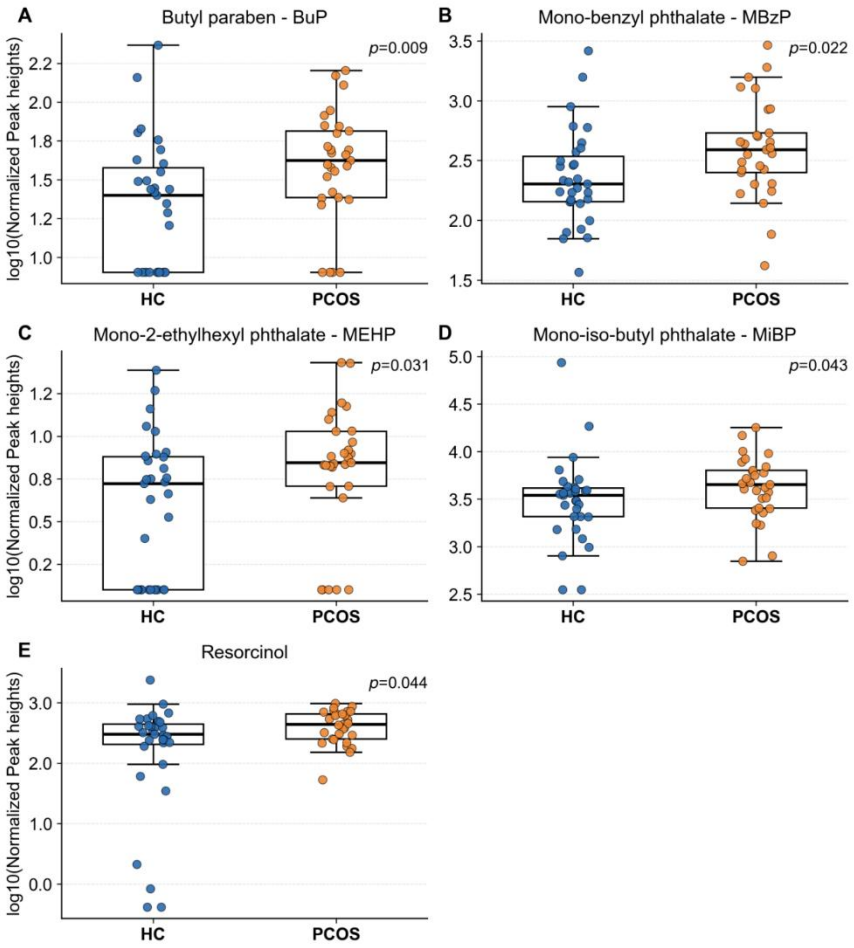


Figure 2. Box-and-whisker plots (A-E) of Log_{10}-transformed normalised peak heights for BoEs with statistically significant differences between HC (n=31, blue) and women with PCOS (n=29, orange), determined by Mann-Whitney U or Welch's t-test ($p < 0.05$). Peak heights were normalised to the internal standard (IS) and corrected for SG prior to log_{10} transformation.

Cumulative exposure assessment showed a significantly higher EDC burden score in women with PCOS compared to HC (17-BoE composite score; Welch t-test, $p = 0.007$), as well as a significantly higher overall phthalate burden score (13 metabolites; Welch t-test, $p = 0.027$). Neither the DEHP subscore ($p = 0.078$) nor the DiNP subscore ($p = 0.191$) reached statistical significance, although both showed a tendency towards higher values in women with PCOS (Figure 3). Detailed statistical results are presented in Table S2-A4.

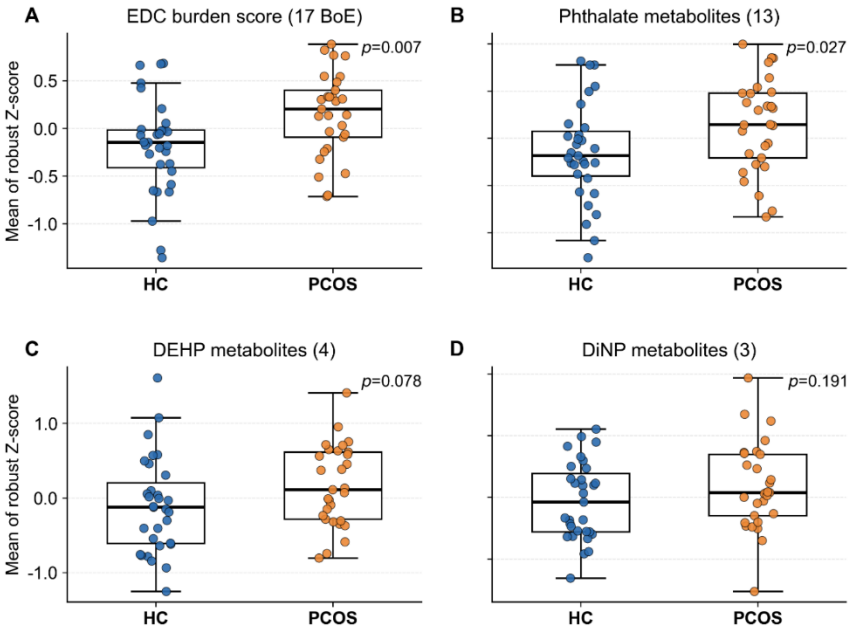


Figure 3. Box-and-whisker plots (A-D) showing composite burden scores in HC (n=31, blue) and women with PCOS (n=29, orange). Z-scores are shown for (A) the overall EDC burden (17 BoEs), (B) phthalate metabolites (13), (C) DEHP metabolites (4), and (D) DiNP metabolites (3). Statistically significant differences were determined by Mann-Whitney U or Welch's t-test ($p < 0.05$). BoE peak heights were normalised to the internal standard (IS), corrected for SG, and $\log_{10}$-transformed. For each BoE, a robust Z-score was calculated across all samples, and the composite burden score for each sample was obtained by averaging these scores across BoE.

In serum, 43 BoEs were annotated, including 23 with level 1 and 20 with level 2 ID confidence (Table S2-A3). After application of the same exclusion and filtering criteria, 10 BoEs met the DF > 60% threshold and were included in the statistical analysis. None differed significantly between women with PCOS and HC (all $p > 0.05$; Table S2-A4). Likewise, the composite PFAS burden score, calculated across four perfluoroalkyl substances (PFNA, PFOA, PFOS, and PFHxS), did not differ significantly between the groups (Welch's t-test, $p = 0.205$).

Spearman correlation analysis revealed strong positive correlations within the urinary phthalate metabolite cluster, particularly among DEHP metabolites (MEHP, oxo-MEHP, OH-MEHP, cx-MEPP) and DiNP metabolites (OH-MINP, oxo-MINP, cx-MINP) (Figure 4). Significant positive correlations were also observed between MiBP and MnBP ($\rho = 0.73$, FDR $q < 0.001$) and between oxybenzone and benzophenone-1 ($\rho = 0.77$, FDR $q < 0.001$). Significant correlations were additionally observed across phthalate metabolites, including between DiNP and DEHP metabolites, between MnBP and DEHP metabolites, and between MBzP, BuP, and oxo-MIDP with DiNP metabolites ($\rho = 0.44$-0.65, FDR $q < 0.01$).

For the BoE determined in serum, significant positive correlations were observed among PFAS (PFNA, PFOS, PFOA, PFHxS; ρ = 0.48-0.79, FDR q < 0.01). Additional serum correlations were identified between propyl paraben (PrP) and 3,5,6-trichloro-2-pyridinol (ρ = 0.51, FDR q < 0.001), and between PrP and PFHxS (ρ = 0.43, FDR q < 0.01). Cross-matrix correlations were largely absent, except for MEP (ρ = 0.73, FDR q < 0.001) and resorcinol (ρ = 0.39, FDR q = 0.021), which both showed significant positive correlations across matrices.

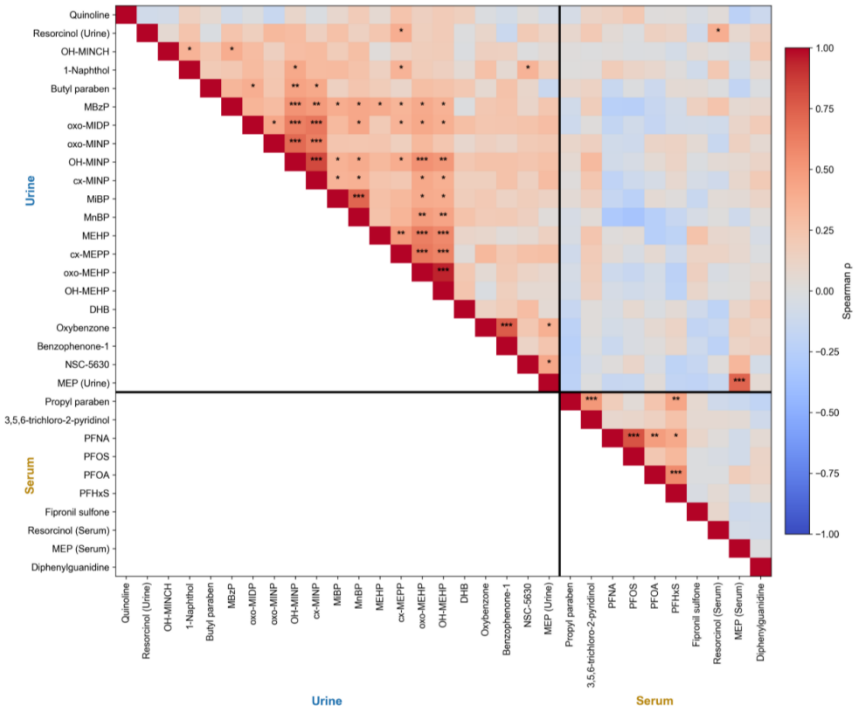


Figure 4. Heatmap of pairwise Spearman correlation coefficients among urinary and serum BoEs (DF > 60 %). Correlations were calculated using $\log_{10}$-transformed normalised values. Urinary and serum BoEs are shown as separate clustered blocks, with BoEs ordered by hierarchical clustering within each matrix. Only the upper triangle of the correlation matrix is displayed. Asterisks denote correlations that remained statistically significant after BH-FDR correction (* q < 0.05, ** q < 0.01, *** q < 0.001).

Metabolomics. Random Forest models were constructed independently for each analytical mode (HILIC ESI+, HILIC ESI−, RPLC ESI+, RPLC ESI−) as an exploratory feature-ranking step for metabolite prioritization. Model performance was modest across all analytical modes, with ROC AUC values ranging from 0.43 to 0.58 (Table S2-A5). Among the evaluated models, HILIC ESI+ showed the best overall performance, with an ROC AUC of 0.58, weighted precision of 0.57, weighted recall of 0.57, and weighted F1-score of 0.56. In contrast, RPLC ESI− performed worst, with an ROC AUC of 0.43, a weighted precision of 0.39, a weighted recall of 0.42, and a weighted F1-score of 0.39. The top 100

features ranked by MDI from each model were selected for annotation, which resulted in 33 annotated metabolites after library matching and *in silico* fragmentation (Table S2-A6).

Univariate statistical analysis of the 33 annotated metabolites identified 10 metabolites that differed significantly between women with PCOS and HC ($p < 0.05$; Table S2-A7; Figure S1-6). The corresponding $\log_2$ fold changes of annotated metabolites between women with PCOS and HC are summarized in Figure 5. The clearest group-level difference was observed within steroid-related metabolites, which were elevated in women with PCOS. These include androstane-3,17-diol 17-sulfate (Welch t-test, $p = 0.0004$), etiocholanolone glucuronide (MWU, p = 0.005), androstenedione (Welch t-test, $p = 0.006$), and pregnanetriol 3α-O-β-D-glucuronide (Welch t-test, $p = 0.012$). Androsterone glucuronide also showed a tendency towards higher levels in women with PCOS without reaching statistical significance ($p = 0.391$; Figure 5). Among fatty acyls, dodecanedioic acid was significantly elevated in women with PCOS (Welch t-test, $p = 0.021$), while 12,13-dihydroxy-9Z-octadecenoic acid (12,13-DiHOME) showed a consistent trend in the same direction without reaching statistical significance. Among carboxylic, amino acids and dipeptides, pipecolic acid (MWU, $p = 0.014$), phenylalanyl-serine (MWU, $p = 0.015$), and lysine (MWU, $p = 0.036$) were significantly elevated in women with PCOS. Leucylalanine and 5-aminolevulinic acid showed a consistent trend in the same direction. Within the glycerophospholipid class, PE 38:4 (MWU, $p = 0.019$) and LPC 22:5 (Welch t-test, $p = 0.038$) were significantly lower in women with PCOS than in HC. The remaining LPC and LPE species (LPC O-24:1, LPC 16:1, LPC 20:4, LPE 20:4, LPE 22:4, LPE P-18:0) showed a consistent pattern of reduction in women with PCOS, although these did not reach statistical significance.

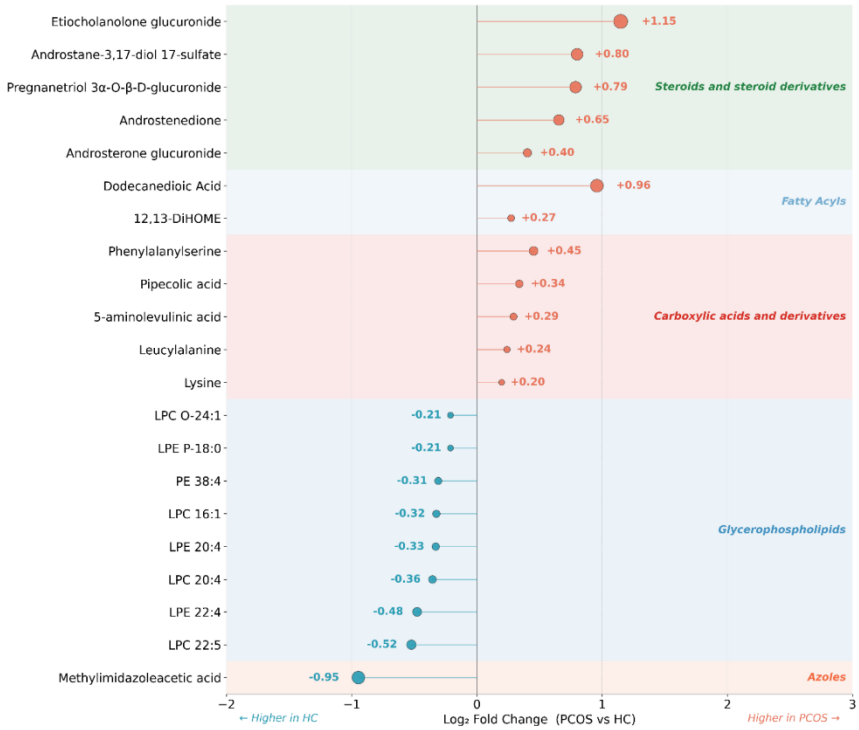


Figure 5. Bubble diverging plot of $\log_2$ fold change (Log_2FC) of annotated serum metabolites identified by Random Forest feature selection, grouped by chemical class. Bubble size is proportional to the absolute Log_2FC value. Metabolites with $Log_2FC > 0$ are elevated in PCOS relative to HC, while those with $Log_2FC < 0$ are elevated in HC. Only metabolites with $|Log_2FC| > 0.2$ are shown.

Spearman correlation analysis among annotated serum metabolites revealed a strong positive correlation cluster encompassing androgen conjugates, including etiocholanolone glucuronide, androsterone glucuronide, pregnanetriol 3α-O-β-D-glucuronide, and androstane-3,17-diol 17-sulfate (ρ = 0.55–0.66, FDR $q < 0.001$; Figure 6). In addition, androstenedione correlated positively with etiocholanolone glucuronide (ρ = 0.45, FDR q = 0.009). A second cluster comprised lysophosphatidylcholines (LPC 22:5, LPC 16:1, LPC 20:4; ρ = 0.60-0.73, FDR $q < 0.001$) and lysophosphatidylethanolamines (LPE 22:4, LPE 20:4; ρ = 0.74, FDR $q < 0.001$), with multiple significant cross-correlations between the two lipid subclasses (ρ = 0.49-0.69, FDR $q < 0.01$). SM 42:5;2O and SM 34:1;2O were significantly positively correlated (ρ = 0.55, FDR $q < 0.001$), and SM 34:1;2O correlated positively with LPC O-24:1 (ρ = 0.47, FDR q = 0.005). Additional significant positive correlations were observed between pipecolic acid and 2-pyrrolidinone (ρ = 0.47, FDR q = 0.005), and between lysine and creatine (ρ = 0.51, FDR q = 0.001).

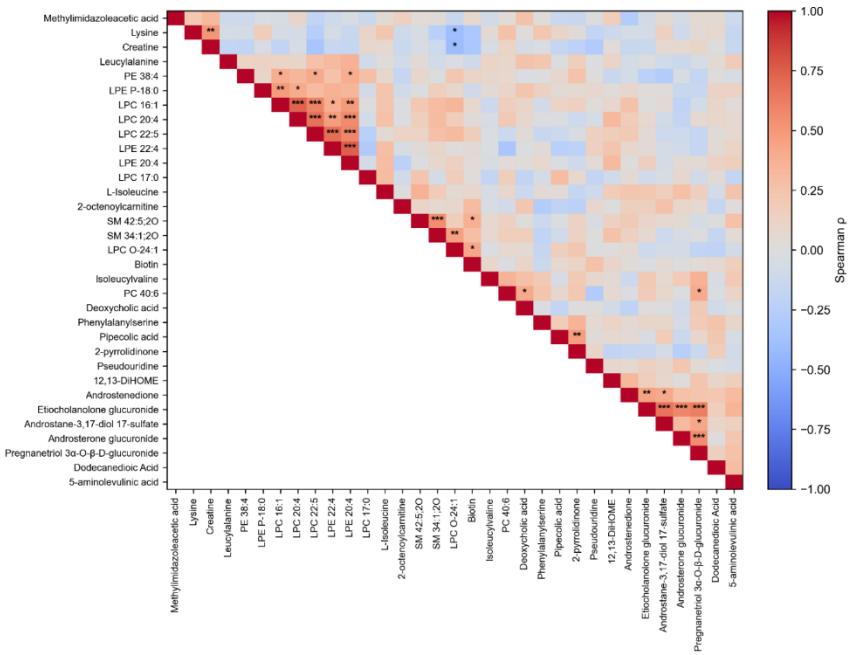


Figure 6. Heatmap of pairwise Spearman correlation coefficients among annotated serum metabolites. Correlations were calculated using $\log_{10}$-transformed peak heights. Analytes are ordered by hierarchical clustering. Only the upper triangle of the correlation matrix is displayed. Asterisks denote correlations that remained statistically significant after BH-FDR correction (* $q < 0.05$, ** $q < 0.01$, *** $q < 0.001$).

To further explore potential links between environmental exposure and serum metabolome, Spearman correlations were calculated between all urinary and serum BoEs and annotated serum metabolites. No statistically significant associations were observed after multiple-testing correction.

4. Discussion

This integrated non-target LC-HRMS analysis identified two complementary PCOS-associated signatures in this cohort: an increased urinary burden of multiple EDC and a serum metabolomic profile characterized by androgen excess and related lipid remodelling.

Women with PCOS showed a significantly higher urinary burden of several phthalate metabolites, together with higher levels of resorcinol and BuP. This pattern was further reflected in higher composite EDC and overall phthalate burden scores at the group level. Such cumulative metrics are particularly relevant in EDC research because real-life exposures occur as complex mixtures rather than as isolated chemicals. Their effects may combine in a dose-additive, and in some cases potentially synergistic, manner when individual compounds converge on shared endocrine targets or

downstream adverse outcomes, even when their primary mechanisms of action are only partly overlapping[37–39]. In the present exposomics profiling workflow, absolute cumulative exposure could not be estimated directly because the NTS approach yields only relative LC-HRMS signal intensities rather than calibrated concentrations, while LC-HRMS response depends strongly on compound-specific ionisation efficiency.. Accordingly, the robust Z-score should be interpreted as a relative measure of cumulative exposure burden rather than an estimate of absolute internal dose.

Metabolites within DEHP and DiNP clusters showed strong positive correlations, consistent with their origin from the same parent compound. Since phthalates are ubiquitous in everyday consumer products, the positive correlations among metabolites from different parent compounds likely reflect shared exposure sources[40], such as cosmetics, plastics, and food-contact materials. The strong positive correlation between oxybenzone and benzophenone-1 likely reflects both common exposure sources and metabolism. Oxybenzone is widely used as a UV filter in sunscreens, cosmetics, and plastics, while benzophenone-1 may occur as a related UV-filter compound and is also a known human metabolite of oxybenzone[41].

Despite no individual serum BoE reached statistical significance, Spearman correlation analysis revealed strong positive intercorrelations among the PFAS compounds (PFNA, PFOS, PFOA, PFHxS), consistent with their well-documented co-occurrence in human serum due to shared environmental sources and their long biological half-lives[42]. Further, propyl paraben significantly correlated with 3,5,6-trichloro-2-pyridinol, a metabolite associated with exposure to organophosphate insecticides. To the best of our knowledge, such correlation has not been reported before, and may indicate a shared route of exposure. Cross-matrix correlations between urinary and serum BoE were largely absent, except for MEP and resorcinol, which were the only analytes detected in both matrices. This was somewhat unexpected, as a higher number of cross-matrix BoE relationships was anticipated. However, only BoE detected with a DF >60% were included in the analysis, which likely limited the number of evaluable pairs. The significant cross-matrix correlations observed for MEP and resorcinol are therefore consistent with concurrent measurement of the same exposure across two biological compartments, rather than indicating independent biological associations, and they support the validity of the sampling and analytical approach. Although serum BoE did not yield significant between-group differences at the individual-compound level, it provided complementary information on co-occurring exposures, strengthening the exposomics characterisation of the cohort.

The BoEs that differed significantly between women with PCOS and HC are discussed below in the context of their potential biological relevance.

Phthalates are widespread organic contaminants extensively used in plastics, cosmetics, and pharmaceuticals[43]. They are metabolized and excreted mainly through urine, with exposure linked to reproductive toxicity, endocrine disruption, and ovarian dysfunction[44]. Epidemiological data from case-control studies comparing women with PCOS to HC remain limited, and reported phthalate concentrations have varied considerably across studies, partly due to differences in the biological matrix[43,45–47]. Our findings (Figure 2) are broadly consistent with results from the TREE cohort, where repeated urinary measurements showed positive associations of MBzP, MEHP, and ∑DEHP with PCOS prevalence, and MiBP, MBzP, and ∑DEHP with polycystic ovary[45]. Notably, MBzP, MEHP, and MiBP were also elevated in women with PCOS in our study (Figure 2). Moreover, the stronger associations observed for urinary phthalate mixtures than for single metabolites in the TREE cohort parallel the

pattern captured here by the overall phthalate burden score (Figure 3). A recent case-control study found significantly higher serum MEHP and DEHP concentrations in women with PCOS compared with HC, further supporting a link between phthalate exposure and PCOS[48]. These associations are biologically plausible because phthalates have been shown to perturb ovarian steroidogenesis and follicular function[23,49,50]. Experimental studies have demonstrated that DEHP can suppress oestradiol and progesterone production, disturb ovulation, and promote polycystic ovarian morphology in rodents[51], while MEHP has been shown to reduce aromatase activity and alter granulosa cell steroidogenesis in ways consistent with hyperandrogenism[52,53]. Although human evidence remains limited and not entirely consistent, the available data support the biological plausibility that phthalates may influence reproductive and metabolic pathways relevant to PCOS pathophysiology. However, further research is needed to confirm causality, particularly in light of potential genetic susceptibility to phthalate exposure as a contributing factor[54]. Establishing this will require larger, well-characterised prospective cohort studies with repeated biomonitoring measurements and standardised PCOS phenotyping.

Parabens are used as antimicrobials and preservatives in cosmetics, personal care products, pharmaceuticals, food, and beverages[55]. Their endocrine activity differs by alkyl chain length, with longer-chain parabens generally showing stronger estrogenic and anti-androgenic effects in vitro, making BuP among the more biologically active members of this class[21,56]. Although direct evidence linking paraben exposure to PCOS remains sparse, the elevated urinary BuP observed in our PCOS group is consistent with its known endocrine-disrupting potential and warrants further investigation[21,57,58].

Resorcinol is used both in industrial applications, such as the production of rubber products, wood adhesives, flame retardants, UV stabilisers, and dyes, and in personal care products, including hair dyes, anti-acne formulations, and chemical peels, making human exposure plausible[59,60]. While evidence linking resorcinol specifically to PCOS remains limited, resorcinol has documented thyroid-disrupting potential through inhibition of thyroid peroxidase, although epidemiological evidence at general-population exposure levels remains scarce[61].

Although the exposomics and metabolomics datasets represent distinct analytical dimensions, both provide relevant information on PCOS. Whereas BoEs describe the internal burden of selected environmental contaminants across the two analysed matrices, serum metabolites provide the end information on the biochemical state associated with the syndrome, helping identify altered pathways relevant to its pathophysiology. PCOS patients showed significant differences in serum metabolites across several biochemical classes. The clearest changes were observed in steroid metabolites, with elevated androstenedione and multiple androgen conjugates, consistent with the central role of androgen excess in PCOS. Alterations were also observed in glycerophospholipid composition and amino acid metabolism, indicating that the detected metabolomic differences involved both endocrine and broader metabolic pathways. Significantly altered serum metabolites are summarized in Table 1 and discussed below by biochemical class.

Steroids and derivatives. Among the annotated metabolites, the clearest group-level difference was observed within steroid-related compounds, with five steroid metabolites elevated in the PCOS patients, consistent with increased steroid turnover, a well-recognized hallmark of the syndrome[62,63]. Four of the elevated steroid metabolites were directly related to androgen metabolism, including

androstenedione and three downstream conjugated metabolites. Increased circulating **androstenedione** is an established biochemical feature of PCOS and has been associated with more pronounced metabolic and reproductive phenotypes. It is also considered diagnostically informative, particularly in women with clinical hyperandrogenism despite normal testosterone concentrations[64–67]. **Etiocholanolone glucuronide**, **androsterone glucuronide**, and **androstane-3,17-diol 17-sulfate** represent downstream conjugated metabolites of androgen catabolism. Higher concentrations of etiocholanolone glucuronide and androsterone glucuronide have previously been reported in PCOS cohorts[64,66,68], while increased androstane 3,17-diol 17-sulfate is consistent with increased downstream androgen reduction, despite not having been previously investigated in PCOS, to the best of our knowledge[69]. **Pregnanetriol 3α-O-β-D-glucuronide** differs from the other detected steroids in that it reflects downstream metabolism of progesterone-derived intermediates rather than direct androgen turnover. Although evidence for this specific conjugate in PCOS is limited, its elevation may indicate that altered steroidogenesis extends beyond androgen pathways. Together, these findings indicate that steroid-related differences in this cohort were not limited to a single androgen precursor but extended across several downstream metabolites.

Glycerophospholipids. Among non-steroid metabolites, glycerophospholipids showed the most coherent direction of change. Dyslipidaemia is one of the most consistent metabolic features of PCOS, and altered glycerophospholipid profiles have been described in both serum and urine[70,71]. A consistent decrease was observed across glycerophospholipid species in the PCOS group. Lower concentrations were observed for several lysophosphatidylcholines (LPCs), such as **LPC O-24:1**, **LPC 16:1**, **LPC 20:4**, and **LPC 22:5**, with LPC 22:5 and LPC 16:1 previously reported in PCOS[72]. Similar decreases in circulating LPC species have also been described in obesity and type 2 diabetes, where Barber et al. associated this pattern primarily with adiposity-related metabolic disturbance rather than insulin resistance itself[73]. Notably, reported directions of change in lysophospholipids are not uniform across PCOS metabolomics studies, which likely reflects differences in adiposity/insulin resistance distributions, fasting status, and analytical coverage[74]. A similar direction was observed for lysophosphatidylethanolamines (LPEs), including **LPE P-18:0**, **LPE 20:4**, and **LPE 22:4**. Among these, lower LPE 20:4 has also been reported previously in PCOS, whereas evidence for the remaining species remains limited[72]. PE 38:4 was also lower in the PCOS group, extending this pattern to phosphatidylethanolamines. The consistent direction across lysophospholipid subclasses supports disturbed membrane phospholipid turnover as a reproducible metabolic feature of PCOS in this cohort.

Fatty acids. Elevated **dodecanedioic acid and 12,13-DiHOME** point to alterations in fatty acid metabolism in PCOS. Increased circulating fatty acid availability, frequently reported in PCOS, particularly in insulin-resistant phenotypes, may exceed mitochondrial oxidative handling capacity and promote diversion toward non-canonical fatty acid oxidation pathways[75]. Although formed through distinct biochemical routes, both metabolites can be interpreted within this broader context. **Dodecanedioic acid** is a representative dicarboxylic acid generated through ω-oxidation, a minor pathway that becomes more relevant when mitochondrial β-oxidation is relatively limited or saturated[76]. Its elevation may reflect increased diversion of fatty acids toward this pathway under conditions of altered lipid utilization, although dodecanedioic acid itself has not been established as a specific biomarker of PCOS. **12,13-DiHOME,** a linoleic acid-derived oxylipin, may reflect either increased substrate availability or altered oxylipin production. Interpretation remains context-dependent, as circulating 12,13-DiHOME has been linked both to favourable metabolic adaptations,

such as enhanced fatty acid uptake, and to adverse cardiometabolic states depending on physiological context[77,78]. Although based on only two metabolites, both changes point in the same direction and support altered fatty-acid handling as part of the broader metabolic disturbance in PCOS.

Amino acid-related metabolites. Within the group of amino acid and peptide metabolites, all annotated compounds were elevated in the PCOS group, suggesting altered amino acid turnover. These included **lysine**, **pipecolic acid**, **phenylalanylserine**, and **leucylalanine**. **Lysine** has repeatedly been associated with insulin-resistant metabolic states, where elevated circulating concentrations are generally interpreted as reflecting impaired amino-acid utilization. Altered lysine concentrations have also been reported in PCOS, although the direction of change has not been consistent across studies[79–83]. This variability likely reflects differences in metabolic phenotype, particularly insulin resistance, adiposity, and cohort composition. **Pipecolic acid**, an intermediate of lysine catabolism, was elevated alongside lysine, which is biochemically consistent with altered lysine turnover. Direct evidence for pipecolic acid in PCOS remains limited, although increased circulating concentrations have been reported in insulin-resistant states[84]. Phenylalanylserine and leucylalanine have to date not been directly linked with PCOS. Their interpretation is therefore based on their constituent amino acids, for which elevated circulating levels of phenylalanine, leucine, and alanine have previously been reported in PCOS[17,79,85,86]. **5-Aminolevulinic acid,** an intermediate of mitochondrial heme biosynthesis, has likewise not been specifically described in PCOS, and its biological relevance in this context remains uncertain. Overall, this pattern suggests altered amino-acid turnover, although the small number of annotated compounds and limited compound-specific evidence warrant cautious interpretation.

Methylimidazoleacetic acid, the main oxidative metabolite of histamine, was decreased in the PCOS group. Direct evidence linking this metabolite to PCOS is currently lacking, and its biological relevance in this context remains uncertain.

Table 1: Summary of serum metabolites altered in PCOS relative to HC, with biochemical classification and supporting evidence from literature.

Metabolite	PCOS vs HC	Biochemical classification	Subclass	Main biochemical pathway	Evidence in PCOS
Etiocholanolone glucuronide	↑	Steroids and derivatives	Steroidal glycosides	Androgen metabolism	↑ (Maliqueo, 2015[68])
Androstane-3,17-diol 17-sulfate	↑		Sulphated steroids	Androgen metabolism, sulfation, and circulation/excretion	Related glucuronidated compounds reported (Fassnacht, 2003[69])
Pregnanetriol 3α-O-β-D-glucuronide	↑		Steroidal glycosides	Progesterone metabolism	No direct evidence
Androstenedione	↑		Androstane steroids	Androgen biosynthesis	↑ (Altinkilic, 2023[64]; Georgopoulos, 2014[65]; Cho, 2017[66])
Androsterone glucuronide	↑		Steroidal glycosides	Androgen metabolism	↑ (Altinkilic, 2023[64]; Cho, 2017[66])
Dodecanedioic Acid	↑	Fatty acyls	Fatty acids and conjugates	Fatty Acid ω-oxidation, peroxisomal β-oxidation	No direct evidence
12,13-DiHOME	↑		Fatty acids and conjugates	Linoleic acid epoxide metabolism	No direct evidence
Phenylalanylserine	↑	Carboxylic acids and derivatives	Amino acids, peptides, and analogues	Proteolysis, amino-acid metabolism	No direct evidence; Phenylalanine reported ↑ (Ye, 2022[79]; Paczkowska, 2023[85]; Yu, 2021[17]; Zhao, 2012[86]), and Serine reported ↑ (Ye, 2022[79])

Pipecolic acid	↑		Amino acids, peptides, and analogues	Lysine degradation	No direct evidence
Lysine	↑		Amino acids, peptides, and analogues	Amino-acid metabolism	Evidence mixed across cohorts: ↓(Sumithra N Unni, 2015[80]); ↑ (Ye, 2022[79]; Tang, 2019[81], Chang, 2017[82])
5-aminolevulinic acid	↑		Amino acids, peptides, and analogues	Heme/porphyrin biosynthesis, mitochondrial metabolism	No direct evidence
Leucylalanine	↑		Amino acids, peptides, and analogues	Proteolysis	No direct evidence; Leucine ↑ (Ye, 2023[79])
LPC O-24:1	↓	Glycerophospholipids	Glycerophosphocholines	Phospholipid remodelling	No direct evidence; dysregulations reported for related species (Yu, 2022[87], Haouls, 2014[88])
LPC 16:1	↓		Glycerophosphocholines	Phosphatidylcholine metabolism	↓ (Zhao, 2014[72])
LPC 20:4	↓		Glycerophosphocholines	Arachidonic acid-containing phospholipid remodelling	↑ (Yu, 2022[87])
LPC 22:5	↓		Glycerophosphocholines	PUFA phospholipid remodelling	↓ (Zhao, 2014[72])
LPE P-18:0	↓		Glycerophosphoethanolamines	PE/plasmogen remodelling	Related species reported ↓(Zhao, 2014[72])
LPE 20:4	↓		Glycerophosphoethanolamines	Arachidonic acid-containing phospholipid remodelling	↓ (Zhao, 2014[72])
LPE 22:4	↓		Glycerophosphoethanolamines	PUFA phospholipid turnover	Related species reported ↓(Zhao, 2014[72])
PE 38:4	↓		Glycerophosphoethanolamines	Membrane phospholipid metabolism	Related species reported ↓ (Haoula, 2014[88])
Methylimidazoleacetic acid	↓	Azoles	Imidazoles	Histidine/histamine metabolism	N/A

Limitations. When interpreting these results, several limitations of the study should be considered. First, the study was conducted in a relatively small cohort, limiting the statistical power, particularly for detecting modest group differences. PCOS is a metabolically heterogeneous syndrome, and despite the study exclusion criteria, variability in metabolic phenotype, including differences in insulin resistance and androgen status, may have contributed to the dispersion within the PCOS group. Second, as samples were collected at a single time point, the observed differences cannot distinguish whether elevated BoE and altered metabolites represent contributing factors to PCOS onset or consequences of the syndrome itself. The study, therefore, identifies associations but does not allow conclusions about temporal sequence or causality. Third, the HRMS-based NTS approach provides relative rather than absolute quantification. Although robust QA/QC procedures were applied, signal intensity depends on compound-specific ionisation efficiency, and cumulative exposure scores therefore reflect relative burden rather than true internal dose. In addition, only compounds detectable under the applied analytical conditions and retained after filtering criteria could be evaluated, meaning that parts of both the exposome and metabolome remain analytically inaccessible.

Significance and future directions. This study provides, to our knowledge, the first integrated NTS assessment of environmental BoE and serum metabolomic alterations in PCOS patients using a dual-matrix, dual-column LC-HRMS workflow. By combining two biological matrices, complementary chromatographic selectivities, and two analytical objectives within the same cohort, the approach

enabled broader chemical coverage than would be achievable with a single-matrix or single-platform design.

The results add two specific observations to the current PCOS field. First, the elevated urinary phthalate burden, together with increased BuP and resorcinol levels, further supports growing evidence that women with PCOS may carry a distinct profile of EDC exposure, particularly when considering cumulative urinary BoEs. Second, the serum metabolomic findings were not limited to elevated androstenedione but also included multiple downstream androgen conjugates together with a coherent decrease in lysophospholipid species, indicating that both altered steroid metabolism and disturbed membrane phospholipid turnover were detectable in this cohort. Furthermore, the results are consistent with targeted studies, which highlight the utility of NTS for identifying biologically meaningful PCOS-associated signals beyond predefined analytes. Taken together, the findings show that exposomics and serum metabolomics contributed complementary information on PCOS in this cohort.

Beyond previously reported metabolite alterations, several metabolites identified in this dataset have not yet been associated with PCOS and may therefore provide new mechanistic insights via NTS approach. These include dodecanedioic acid (ω-oxidation/peroxisomal β-oxidation), 12,13-DiHOME (linoleic-acid oxylipin/lipokine), pipecolic acid (lysine-pathway), 5-aminolevulinate (heme biosynthesis), and methylimidazoleacetic acid (histamine turnover). These signals should be interpreted as hypothesis-generating markers that point to biologically plausible pathways, including fatty-acid overflow and lipid signalling, altered amino-acid utilisation, mitochondrial/heme metabolism, and immune–metabolic processes. Future studies should confirm these candidates at higher annotation confidence, quantify them using targeted assays, and evaluate their added biological or clinical relevance beyond established endocrine and metabolic markers in independent, ideally longitudinal cohorts. Future work should also focus on further integration with additional molecular layers, such as proteomics or transcriptomics, which may help clarify whether the observed exposure patterns relate to specific biological pathways relevant to PCOS pathophysiology.

This work aligns with the objectives of the European Partnership for the Assessment of Risks from Chemicals (PARC) by demonstrating the value of integrated HRMS-based NTS for advancing human biomonitoring beyond predefined target analytes. The combination of BoE profiling with downstream molecular readouts illustrates how multi-layered approaches may support the identification of biologically relevant exposure signatures, improve understanding of cumulative and mixture-related effects, and contribute to the development of next-generation human biomonitoring strategies. In this context, the present workflow may serve as a proof-of-concept for future PARC-related studies aiming to integrate chemical exposure assessment with mechanistic health information in support of prevention and risk assessment.

Abbreviations

ACN, acetonitrile; AU, arbitrary units; BH-FDR, Benjamini-Hochberg false discovery rate; BMI, body mass index; BoE, biomarker of exposure; DDA, data-dependent acquisition; DF, detection frequency; EDCs, endocrine-disrupting chemicals; EtOAc, ethyl acetate; HC, healthy controls; HCD, higher-energy collisional dissociation; HESI, heated electrospray ionization; HILIC, hydrophilic interaction liquid

chromatography; HRMS, high-resolution mass spectrometry; IS, internal standard; LC-HRMS, liquid chromatography-high-resolution mass spectrometry; MDI, mean decrease in impurity; MeOH, methanol; MS, mass spectrometry; MS/MS, tandem mass spectrometry; NTS, non-targeted screening; PCOS, polycystic ovary syndrome; PFAS, per- and polyfluoroalkyl substances; QC, quality control; RF, Random Forest; ROC AUC, area under the receiver operating characteristic curve; RPLC, reversed-phase liquid chromatography; RSD, relative standard deviation; SG, specific gravity; SPE, solid-phase extraction.

Supporting information

-S1: Materials and chemicals, data preprocessing, modelling, class distribution of annotated BoE, and results of univariate statistical analysis of annotated metabolites (DOC).

-S2: Tables of reference standards, quality control results, identified BoEs, exposomics statistical results, Random Forest model performance, identified metabolites, and metabolomics statistical results (XLS).

Author contributions

ŽR and HP contributed equally and share the first authorship. Conceptualization: ŽR, HP, TK; Methodology: ŽR, HP, TK; Software: ŽR, HP, ŽT; Validation: ŽR, HP; Formal analysis: ŽR, HP; Investigation: ŽR, HP, IVK, MS, SIK; Resources: TK, IVK, MH; Writing – original draft: ŽR, HP, TK; Writing – review and editing: all; Visualization: ŽR, HP, SS, TK; Supervision: TK, MH; Project administration: TK, IVK, MH; Funding acquisition: MH, TK, IVK.

Acknowledgments

This work was supported by the project Partnership for the Assessment of Risks from Chemicals (PARC) funded by the European Union research and innovation program Horizon Europe [grant agreement 101057014]. The funding by the Slovenian Research and Innovation Agency – ARIS through the program group P-0134, and research projects J3-2530 and J7-50230 is acknowledged. Žan Rekar acknowledges ARIS for the Young Researcher grant. Žiga Tkalec acknowledges Slovenian Research and Innovation Agency (ARIS) under »krepitev mednarodne mobilnosti slovenskih raziskovalcev in raziskovalnih organizacij ter za spodbujanje mednarodne vpetosti slovenskih prijaviteljev« (C3.K8.IC) v okviru Načrta za okrevanje in odpornost (NOO) grant agreement MN-0034-106.

5. References

(1) Bozdag, G.; Mumusoglu, S.; Zengin, D.; Karabulut, E.; Yildiz, B. O. The Prevalence and Phenotypic Features of Polycystic Ovary Syndrome: A Systematic Review and Meta-Analysis. *Hum Reprod* **2016**, *31* (12), 2841–2855. https://doi.org/10.1093/humrep/dew218.

(2) Azziz, R.; Woods, K. S.; Reyna, R.; Key, T. J.; Knochenhauer, E. S.; Yildiz, B. O. The Prevalence and Features of the Polycystic Ovary Syndrome in an Unselected Population. *J Clin Endocrinol Metab* **2004**, *89* (6), 2745–2749. https://doi.org/10.1210/jc.2003-032046.

(3) Stener-Victorin, E.; Teede, H.; Norman, R. J.; Legro, R.; Goodarzi, M. O.; Dokras, A.; Laven, J.; Hoeger, K.; Piltonen, T. T. Polycystic Ovary Syndrome. *Nature Reviews Disease Primers* **2024**, *10* (1), 27. https://doi.org/10.1038/s41572-024-00511-3.

(4) Revised 2003 Consensus on Diagnostic Criteria and Long-Term Health Risks Related to Polycystic Ovary Syndrome. *Fertility and Sterility* **2004**, *81* (1), 19–25. https://doi.org/10.1016/j.fertnstert.2003.10.004.

(5) Teede, H. J.; Tay, C. T.; Laven, J. J. E.; Dokras, A.; Moran, L. J.; Piltonen, T. T.; Costello, M. F.; Boivin, J.; Redman, L. M.; Boyle, J. A.; Norman, R. J.; Mousa, A.; Joham, A. E.; on behalf of the International PCOS Network. Recommendations From the 2023 International Evidence-Based Guideline for the Assessment and Management of Polycystic Ovary Syndrome. *J Clin Endocrinol Metab* **2023**, *108* (10), 2447–2469. https://doi.org/10.1210/clinem/dgad463.

(6) Zhang, H.; Wang, W.; Zhao, J.; Jiao, P.; Zeng, L.; Zhang, H.; Zhao, Y.; Shi, L.; Hu, H.; Luo, L.; Fukuzawa, I.; Li, D.; Li, R.; Qiao, J. Relationship between Body Composition, Insulin Resistance, and Hormonal Profiles in Women with Polycystic Ovary Syndrome. *Front. Endocrinol.* **2023**, *13*, 1085656. https://doi.org/10.3389/fendo.2022.1085656.

(7) Helvaci, N.; Yildiz, B. O. Polycystic Ovary Syndrome as a Metabolic Disease. *Nature Reviews Endocrinology* **2025**, *21* (4), 230–244. https://doi.org/10.1038/s41574-024-01057-w.

(8) Wolf, W. M.; Wattick, R. A.; Kinkade, O. N.; Olfert, M. D. Geographical Prevalence of Polycystic Ovary Syndrome as Determined by Region and Race/Ethnicity. *International Journal of Environmental Research and Public Health* **2018**, *15* (11).

(9) Azziz, R.; Carmina, E.; Dewailly, D.; Diamanti-Kandarakis, E.; Escobar-Morreale, H. F.; Futterweit, W.; Janssen, O. E.; Legro, R. S.; Norman, R. J.; Taylor, A. E.; Witchel, S. F. The Androgen Excess and PCOS Society Criteria for the Polycystic Ovary Syndrome: The Complete Task Force Report. *Fertility and Sterility* **2009**, *91* (2), 456–488. https://doi.org/10.1016/j.fertnstert.2008.06.035.

(10) Christ, J. P.; Cedars, M. I. Current Guidelines for Diagnosing PCOS. *Diagnostics* **2023**, *13* (6). https://doi.org/10.3390/diagnostics13061113.

(11) Fauser, B. C. J. M.; Tarlatzis, B. C.; Rebar, R. W.; Legro, R. S.; Balen, A. H.; Lobo, R.; Carmina, E.; Chang, J.; Yildiz, B. O.; Laven, J. S. E.; Boivin, J.; Petraglia, F.; Wijeyeratne, C. N.; Norman, R. J.; Dunaif, A.; Franks, S.; Wild, R. A.; Dumesic, D.; Barnhart, K. Consensus on Women's Health Aspects of Polycystic Ovary Syndrome (PCOS): The Amsterdam

ESHRE/ASRM-Sponsored 3rd PCOS Consensus Workshop Group. *Fertility and Sterility* **2012**, *97* (1), 28-38.e25. https://doi.org/10.1016/j.fertnstert.2011.09.024.

(12) Hajam, Y. A.; Rather, H. A.; Neelam; Kumar, R.; Basheer, M.; Reshi, M. S. A Review on Critical Appraisal and Pathogenesis of Polycystic Ovarian Syndrome. *Endocrine and Metabolic Science* **2024**, *14*, 100162. https://doi.org/10.1016/j.endmts.2024.100162.

(13) Chen, W.; Pang, Y. Metabolic Syndrome and PCOS: Pathogenesis and the Role of Metabolites. *Metabolites* **2021**, *11* (12). https://doi.org/10.3390/metabo11120869.

(14) Zhou, M.; Yu, J.; Li, X.; Ruan, Z.; Yu, S. Role of the Gut Microbiota and Innate Immunity in Polycystic Ovary Syndrome: Current Updates and Future Prospects. *Journal of Cellular and Molecular Medicine* **2024**, *28* (8), e18258. https://doi.org/10.1111/jcmm.18258.

(15) Rajska, A.; Buszewska-Forajta, M.; Rachoń, D.; Markuszewski, M. J. Metabolomic Insight into Polycystic Ovary Syndrome—An Overview. *International Journal of Molecular Sciences* **2020**, *21* (14). https://doi.org/10.3390/ijms21144853.

(16) Patel, J.; Chaudhary, H.; Chudasama, A.; Panchal, J.; Trivedi, A.; Panchal, S.; Joshi, T.; Joshi, R. Comparing the Metabolomic Landscape of Polycystic Ovary Syndrome within Urban and Rural Environments. *Communications Medicine* **2025**, *5* (1), 253. https://doi.org/10.1038/s43856-025-00985-6.

(17) Yu, Y.; Tan, P.; Zhuang, Z.; Wang, Z.; Zhu, L.; Qiu, R.; Xu, H. Untargeted Metabolomic Approach to Study the Serum Metabolites in Women with Polycystic Ovary Syndrome. *BMC Medical Genomics* **2021**, *14* (1), 206. https://doi.org/10.1186/s12920-021-01058-y.

(18) Zhao, T.; Xiao, X.; Li, L.; Zhu, J.; He, W.; Zhang, Q.; Wu, J.; Wu, X.; Yuan, T. Changes in the Serum Metabolomics of Polycystic Ovary Syndrome before and after Compound Oral Contraceptive Treatment. *Front. Endocrinol.* **2024**, *15*, 1354214. https://doi.org/10.3389/fendo.2024.1354214.

(19) Li, J.; Xie, L.-M.; Song, J.-L.; Yau, L.-F.; Mi, J.-N.; Zhang, C.-R.; Wu, W.-T.; Lai, M.-H.; Jiang, Z.-H.; Wang, J.-R.; Ma, H.-X. Alterations of Sphingolipid Metabolism in Different Types of Polycystic Ovary Syndrome. *Scientific Reports* **2019**, *9* (1), 3204. https://doi.org/10.1038/s41598-019-38944-6.

(20) Halama, A.; Aye, M. M.; Dargham, S. R.; Kulinski, M.; Suhre, K.; Atkin, S. L. Metabolomics of Dynamic Changes in Insulin Resistance Before and After Exercise in PCOS. *Front. Endocrinol.* **2019**, *10*, 116. https://doi.org/10.3389/fendo.2019.00116.

(21) Srnovršnik, T.; Virant-Klun, I.; Pinter, B. Polycystic Ovary Syndrome and Endocrine Disruptors (Bisphenols, Parabens, and Triclosan)—A Systematic Review. *Life* **2023**, *13* (1). https://doi.org/10.3390/life13010138.

(22) Jala, A.; Varghese, B.; Kaur, G.; Rajendiran, K.; Dutta, R.; Adela, R.; Borkar, R. M. Implications of Endocrine-Disrupting Chemicals on Polycystic Ovarian Syndrome: A Comprehensive Review. *Environmental Science and Pollution Research* **2022**, *29* (39), 58484–58513. https://doi.org/10.1007/s11356-022-21612-0.

(23) Jozkowiak, M.; Piotrowska-Kempisty, H.; Kobylarek, D.; Gorska, N.; Mozdziak, P.; Kempisty, B.; Rachon, D.; Spaczynski, R. Z. Endocrine Disrupting Chemicals in Polycystic Ovary Syndrome: The Relevant Role of the Theca and Granulosa Cells in the Pathogenesis of the Ovarian Dysfunction. *Cells* **2022**, *12* (1). https://doi.org/10.3390/cells12010174.

(24) Kandaraki, E.; Chatzigeorgiou, A.; Livadas, S.; Palioura, E.; Economou, F.; Koutsilieris, M.; Palimeri, S.; Panidis, D.; Diamanti-Kandarakis, E. Endocrine Disruptors and Polycystic Ovary Syndrome (PCOS): Elevated Serum Levels of Bisphenol A in Women with PCOS. *J Clin Endocrinol Metab* **2011**, *96* (3), E480–E484. https://doi.org/10.1210/jc.2010-1658.

(25) Srnovršnik, T.; Pinter, B.; Horvat, M.; Tratnik, J. S.; Falnoga, I.; Mazej, D.; Verdenik, I.; Virant-Klun, I. Association of Trace Elements with Polycystic Ovary Syndrome in Women—A Case-Control Study. *Metabolites* **2025**, *15* (2). https://doi.org/10.3390/metabo15020079.

(26) Plešnik, H.; Rekar, Ž.; Stevanović, S.; Virant-Klun, I.; Imamović Kumalić, S.; Sladič, M.; Mazej, D.; Tratnik, J. S.; Horvat, M.; Kosjek, T. Nontargeted Urinary Profiling Strategy for Endocrine-Disrupting Chemicals in Women with Ovarian Malignancies. *Environ. Sci. Technol.* **2025**, *59* (17), 8380–8390. https://doi.org/10.1021/acs.est.4c13290.

(27) Tkalec, Ž.; Codling, G.; Tratnik, J. S.; Mazej, D.; Klánová, J.; Horvat, M.; Kosjek, T. Suspect and Non-Targeted Screening-Based Human Biomonitoring Identified 74 Biomarkers of Exposure in Urine of Slovenian Children. *Environmental Pollution* **2022**, *313*, 120091. https://doi.org/10.1016/j.envpol.2022.120091.

(28) Schmid, R.; Heuckeroth, S.; Korf, A.; Smirnov, A.; Myers, O.; Dyrlund, T. S.; Bushuiev, R.; Murray, K. J.; Hoffmann, N.; Lu, M.; Sarvepalli, A.; Zhang, Z.; Fleischauer, M.; Dührkop, K.; Wesner, M.; Hoogstra, S. J.; Rudt, E.; Mokshyna, O.; Brungs, C.; Ponomarov, K.; Mutabdžija, L.; Damiani, T.; Pudney, C. J.; Earll, M.; Helmer, P. O.; Fallon, T. R.; Schulze, T.; Rivas-Ubach, A.; Bilbao, A.; Richter, H.; Nothias, L.-F.; Wang, M.; Orešič, M.; Weng, J.-K.; Böcker, S.; Jeibmann, A.; Hayen, H.; Karst, U.; Dorrestein, P. C.; Petras, D.; Du, X.; Pluskal, T. Integrative Analysis of Multimodal Mass Spectrometry Data in MZmine 3. *Nature Biotechnology* **2023**, *41* (4), 447–449. https://doi.org/10.1038/s41587-023-01690-2.

(29) Schymanski, E. L.; Jeon, J.; Gulde, R.; Fenner, K.; Ruff, M.; Singer, H. P.; Hollender, J. Identifying Small Molecules via High Resolution Mass Spectrometry: Communicating Confidence. *Environ. Sci. Technol.* **2014**, *48* (4), 2097–2098. https://doi.org/10.1021/es5002105.

(30) *MassBank of North America*. https://mona.fiehnlab.ucdavis.edu/ (accessed 2025-11-27).

(31) Horai, H.; Arita, M.; Kanaya, S.; Nihei, Y.; Ikeda, T.; Suwa, K.; Ojima, Y.; Tanaka, K.; Tanaka, S.; Aoshima, K.; Oda, Y.; Kakazu, Y.; Kusano, M.; Tohge, T.; Matsuda, F.; Sawada, Y.; Hirai, M. Y.; Nakanishi, H.; Ikeda, K.; Akimoto, N.; Maoka, T.; Takahashi, H.; Ara, T.; Sakurai, N.; Suzuki, H.; Shibata, D.; Neumann, S.; Iida, T.; Tanaka, K.; Funatsu, K.; Matsuura, F.; Soga, T.; Taguchi, R.; Saito, K.; Nishioka, T. MassBank: A Public Repository for Sharing Mass Spectral Data for Life Sciences. *Journal of Mass Spectrometry* **2010**, *45* (7), 703–714. https://doi.org/10.1002/jms.1777.

(32) Wishart, D. S.; Guo, A.; Oler, E.; Wang, F.; Anjum, A.; Peters, H.; Dizon, R.; Sayeeda, Z.; Tian, S.; Lee, B. L.; Berjanskii, M.; Mah, R.; Yamamoto, M.; Jovel, J.; Torres-Calzada, C.; Hiebert-Giesbrecht, M.; Lui, V. W.; Varshavi, D.; Varshavi, D.; Allen, D.; Arndt, D.; Khetarpal, N.; Sivakumaran, A.; Harford, K.; Sanford, S.; Yee, K.; Cao, X.; Budinski, Z.; Liigand, J.; Zhang, L.; Zheng, J.; Mandal, R.; Karu, N.; Dambrova, M.; Schiöth, H. B.; Greiner, R.; Gautam, V. HMDB 5.0: The Human Metabolome Database for 2022. *Nucleic Acids Research* **2022**, *50* (D1), D622–D631. https://doi.org/10.1093/nar/gkab1062.

(33) Wang, M.; Carver, J. J.; Phelan, V. V.; Sanchez, L. M.; Garg, N.; Peng, Y.; Nguyen, D. D.; Watrous, J.; Kapono, C. A.; Luzzatto-Knaan, T.; Porto, C.; Bouslimani, A.; Melnik, A. V.; Meehan, M. J.; Liu, W.-T.; Crüsemann, M.; Boudreau, P. D.; Esquenazi, E.; Sandoval-Calderón, M.; Kersten, R. D.; Pace, L. A.; Quinn, R. A.; Duncan, K. R.; Hsu, C.-C.; Floros, D. J.; Gavilan, R. G.; Kleigrewe, K.; Northen, T.; Dutton, R. J.; Parrot, D.; Carlson, E. E.; Aigle, B.; Michelsen, C. F.; Jelsbak, L.; Sohlenkamp, C.; Pevzner, P.; Edlund, A.; McLean, J.; Piel, J.; Murphy, B. T.; Gerwick, L.; Liaw, C.-C.; Yang, Y.-L.; Humpf, H.-U.; Maansson, M.; Keyzers, R. A.; Sims, A. C.; Johnson, A. R.; Sidebottom, A. M.; Sedio, B. E.; Klitgaard, A.; Larson, C. B.; Boya P, C. A.; Torres-Mendoza, D.; Gonzalez, D. J.; Silva, D. B.; Marques, L. M.; Demarque, D. P.; Pociute, E.; O'Neill, E. C.; Briand, E.; Helfrich, E. J. N.; Granatosky, E. A.; Glukhov, E.; Ryffel, F.; Houson, H.; Mohimani, H.; Kharbush, J. J.; Zeng, Y.; Vorholt, J. A.; Kurita, K. L.; Charusanti, P.; McPhail, K. L.; Nielsen, K. F.; Vuong, L.; Elfeki, M.; Traxler, M. F.; Engene, N.; Koyama, N.; Vining, O. B.; Baric, R.; Silva, R. R.; Mascuch, S. J.; Tomasi, S.; Jenkins, S.; Macherla, V.; Hoffman, T.; Agarwal, V.; Williams, P. G.; Dai, J.; Neupane, R.; Gurr, J.; Rodríguez, A. M. C.; Lamsa, A.; Zhang, C.; Dorrestein, K.; Duggan, B. M.; Almaliti, J.; Allard, P.-M.; Phapale, P.; Nothias, L.-F.; Alexandrov, T.; Litaudon, M.; Wolfender, J.-L.; Kyle, J. E.; Metz, T. O.; Peryea, T.; Nguyen, D.-T.; VanLeer, D.; Shinn, P.; Jadhav, A.; Müller, R.; Waters, K. M.; Shi, W.; Liu, X.; Zhang, L.; Knight, R.; Jensen, P. R.; Palsson, B. Ø.; Pogliano, K.; Linington, R. G.; Gutiérrez, M.; Lopes, N. P.; Gerwick, W. H.; Moore, B. S.; Dorrestein, P. C.; Bandeira, N. Sharing and Community Curation of Mass Spectrometry Data with Global Natural Products Social Molecular Networking. *Nature Biotechnology* **2016**, *34* (8), 828–837. https://doi.org/10.1038/nbt.3597.

(34) Dührkop, K.; Fleischauer, M.; Ludwig, M.; Aksenov, A. A.; Melnik, A. V.; Meusel, M.; Dorrestein, P. C.; Rousu, J.; Böcker, S. SIRIUS 4: A Rapid Tool for Turning Tandem Mass

Spectra into Metabolite Structure Information. *Nature Methods* **2019**, *16* (4), 299–302. https://doi.org/10.1038/s41592-019-0344-8.

(35) Kanehisa, M.; Goto, S. KEGG: Kyoto Encyclopedia of Genes and Genomes. *Nucleic Acids Res* **2000**, *28* (1), 27–30. https://doi.org/10.1093/nar/28.1.27.

(36) Hastings, J.; Owen, G.; Dekker, A.; Ennis, M.; Kale, N.; Muthukrishnan, V.; Turner, S.; Swainston, N.; Mendes, P.; Steinbeck, C. ChEBI in 2016: Improved Services and an Expanding Collection of Metabolites. *Nucleic Acids Res* **2016**, *44* (D1), D1214–D1219. https://doi.org/10.1093/nar/gkv1031.

(37) Kortenkamp, A. Ten Years of Mixing Cocktails: A Review of Combination Effects of Endocrine-Disrupting Chemicals. *Environ Health Perspect* **2007**, *115* (Suppl 1), 98–105. https://doi.org/10.1289/ehp.9357.

(38) Kortenkamp, A. Low Dose Mixture Effects of Endocrine Disrupters: Implications for Risk Assessment and Epidemiology. *International Journal of Andrology* **2008**, *31* (2), 233–240. https://doi.org/10.1111/j.1365-2605.2007.00862.x.

(39) Christiansen, S.; Scholze, M.; Dalgaard, M.; Vinggaard, A. M.; Axelstad, M.; Kortenkamp, A.; Hass, U. Synergistic Disruption of External Male Sex Organ Development by a Mixture of Four Antiandrogens. *Environ Health Perspect* **2009**, *117* (12), 1839–1846. https://doi.org/10.1289/ehp.0900689.

(40) Runkel, A. A.; Mazej, D.; Snoj Tratnik, J.; Tkalec, Ž.; Kosjek, T.; Horvat, M. Exposure of Men and Lactating Women to Environmental Phenols, Phthalates, and DINCH. *Chemosphere* **2022**, *286*, 131858. https://doi.org/10.1016/j.chemosphere.2021.131858.

(41) Mustieles, V.; Balogh, R. K.; Axelstad, M.; Montazeri, P.; Márquez, S.; Vrijheid, M.; Draskau, M. K.; Taxvig, C.; Peinado, F. M.; Berman, T.; Frederiksen, H.; Fernández, M. F.; Marie Vinggaard, A.; Andersson, A.-M. Benzophenone-3: Comprehensive Review of the Toxicological and Human Evidence with Meta-Analysis of Human Biomonitoring Studies. *Environment International* **2023**, *173*, 107739. https://doi.org/10.1016/j.envint.2023.107739.

(42) Panel), E. P. on C. in the F. C. (EFSA C.; Schrenk, D.; Bignami, M.; Bodin, L.; Chipman, J. K.; del Mazo, J.; Grasl-Kraupp, B.; Hogstrand, C.; Hoogenboom, L. (Ron); Leblanc, J.-C.; Nebbia, C. S.; Nielsen, E.; Ntzani, E.; Petersen, A.; Sand, S.; Vleminckx, C.; Wallace, H.; Barregård, L.; Ceccatelli, S.; Cravedi, J.-P.; Halldorsson, T. I.; Haug, L. S.; Johansson, N.; Knutsen, H. K.; Rose, M.; Roudot, A.-C.; Van Loveren, H.; Vollmer, G.; Mackay, K.; Riolo, F.; Schwerdtle, T. Risk to Human Health Related to the Presence of Perfluoroalkyl Substances in Food. *EFSA Journal* **2020**, *18* (9), e06223. https://doi.org/10.2903/j.efsa.2020.6223.

(43) Neuvonen, R.; Huovinen, M.; Dorman, D. C.; Laitinen, H.; Sahlman, H. Phthalates and Polycystic Ovary Syndrome – Systematic Literature Review. *Reproductive Toxicology* **2023**, *121*, 108473. https://doi.org/10.1016/j.reprotox.2023.108473.

(44) Zhang, Y.-J.; Guo, J.-L.; Xue, J.; Bai, C.-L.; Guo, Y. Phthalate Metabolites: Characterization, Toxicities, Global Distribution, and Exposure Assessment. *Environmental Pollution* **2021**, *291*, 118106. https://doi.org/10.1016/j.envpol.2021.118106.

(45) Zhang, M.; Liu, C.; Yuan, X.-Q.; Cui, F.-P.; Miao, Y.; Yao, W.; Qin, D.-Y.; Deng, Y.-L.; Chen, P.-P.; Zeng, J.-Y.; Liu, X.-Y.; Wu, Y.; Li, C.-R.; Lu, W.-Q.; Li, Y.-F.; Zeng, Q. Individual and Joint Associations of Urinary Phthalate Metabolites with Polycystic Ovary and Polycystic Ovary Syndrome: Results from the TREE Cohort. *Environmental Toxicology and Pharmacology* **2023**, *102*, 104233. https://doi.org/10.1016/j.etap.2023.104233.

(46) Al-Saleh, I. The Relationship between Urinary Phthalate Metabolites and Polycystic Ovary Syndrome in Women Undergoing in Vitro Fertilization: Nested Case-Control Study. *Chemosphere* **2022**, *286*, 131495. https://doi.org/10.1016/j.chemosphere.2021.131495.

(47) Zhou, W.; Lei, S.; Lv, H.; Jiang, Y.; Sun, T.; Zhang, Y.; Ma, H.; Wu, J.; Lin, Y. Association of Urinary Phthalate Metabolites and Polycystic Ovary Syndrome in Women Undergoing in Vitro Fertilization. *Reproductive Toxicology* **2025**, *137*, 109041. https://doi.org/10.1016/j.reprotox.2025.109041.

(48) Patel, J.; Chaudhary, H.; Panchal, S.; Rajput, K.; Joshi, R. Investigating the Impact of Phthalate Exposure on Endocrine Function in Women with Polycystic Ovary Syndrome. *BMC Endocrine Disorders* **2026**, *26* (1), 42. https://doi.org/10.1186/s12902-026-02166-5.

(49) Craig, Z. R.; Wang, W.; Flaws, J. A. Endocrine-Disrupting Chemicals in Ovarian Function: Effects on Steroidogenesis, Metabolism and Nuclear Receptor Signaling. *Reproduction* **2011**, *142* (5), 633–646. https://doi.org/10.1530/REP-11-0136.

(50) Hannon, P. R.; Flaws, J. A. The Effects of Phthalates on the Ovary. *Front. Endocrinol.* **2015**, *6*. https://doi.org/10.3389/fendo.2015.00008.

(51) Davis, B. J.; Maronpot, R. R.; Heindel, J. J. Di-(2-Ethylhexyl) Phthalate Suppresses Estradiol and Ovulation in Cycling Rats. *Toxicology and Applied Pharmacology* **1994**, *128* (2), 216–223. https://doi.org/10.1006/taap.1994.1200.

(52) Reinsberg, J.; Wegener-Toper, P.; van der Ven, K.; van der Ven, H.; Klingmueller, D. Effect of Mono-(2-Ethylhexyl) Phthalate on Steroid Production of Human Granulosa Cells. *Toxicology and Applied Pharmacology* **2009**, *239* (1), 116–123. https://doi.org/10.1016/j.taap.2009.05.022.

(53) Lovekamp-Swan, T.; Davis, B. Mechanisms of Phthalate Ester Toxicity in the Female Reproductive System. *Environ Health Perspectives* **2003**, *111* (2), 139–145. https://doi.org/10.1289/ehp.5658.

(54) Stajnko, A.; Runkel, A. A.; Kosjek, T.; Snoj Tratnik, J.; Mazej, D.; Falnoga, I.; Horvat, M. Assessment of Susceptibility to Phthalate and DINCH Exposure through CYP and UGT Single Nucleotide Polymorphisms. *Environment International* **2022**, *159*, 107046. https://doi.org/10.1016/j.envint.2021.107046.

(55) Tkalec, Ž.; Kosjek, T.; Snoj Tratnik, J.; Stajnko, A.; Runkel, A. A.; Sykiotou, M.; Mazej, D.; Horvat, M. Exposure of Slovenian Children and Adolescents to Bisphenols, Parabens and Triclosan: Urinary Levels, Exposure Patterns, Determinants of Exposure and Susceptibility. *Environment International* **2021**, *146*, 106172. https://doi.org/10.1016/j.envint.2020.106172.

(56) Boberg, J.; Taxvig, C.; Christiansen, S.; Hass, U. Possible Endocrine Disrupting Effects of Parabens and Their Metabolites. *Reproductive Toxicology* **2010**, *30* (2), 301–312. https://doi.org/10.1016/j.reprotox.2010.03.011.

(57) Özer, Ö. F.; İbrahimoğlu, A. Z.; Gül, A. Z.; Demirel, M.; Ateş, S.; Taha, H. S.; İbrahimoğlu, M.; Selek, Ş. Mass Spectrometry-Based Untargeted Metabolomics Study of Polycystic Ovary Syndrome. *Journal of Ovarian Research* **2025**, *18* (1), 255. https://doi.org/10.1186/s13048-025-01842-9.

(58) ŠIMKOVÁ, M.; VÍTKŮ, J.; KOLÁTOROVÁ, L.; VRBÍKOVÁ, J.; VOSÁTKOVÁ, M.; VČELÁK, J.; DUŠKOVÁ, M. Endocrine Disruptors, Obesity, and Cytokines - How Relevant Are They to PCOS? *Physiol Res* **2020**, *69* (Suppl 2), S279–S293. https://doi.org/10.33549/physiolres.934521.

(59) Sciarrillo, R.; Falzarano, A.; Gallicchio, V.; Carrella, F.; Chianese, T.; Mileo, A.; De Falco, M. Resorcinol as “endocrine Disrupting Chemical": Are Thyroid-Related Adverse Effects Adequately Documented in Reptiles? *In Vivo* Experimentation in Lizard *Podarcis Siculus*. *Chemosphere* **2024**, *364*, 143009. https://doi.org/10.1016/j.chemosphere.2024.143009.

(60) *Resorcinol: Volume 71*; 2012.

(61) Pasquier, E.; Viguié, C.; Fini, J.-B.; Mhaouty-Kodja, S.; Michel-Caillet, C. Limits of the Regulatory Evaluation of Resorcinol as a Thyroid Disruptor: When Limited Experimental Data Challenge Established Effects in Humans. *Environmental Research* **2023**, *222*, 115330. https://doi.org/10.1016/j.envres.2023.115330.

(62) Ye, W.; Xie, T.; Song, Y.; Zhou, L. The Role of Androgen and Its Related Signals in PCOS. *J Cell Mol Med.* **2021**, *25* (4), 1825–1837. https://doi.org/10.1111/jcmm.16205.

(63) Ghafari, A.; Maftoohi, M.; Samarin, M. E.; Barani, S.; Banimohammad, M.; Samie, R. The Last Update on Polycystic Ovary Syndrome(PCOS), Diagnosis Criteria, and Novel Treatment. *Endocrine and Metabolic Science* **2025**, *17*, 100228. https://doi.org/10.1016/j.endmts.2025.100228.

(64) Altinkilic, E. M.; du Toit, T.; Sakin, Ö.; Attar, R.; Groessl, M.; Flück, C. E. The Serum Steroid Signature of PCOS Hints at the Involvement of Novel Pathways for Excess Androgen Biosynthesis. *The Journal of Steroid Biochemistry and Molecular Biology* **2023**, *233*, 106366. https://doi.org/10.1016/j.jsbmb.2023.106366.

(65) Georgopoulos, N. A.; Papadakis, E.; Armeni, A. K.; Katsikis, I.; Roupas, N. D.; Panidis, D. Elevated Serum Androstenedione Is Associated with a More Severe Phenotype in Women with Polycystic Ovary Syndrome (PCOS). *Hormones* **2014**, *13* (2), 213–221. https://doi.org/10.1007/BF03401335.

(66) Cho, L.-W.; Sathyapalan, T.; Kilpatrick, E. S.; Keevil, B. G.; Miller, A. G.; Coady, A. M.; Ahmed, L.; Atkin, S. L. Androsterone Glucuronide to Dehydroepiandrosterone Sulphate Ratio Is Discriminatory for Obese Caucasian Women with Polycystic Ovary Syndrome. *BMC Endocrine Disorders* **2017**, *17* (1), 26. https://doi.org/10.1186/s12902-017-0177-3.

(67) Bizuneh, A. D.; Joham, A. E.; Teede, H.; Mousa, A.; Earnest, A.; Hawley, J. M.; Smith, L.; Azziz, R.; Arlt, W.; Tay, C. T. Evaluating the Diagnostic Accuracy of Androgen Measurement in Polycystic Ovary Syndrome: A Systematic Review and Diagnostic Meta-Analysis to Inform Evidence-Based Guidelines. *Hum Reprod Update* **2025**, *31* (1), 48–63. https://doi.org/10.1093/humupd/dmae028.

(68) Maliqueo, M.; Sundström Poromaa, I.; Vanky, E.; Fornes, R.; Benrick, A.; Åkerud, H.; Stridsklev, S.; Labrie, F.; Jansson, T.; Stener-Victorin, E. Placental STAT3 Signaling Is Activated in Women with Polycystic Ovary Syndrome. *Hum Reprod* **2015**, *30* (3), 692–700. https://doi.org/10.1093/humrep/deu351.

(69) Fassnacht, M.; Schlenz, N.; Schneider, S. B.; Wudy, S. A.; Allolio, B.; Arlt, W. Beyond Adrenal and Ovarian Androgen Generation: Increased Peripheral 5α-Reductase Activity in Women with Polycystic Ovary Syndrome. *J Clin Endocrinol Metab* **2003**, *88* (6), 2760–2766. https://doi.org/10.1210/jc.2002-021875.

(70) Sun, L.; Hu, W.; Liu, Q.; Hao, Q.; Sun, B.; Zhang, Q.; Mao, S.; Qiao, J.; Yan, X. Metabonomics Reveals Plasma Metabolic Changes and Inflammatory Marker in Polycystic Ovary Syndrome Patients. *J. Proteome Res.* **2012**, *11* (5), 2937–2946. https://doi.org/10.1021/pr3000317.

(71) Wang, W.; Wang, S.; Tan, S.; Wen, M.; Qian, Y.; Zeng, X.; Guo, Y.; Yu, C. Detection of Urine Metabolites in Polycystic Ovary Syndrome by UPLC Triple-TOF-MS. *Clinica Chimica Acta* **2015**, *448*, 39–47. https://doi.org/10.1016/j.cca.2015.06.008.

(72) Zhao, X.; Xu, F.; Qi, B.; Hao, S.; Li, Y.; Li, Y.; Zou, L.; Lu, C.; Xu, G.; Hou, L. Serum Metabolomics Study of Polycystic Ovary Syndrome Based on Liquid Chromatography–Mass Spectrometry. *J. Proteome Res.* **2014**, *13* (2), 1101–1111. https://doi.org/10.1021/pr401130w.

(73) Barber, M. N.; Risis, S.; Yang, C.; Meikle, P. J.; Staples, M.; Febbraio, M. A.; Bruce, C. R. Plasma Lysophosphatidylcholine Levels Are Reduced in Obesity and Type 2 Diabetes. *PLoS ONE* **2012**, *7* (7), e41456. https://doi.org/10.1371/journal.pone.0041456.

(74) Popa Ilie, I. R.; Herdean, A. M.; Herdean, A. I.; Georgescu, C. E. Lipidomic Biomarkers in Polycystic Ovary Syndrome: An Overview. *Annales d'Endocrinologie* **2023**, *84* (1), 69–80. https://doi.org/10.1016/j.ando.2022.07.675.

(75) Tian, Y.; Zhang, J.; Li, M.; Shang, J.; Bai, X.; Zhang, H.; Wang, Y.; Chen, H.; Song, X. Serum Fatty Acid Profiles Associated with Metabolic Risk in Women with Polycystic Ovary Syndrome. *Front. Endocrinol.* **2023**, *14*, 1077590. https://doi.org/10.3389/fendo.2023.1077590.

(76) Ranea-Robles, P.; Houten, S. M. The Biochemistry and Physiology of Long-Chain Dicarboxylic Acid Metabolism. *Biochem J* **2023**, *480* (9), 607–627. https://doi.org/10.1042/BCJ20230041.

(77) Cao, N.; Wang, Y.; Bao, B.; Wang, M.; Li, J.; Dang, W.; Hua, B.; Song, L.; Li, H.; Li, W. 12,13-diHOME and Noradrenaline Are Associated with the Occurrence of Acute Myocardial Infarction in Patients with Type 2 Diabetes Mellitus. *Diabetol Metab Syndr* **2023**, *15* (1), 142. https://doi.org/10.1186/s13098-023-01115-9.

(78) Tang, X.; Wang, J.; Ouyang, X.; Chen, Q.; Dong, R.; Luo, Y.; Zhong, J.; Huang, Z.; Peng, L.; Xie, X.; Zhu, J.; Zheng, Z.; Li, S. Coronary Sinus Metabolite 12,13-diHOME Is a Novel Biomarker for Left Atrial Remodeling in Patients With Atrial Fibrillation. *Circ: Arrhythmia and Electrophysiology* **2024**, *17* (6). https://doi.org/10.1161/CIRCEP.123.012486.

(79) Ye, Z.; Zhang, C.; Wang, S.; Zhang, Y.; Li, R.; Zhao, Y.; Qiao, J. Amino Acid Signatures in Relation to Polycystic Ovary Syndrome and Increased Risk of Different Metabolic Disturbances. *Reproductive BioMedicine Online* **2022**, *44* (4), 737–746. https://doi.org/10.1016/j.rbmo.2021.11.012.

(80) Unni, C. S. N.; Lakshman, L. R.; Vaidyanathan, K.; Subhakumari, K. N.; Menon, N. L. Alterations in the Levels of Plasma Amino Acids in Polycystic Ovary Syndrome- A Pilot Study. *Indian J Med Res* **2015**, *142* (5), 549–554. https://doi.org/10.4103/0971-5916.171281.

(81) Tang, L.; Yuan, L.; Yang, G.; Wang, F.; Fu, M.; Chen, M.; Liu, D. Changes in Whole Metabolites after Exenatide Treatment in Overweight/Obese Polycystic Ovary Syndrome Patients. *Clin Endocrinol (Oxf)* **2019**, *91* (4), 508–516. https://doi.org/10.1111/cen.14056.

(82) Chang, A. Y.; Lalia, A. Z.; Jenkins, G. D.; Dutta, T.; Carter, R. E.; Singh, R. J.; Sreekumaran Nair, K. Combining a Nontargeted and Targeted Metabolomics Approach to Identify Metabolic Pathways Significantly Altered in Polycystic Ovary Syndrome. *Metabolism* **2017**, *71*, 52–63. https://doi.org/10.1016/j.metabol.2017.03.002.

(83) Cree-Green, M.; Carreau, A.-M.; Rahat, H.; Garcia-Reyes, Y.; Bergman, B. C.; Pyle, L.; Nadeau, K. J. Amino Acid and Fatty Acid Metabolomic Profile during Fasting and Hyperinsulinemia in Girls with Polycystic Ovarian Syndrome. *American Journal of Physiology-Endocrinology and Metabolism* **2019**, *316* (5), E707–E718. https://doi.org/10.1152/ajpendo.00532.2018.

(84) He, Q.; Shu, H.; Peng, Y.; Xu, Y.; Liu, L.; Zhou, J.; Zhao, J.; Xiong, X.; Li, C. Untargeted Metabolomics Analysis of Plasma Metabolic Characteristics in Patients with Acne and Insulin Resistance. *Amino Acids* **2023**, *55* (10), 1417–1428. https://doi.org/10.1007/s00726-023-03320-2.

(85) Paczkowska, K.; Rachoń, D.; Berg, A.; Rybka, J.; Kapczyńska, K.; Bolanowski, M.; Daroszewski, J. Alteration of Branched-Chain and Aromatic Amino Acid Profile as a Novel Approach in Studying Polycystic Ovary Syndrome Pathogenesis. *Nutrients* **2023**, *15* (19).

(86) Zhao, Y.; Fu, L.; Li, R.; Wang, L.-N.; Yang, Y.; Liu, N.-N.; Zhang, C.-M.; Wang, Y.; Liu, P.; Tu, B.-B.; Zhang, X.; Qiao, J. Metabolic Profiles Characterizing Different Phenotypes of Polycystic Ovary Syndrome: Plasma Metabolomics Analysis. *BMC Medicine* **2012**, *10* (1), 153. https://doi.org/10.1186/1741-7015-10-153.

(87) Yu, Z.; Qin, E.; Cheng, S.; Yang, H.; Liu, R.; Xu, T.; Liu, Y.; Yuan, J.; Yu, S.; Yang, J.; Liang, F. Gut Microbiome in PCOS Associates to Serum Metabolomics: A Cross-Sectional Study. *Scientific Reports* **2022**, *12* (1), 22184. https://doi.org/10.1038/s41598-022-25041-4.

(88) Haoula, Z.; Ravipati, S.; Stekel, D. J.; Ortori, C. A.; Hodgman, C.; Daykin, C.; Raine-Fenning, N.; Barrett, D. A.; Atiomo, W. Lipidomic Analysis of Plasma Samples from Women with Polycystic Ovary Syndrome. *Metabolomics* **2014**, *11* (3), 657–666. https://doi.org/10.1007/s11306-014-0726-y.

3.2 The Use of HILIC-based Workflows for Metabolite Profiling in Other Biological Matrices

3.2.1 Foliar application of protein hydrolysates promotes growth and affects leaf ionome in olive

Published: Pasković, I., Andlovic, M., Plešnik, H., Vavpetič, P., Žurga, P., Popović, L., Šala, M., Franić, M., Dlačić, I., Goreta Ban, S., Polić Pasković, M., Kosjek, T., Pongrac, P., Horticulturae, 2026

In this study, protein-hydrolysate biostimulants were evaluated with respect to their effects on olive plant physiology. My contribution focused on the development and application of a HILIC–LC–MS workflow for profiling amino acids and short peptides in olive leaf extracts, generating the analytical data used to assess biostimulant-induced metabolic changes. Using this approach, 17 amino acids were identified with Schymanski level 1 confidence through confirmation with analytical reference standards and subsequently quantified. In addition, 54 di- and tripeptides were annotated at Schymanski level 2 confidence based on MS/MS spectral library matching.

Although the biological application is agronomic and differs from the human studies presented in previous chapters, this work indirectly addresses Hypothesis 3, which states that HILIC-based non-targeted screening provides broader chemical-space coverage than RP-based workflows alone. While formulated in the context of exogenous compounds, the findings show that the same principle extends to endogenous metabolites. This is exemplified by amino acids and short peptides, which formed a central part of the metabolomic response and showed good retention in the optimized HILIC method. The results further demonstrate that non-targeted analysis reveals substantially more molecular features than a predefined targeted panel, particularly in the oligopeptide fraction, where numerous sequence combinations are accessible only through non-targeted screening. In this sense, the study illustrates the added value of non-targeted approaches independent of matrix or application field.

Furthermore, the key elements of the HILIC-based workflow, including instrumental method, quality-control strategy, sequence design, and data processing, proved transferable. With the exception of matrix-specific sample preparation, the workflow established here was later adapted for the human metabolomics and exposure science studies presented in this thesis, supporting the broader objective of harmonizing non-targeted screening through re-use of validated analytical and computational components rather than redeveloping complete pipelines for each application.

horticulturae

MDPI

Article

Foliar Application of Protein Hydrolysates Promotes Growth and Affects Leaf Ionome in Olive

Igor Pasković [1], Maša Andlovic [2], Helena Plešnik [3], Primož Vavpetič [3], Paula Žurga [4], Ljiljana Popović [5], Martin Šala [6], Mario Franić [1], Ivan Dlačić [1], Smiljana Goreta Ban [1], Marija Polić Pasković [1,*], Tina Kosjek [3] and Paula Pongrac [2,3]

[1] Institute of Agriculture and Tourism, Karla Huguesa 8, 52440 Poreč, Croatia; paskovic@iptpo.hr (I.P.); mario@iptpo.hr (M.F.); ivan@iptpo.hr (I.D.); smilja@iptpo.hr (S.G.B.)
[2] Biotechnical Faculty, University of Ljubljana, Jamnikarjeva 101, 1000 Ljubljana, Slovenia; masa.andlovic@bf.uni-lj.si (M.A.); paula.pongrac@bf.uni-lj.si (P.P.)
[3] Jožef Stefan Institute, Jamova cesta 39, 1000 Ljubljana, Slovenia; helena.plesnik@ijs.si (H.P.); primoz.vavpetic@ijs.si (P.V.); tina.kosjek@ijs.si (T.K.)
[4] Teaching Institute of Public Health of Primorsko-Goranska County, Krešimirova 52a, 51000 Rijeka, Croatia; paula.zurga@zzjzpgz.hr
[5] Faculty of Technology, University of Novi Sad, Bulevar cara Lazara 1, 21000 Novi Sad, Serbia; ljiljana04@tf.uns.ac.rs
[6] National Institute of Chemistry, Hajdrihova 18, 1000 Ljubljana, Slovenia; martin.sala@ki.si
* Correspondence: mpolic@iptpo.hr

Abstract

The foliar application of various biostimulants, such as protein hydrolysates (PHs), has been associated with improved nutrient uptake efficiency and stress tolerance in perennial crops, like olive (*Olea europaea* L.). In this study, PHs obtained by enzymatic hydrolysis by Alcalase Pure (referred to as treatment H1), Alcalase Pure and Flavourzyme (referred to as treatment H2), or Alcalase Pure and Protana™ Prime (referred to as treatment H3) with proteins from pumpkin seed cake were tested for their potential beneficial growth, performance, and nutrition effects in one-year-old olive seedlings grown under controlled conditions. Amino acid and element compositions were evaluated in the PHs, which were used for foliar application six times at eight-day intervals. Control (C) plants were treated the same way, but without PHs. Shoot and root growth, leaf reflectance indices, and the composition of micro and macronutrients in different organs and leaf tissues were determined. Plants in the H2 treatment grew significantly better than C plants. They had the highest Photochemical Reflectance Index and a Chlorophyll-Normalized Difference Vegetation Index similar to that of C plants, indicating an optimal growth/photosynthesis balance. A decrease in the concentration of several mineral elements in the lower epidermis in H2- and H3-treated plants compared to C and H1-treated plants was accompanied by their increase in the spongy mesophyll, indicating their redistribution to support increased metabolism, resulting in increased shoot growth in these two treatments. Arguably, these observed effects could be attributed to the amino acid profile of the H2 mixture, which had the highest concentration of L-proline, L-arginine, and L-lysine among the three PH mixtures, and a higher L-asparagine concentration than the H1 mixture. Overall, the results highlight the applicative potential of tailored PH formulations for the optimization of growth, mineral element composition, and physiological performance in olive cultivation.

Keywords: hydrolyzed proteins; pumpkin cake; biostimulants; element localization; olive cultivation

Check for updates

Academic Editor: Yang Liu

Received: 3 December 2025
Revised: 22 January 2026
Accepted: 27 January 2026
Published: 29 January 2026

Copyright: © 2026 by the authors. Licensee MDPI, Basel, Switzerland. This article is an open access article distributed under the terms and conditions of the Creative Commons Attribution (CC BY) license.

1. Introduction

Cultivation of olives (*Olea europaea* L.) is the basis of Mediterranean agriculture and is tightly linked with the local economy and cultural heritage. In addition to olive fruits and olive oil, various by-products of olive cultivation, such as twigs, leaves, and pomace, all rich in bioactive compounds, have been integrated into the production of functional foods, food supplements, phytochemicals, and nutraceuticals [1]. The long-term sustainability of olive production is being perturbed by unpredictable climate changes, which are exacerbating soil degradation, depleting water resources, and facilitating the emergence of new pathogens [2,3]. Among the factors enabling stable olive cultivation under these stress conditions is the nutritional status of olive trees, as this ensures optimal vegetative and reproductive growth while enhancing resilience. Therefore, research exploring the links between olive leaf nutrition and stress has attracted significant interest [4].

In this context, biostimulants, i.e., substances or microorganisms that stimulate natural processes to enhance nutrient uptake, nutrient-use efficiency, stress tolerance, and crop quality, regardless of their nutrient content [5], have been extensively explored as innovative tools for enhancing plant growth and improving stress tolerance. Du Jardin [6] highlighted that biostimulants seem to offer a unique opportunity to bridge plant nutrition and plant health, emphasizing the need to extend 'plant care' to the strengthening of the plants' capacity to withstand adverse environments and to cope with the scarcity of nutrients and water resources, which are all challenges amplified by climate change. Among the seven main categories of biostimulants, protein hydrolysates (PHs) have been shown to enhance crop performance, particularly under stressful environmental conditions [7,8]. This ability has been attributed to a higher ratio of peptides to free amino acids and a greater proportion of L-amino acids obtained from the enzymatic hydrolysis of plant-derived PH mixtures compared to animal-derived PHs, which are typically produced by acid hydrolysis [8].

General modes of indirect action in biostimulants remain poorly resolved because of the complexity of factors such as the quality and composition of proteins from different plant sources, the enzymes used, the conditions of hydrolysis, the methods of application, and the types of stress. Combining mineral fertilizers, biofertilizers, or different biostimulants (including amino acids) in olive orchards has already been shown to improve fruit and olive oil quality [9] simultaneously. This is presumably a consequence of (in)directly optimizing the supply of essential mineral nutrients and/or other regulators of plant metabolism supporting the physiological and biochemical processes that drive growth, flowering, fruit set, and oil accumulation [10]. In a conventional olive orchard, the most applied nutrient is nitrogen (N), which, due to its role in protein and chlorophyll synthesis, promotes photosynthesis and yield [11]. By contrast, phosphorus (P) deficiency is not very common in olive orchards, while potassium (K) deficiency is considered the most prevalent nutritional disorder in rainfed olive cultivation [10]. Through the key involvement of K in stomatal regulation, osmotic adjustment, and carbohydrate distribution, K nutritional status in olives critically contributes to drought stress resilience [12,13], and, through interactions with amino acid metabolism and the stimulation of IAA-oxidase activity, K affects flowering [11]. Calcium (Ca) is essential for maintaining plant structural integrity and preventing pathogen entry, while magnesium (Mg), as part of chlorophyll, plays a crucial role in photosynthesis [14], but they are rarely applied. Sulphur (S) is an essential nutrient for many physiological functions, such as protein synthesis and enzyme activation [15]. It therefore affects the biosynthesis of different primary and secondary metabolites, which are vital for plant growth and development [14]. Micronutrients such as iron (Fe), manganese (Mn), copper (Cu), and zinc (Zn) are essential for enzymatic activity and metabolic regulation [14,16], with boron (B) supporting olive reproductive development [17], and these are also seldom used to improve olive production. Deficiencies or imbalances in any of

https://doi.org/10.3390/horticulturae12020151

these nutrients impair tree vigor, fruiting, and oil quality, and can increase susceptibility to diseases such as olive leaf spot [4].

This study investigated the effects of the foliar application of PHs obtained by the enzymatic hydrolysis of pumpkin (*Cucurbita pepo* var. styriaca) seed cake proteins and assessed their impact on the shoot and root growth of one-year olive seedlings, leaf reflectance, and the composition of micro and macronutrients in different organs and leaf tissues. We hypothesize that tailored PHs will enhance growth and modulate ionome distribution in olive seedlings.

2. Materials and Methods

2.1. Protein Hydrolysates and Their Characterization

Proteins were isolated from pumpkin seed cake, as previously described in detail [18]. This protein isolate was hydrolyzed with the enzymes Alcalase® Pure (Novozymes, Bagsværd, Denmark, treatment referred to as H1), enzymes Alcalase® Pure and Flavourzyme® (Novozymes, Bagsværd, Denmark, treatment referred to as H2), or enzymes Alcalase® Pure and Protana™ Prime® (Novozymes, Bagsværd, Denmark, treatment referred to as H3). First, a suspension of 1.5 g of isolated proteins in 100 mL was prepared by suspending the required amount of protein isolates in 0.2 mol L^{-1} TRIS–HCl buffer solution at pH 9.0. Enzymatic hydrolysis was carried out at 50 °C for 180 min with an enzyme-to-substrate ratio of 1/50. The degree of hydrolysis was determined by the trichloroacetic acid method: the obtained suspension of hydrolyzed proteins was mixed with trichloroacetic acid (0.44 mol L^{-1}) in a 1:1 volume ratio and incubated at 4 °C for 30 min, after which the mixture was centrifuged (Eppendorf miniSpin Plus (Eppendorf, Hamburg, Germany), 14,500 rpm, 10 min). Protein content was determined in both fractions using the method described by [18], with bovine serum albumin as the standard protein. The degree of hydrolysis was calculated as the ratio of 0.22 mol L^{-1} trichloroacetic acid-soluble proteins to total proteins in the hydrolysate, expressed as a percentage.

Characterization of the PHs used in this study comprised targeted and non-targeted amino acid and dipeptide profiling and element composition assessment. For targeted and non-targeted amino acid and dipeptide analysis, ammonium formate and formic acid were purchased from Sigma Aldrich (St Louis, MO, USA), LC-MS-grade acetonitrile (ACN) and LC-MS-grade water were purchased from J. T. Baker (Phillipsburg, NJ, USA) and the amino acid standards (≥98%) used for analysis included L-valine, L-leucine, L-isoleucine, L-threonine, L-serine, L-proline, L-methionine, L-glutamic acid, L-phenylalanine, L-lysine, L-tyrosine, 4-Aminobutyric acid, L-asparagine, L-glutamine, L-cysteic acid, glycine, and L-arginine (all Sigma Aldrich). The internal standard, Stable Isotope Labeled Amino Acid Mix Solution 1, containing labeled variants of 17 amino acids, was obtained from Supelco (Buchs, Switzerland). The samples were prepared by 10-time dilution with acetonitrile containing 10% Milli-Q water. A mixture of isotopically labeled amino acids was added as an internal standard to each sample, yielding a final concentration of 500 µg L^{-1}. Calibration standards were prepared at concentrations of 10, 50, 100, 250, 500, and 750 µg L^{-1} of each amino acid. The internal standard mixture was added to all calibration levels in the same way as for the samples.

Chromatographic separation was performed on a Vanquish UHPLC system (Thermo Fisher Scientific, Waltham, MA, USA) using an Acquity BEH Amide column (Waters, 2.1 × 100 mm, 1.7 µm) maintained at 35 °C. Mobile phase A consisted of acetonitrile, and mobile phase B of 20 mM ammonium formate with 0.1% formic acid. The gradient program was as follows: 0–2 min, 10% B; 2–16 min, 10–45% B; 16–17 min, 45–10% B; followed by re-equilibration at 10% B until 30 min. The flow rate was 0.40 mL $min^{-1,}$ and the injection volume was 5 µL. Mass spectrometric detection was performed using a high-resolution

Orbitrap instrument (Thermo Fisher Scientific, Waltham, MA, USA) equipped with a heated electrospray ionization (HESI) source. The instrument was operated in either positive or negative ionization mode, using identical acquisition settings, except for polarity. The spray voltage was 3500 V, and the sheath, auxiliary, and sweep gas flows were 50, 50, and 1 (arbitrary units), respectively. The ion transfer tube and vaporizer temperatures were 325 °C and 350 °C. EASY-IC™ internal calibration and Advanced Peak Determination were enabled. Full MS scans were acquired at 120,000 resolving power (m/z 200) over m/z 70–1000 in centroid mode. Data-dependent MS/MS (dd-MS^2) was performed with eight dependent scans per cycle, using a 1.5 m/z isolation window and stepped HCD energies of 30, 50, and 150, recorded at 30,000 resolving power. Dynamic exclusion was enabled (repeat count 1, exclusion duration 9 s, $\pm$5 ppm tolerance, isotopes excluded).

Data processing was performed in MZmine 4.8.0 using the following workflow: (i) mass detection with noise levels set to 50,000 for MS^1 and 25,000 for MS^2; (ii) chromatogram building with a minimum of 5 consecutive scans, a minimum consecutive-scan intensity of 50,000, a minimum absolute peak height of 50,000, and an m/z tolerance of 0.0020 m/z or 10.0 ppm; (iii) retention-time smoothing using the Savitzky–Golay algorithm; (iv) peak deconvolution using the Local Minimum feature resolver with an 85% chromatographic threshold, a minimum RT search range of 0.15 min, a minimum absolute height of 50,000, a minimum peak-top-to-edge ratio of 2.0, a peak duration range of 0.00–4.51 min, and a minimum of 4 scans per feature; (v) ^{13}C isotope filtering with an m/z tolerance of 3.0 ppm, an RT tolerance of 0.20 min, a maximum charge state of 1, and assignment of the most intense isotope as the representative feature; (vi) join aligner with an m/z tolerance of 0.0015 m/z or 5.0 ppm, an RT tolerance of 0.5 min, with no requirement for matching charge state or identification and without isotope-pattern or spectral-similarity comparison; (vii) peak finder with 1% intensity tolerance, m/z tolerance of 0.0010 m/z or 5.0 ppm, RT tolerance of 0.5 min, and a minimum of 4 scans; and (viii) duplicate peak filtering using the "new average" mode with an m/z tolerance of 0.0008 m/z or 1.5 ppm and an RT tolerance of 0.10 min. Feature heights were first normalized using the closest eluting IS (normalized intensities).

For targeted analysis, quantitative measurements of amino acids for which authentic standards were available were performed, and calibration curves were prepared. Identification was confirmed by matching retention time and MS/MS spectra to the injected standards (Schymanski level 1) [19]. Calibration curves were fitted using linear regression; valine showed an R^2 of 0.94, whereas all other amino acids exhibited R^2 values of 0.99 or higher. The LLOQ was defined as the lowest calibration level with S/N > 3.

For non-targeted analysis, MS/MS spectra were matched against the MoNA (MassBank of North America) experimental library using the same mass-accuracy criteria as in the targeted workflow (precursor < 5 ppm; fragments < 10 ppm). These features were reported at Schymanski's level 2 confidence [19]. Annotation was restricted to di- and tripeptides, and matches outside this compound class were not reported.

Concentrations of Mg, K, Ca, Mn, Fe, Cu, Zn, and B in PHs were determined directly in PHs using inductively coupled plasma mass spectrometry, as described previously [20].

2.2. Experimental Setup and Plant Material

Sixteen one-year-old olive (*Olea europaea* L. cv. Leccino) seedlings, purchased from Darko Nursery (Rovinj, Croatia) as certificated plant material, were potted into 3.5 L pots filled with perlite and Potground H (Klasmann-Deilmann GmbH, Geeste, Germany) substrate mixture (1/3 v/v). Their leaves were carefully washed with a paper towel moistened with distilled water to remove visible deposits. Plants were allowed to acclimatize to a 12/12 day/night cycle with a 25/15 °C temperature regime for two weeks before start-

https://doi.org/10.3390/horticulturae12020151

ing the foliar treatments, which were applied six times at eight-day intervals. Each time, the plants were entirely sprayed with approximately 200 mL of the solution until runoff. Control plants (C) received a treatment consisting of distilled water with a wetting agent (0.15 mL L^{-1}; Optimus, AgroChem Max, Zagreb, Croatia), whereas PH-treated plants received distilled water, the same wetting agent, and the H1, H2, or H3 hydrolysates, diluted so that each solution contained 1.2 g L^{-1} of total soluble proteins. After spraying, all four plants per treatment were allowed to dry, then arranged in a randomized complete block design. At the start and at the end of the experiment, the elongation of the central shoot was measured. Eight days after the final foliar application, the six leaf reflectance indices listed in Table 1 were measured using the CI-710 SpectraVue Leaf Spectrometer (CID Bio-Science Inc., Camas, WA, USA), and plants were harvested. One leaf per plant (yielding four leaves per treatment) was sampled for tissue-specific elemental analysis and prepared by cryo-fixation, cryo-sectioning, and freeze-drying, as described previously [21]. To minimize the within-leaf variation, pieces of leaves (circa 5 × 5 mm^2) were sampled on the same leaf area, namely on the bottom half of the leaf, including the main vein and the neighboring leaf blade. For bulk analyses, shoots were separated into young leaves (i.e., those that developed during the experiment), old leaves, and stems; washed with tap water, then with distilled water containing 1% acetic acid, and finally with distilled water; frozen in liquid nitrogen; and freeze-dried at −96 °C and 0.0012 mbar for three days in Scanvac, CoolSafe (LaboGene, Allerød, Denmark). Roots were gently removed from the substrate, carefully washed, and scanned using WinRhizo software (version 2017a, Quebec City, QC, Canada) for morphological analysis: root length, root surface area, root volume, and average root diameter were measured, and then the roots were oven-dried at 35 °C for three days until reaching a constant mass [22].

Table 1. Overview of reflectance indices and calculation formulas, with data ranges, according to the internal firmware index definitions of the CI-710 SpectraVue Leaf Spectrometer (CID Bio-Science, Camas, WA, USA).

Index	Full Name	Formula	Range During Vegetation
CNDVI	Chlorophyll-Normalized Difference Vegetation Index	$(W_{750} - W_{705})/(W_{750} + W_{705})$	−1 to 1 (commonly 0.2–0.8)
PRI	Photochemical Reflectance Index	$(W_{531} - W_{570})/(W_{531} + W_{570})$	−1 to 1 (commonly −0.2–0.2)
GI	Greenness Index	W_{554}/W_{677}	–
SIPI	Structure Insensitive Pigment Index	$(W_{800} - W_{445})/(W_{800} + W_{680})$	0–2 (commonly 0.8–1.8)
WBI	Water Band Index	W_{900}/W_{970}	0.8–1.2
PSRI	Plant Senescence Reflectance Index	$(W_{680} - W_{500})/W_{750}$	−1 to 1 (commonly −0.1–0.2)

2.3. Bulk Element Analysis in Plant Material

All plant material was ground and homogenized to a fine powder using a 0.2 mm sieve in the Ultra Centrifugal mill ZM 200 (Retsch Maschinen GmbH, Setzingen, Germany). As described previously [1], a precisely measured 0.200 g of plant material was digested with 5 mL of 65% HNO_3 at 200 °C for 20 min using a Multiwave 3000 (Anton Paar, Graz, Austria), then diluted to 25 mL with ultrapure water. Manganese, Cu, Fe, Zn, and B were determined by inductively coupled plasma mass spectrometry (NexION 300X, PerkinElmer, Shelton, CT, USA), and Ca, K, and Mg by flame atomic absorption spectrometry (AAS800, PerkinElmer). Calibration utilized certified standards; only curves with an R^2 value greater than 0.999 were accepted.

https://doi.org/10.3390/horticulturae12020151

2.4. Leaf Tissue-Specific Element Analysis

Quantitative distribution of P, S, chlorine (Cl), K, Ca, Mn, Fe, Cu, and Zn in cross-sections of leaves was determined using micro-proton induced X-ray emission (micro-PIXE) at the ion accelerator (High Voltage Engineering Europa B.V., Amersfoort, The Netherlands) of the Jožef Stefan Institute (Ljubljana, Slovenia) as described previously [21]. In short, accelerated protons were focused to approximately 1×1 μm^2 beam size, scanning the sections sandwiched between the Pioloform foils stretched over an aluminum holder placed in a vacuum chamber. The interaction between protons and atoms in the sample induces X-ray emissions characteristic of each element. X-rays were detected by a four-segmented SDD detector (PNDetector, Münich, Germany), and spectra were recorded using Oxford Microbeam Data Acquisitio-3 (OMDAQ-3, Oxford Microbeams Ltd., Bicester, UK) software, which saves pixel-by-pixel spectra in a list mode file. These spectra were processed in GeoPIXE II software [23], where distribution maps were generated, and ASCII files with pixel-by-pixel concentrations in a matrix were exported. Tissue-specific concentrations were extracted from these matrices using Fiji (version 1.54p) [24] by importing as a Text Image followed by selecting the cell type (i.e., tissue) in the image—namely the whole section (W), upper epidermis (UE), lower epidermis (LE), palisade mesophyll (PM), and spongy mesophyll (SM—as previously described in detail [21]); using the Brush tool; and saving the selection to the Region of Interest Manager to calculate average concentrations in the selected tissues. Epidermises were selected based on Ca maps, considering the outermost layer of the sample, while mesophylls were discerned based on S distribution maps, namely, palisade mesophyll was recognized by its high S concentration and elongated structures (cells), while spongy mesophyll comprised the remaining area of the leaf, with lower S concentrations and more round structures (cells). None of the tissues were overlapping in this selection.

2.5. Statistical Analysis

Bar charts displaying means (n = 4) ± standard errors were generated using SigmaPlot version 12.0 (Systat Software, San Jose, CA, USA). Statistical analyses were performed using TIBCO Statistica version 14.1.0.8 (TIBCO StatSoft, Palo Alto, CA, USA). Data were analyzed using a randomized complete block design (RCBD), with treatment as the main effect and replicates included as blocks. The use of four biological replicates per treatment (n = 4), with each replicate corresponding to a single plant, follows a previously used experimental approach in olive studies, in which individual plants were treated as independent experimental units [1,21]. In the present study, replication and total number of seedlings were additionally constrained by the physical capacity of the growth chamber and the strong focus on micro-PIXE analysis, which requires extensive beam time per sample and therefore inherently limits the number of analyzable specimens. Normality was assessed on ANOVA residuals using Q–Q plots and the Shapiro–Wilk test, whereas homogeneity of variances was evaluated using Levene's type-test based on absolute ANOVA residuals [25]. When ANOVA assumptions were satisfied for the original or transformed data, parametric RCBD ANOVA followed by Fisher's least significant difference (LSD) test was applied ($p < 0.05$). If assumptions were still violated after transformation, the original data were rank-transformed and analyzed using RCBD ANOVA on ranks, as commonly applied in ecological studies [26], with Bonferroni-adjusted pairwise comparisons. Post hoc power analyses for leaf tissue and plant organ-specific elemental concentrations were performed in R (version 4.4.1) [27] using RStudio (version 2024.09.0) [28] and are reported in Supplementary Table S1.

https://doi.org/10.3390/horticulturae12020151

3. Results

First, we characterized the amino acid, peptide, and mineral element compositions of the PHs used in the experiment. The amino acid compositions of the three PH treatments revealed apparent differences between these PHs, with the degree of hydrolysis not necessarily correlating with the concentration of specific amino acids (Table 2). For example, H2 contained 3.2-, 2.1-, and 1.7-fold higher concentrations of L-asparagine, L-lysine, and L-glycine, respectively, than H1, although H1 had a 1.25-fold higher degree of hydrolysis than H2. Differences in all amino acid concentrations between H1 and H3 were below 1.2-fold, consistent with their differences in hydrolysis degree. There were 54 di- and tripeptides detected with different abundances (Table 2). The most numerous (7) were arginine-containing dipeptides, with arginine-isoleucine being most abundant in all three PHs, with H1 containing the highest values.

Table 2. Degree of hydrolysis (averages of n = 4 ± standard error are shown), concentration of amino acids, and non-targeted peptide profiles (normalized data) measured in protein hydrolysates (H1, H2, and H3) used in the experiment. Different letters above columns represent statistically significant differences between treatments (One-Way ANOVA and LSD post hoc test at $p < 0.05$). <LLOQ, lower limit of quantification, n.d., not detected.

		H1	H2	H3
Degree of hydrolysis		88.8 ± 0.51 [a]	71.0 ± 0.38 [c]	77.4 ± 0.25 [b]
Amino acids (mg L^{-1})	L-glycine	7.95	13.8	18.1
	4-amino butanoic acid	137	64	42.9
	L-proline	<LLOQ	1.39	0.611
	L-threonine	<LLOQ	<LLOQ	<LLOQ
	trans-4-hydroxy-L-proline	4.43	4.37	3.22
	L-leucine	22	21.2	17.4
	L-asparagine	9.3	29.9	32.2
	L-glutamine	64.7	78	71
	L-lysine	6.86	14.1	11.2
	L-methionine	8.02	5.32	5.21
	L-phenylalanine	28.1	24	20.9
	L-cysteic acid	<LLOQ	<LLOQ	<LLOQ
	L-arginine	24.5	40.7	31.9
	L-tyrosine	21.9	21.8	21
	L-serine	15.2	22.5	20.7
	L-valine	20.8	20.5	14
	L-glutamic acid	2.5	3.51	8.59
Compounds (abundance)	alanine—glutamine	365	348	150
	alanine—leucine	138	116	47.8
	alanine—methionine	46.9	27.8	9.39
	alanine—phenylalanine	144	86.5	41.3
	arginine—alanine	80.2	22.7	25.2
	arginine—glycine	16.2	8.98	7.87
	arginine—isoleucine	24,412	7348	8406
	arginine—methionine	1613	542	287
	arginine—proline	1.72	4.85	1.01
	arginine—serine	10.4	2.53	2.92
	arginine—valine	1465	561	477
	asparagine—leucine	557	268	114
	glutamine—glutamine	151	164	54
	glycine—leucine	847	460	126
	glycine—leucine	752	450	347
	isoleucine—glutamic acid	49	78	85

https://doi.org/10.3390/horticulturae12020151

Table 2. *Cont.*

		H1	H2	H3
Compounds (abundance)	isoleucine—leucine	362	359	211
	isoleucine—proline	353	232	56
	leucine—asparagine	226	133	100
	leucine—leucine—tryptophan	63	60	33
	leucine—phenylalanine	409	250	205
	lysine—leucine	1398	405	125
	3-methyl-histidine	1.1	n.d.	1.37
	methyl-lysine	n.d.	n.d.	n.d.
	methionine—leucine	22.9	32.6	5.4
	methionine—phenylalanine	45.6	33.2	15.2
	phenylalanine—alanine—leucine	81.6	29.6	12.6
	phenylalanine—glycine	342	194	153
	phenylalanine—isoleucine	159	74	38
	phenylalanine—phenylalanine	20.6	6.7	5.5
	proline—glutamine	207	404	28
	proline—histidine	2.53	55.9	28.1
	proline—valine	133	392	26
	serine—leucine	139	68.9	25.4
	serine—phenylalanine	124	60.5	19
	threonine—leucine	27.5	34.9	24.5
	threonine—phenylalanine	18.2	13.7	13.9
	tryptophan—leucine	61.5	39	41
	tyrosine—arginine	1639	322	196
	tyrosine—isoleucine	18.9	15.4	5.26
	valine—glutamine	202	84	51
	valine—isoleucine	166	244	127
	5-hydroxytryptophano	236	346	397
	pyroglutamyl—isoleucine	272	326	96
	glycine—phenylalanine	162	138	95
	serine—isoleucine	160	52.6	13.5
	arginine—leucine	785	328	465
	leucine—leucine	92	124	70
	threonine—isoleucine	60.6	46.1	46.8
	alanine—isoleucine	54.8	60	23.1
	glycine—valine	32.1	61.6	24.1
	glycine—glutamine	150	109	110
	threonine—glutamine	128	103	86.7
	serine—asparagine	121	109	95.2

By contrast, there were minimal differences in element composition between the three PHs, with H3 tending to have the lowest values, especially of micronutrients (Table 3).

Table 3. Concentrations of elements in protein hydrolysates (H1, H2, and H3) used in the experiment. Averages (n = 4) ± standard errors are shown. Different letters above columns represent statistically significant differences between treatments (One-Way ANOVA and LSD post hoc test at $p < 0.05$).

		H1			H2			H3		
mg L^{-1}	Mg	13.94	±	0.421 ^{a}	14.7	±	0.245 ^{a}	13.2	±	0.610 ^{a}
	K	2.43	±	0.058 ^{b}	2.66	±	0.0129 ^{a}	1.51	±	0.100 ^{c}
	Ca	42.54	±	0.896 ^{a}	42.8	±	0.525 ^{a}	42.7	±	0.407 ^{a}
	Zn	1.83	±	0.099 ^{a}	0.955	±	0.025 ^{b}	0.481	±	0.021 ^{c}
µg L^{-1}	Mn	6.99	±	0.690 ^{ab}	8.02	±	0.209 ^{a}	4.83	±	0.135 ^{b}

https://doi.org/10.3390/horticulturae12020151

Table 3. *Cont.*

	H1			H2			H3		
Fe	63.1	±	5.56 [b]	90.3	±	6.06 [a]	42.2	±	1.24 [c]
Cu	77.3	±	5.06 [b]	102	±	3.59 [a]	28.6	±	2.64 [c]
B	7.26	±	0.678 [a]	4.56	±	0.754 [b]	3.78	±	0.859 [b]

3.1. Shoot and Root Growth and Leaf Reflectance

Shoot and root growth and leaf reflectance were assessed in the one-year-old olive seedlings sprayed with the three PHs under control conditions. Olive seedlings did not show any toxicity or deficiency symptoms throughout the experiment (Figure 1a). Shoot growth (height) was significantly enhanced in the H2 and H3 treatments by 20–30% ($p < 0.05$) compared to the C or H1 treatments (Figure 1a). Among the reflectance indices measured, significant treatment effects were observed for the Chlorophyll-Normalized Difference Vegetation Index (CNDVI), greenness index (GI), photochemical reflectance index (PRI), and structure insensitive pigment index (SIPI), and not for the water band index (WBI) and plant senescence reflectance index (PSRI; Figure 1a). Control- and H2-treated plants had higher CNDVI values than H1- and H3-treated plants, while PRI was significantly higher in the H2 treatment compared to other treatments (Figure 1a). The GI and SIPI showed contrasting trends: GI was the lowest, while SIPI was the highest in C plants compared to other treatments (Figure 1a).

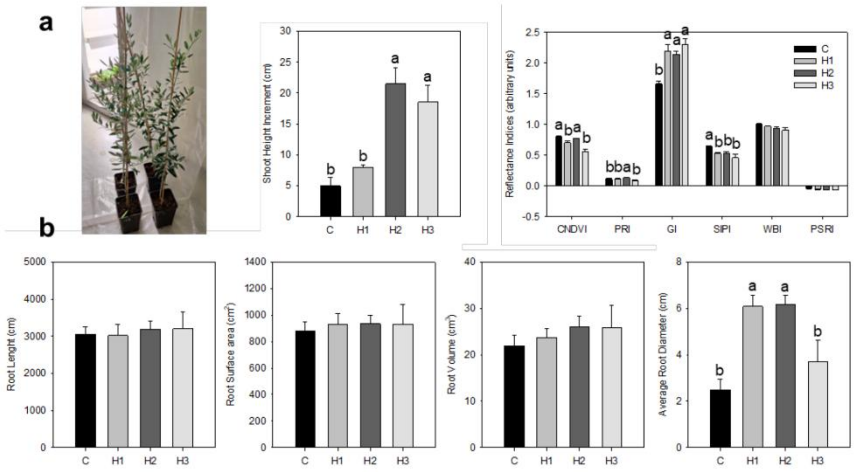


Figure 1. Shoot growth and reflectance indices (**a**) and root growth parameters (**b**) in one-year-old seedlings of olive (*Olea europaea* cv. *Leccino*) to which water and a wetting agent (control, C) or additional protein hydrolysates (H1 − H3, detailed amino acid, peptide and element composition is provided in Tables 2 and 3) were foliarly applied six times in eight-day intervals under controlled conditions. Means (n = 4) ± standard errors are shown. Different letters indicate significant differences according to main-effects ANOVA with Fisher's LSD test ($p < 0.05$). Reflectance indices are defined in Table 1.

In contrast to root length, root surface area, and root volume, the average root diameter was significantly affected by treatments: it was higher in H1- and H2-treated plants than in C and H3-treated plants (Figure 1b).

3.2. Element Composition of Olive Organs

At harvest, young and old leaves were separated in addition to sampling stems and roots for mineral element composition of one-year olive seedlings sprayed with three different PHs under controlled conditions. There were apparent differences in mineral element concentrations between olive organs: all micronutrients analyzed, except B, were higher in roots than in other organs, Mg, Ca, and B concentrations were higher in old leaves than in other organs, and K concentrations were higher in young leaves than in other organs (Figure 2).

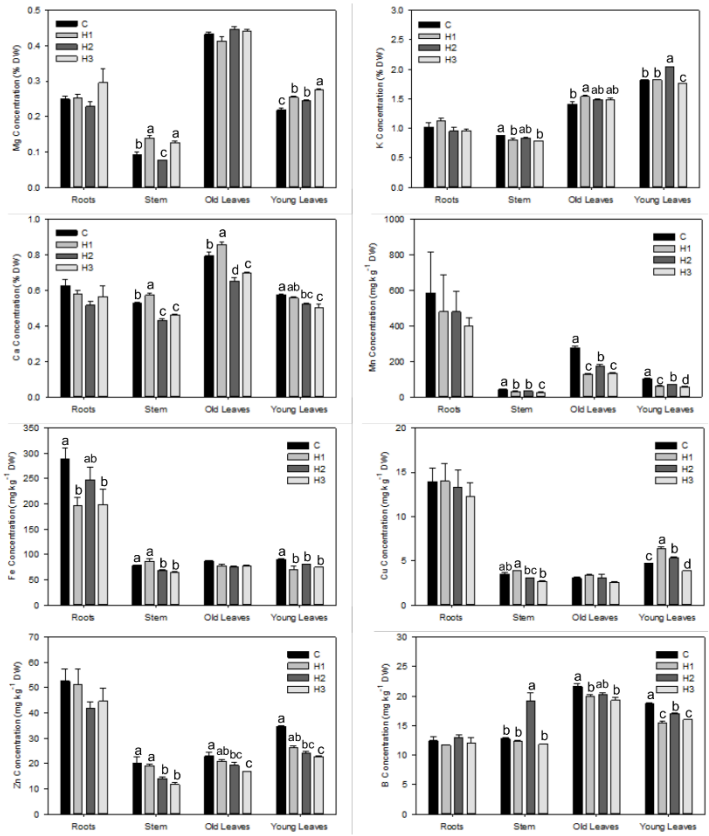


Figure 2. Bulk concentrations of magnesium (Mg), potassium (K), calcium (Ca), iron (Fe), manganese (Mn), copper (Cu), zinc (Zn) and boron (B) in roots, stem, young, and old leaves of one-year-old seedlings of olive (*Olea europaea* cv. *Leccino*) to which water and a wetting agent (control, C) or additional protein hydrolysates (H1 − H3, detailed amino acid, peptide and element composition is provided in Tables 2 and 3) were foliarly applied six times in eight-day intervals under controlled conditions. Averages (n = 4) ± standard errors are shown. Different letters indicate significant differences according to main-effects ANOVA with Fisher's LSD test or rank-based main-effects ANOVA with Bonferroni-adjusted pairwise comparisons ($p < 0.05$). DW, dry weight.

https://doi.org/10.3390/horticulturae12020151

In roots, the only significant treatment effects were observed for Fe concentrations: C plants had the highest concentrations, H1- and H3-treated plants had significantly lower concentrations, and H2-treated plants had intermediate values (Figure 2).

By contrast, there was a significant effect of treatments on all mineral elements in the stem; however, no general trend could be found (Figure 2). Magnesium concentrations were the highest in H1 and H3-treated plants, followed by C plants and finally by H2-treated plants. Potassium concentrations were the highest in C plants and declined in the treatments, except in H2-treated plants, where they were intermediate. Calcium concentrations in stems were the highest in H1-treated plants, followed by C plants and finally by H2 and H3-treated plants. Manganese concentrations in the stems were highest in C plants and declined in H1- and H2-treated plants and in H3-treated plants. There was a common trend in Fe and Zn concentrations in the stems, with C plants and H1-treated plants having higher concentrations than H2 and H3-treated plants. A significant increase in stem B concentrations was observed in H2-treated plants.

In old leaves, Mg, Fe, and Cu concentrations were not affected by treatments (Figure 2). Similarly to the results in the stems, no general trend in PH effects on the concentration of the analyzed mineral elements in old leaves could be deduced. H1-treated plants had significantly higher K concentrations in their old leaves than C plants, but not higher than H2- and H3-treated plants, while Ca concentrations in old leaves were the highest in H1-treated plants, followed by C plants, and were significantly lower in H2- and H3-treated plants. Manganese, Zn, and B concentrations were higher in the old leaves of C plants than in those of the other two treatments (Figure 2).

In young leaves, all measured mineral nutrients were significantly affected by the treatments (Figure 2). A trend of increasing concentrations from C plants to H3-treated plants can be observed for Mg concentrations and a decrease for Ca, Mn, Fe, Zn, and B concentrations, whereas H2-treated plants had significantly higher K concentrations and H1-treated plants had higher Cu concentrations than plants in other treatments (Figure 2).

3.3. Element Composition of Leaf Tissues

While bulk element concentrations depict the general nutrition status of the one-year old olive seedlings sprayed with three PHs under control conditions, there may be tissue-specific changes in the leaf tissues. Therefore, mineral element localization analyses were used to capture responses at the tissue level in leaves. Phosphorus, S, Cl, K, Ca, Mn, Fe, Cu, and Zn were detected, and their tissue allocation in olive leaf cross sections was captured (Figures 3 and 4). From quantitative distribution images, concentrations in the whole section (W), lower epidermis (LE), upper epidermis (UE), palisade mesophyll (PM), and spongy mesophyll (SM) were measured. For P, S, Cl, K, and Ca, concentrations are given as weight %, whereas for Mn, Fe, Cu, and Zn, concentrations are given as mg kg^{-1} of dry weight.

Of all mineral elements analyzed, P was the only element for which there was a significant effect of treatments observed in all leaf tissues: there was significantly less P in W, PM, and SM in H1- and H3-treated plants than in C and H2-treated plants, whereas in epidermises there was negative effect on P concentrations in all three treatments compared to C (Figure 3). An opposite trend, although not significant in all instances, was observed for Cl concentrations: higher values were found in the leaf tissues of H1- and/or H3-treated plants than in C and/or H1-treated plants (Figure 3). An apparent decrease in S, K, and Ca concentrations was observed in the LE of leaves from H2- and H3-treated plants compared to C and H1-treated plants (Figure 3). This observation was not mirrored in UE. Potassium concentrations increased in SM, with the highest values observed in the H2 and H3 treatments, which were significantly higher than in the untreated C plants.

https://doi.org/10.3390/horticulturae12020151

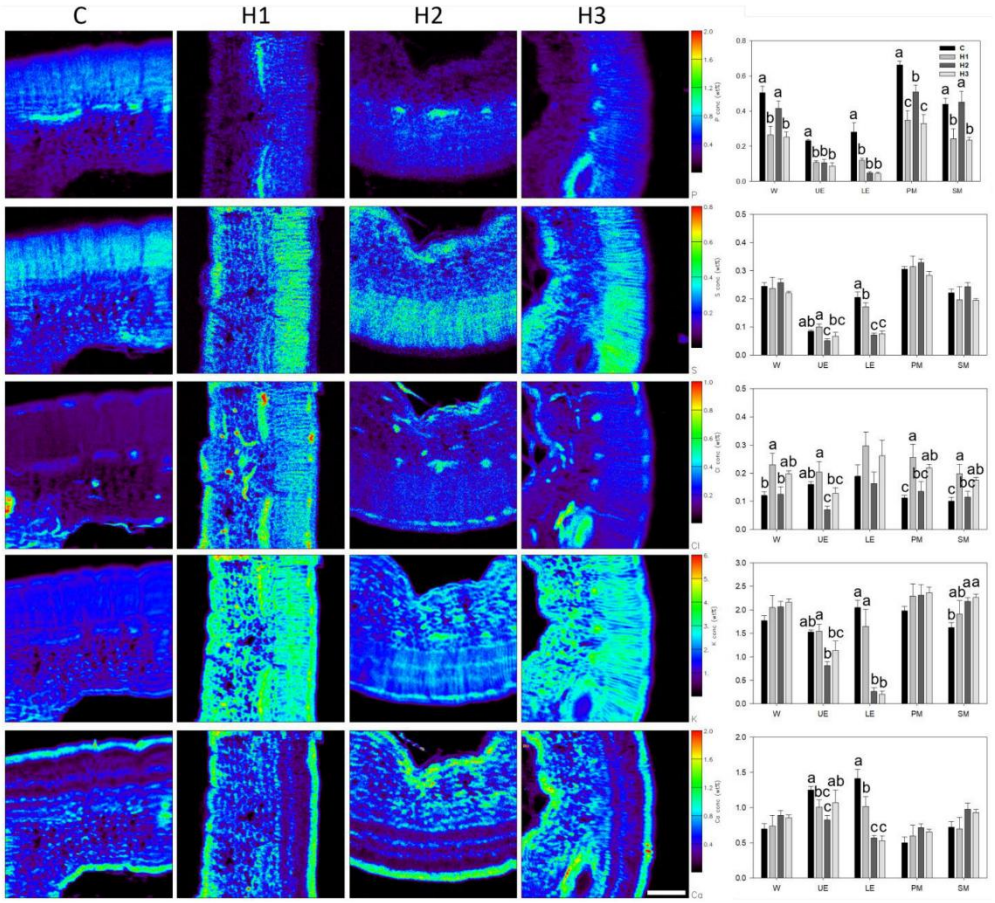


Figure 3. Representative distribution maps and tissue-specific concentrations (in % dry weight) of phosphorus (P), sulphur (S), chlorine (Cl), potassium (K) and calcium (Ca) in the cross-sections of leaves of one-year-old seedlings of olive (*Olea europaea* cv. *Leccino*) to which water and a wetting agent (control, C) or additional protein hydrolysates (H1–H3, detailed amino acid, peptide and element composition is provided in Tables 2 and 3) were foliarly applied six times in eight-day intervals under controlled conditions. Bar charts represent averages (n = 4) ± standard errors. W, whole section; UE, upper epidermis; LE, lower epidermis; PM, palisade mesophyll; SM, spongy mesophyll. Different letters indicate significant differences according to main-effects ANOVA with Fisher's LSD test or rank-based main-effects ANOVA with Bonferroni-adjusted pairwise comparisons ($p < 0.05$). Scale bar indicates 100 µm and is the same for all maps.

The allocation of micronutrients was only significantly affected by treatments in the epidermises (Figure 4). There was an apparent trend of C plants having the highest concentrations of Mn and Cu in UE and of C and H1-treated plants having higher Cu in LE. Also, C plants exhibited higher Fe concentrations than H2 plants in both epidermises. Manganese and Zn concentrations decreased from C plants toward H2- and/or H3-treated plants (Figure 4).

https://doi.org/10.3390/horticulturae12020151

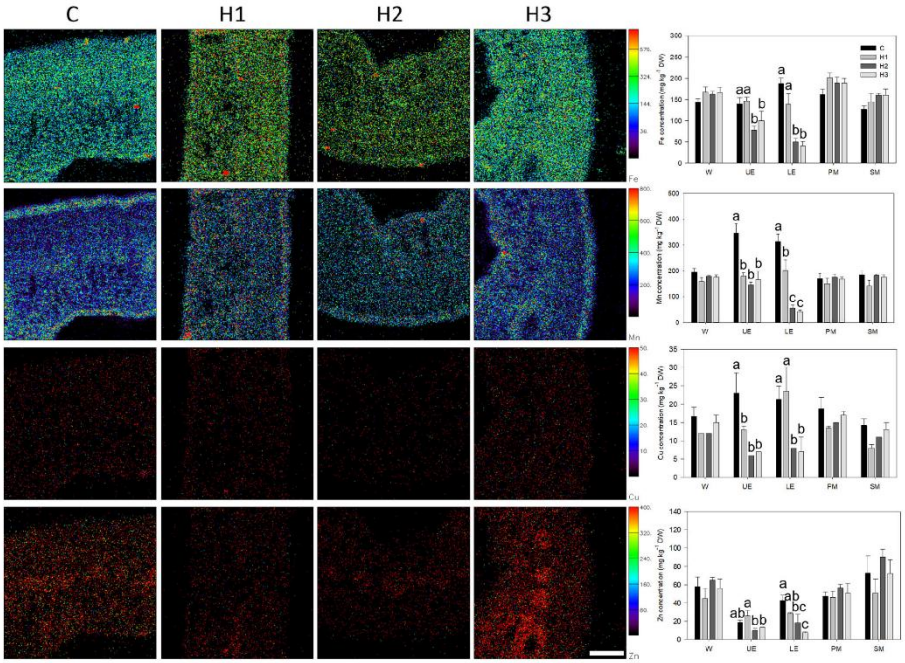


Figure 4. Representative distribution maps and tissue-specific concentrations (in mg kg^{-1} dry weight) of iron (Fe), manganese (Mn), copper (Cu) and zinc (Zn) in the cross-sections of leaves of one-year-old seedlings of olive (*Olea europaea* cv. *Leccino*) to which water and a wetting agent (control, C) or additional protein hydrolysates (H1 − H3, detailed amino acid, peptide and element composition is provided in Tables 2 and 3) were foliarly applied six times in eight-day intervals under controlled conditions. Bar charts represent averages (n = 4) ± standard errors. W, whole section; UE, upper epidermis; LE, lower epidermis; PM, palisade mesophyll; SM, spongy mesophyll. Different letters indicate significant differences according to main-effects ANOVA with Fisher's LSD test or rank-based main-effects ANOVA with Bonferroni-adjusted pairwise comparisons ($p < 0.05$). Scale bar indicates 100 µm and is the same for all maps.

4. Discussion

4.1. Protein Hydrolysates

The biological and functional properties of PHs are strongly influenced by factors such as degree of hydrolysis, enzyme specificity, and protein substrate type [29]. Using a single protein isolate from pumpkin seed cake, a protein-rich by-product of pumpkin oil production [30] popular in the region, and three different enzyme combinations, we obtained three mixtures. They comprised different amino acid compositions with large di and tripeptide diversity (Table 2) and low element concentrations (Table 3). Enzymatic hydrolysis was used because it is a gentle process for preparing food PHs with fewer undesirable side effects. Three different enzymes were used. Alcalase is an endopeptidase that cleaves peptide bonds at the C-terminal amino acid and was the most effective, resulting in the highest degree of hydrolysis. In contrast, Flavourzyme is both an endo- and exopeptidase that cleaves at the N-terminal of peptide chains. Protana (also known as Protamex) is a broad-spectrum endoprotease that hydrolyses proteins into smaller peptides and amino acids. Alcalase tends to produce smaller peptides more readily than Protana, which aligns

with studies on Whey Protein Isolate, soybean, and fish protein [31–33]. This behavior can be attributed to the type of enzyme. Alcalase has greater activity than Protana due to its higher specificity for serine residues and its endoproteolytic activity [34], and is known to produce mainly small, hydrophobic peptides [35].

4.2. Effects of Protein Hydrolysates on Growth and Leaf Reflectance Composition in One-Year Old Olive Seedlings

Foliar application of the PHs was expected to elicit local and systemic responses in one-year-old olive seedlings. The increased shoot height in the H2 and H3 treatments compared to the C and H1 treatments was accompanied by the H2 treatment showing more favorable reflectance indices (Figure 1a), indicating that the H2 treatment had the most significant effect on above-ground plant fitness. These responses are consistent with improved chlorophyll status, enhanced photosynthetic performance, and reduced stress intensity [36,37] in H2-treated plants compared to other treatments. Moreover, the average root diameter was higher in plants from the H2 treatment than in plants from the C (Figure 1b), corroborating conclusions from the above-ground observations. Because PH mixtures were used in this experiment, only limited mechanistic inferences are possible. Because element concentrations in the PH mixtures were so low (Table 3) and there was little meaningful correlation with bulk element concentrations, the amino acid and or di and tripeptide composition of the PHs was examined for pivotal candidates, considering observed effects individually. For example, positive shoot height effects observed for H2 and H3 may be a consequence of their 3.22-fold and 3.47-fold higher concentrations of L-asparagine than in the H1 mixture, respectively. This N-containing amino acid has recently been reported to have a biostimulant effect on leaf area in *Arabidopsis thaliana* [38], but no mechanistic interaction was proposed. The superiority of the H2 mixture over both H1 and H3 mixtures in reflectance indices (Figure 1) may be associated with a 2.3-fold higher L-proline concentration in H2 over H3 (in the H1 mixture, no L-proline was detected), despite low absolute levels. Proline is a well-known compatible osmolyte and potential reactive oxygen species (ROS) scavenger [39], and its exogenous application in numerous fruit trees has shown significant enhanced fruit qualities [40]. However, given the low absolute concentrations detected, its quantitative contribution to the observed responses remains uncertain. A further amino acid candidate for the observed differences in reflectance indices may be the higher L-arginine concentration found in H2 compared to H3 and H1 mixtures, as arginine is a key N-containing amino acid [41] and has been shown to alleviate the reduction in photosynthesis and antioxidant activity induced by drought stress in maize seedlings [42]. Furthermore, in N-deficient apple, hydroponically supplied arginine was shown to promote photosynthesis capacity, alter amino acid metabolism, and improve tolerance to N deficiency, possibly through improving the uptake and translocation of N, P, and K [43]. In addition, the fourth amino acid candidate is L-lysine, which has been typically applied as a biostimulant in a complex with Zn, resulting in better photosynthesis efficiency in water-stressed maize [44] or with Fe, boosting photosynthetic pigments in cadmium-stressed canola [45]. Less is known about the effects of L-lysine in woody species, including olive [46].

The long-distance effect (i.e., root growth parameters) of treatments was only measurable in the average root diameter, which was higher in the H1 and H2 treatments compared to the C and H3 treatments (Figure 1b). One of the amino acids, the concentrations of which were higher in the H1 and H2 mixtures than in the H3 mixture, was L-valine (Table 2). Exogenous valine has been shown to promote root growth and to inhibit the shoot growth of peach seedlings [47]. The shoot growth inhibition was prevented in these peach seedlings if isoleucine was sprayed. While the L-isoleucine was not detected in the PHs, there were 11 isoleucine-containing dipeptides found, and arginine-isoleucine was most abundant of

all, with the H1 mixture containing the highest values (Table 2). It seems that isoleucine in dipeptide form does not have the same effect as exogenously applied isoleucine, as in H1-treated olive seedlings, shoot growth did not reach that of H2- and H3-treated plants. These observations clearly imply that tailoring optimized PH combinations will be very challenging and will probably be species-specific.

So far, we have examined only amino acids whose concentrations were higher in the H2 mixture compared to the H1 or H3 mixtures. However, it may as well be that the concentration of an individual amino acid is not responsible for an observed effect, but rather that their combination(s) is. While experiments with individual amino acids or defined mixtures would be required to draw firm mechanistic conclusions, our aim is to design an agronomically acceptable biostimulant from an agronomic waste product, valorizing it and enabling its use in sustainable agronomic practice.

4.3. Effects of Protein Hydrolysates on Mineral Element Composition in One-Year Old Olive Seedlings

Young leaves were defined as those that developed during the experiment; therefore, we assumed they had been treated to a lesser extent than older leaves. In addition, young (developing) leaves are considered a mineral sink for elements, particularly those with greater phloem mobility, such as K, P, Mg, and Zn [48]. As there is a continuous shift in sink/source relationship within a plant, the element composition of any of the plant parts measured at a selected time point is a consequence of several physiological processes, including uptake, storage, and (re)translocation, in line with the current demands of the tissue. Additional external applications of mineral elements that cannot be traced in vivo further complicate the picture. In this study, the PHs did not contain large quantities of mineral elements (Table 3); therefore, extensive increases in total element concentrations were not expected to be due to the foliar application itself. Indeed, only occasionally did the concentration of the measured elements in any of the plant parts increase (Figure 2). Rather, changes in mineral composition were an indirect consequence of amino acid and di- and tripeptide activity as signaling molecules, or of their interactions with physiological processes linked to mineral nutrition. One example of such an interaction reports that exogenously applied valine inhibited the growth of peach tree shoots by regulating the balance between sucrose non-fermenting-1-related protein kinase and target of rapamycin kinase [47]. The latter plays a key role in responses to starvation and induces autophagy in plants [49], a process involved in responses to mineral deficiency and/or senescence.

In olive seedlings, the pH treatments did not change the overall predominant allocation of mineral elements to a specific plant organ. All micronutrients analyzed, except B, were higher in the roots than in other organs. Mg, Ca, and B concentrations were higher in old leaves than in other organs, whereas K concentrations were higher in young leaves than in other organs (Figure 2). At least observations of differences between old and young leaves (concentrations in stems and roots are rarely reported, as their removal from slow-growing trees, such as olives, means the termination of the experiment) can be confirmed in the literature [50,51]. The robustness of these organ-level allocation patterns varied among elements and tissues, as indicated by the observed power analysis (Supplementary Table S1). In particular, K allocation to young leaves was supported by high statistical power, whereas the root accumulation of micronutrients was associated with lower power and should therefore be interpreted cautiously. Looking at PH-specific effects on bulk mineral elements concentrations reveals that a similar distinctive beneficial effect was observed for the growth and leaf reflectance indices for the H2 treatment in comparison to C plants, which was observed for K concentration in young leaves and B concentration in the stems (Figure 2). Increases in K concentrations after foliar application of PHs were reported in pea plants (*Pisum sativum*) in a field experiment [52], an increase in K channel

expression when PHs were added to the nutrient solution of growing tomato plants [53] and under saline stress conditions, plants treated with biostimulants showed higher levels of K and proline compared to untreated controls [8]. All these reports are in line with our observation, but only for the H2 treatment of young leaves and the H1 treatment of old leaves. Within leaf tissues, K concentrations in SM were higher in H2-treatment (and in H3 treatment) than in C plants (Figure 3). Interestingly, these two treatments had significantly less K in LE than C and H1-treated plants, which suggests a redistribution of K from LE towards the SM if high short-distance transport of K resembles the high long-distance phloem mobility of K [48]. Such redistribution likely reflects more vigorous metabolic and osmotic activity in the SM of H2- and H3-treated plants, which is consistent with the physiological role of K in supporting cell expansion, turgor maintenance, and photosynthetic performance during active growth [54–57], which was clearly observed in olive seedlings treated with the H2 and H3 mixtures (Figure 1). However, while the reduction in K in the LE was supported by high statistical power, the increase in the SM was associated with moderate power and should therefore be interpreted with appropriate restraint.

Nevertheless, there were instances when H2-treated plants had significantly lower concentrations than C plants (e.g., in the stem, all elements except B) or when this was observed in conjunction with H3-treated plants (e.g., in old and young leaves for Ca, and young leaves for Fe), making robust mechanistic interpretation difficult. In general, it seems that, for all elements, LE was mainly negatively affected by PH treatments, particularly by H2 and H3 treatments, as consistently lower concentrations of all elements, except for Cl, were observed in C-treated plants (Figures 3 and 4). Again, the higher L-arginine and L-proline concentration in H2 and H3 mixtures compared to the H1 mixture could play a synergistic role in element relocation from epidermis to mesophyll. Arginine is a precursor of polyamines, a class of phytohormones that regulate the voltage-dependent inward K^+ channel in the plasma membrane of guard cells and induce stomatal closure [58], thereby limiting transpiration and hence the delivery of essential elements to the leaves. Local element deficiency may be remedied by the redistribution of those elements from the epidermis to the metabolically active mesophyll. Polyamines can increase ROS levels in guard cells [59], which can be scavenged by the applied L-proline, thereby maintaining the physiological stability of olive leaves. However, since polyamine levels and stomatal parameters were not measured in this study, these interpretations remain hypothetical and are presented as possible explanatory mechanisms.

Peculiar was a contrasting treatment response in mesophyll concentrations of P and Cl (Figure 3), with P concentrations higher in C and H2-treated plants than in H1- and H3-treated plants. In comparison, Cl concentrations were higher in H1- and/or H3-treated plants than in C plants. While treatment-related differences observed in the stem and for Ca and Fe in old and young leaves were generally supported by high observed statistical power, the contrasting Cl mesophyll responses and LE effects were associated with moderate to low power, respectively (Supplementary Table S1), limiting the interpretability of these tissue-specific patterns. Although the uptake of P and Cl by roots was reported to be antagonistic [60,61], their tissue-specific allocation in leaves and the effects of treatments should be investigated further.

5. Conclusions

The foliar application of PHs from valorized agronomic waste (pumpkin seed cake), particularly the H2 and H3 mixtures, to one-year-old olive seedlings under controlled conditions resulted in improved shoot growth and reflectance index compared with untreated C plants, reflecting improvement in photosynthetic activity. Considering also the element composition of plant parts, the H2 mixture appears the most promising foliar

PHs treatment, suitable for improving nutrient uptake and photosynthetic performance of olives without significantly affecting bulk ionome homeostasis. At the leaf tissue level, conspicuous redistribution of elements from epidermis to mesophyll was observed, presumably to support increased metabolic demands that sustained increased shoot growth. Arguably, these observed effects could be attributed to the amino acid profile of the H2 mixture, which has the highest concentration of L-proline, L-arginine, and L-lysine among the three PHs mixtures, and a higher L-asparagine concentration than the H1 mixture. Further mechanistic experiments are required to resolve modes of action of PHs and/or individual amino acids, and a field experiment to corroborate the beneficial physiological effects observed in this experiment and to evaluate agronomic effects, particularly the potential benefits to yield and olive oil quality.

Supplementary Materials: The following supporting information can be downloaded at https://www.mdpi.com/article/10.3390/horticulturae12020151/s1, Table S1: Post hoc power analysis of treatment effects for organ-level and tissue-specific elemental variables analyzed using a randomized complete block design.

Author Contributions: Conceptualization: I.P., P.P., L.P., and M.P.P.; validation and formal analysis: P.Ž., M.Š., M.P.P., P.P., P.V., M.A., L.P., M.F., I.D., and H.P.; investigation: I.P., I.D., L.P., M.A., and M.P.P.; resources: I.P., L.P., S.G.B., P.Ž., and P.P.; data curation: I.P., P.P., H.P., P.V., P.Ž., M.F., L.P., S.G.B., T.K., M.Š., and M.P.P.; writing—original draft preparation: I.P., L.P., and M.P.P.; writing—review and editing: I.P., P.P., T.K., and M.P.P.; visualization: P.P. and M.P.P.; supervision: I.P. and P.P.; project administration: I.P., P.P., and M.P.P.; funding acquisition: I.P. and P.P. All authors have read and agreed to the published version of the manuscript.

Funding: This work was funded by the Croatian Science Foundation (CSF (HRZZ)) and the Slovenian Research and Innovation Agency (ARIS) under the WEAVE initiative bilateral project HRZZ- IP-2022-10-8305 and N4-0346 (PROGRESS) and through core ARIS funding (P1-0212). Access to micro-PIXE facility (ID 34772) was enabled by the European Union as part of the Horizon Europe call HORIZON-INFRA-2021-SERV-01 under grant agreement number 101058414 and co-funded by UK Research and Innovation (UKRI) under the UK government's Horizon Europe funding guarantee (grant number 10039728) and by the Swiss State Secretariat for Education, Research and Innovation (SERI) under contract number 22.00187. Views and opinions expressed are, however, those of the author(s) only and do not necessarily reflect those of the European Union, the UK Science and Technology Facilities Council, or the Swiss State Secretariat for Education, Research and Innovation (SERI). Neither the European Union nor the granting authorities can be held responsible for them. The authors acknowledge the financial support from the Slovenian Research and Innovation Agency (ARIS), research core funding No. P1-0034. In addition, the work of PhD student M.P.P. was supported by the "Young researchers career development project-training of doctoral students" program under the CSF project no. HRZZ-DOK-2021-02-5517 and HRZZ-MOBDOK-2023-3103, and the work of PhD student I.D. was supported by the "Young researchers career development project-training of doctoral students" program under the CSF project no. HRZZ DOK-NPOO-2023-10-1951.

Data Availability Statement: The raw data supporting the conclusions of this article will be made available by the authors on request.

Conflicts of Interest: The authors declare no conflicts of interest.

References

1. Polić Pasković, M.; Herak Ćustić, M.; Lukić, I.; Marcelić, Š.; Žurga, P.; Vidović, N.; Major, N.; Goreta Ban, S.; Pecina, M.; Ražov, J.; et al. Foliar nutrition strategies for enhancing phenolic and amino acid content in olive leaves. *Plants* **2024**, *13*, 3514. [CrossRef] [PubMed]
2. Martins, S.; Pereira, S.; Dinis, L.-T.; Brito, C. Enhancing olive cultivation resilience: Sustainable long-term and short-term adaptation strategies to alleviate climate change impacts. *Horticulturae* **2024**, *10*, 1066. [CrossRef]

3. Saifi, R.; Kokiçi, H.; Saifi, H.; Akça, I.; Benabdelkader, M.; Xhemali, B.; Çota, E.; Hadjeb, A. Does climate change heighten the risk of *Xylella fastidiosa* infection? In *Plant Quarantine Challenges Under Climate Change Anxiety*; Springer: Cham, Switzerland, 2024; pp. 331–358. [CrossRef]
4. Fernández-Escobar, R. Olive nutritional status and tolerance to biotic and abiotic stresses. *Front. Plant Sci.* **2019**, *10*, 1151. [CrossRef] [PubMed]
5. Calvo, P.; Nelson, L.; Kloepper, J.W. Agricultural uses of plant biostimulants. *Plant Soil* **2014**, *383*, 3–41. [CrossRef]
6. Carillo, P.; Avice, J.-S.; Vasconcelos, M.W.; du Jardin, P.; Brown, P.H. Biostimulants in Agriculture: Editorial. *Physiol. Plant.* **2025**, *177*, e70046. [CrossRef]
7. Du Jardin, P. Plant biostimulants: Definition, concept, main categories and regulation. *Sci. Hortic.* **2015**, *196*, 3–14. [CrossRef]
8. Colla, G.; Hoagland, L.; Ruzzi, M.; Cardarelli, M.; Bonini, P.; Canaguier, R.; Rouphael, Y. Biostimulant action of protein hydrolysates: Unravelling their effects on plant physiology and microbiome. *Front. Plant Sci.* **2017**, *8*, 2202. [CrossRef]
9. Tadayon, M.S.; Asgharzadeh, A.; Mousavi, S.M.; Saghafi, K. Synergistic effects of chemical and biochemical fertilisation on yield enhancement and oil quality optimisation in 'Zard' olive cultivars. *Front. Plant Sci.* **2025**, *16*, 1455921. [CrossRef]
10. Zipori, I.; Erel, R.; Yermiyahu, U.; Ben-Gal, A.; Dag, A. Sustainable management of olive orchard nutrition: A review. *Agriculture* **2020**, *10*, 11. [CrossRef]
11. Erel, R.; Dag, A.; Ben-Gal, A.; Schwartz, A.; Yermiyahu, U. Flowering and fruit set of olive trees in response to nitrogen, phosphorus, and potassium. *J. Am. Soc. Hortic. Sci.* **2008**, *133*, 639–647. [CrossRef]
12. Hawkesford, M.J.; Cakmak, I.; Coskun, D.; De Kok, L.J.; Lambers, H.; Schjoerring, J.K.; White, P.J. Functions of macronutrients. In *Marschner's Mineral Nutrition of Plants*; Academic Press: Cambridge, MA, USA, 2023; pp. 201–281.
13. Hasanuzzaman, M.; Bhuyan, M.H.M.B.; Nahar, K.; Hossain, M.S.; Mahmud, J.A.; Hossen, M.S.; Masud, A.A.C.; Moumita; Fujita, M. Potassium: A vital regulator of plant responses and tolerance to abiotic stresses. *Agronomy* **2018**, *8*, 31. [CrossRef]
14. Tariq, A.; Zeng, F.; Graciano, C.; Ullah, A.; Sadia, S.; Ahmed, Z.; Murtaza, G.; Ismoilov, K.; Zhang, Z. Regulation of metabolites by nutrients in plants. In *Plant Ionomics: Sensing, Signalling, and Regulation*; John Wiley & Sons Ltd.: Hoboken, NJ, USA, 2023; pp. 1–18. [CrossRef]
15. de Paiva Foletto-Felipe, M.; Abrahão, J.; Contesoto, I.C.; Ferro, A.P.; Grizza, L.H.E.; Menezes, P.V.M.C.; Wagner, A.L.S.; Seixas, F.A.V.; de Oliveira, M.A.S.; Tomazini, L.F.; et al. Inhibition of sulfur assimilation by S-benzyl-L-cysteine: Impacts on growth, photosynthesis, and leaf proteome of maize plants. *Plant Physiol. Biochem.* **2024**, *216*, 109173. [CrossRef]
16. Broadley, M.; Brown, P.; Cakmak, I.; Rengel, Z.; Zhao, F. Function of nutrients: Micronutrients. In *Marschner's Mineral Nutrition of Higher Plants*; Academic Press: Cambridge, MA, USA, 2023; pp. 191–248.
17. Perica, S.; Brown, P.H.; Connell, J.H.; Nyomora, A.M.; Dordas, C.; Hu, H.; Stangoulis, J. Foliar boron application improves flower fertility and fruit set of olive. *HortScience* **2001**, *36*, 714–716. [CrossRef]
18. Čakarević, J.; Šeregelj, V.; Tumbas Šaponjac, V.; Ćetković, G.; Čanadanović Brunet, J.; Popović, S.; Hadnađev Kostić, M.; Popović, L. Encapsulation of beetroot juice: A study on the application of pumpkin oil cake protein as new carrier agent. *J. Microencapsul.* **2020**, *37*, 121–133. [CrossRef] [PubMed]
19. Schymanski, E.L.; Jeon, J.; Gulde, R.; Fenner, K.; Ruff, M.; Singer, H.P.; Hollender, J. Identifying small molecules via high resolution mass spectrometry: Communicating confidence. *Environ. Sci. Technol.* **2014**, *48*, 2097–2098. [CrossRef]
20. Šelih, V.S.; Šala, M.; Drgan, V. Multi-element analysis of wines by ICP-MS and ICP-OES and their classification according to geographical origin in Slovenia. *Food Chem.* **2014**, *153*, 414–423. [CrossRef]
21. Pongrac, P.; Kelemen, M.; Vogel-Mikuš, K.; Vavpetič, P.; Pelicon, P.; Žurga, P.; Vidović, N.; Polić Pasković, M.; Smiljana, G.B.; Lukić, I.; et al. Tissue-specific calcium and magnesium allocation to explain differences in bulk concentration in leaves of one-year-old seedlings of two olive (*Olea europaea* L.) cultivars. *Plant Physiol. Biochem.* **2023**, *194*, 619–626. [CrossRef]
22. Pasković, I.; Pecina, M.; Bronić, J.; Perica, S.; Ban, D.; Ban, S.G.; Pošćić, F.; Palčić, I.; Herak Ćustić, M. Synthetic zeolite A as zinc and manganese fertilizer in calcareous soil. *Commun. Soil Sci. Plant Anal.* **2018**, *49*, 1072–1082. [CrossRef]
23. Ryan, C.G. Quantitative trace element imaging using PIXE and the nuclear microprobe. *Int. J. Imaging Syst. Technol.* **2000**, *11*, 219–230. [CrossRef]
24. Schindelin, J.; Arganda-Carreras, I.; Frise, E.; Kaynig, V.; Longair, M.; Pietzsch, T.; Preibisch, S.; Rueden, C.; Saalfeld, S.; Schmid, B.; et al. Fiji: An open-source platform for biological-image analysis. *Nat. Methods* **2012**, *9*, 676–682. [CrossRef]
25. R Core Team. *R: A Language and Environment for Statistical Computing*; R Foundation for Statistical Computing: Vienna, Austria, 2024. Available online: https://www.R-project.org/ (accessed on 4 January 2026).
26. RStudio Team. *RStudio: Integrated Development Environment for R*; Posit Software, PBC: Boston, MA, USA, 2024. Available online: https://posit.co/ (accessed on 4 January 2026).
27. O'Neill, M.E.; Mathews, K.L. Levene tests of homogeneity of variance for general block and treatment designs. *Biometrics* **2002**, *58*, 216–224. [CrossRef] [PubMed]
28. Urcelay, C.; Díaz, S.; Gurvich, D.E.; Chapin, F.S., III; Cuevas, E.; Domínguez, L.S. Mycorrhizal community resilience in response to experimental plant functional type removals in a woody ecosystem. *J. Ecol.* **2009**, *97*, 1291–1301. [CrossRef]

https://doi.org/10.3390/horticulturae12020151

29. Bkhairia, I.; Mhamdi, S.; Jridi, M.; Nasri, M. New acidic proteases from *Liza aurata* viscera: Characterization and application in gelatin production. *Int. J. Biol. Macromol.* **2016**, *92*, 533–542. [CrossRef] [PubMed]
30. Hadidi, M.; Tarahi, M.; Günther Innerhofer, M.; Pitscheider, I.; Löscher, A.; Pignitter, M. Pumpkin seed as a sustainable source of plant-based protein for novel food applications. *Crit. Rev. Food Sci. Nutr.* **2025**, *65*, 8566–8591. [CrossRef]
31. Da Rocha, M.; Alemán, A.; Baccan, G.C.; López-Caballero, M.E.; Gómez-Guillén, C.; Montero, P.; Prentice, C. Anti-inflammatory, antioxidant, and antimicrobial effects of underutilized fish protein hydrolysate. *J. Aquat. Food Prod. Technol.* **2018**, *27*, 592–608. [CrossRef]
32. Hoa, N.T.Q.; Dao, D.T.A. Release bioactive peptides from enzymatic hydrolysated soybean by Alcalase and Protamex using response surface methodology. *Viet. J. Sci. Technol.* **2017**, *55*, 137–149. [CrossRef]
33. Innocente, N.; Calligaris, S.; Di Filippo, G.; Melchior, S.; Marino, M.; Nicoli, M.C. Process design for the production of peptides from whey protein isolate with targeted antimicrobial functionality. *Int. J. Food Sci. Technol.* **2023**, *58*, 2505–2517. [CrossRef]
34. Schlegel, K.; Sontheimer, K.; Hickisch, A.; Wani, A.A.; Eisner, P.; Schweiggert-Weisz, U. Enzymatic hydrolysis of lupin protein isolates—Changes in the molecular weight distribution, technofunctional characteristics, and sensory attributes. *Food Sci. Nutr.* **2019**, *7*, 2747–2759. [CrossRef]
35. Tacias-Pascacio, V.G.; Morellon-Sterling, R.; Siar, E.-H.; Tavano, O.; Berenguer-Murcia, Á.; Fernandez-Lafuente, R. Use of Alcalase in the production of bioactive peptides: A review. *Int. J. Biol. Macromol.* **2020**, *165*, 2143–2196. [CrossRef]
36. Peñuelas, J.; Gamon, J.A.; Fredeen, A.L.; Merino, J.; Field, C.B. Reflectance indices associated with physiological changes in nitrogen- and water-limited sunflower leaves. *Remote Sens. Environ.* **1995**, *48*, 135–146. [CrossRef]
37. Gamon, J.A.; Peñuelas, J.; Field, C.B. A narrow-waveband spectral index that tracks diurnal changes in photosynthetic efficiency. *Remote Sens. Environ.* **1992**, *41*, 35–44. [CrossRef]
38. Lardos, M.; Marmagne, A.; Bonadé Bottino, N.; Caris, Q.; Béal, B.; Chardon, F.; Masclaux-Daubresse, C. Discovery of the biostimulant effect of asparagine and glutamine on plant growth in *Arabidopsis thaliana*. *Front. Plant Sci.* **2024**, *14*, 1281495. [CrossRef] [PubMed]
39. Renzetti, M.; Funck, D.; Trovato, M. Proline and ROS: A unified mechanism in plant development and stress response? *Plants* **2025**, *14*, 2. [CrossRef] [PubMed]
40. Shehata, R.S. Proline in action: Enhancing fruit quality. *DYSONA–Appl. Sci.* **2025**, *6*, 8–15. [CrossRef]
41. Ávila, C.; Llebrés, M.T.; Cánovas, F.M.; Castro-Rodríguez, V. Arginine, a key amino acid for nitrogen nutrition and metabolism of forest trees. *J. Exp. Bot.* **2025**, *76*, 5238–5251. [CrossRef]
42. Sun, Y.; Miao, F.; Wang, Y.; Liu, H.; Wang, X.; Wang, H.; Guo, J.; Shao, R.; Yang, Q. L-Arginine alleviates the reduction in photosynthesis and antioxidant activity induced by drought stress in maize seedlings. *Antioxidants* **2023**, *12*, 482. [CrossRef]
43. Chen, Q.; Wang, Y.; Zhang, Z.; Liu, X.; Li, C.; Ma, F. Arginine Increases Tolerance to Nitrogen Deficiency in Malus hupehensis via Alterations in Photosynthetic Capacity and Amino Acids Metabolism. *Front. Plant Sci.* **2022**, *12*, 772086. [CrossRef]
44. Li, S.; Peng, F.; Xiao, Y.; Gong, Q.; Bao, Z.; Li, Y.; Wu, X. Mechanisms of high concentration valine-mediated inhibition of peach tree shoot growth. *Front. Plant Sci.* **2020**, *11*, 603067. [CrossRef]
45. Maillard, A.; Diquélou, S.; Billard, V.; Laîné, P.; Garnica, M.; Prudent, M.; Garcia-Mina, J.M.; Yvin, J.C.; Ourry, A. Leaf mineral nutrient remobilisation during leaf senescence and modulation by nutrient deficiency. *Front. Plant Sci.* **2015**, *6*, 317. [CrossRef]
46. Gao, Y.; Qin, Y.; Liu, Z.; Li, C.; Ma, F. Target of rapamycin (TOR) regulates the response to low nitrogen stress via autophagy and hormone pathways in *Malus hupehensis*. *Hortic. Res.* **2022**, *9*, uhac143. [CrossRef]
47. Fernández-Escobar, R.; Moreno, R.; García-Creus, M. Seasonal changes of mineral nutrients in olive leaves during the alternate-bearing cycle. *Sci. Hortic.* **1999**, *82*, 25–45. [CrossRef]
48. Shehzad, F.; Ali, Q.; Ali, S.; Al-Misned, F.A.; Maqbool, S. Fertigation with Zn-Lysine confers better photosynthetic efficiency and yield in water-stressed maize: Water relations, antioxidative defense mechanism and nutrient acquisition. *Plants* **2022**, *11*, 404. [CrossRef]
49. Okla, M.K.; Saleem, M.H.; Saleh, I.A.; Zomot, N.; Perveen, S.; Parveen, A.; Abasi, F.; Ali, H.; Ali, B.; Alwasel, Y.A.; et al. Foliar application of iron-lysine to boost growth attributes, photosynthetic pigments and biochemical defense system in canola (*Brassica napus* L.) under cadmium stress. *BMC Plant Biol.* **2023**, *23*, 648. [CrossRef] [PubMed]
50. Henderson, B.C.; Sanderson, J.M.; Fowles, A. A review of the foliar application of individual amino acids as biostimulants in plants. *Discov. Agric.* **2025**, *3*, 69. [CrossRef] [PubMed]
51. Alcazar, R.; Amorós Ortiz-Villajos, J.Á.; Pérez de los Reyes, C.; García Navarro, F.J.; Bravo Martín-Consuegra, S. Major and trace element content of olive leaves. *Olivæ* **2014**, *119*, 1–7. [CrossRef]
52. Osman, A.; Merwad, A.-R.M.; Mohamed, A.H.; Sitohy, M. Foliar spray with pepsin- and papain-whey protein hydrolysates promotes productivity of pea plants. *Molecules* **2021**, *26*, 2805. [CrossRef]
53. Ertani, A.; Schiavon, M.; Nardi, S. Transcriptome-wide identification of differentially expressed genes in *Solanum lycopersicon* L. in response to an alfalfa-protein hydrolysate using microarrays. *Front. Plant Sci.* **2017**, *8*, 1159. [CrossRef]

54. Hu, W.; Lu, Z.; Meng, F.; Li, X.; Cong, R.; Ren, T.; Sharkey, T.; Lu, J. The reduction in leaf area precedes that in photosynthesis under potassium deficiency: The importance of leaf anatomy. *New Phytol.* **2020**, *227*, 1749–1763. [CrossRef]
55. Wang, M.; Zheng, Q.; Shen, Q.; Guo, S. The critical role of potassium in plant stress response. *Int. J. Mol. Sci.* **2013**, *14*, 7370–7390. [CrossRef]
56. Sardans, J.; Peñuelas, J. Potassium control of plant functions: Ecological and agricultural implications. *Plants* **2021**, *10*, 419. [CrossRef]
57. Shabala, S.; Shabala, L. Ion transport and osmotic adjustment in plants and bacteria. *Biomol. Concepts* **2011**, 2, 407–419. [CrossRef]
58. Liu, K.; Fu, H.; Bei, Q.; Luan, S. Inward potassium channel in guard cells as a target for polyamine regulation of stomatal movements. *Plant Physiol.* **2000**, *124*, 1315–1326. [CrossRef]
59. Agurla, S.; Gayatri, G.; Raghavendra, A.S. Polyamines increase nitric oxide and reactive oxygen species in guard cells of *Arabidopsis thaliana* during stomatal closure. *Protoplasma* **2018**, *255*, 153–162. [CrossRef]
60. Chabra, R.; Ringoet, A.; Lamberts, D. Kinetics and interaction of chloride and phosphate absorption by intact tomato plants (*Lycopersicon esculentum* Mill.) from a dilute nutrient solution. *Z. Pflanzenphysiol.* **1976**, *78*, 253–261. [CrossRef]
61. Hang, Z. Influence of chloride on the uptake and translocation of phosphorus in potato. *J. Plant Nutr.* **1993**, *16*, 1733–1737. [CrossRef]

Disclaimer/Publisher's Note: The statements, opinions and data contained in all publications are solely those of the individual author(s) and contributor(s) and not of MDPI and/or the editor(s). MDPI and/or the editor(s) disclaim responsibility for any injury to people or property resulting from any ideas, methods, instructions or products referred to in the content.

https://doi.org/10.3390/horticulturae12020151

3.3 HILIC in Targeted Compound Monitoring for Pharmacotherapy and TDM

3.3.1 An effective validation of analytical method for determination of a polar complexing agent: the illustrative case of cytotoxic bleomycin

Published: Plesnik, H., Bosnjak, M., Cemazar, M., Sersa, G., Kosjek, T., Analytical and Bioanalytical Chemistry, 2023

This paper directly addresses Hypothesis 1, which posits that HILIC-based chromatographic approaches are necessary for the reliable quantitative analysis of highly polar and structurally complex compounds that fall outside the effective scope of conventional reversed-phase workflows. The hypothesis is examined and confirmed through the development and validation of a quantitative LC–MS/MS method for bleomycin in plasma and serum, using the compound as a representative example of a broader class of analytically challenging therapeutics.

Bleomycin is employed in this thesis not because of its clinical relevance alone, but because it concentrates several recurring analytical difficulties into a single case: extreme polarity, from which follows poor RP retention, pronounced metal-complexing behavior, light sensitivity, and formulation heterogeneity. In addition, the absence of certified reference materials and interlaboratory comparison data places further constraints on method validation and long-term performance control. Together, these characteristics make bleomycin a suitable model compound for testing whether polarity-aware chromatographic and sample preparation choices can resolve limitations commonly encountered in quantitative bioanalysis of polar drugs.

The method developed in this study demonstrates that these challenges can be managed within a clinically realistic analytical framework. Adequate retention and reproducible separation are achieved using a BEH Amide HILIC column, confirming the necessity of HILIC for this analyte class and thereby supporting Hypothesis 1. Sample preparation is deliberately kept simple and robust, relying on protein precipitation and phospholipid removal, followed by UHPLC–MS/MS analysis on a QTrap platform. Quantification focuses on the BLM-A2 fraction, which dominates the clinical formulation, while additional fractions are used for qualitative confirmation. Importantly, bleomycin is quantified in its copper-complexed form, with controlled complexation enforced during sample preparation, reflecting its chemical behavior in biological matrices rather than treating metal binding as a secondary effect.

The achieved sensitivity is sufficient for therapeutic drug monitoring in plasma and serum, and method performance was monitored over time using control charts to ensure consistency. Stability experiments further define practical limits for sample handling and storage. Taken together, these results confirm Hypothesis 1 by demonstrating that HILIC-based methods are not merely advantageous but required for the development of robust, quantitative assays for highly polar drugs such as bleomycin.

Within the structure of the thesis, this work establishes the pharmacotherapy-oriented foundation for later non-targeted studies by showing, in a controlled quantitative setting, how polarity-driven analytical constraints can be systematically addressed.

Analytical and Bioanalytical Chemistry (2023) 415:2737–2748
https://doi.org/10.1007/s00216-023-04675-x

RESEARCH PAPER

An effective validation of analytical method for determination of a polar complexing agent: the illustrative case of cytotoxic bleomycin

Helena Plesnik[1,2] · Masa Bosnjak[3,4] · Maja Cemazar[3,5] · Gregor Sersa[3,6] · Tina Kosjek[1,2]

Received: 5 January 2023 / Revised: 2 March 2023 / Accepted: 28 March 2023 / Published online: 12 April 2023
© The Author(s) 2023

Abstract
The effectiveness of highly polar agents in cancer treatment is well recognized, but their physicochemical properties make their analytical determination a demanding task. Their analysis requires peculiar sample preparation and chromatographic separation, which heavily impacts the precision of such an analytical method. As a case study, we chose a polar cytotoxic bleomycin, which is a mixture of complexing congeners with relatively high molecular mass, a fact that creates an added challenge in regard to its detection via electrospray mass spectrometry. These issues combined lead to a deprived method performance, so the aim of this study is manifold, i.e., to optimize, validate, and establish quality performance measures for determination of bleomycin in pharmaceutical and biological specimens. Quantification of bleomycin is done at diametrically different concentration levels: at the concentrations relevant for analysis of pharmaceutical dosage forms it is based on a direct reversed-phase HPLC-UV detection, involving minimum sample pretreatment. On the contrary, analysis of bleomycin in biological specimens requires phospholipid removal and protein precipitation followed by HILIC chromatography with MS/MS detection of bleomycin A2 and B2 copper complexes being the predominant species. This study further attempts to solve the traceability issue in the absence of certified reference standards, determines measurement uncertainty, investigates BLM stability and method performance characteristics, and, last but not least, provides an explanatory example of how a method quality assurance procedure should be established in case of an exceedingly complex analytical method.

Keywords Liquid chromatography · Mass spectrometry · Biological · Pharmaceutical · Measurement uncertainty · Stability

Abbreviations

BLM	Bleomycin
LLOQ	Lower limit of quantification
BLM-A2-Cu	Bleomycin A2 fraction copper complex
BLM-B2-Cu	Bleomycin B2 fraction copper complex
ACN	Acetonitrile
ECT	Electrochemotherapy
BLMH	Bleomycin hydrolase

✉ Tina Kosjek
tina.kosjek@ijs.si

1 Department of Environmental Sciences, Jozef Stefan Institute, Jamova 39, 1000 Ljubljana, Slovenia

2 International Postgraduate School Jozef Stefan, Jamova cesta 39, 1000 Ljubljana, Slovenia

3 Department of Experimental Oncology, Institute of Oncology Ljubljana, Zaloska 2, 1000 Ljubljana, Slovenia

4 Faculty of Pharmacy, University of Ljubljana, Askerceva 7, 1000 Ljubljana, Slovenia

5 Faculty of Health Sciences, University of Primorska, Polje 42, 6310 Izola, Slovenia

6 Faculty of Health Sciences, University of Ljubljana, Zdravstvena pot 5, 1000 Ljubljana, Slovenia

Introduction

Bleomycin (BLM) is a common term for a group of structurally related cytostatic antibiotics, isolated from *Streptomyces verticillus*. Due to its high cytotoxicity, it is used in the treatment of various neoplasms, particularly squamous carcinoma, lymphoma, and testicular carcinoma [1]. It was recently proven to also be effective against vascular malformations [2]. Although injected in the apo form, the cytotoxic activity is exhibited by its metal complexes or metallobleomycins. These generate reactive oxygen species and thereby oxidatively damage DNA, causing single- and double-strand breaks, ultimately destroying the cell [3]. The exact mechanism of action has however yet to be fully elucidated.

To achieve the desired cytotoxic effect in patients, a sufficient amount of bleomycin must reach its site of action, located inside the cell nuclei. The transition of bleomycin through cell membranes is however hindered due to its size and rather hydrophilic nature. Therefore, only a small portion of molecules is able to enter the cells. Simply increasing the administered dose to reach the desired effect does not present a viable solution as doing so would also amplify the toxic side effects, already observed at the currently used doses in a significant fraction of patients (with up to 46% experiencing significant morbidity) [4]. This problem is stimulating the development of new approaches, one promising example being electrochemotherapy (ECT), where electrical pulses are applied to transiently increase the permeability of cell membranes, thereby facilitating the passage of BLM into cells [5]. ECT is still being optimized but has already been proven to be effective in tumor as well as vascular malformations therapy [2, 6, 7]. Another obstacle to achieving sufficiently high concentrations of bleomycin at the site of its action is the presence of bleomycin hydrolase (BLMH), a cytoplasmic protease, causing deamination and thereby inactivation of bleomycin. Despite being tissue nonspecific, this enzyme is overexpressed in some tumors and further reduces the amount of intact bleomycin reaching its site of action [8, 9].

Quantitative analyses of bleomycin for assay testing of its pharmaceutical form (injection solution powder) are, as pure and rather concentrated solutions can be prepared with the powder, routinely performed using simple methods based on HPLC separation with UV detection as described in the European Pharmacopoeia and require little to no pretreatment [10]. A different approach must be considered with clinical samples. Biological matrices such as blood or tissue are namely relatively complex, which implies extensive sample preparation. In addition, BLM is present at considerably lower concentrations in such samples, requiring the use of highly sensitive instruments. The newest published method, meeting such requirements, describes sample preparation employing solid-phase extraction and is based on UHPLC-MS/MS, and reaches a lower limit of quantification (LLOQ) in the ng/mL range [11].

High-quality analytical procedures are of critical importance for monitoring bleomycin concentrations in patients undergoing already established treatment regimes, but also support their further optimization or development of new therapeutic approaches. Developing a well-performing analytical method comes with various challenges, one of them being the heterogeneity of bleomycin, which is not a single molecule but rather a compost of multiple very similar fractions (A1–A6; B1–B5), only varying in the structure of the C-terminal substituent [12]. Its structure with main functional domains is shown in Fig. 1. Clinically administered bleomycin (Bleomycin Sulphate USP) largely consists of BLM-A2 (55–70%) and BLM-B2 (25–32%) fractions, but trace amounts of others may also be present [10, 12, 13].

Bleomycin's tendency to form complexes with a range of redox-active metals (Fe, Cu, Ni, Mn, and Zn) plays an important role in its biological activity [1]. The highest binding affinity is shown towards copper ions, which bind in vivo as well as in vitro [11, 14]. Therefore, although administered in a metal-free form, BLM in the blood is present in the form of a copper complex. Complex formation needs to be accounted for in the case of mass spectrometric detection, as metallobleomycins differ from their corresponding native molecules in mass.

A limited number of analytical methods have been developed for the detection of bleomycin in biological samples. The early methods mainly utilized HPLC separation and identification techniques such as UV absorption, radioimmunoassay, and fluorescence detection, which demonstrate

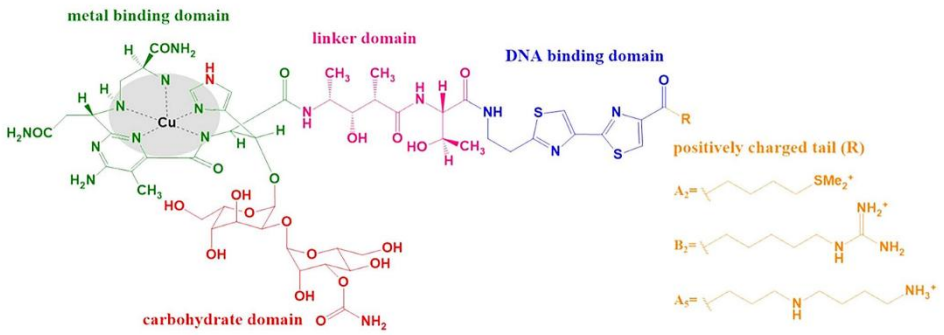


Fig. 1 Structure of a BLM-Cu complex (adapted from [1])

limited selectivity being unable to distinguish between BLM fractions [13, 15–17]. Striving towards better selectivity, some studies have been able to develop methods that managed to separate the predominant fractions of bleomycin (A2 and B2), using ion-paired reversed-phase HPLC [12, 13, 18, 19]. They however demonstrated either a relatively high detection limit [13] or a narrow linear concentration range [12]. After comparing the formerly often-used reversed-phase to hydrophilic interaction chromatography (HILIC), specifically designed for the analysis of polar compounds, Galba et al. [20] demonstrated the advantages of the latter. In addition to better retention, separation efficiency, and selectivity, the use of a HILIC column eliminates the need for adding ion-pairing reagents in the mobile phase. Similarly, our group resorted to a HILIC-like BEH Amide column, developing a method with high-resolution MS (HRMS) quantitative determination of the main bleomycin fractions that successfully separates their Cu(II) complexes [11]. Bleomycin's high affinity towards copper ions and their presence in biological samples make the complex a sensible choice of analyte. Despite providing results with high selectivity, sensitivity, and low detection limits for both predominant bleomycin fractions, it relies on an HR mass analyzer, not readily available or widespread in the clinical setting. A method using more accessible instrumentation would therefore mean a great advantage, allowing its wider use.

The method for the quantitative determination of BLM in biological tissues was published in 2016 and was for the time being the only reliable choice for such analysis at clinical levels. Since then, new sorbent materials have been brought to the market, and along grew the need for simplification in terms of labor invested, time, and materials consumed, thus facilitating the analyses of sizeable batches of samples. This study reveals the results of analytical method optimization and its revalidation compliant with the European Medicines Agency (EMA) guidelines [21]. Furthermore, it attempts to solve the traceability issue, determines measurement uncertainty, investigates BLM stability and method performance characteristics, and, last but not least, this study sets an explanatory example of how method quality assurance procedure should be established in the case of an exceedingly complex analytical method.

Experimental/materials and methods

Caution: BLM is cytotoxic, genotoxic, teratogenic, and mutagenic *and should be handled with care* [22, 23].

Chemicals and materials

Primary reference standard: bleomycin sulfate salt (CAS No.: 9041-93-4) was purchased in a metal-free form with a declared purity of 95.7% (C55H84N17O21S3 × H2SO4) from Santa Cruz Biotechnology, Inc. (Dallas, TX). Cross-check reference standard bleomycin sulfate, also in metal-free form, was purchased with as declared purity of ≥95% from Cayman Chemical (Ann Arbor, MI). The pharmaceutical dosage form Bleomedac®, a powder solution for injection with the declared amount of bleomycin sulfate 15,000 IU that corresponds to the biological activity of 15 mg BLM, is produced by Medac GmbH (Wedel, Germany). Bleomycin A5 hydrochloride (C57H89N19O21S2 × HCl, CAS: 55658-47-4) used as an internal standard was purchased from LKT Laboratories, Inc. (St. Paul, MN) in a metal-free form and had a declared purity of ≥ 90%. The agent for control of metal complex formation was CuSO4 × 5H2O (Alkaloid Skopje, Macedonia). Mobile phase additives ammonium formate (≥99.0%) and formic acid (99%) were purchased at Sigma-Aldrich Corp. and Carlo Erba (Val de Reuil, France), respectively, both of LC-MS purity grade. Acetonitrile and water used as the mobile phases were of LC-MS purity, and all solvents used in sample prep (methanol, water, acetonitrile) were of analytical grade purity.

Normal human serum was purchased from Sigma-Aldrich (St. Louis, MO, USA). Blood plasma was acquired by using Vacutainer® heparin collection tubes.

The chromatographic columns used were Acquity UPLC BEH Amide column with dimensions 130 Å, 1.7 µm, 2.1 mm × 50 mm (Waters Corp., Milford, MA, USA) and Zorbax® Eclipse XDB-C18 column with dimensions 5 µm, 4.6 mm × 150 mm. For sample preparation, the following sorbent forms were used: Oasis HLB 96-well plates (30 mg sorbent per well, 30 µm), Oasis HLB 1cc (30 mg) extraction cartridges, and Ostro protein precipitation and phospholipid removal plates, 25 mg (Waters Corp.). Filtering of the samples before the analysis was performed on 0.2 µm Phenex^{TM} regenerated cellulose membrane syringe filters (Phenomenex, Torrance, CA).

The software used included ChemDraw 14.0 (Perkin-Elmer Corp., Norwalk, CT) and Analyst 1.6.3 (AB Sciex, Framingham, MA).

Preparation of standard and working solutions

The stock solution of BLM was prepared by dissolving 10 mg of bleomycin sulfate primary reference standard in 10 mL of methanol and Milli-Q water mixture (8:2) and was kept at −18 °C. The stock solution of the cross-check reference standard was prepared the same way. The working standards at concentrations 0.1, 1, 5, and 10 µg/mL were freshly prepared before the analysis by diluting the BLM stock solution in 0.1% formic acid.

The internal standard (bleomycin A5) was prepared as a stock solution by dissolving 5 mg in 10 mL of methanol and Milli-Q water mixture (8:2) and was kept at −18 °C. The

working standard was freshly prepared every time prior to analysis by diluting the stock solution to the concentration of 5 µg/mL.

The LC-MS method calibration and quality control standards were prepared by spiking the serum or plasma, their concentrations ranging from 6 to 1500 ng/mL. The HPLC method validation standards were prepared in concentrations 2.5–40 µg/mL BLM in Milli-Q water.

CuSO4, the agent for control of metal complex formation, was prepared by dissolving 1.22 mg of CuSO4·5H2O in 20 mL of Milli-Q water and further diluted to 3.05 µg/mL. It was later added into serum in a molar concentration that exceeded that of the analyte at the highest calibration point and internal standard combined.

NH4COO- measuring 200 mM was prepared by diluting 1.261 g in 100 mL of Milli-Q water. The aqueous mobile phase for the LC-MS method (10 mM ammonium formate with 0.1% formic acid) was prepared by 20 times diluting 200 mM ammonium formate and addition of 500 µL formic acid per 500 mL of buffer solution. The aqueous mobile phase for the HPLC method (20 mM ammonium formate with 0.1% formic acid) was prepared by 10 times diluting 200 mM NH4COOH and addition of 500 µL formic acid per 500 mL of buffer solution.

Sample preparation

Two hundred microliters of either plasma or serum was put into 1.5-mL polypropylene microcentrifuge tubes. Forty microliters of $CuSO_4$ (3.05 µg/mL) and 24 µL of BLM-A5 (5 µg/mL) were added. The mixture was vortexed and then transferred into Ostro™ 96-well plate wells. Protein precipitation was achieved by the addition of 900 µL ice-cold acetonitrile with 0.1% formic acid. In-well mixing was performed with vigorous pipette aspiration and subsequently pushed through the Ostro™ sorbent at 60 psi N_2 for 5 min using a positive pressure manifold. Finally, the eluates were filtered through 0.2 µm reverse cellulose filters, generating a protein-, phospholipid-, and particulate-free solution. Since bleomycin has been proven to be light-sensitive [24], measures have been taken during all sample preparation steps to avoid direct light exposure.

Instrumental analysis

Two analytical methods were optimized for the quantitative analysis of BLM. The analysis of biological samples with more complex matrices and at lower concentration levels was performed on a UHPLC-MS/MS system, while a simpler method employing an HPLC system with DAD detection was used to analyze BLM content in injection solution (Bleomedac®) at higher concentration levels.

Ultra-high-performance liquid chromatography–tandem mass spectrometry

For the instrumental analysis of trace level BLM in complex samples, an ultra-high-performance liquid chromatograph (UHPLC, Shimadzu, Kyoto, Japan) coupled to a hybrid quadrupole-linear ion trap mass spectrometry analyzer QTRAP 4500 (Sciex, Framingham, MA, USA) with positive electrospray ionization (ESI+) was utilized. Acquity™ UPLC BEH Amide Column (1.7 µm, 2.1 mm × 50 mm) (Waters, Milford, MA, USA) column was used for separation. Separation was achieved using the gradient method and the following mobile phase composition: acetonitrile (mobile phase A) and 10 mM ammonium formate with 0.1% formic acid (mobile phase B). The gradient program started with 5% B, first increased to 50% at 2 min, and then further to 60% at 4 min. It then decreased back to 5% where it remained until 6 min. The total mobile phase flow rate was 0.3 mL/min. The column temperature was kept at 40 °C. An injection volume was 1.0 µL.

The ion source parameters were maintained as follows: ion spray voltage +5500 V; source temperature 650 °C; declustering potential (DP) 126 V; curtain gas (CUR) 40 psi; ion source gas 1 (GS1) 40 psi; ion source gas 2 (GS2) 25 psi. Ions were acquired in multiple reaction monitoring (MRM) mode; the transitions are together with the compound-specific parameters presented in Table 1.

High-performance liquid chromatography

To perform this analysis, a high-performance liquid chromatograph coupled with a diode array detector (1260 Infinity Agilent Technologies, Santa Clara, CA, USA) was used. The separation was achieved using the Zorbax Eclipse C-18 column (150 mm × 4.6 mm, 5 µm) (Agilent Technologies, Santa Clara, CA, USA), which was kept at 40 °C. The injection volume was 10 µL. Gradient elution was performed with the following mobile phases: (A) 0.1% HCOOH in acetonitrile (mobile phase A) and 0.1% HCOOH in 20 mM NH4COOH formate buffer (mobile phase B). The gradient started with 95% B, which decreased down to 55% from minute 1 to 6 min; then, it increased back to 95% B at 6.5 min and was kept so until 9 min. The flow rate was 1 mL/min and the detector wavelength was set to 291 nm.

Table 1 MRM parameters for the LC-MS/MS method

Compound	Q1 mass	Q3 mass	Time (ms)	CE (V)	CXP (V)
BLM-A2-Cu	738.4	707.2	500.0	23.0	4.0
BLM-B2-Cu	743.8	707.3	200.0	39.0	10.0
BLM-A5-Cu	752.3	715.7	200.0	37.0	8.0
BLM-A5-Cu	752.3	294.9	100.0	71.0	12.0

Validation protocols

To confirm the *selectivity* of the method, blank and zero samples were evaluated. The blanks were prepared in appropriate matrices (serum or plasma) with the addition of internal standard but were not spiked with the analyte. The zero samples were prepared identically, though without the internal standard. The EMA criteria [21] for method validation require analyte peak areas in blanks to be ≤ 20% of the mean LLOQ analyte peak area and IS peak areas of the blanks below 5% of the average IS peak area of the calibrators and QCs.

Carryover was examined by analyzing solvent blanks after the measurement of the highest calibrator (1500 ng/mL). The blank analyte peak area, observed in the blanks should, according to the guidelines, not exceed 20% of the analyte peak area in the LLOQ. Likewise, the blank IS peak area should not exceed 5% of the mean IS peak area of the calibration standards and QC.

Linearity of the LC-MS was determined by analyzing matrix-matched calibration curves, made up of ten serum samples, spiked at different concentration levels in the range of 2.5–250 ng/mL in the final extract, corresponding to concentrations of 15–1500 ng/mL in serum as might be expected in real samples. For the HPLC method, the calibration curve consisted of six spiked samples, covering a concentration range of 2.5–40 µg/mL. The correlation between peak area ratio and bleomycin concentration was characterized by linear regression. EMA guidelines [21] consider a calibration to be acceptable if at least 75% of the calibrators fall within ± 15% (or 20% for the LLOQ) of their nominal concentrations.

Sensitivity of the method is defined in the FDA guidelines [25] as the lowest analyte concentration in the matrix that can be measured with acceptable accuracy and precision described by LLOQ. The determined LLOQ concentration was evaluated by analyzing three replicates of LLOQ concentration with each calibration curve, the mean of which should be within ±20% of the nominal concentration for at least 50% of the replicates.

Accuracy, described by trueness and precision, was evaluated by analyzing QC standards for three replicates at two different concentration levels. Precision reflected inter- and intra-day repeatability, the latter was evaluated by assessing injection and method repeatability. Injection repeatability was assessed as part of precision determination by successively injecting the same matrix-matched calibration standard three times while the method repeatability test included analyses of identically prepared (QC) samples at two concentrations, each in 3 replicates.

Inter-day precision and accuracy were part of the experiment following the method's performance over a longer period of time. This was done by establishing a control chart, and recording quantification results for the quality control samples at two different concentrations, at a low (method LLOQ) and an intermediate concentration of the analyte, both in triplicates. Acceptance criteria, according to EMA guidelines [21] were (1) accuracy: mean concentration of QC samples must be within 15% of their nominal concentration (20% for QC at LLOQ). (2) Precision: each QC level should have a coefficient of variation (% CV) of no more than 15% and at the LLOQ no more than 20%.

Extraction recovery was calculated as an IS normalized response ratio of human serum spiked at LLOQ level and at 600 ng/mL before vs after extraction. The internal standard was added before the analysis in both cases to cover for instrumental drift.

Stability in serum and plasma

Long-term stability: eight 200 µL replicates of each, blank human plasma and serum, were spiked with BLM, generating concentrations of 1200 ng/mL. Duplicates were evaluated against freshly prepared matrix-matched calibration standards at four different time points: at 0, after 52, 90, and 123 days stored at −20 °C, protected from light.

Freeze-thaw stability: bleomycin freeze-thaw stability was evaluated for a total of six freeze/thaw cycles, from −20 °C to room temperature. Spiked blank serum and plasma samples were subjected to six cycles. The samples were compared against freshly prepared calibration standards.

Stability in injection solution

Long-term stability: bleomycin injection solution, obtained by dissolving the contents of one vial of Bleomedac® powder with 15,000 IU bleomycin in 5 mL of saline, was divided into aliquots; eight were stored in a freezer at −20 °C and another eight in a cooler at 8 °C. Duplicates were diluted (100 times; generating samples with 30 IU of BLM per mL; referring to biological potency) and analyzed against freshly prepared calibration standards after 0, 58, 98, and 141 days.

Freeze-thaw stability: injection solution with bleomycin was evaluated for six freeze/thaw cycles, prepared in the same way as plasma and serum.

Measurement uncertainty (*MU*) was estimated for both methods based on QC samples at two different analyte concentrations, which were acquired at different time points. MU took into account accuracy errors as well as the reproducibility of QCs. This covered uncertainty contributed by different analysts, days of analysis, and uncertainty in concentration contributed by the preparation of standards and calibration samples. An extended description of the calculation is reported in the Supplementary material.

Traceability: due to the lack of existing certified reference materials, otherwise necessary to demonstrate traceability,

samples, prepared with BLM standards from two different producers (Cayman chemical and Santa Cruz Biotechnology), were compared. They were prepared at 600 ng/mL in three parallels for each.

Results and discussion

LC-MS-based method

Optimization

Instrumental analysis The UHPLC-MS/MS method was essentially based on our previous method [11], which we transferred from an HRMS to a more sensitive and more robust MSMS system, a QTRAP MS, which is also more widely available in the clinical settings and generic analytical laboratories. The separation conditions were HILIC-like using the BEH Amide column. Several mobile phases and gradients were tested throughout the optimization process, but they all generated poorer peak shapes, hence the decision to keep ammonium formate buffer (10 mM NH_4COO with 0.1% v/v formic acid, pH 3.3) and acetonitrile. A range of injection volumes was tested, determining 1 µL to fit best for the applied analyte concentration range. An increase to 10 µL might however be preferable for concentrations at the lower end of the applied concentration range. An overview of the tested and selected instrumental operational parameters is presented in Table S - 1.

Extraction and clean-up protocols The existing sample preparation procedures developed for the clean-up of biological samples are time-consuming and laborious. Our main objective was therefore to develop a simplified protocol, which would facilitate the preparation of larger sample batches while still providing satisfactory clean-up and high recoveries. Three different procedures were compared based on their performance and overall complexity; the respective workflows are summarized in Fig. 2.

The simplest workflow (a), solely focused on removing protein, entailed straightforward acetonitrile-mediated protein precipitation, followed by centrifugation. An alternative method (b) provided the removal of protein as well as phospholipids, together comprising the main matrix interferences leading to ion suppression in MS analysis. Performed on a 96-well plate system, in-well deproteinization, achieved by forcefully adding ice-cold acetonitrile, was combined with subsequent removal of phospholipids through adsorption on C18 sorbent. The third method (c), classical SPE, was also performed on 96-well plate systems at positive N2 pressure. The universal polymeric HLB sorbent provided the removal of a wide range of matrix impurities.

The SPE method was originally considered to be the method of choice due to its ability to remove the largest spectrum of impurities in comparison to the other applied methods, including nonvolatile salts, which interfere with the MS analysis. The SPE protocol used hydrophilic-lipophilic-balanced (HLB) sorbent, packed into cartridges [11], and was within this study upgraded to a 96-well plate

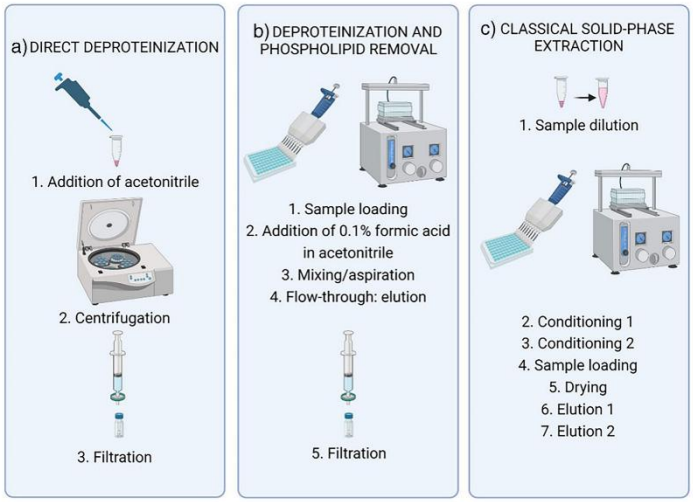


Fig. 2 Sample preparation workflows

format, allowing preparation of a larger number of samples simultaneously, which drastically simplifies and speeds up the sample prep procedure. The SPE protocol was further optimized by modifying the composition of elution solvents. Different compositions of Milli-Q water, methanol, and acetonitrile were tested to determine, which provides the best results in terms of chromatographic peak shapes and recoveries (maximum elution efficiency and reduction in matrix effect). In HILIC chromatography, the peak shape is drastically affected by the choice of a reconstitution solvent. Yet, it was observed that the elution solvent cannot be completely reconstituted, since drying of the entire solvent leads to extensive losses of BLM as reported by Kosjek et al. [11], which is likely the consequence of its sorption to glass surfaces. It is therefore obvious that the resulting suboptimal composition of elution solvent in turn affects the peak shape and chromatographic separation. Therefore, we aimed for the elution phase to contain as much ACN solvent as possible, limiting the MQ content in the final extract to a maximum of 30% in order to get acceptable peak shapes. However, since ACN performs rather poorly as an elution solvent (with both methanol and Milli-Q water eluting BLM at much higher efficiencies), the choice of the elution solvent composition was a compromise between the two factors, the optimal being methanol/Milli-Q water 1:1 (0.5 mL) followed by acetonitrile (0.5 mL). The comparison of all tested elution solvents (Table S - 2) as well as the final SPE protocol is presented in Supplementary material 2.2.1.

As an easier and faster alternative to initially employed SPE, the use of Ostro plates was considered, offering a combination of in-well protein precipitation with acetonitrile and subsequent phospholipid removal. The process, also performed on 96-well plates, is in this case advantageous as it is simpler and more rapid than the SPE. We followed the producer-recommended protocol, only implementing one slight modification. The concentration of formic acid added to the precipitating agent acetonitrile was reduced to 0.1% instead of 1% to avoid its negative impact on chromatographic peak shape.

Simplifying the pretreatment further by eliminating the extraction step an even more straightforward procedure was tested. Cold acetonitrile was added to the spiked serum or plasma, precipitating the protein, which was followed by centrifugation and finally filtering. The great repeatability as well as high recoveries (see Fig. S - 1) exhibited by this method would make it a preferred choice for serum samples. In the more complex plasma matrix, however, this is not the case as sufficient clean-up is not provided. More background noise in the chromatograms resulted in unfavorably high LLOQ. Additionally, the remainder of the matrix that is not removed causes signal suppression with the average response in spiked serum samples being over 30% lower than in serum samples at the same BLM concentration (see Table S - 3). Additionally, somewhat poorer repeatability is observed at low concentrations.

Figure S - 1 summarizes the performance parameters of the three described sample preparation methods (SPE, deproteinization with phospholipid removal on Ostro® plates, and direct deproteinization). All three sample prep protocols provided sufficient clean-up for serum. For plasma, however, the direct deproteinization method proved unsuitable, suggesting extraction step be necessary. The direct deproteinization method did however provide the highest recoveries, while these were not significantly different among the other methods. The variation coefficients are the lowest for the SPE method. Factoring in the simplicity and brevity of the procedure, the sample preparation method of choice was the one using phospholipid removal plates.

Further considerations *Vial material*: possible effect of analyte sorption onto the surface of glass vials on quantitative results was studied by comparing glass and polypropylene plastic vials. Having observed no significant quantitative differences between the two, we assumed the container surfaces do not impact analysis.

Addition of $CuSO_4$ (agent for control of metal complex formation): copper is ubiquitously present in the human body. As BLM has been shown to instantly form equimolar complexes in contact with copper ions [26] and the formation of such chelates in vivo is therefore practically inevitable in vivo, we determined BLM as well as the internal standard (BLM-A5) as BLM-copper complexes. The total copper content in blood plasma and serum is about 1000 ng/mL (15.7 nmol/mL) [27]. A large fraction thereof is bound to various protein species, either specifically (ceruloplasmin) or non-specifically (e.g., albumin). In sick individuals, the equilibrium between the bound and non-bound fractions can be altered [27]. To make sure that there were enough copper (Cu^{2+}) ions available for the complexation of BLM, a surplus of $CuSO_4$ (0.05µmol/sample) was added as an agent for control of metal complex formation. The samples with the addition of copper revealed about 18% higher abundancies of the analyte in comparison to those where Cu^{2+} was not added (see Fig. S - 2), indicating the necessity of this addition.

Importance of the anticoagulant choice for plasma preparation: we found the choice of blood collection tubes in sample withdrawal crucially important for the further analysis of the BLM-Cu complex. The most commonly used anticoagulant in plasma preparation is K2EDTA or K3EDTA, typically packed in purple-cap blood collection tubes for clinical hematology. A possible alternative is green-cap collection tube containing lithium heparin as an anticoagulant for plasma preparation, whereas a yellow-cap tube containing a clot activator and gel is used for serum separation.

EDTA being a known chelating agent potentially affects quantification results by reducing the availability of free copper to BLM and in turn preventing the complexation of the entire BLM present. To assess whether this is of significance, plasma prepared with purple-cap and green-cap tubes was compared. Spiked samples were prepared at 600 ng/mL in triplicates for each plasma type. The clear difference between the average responses, being 88% lower for EDTA plasma, favors the use of heparin plasma (see Fig. S - 2).

Implementation of a new internal standard: the importance of an internal standard to normalize for potential errors and drifts that arise during sample preparation and LC-MS analysis, and to correct for matrix effects in MS detection, is indisputable. An isotopically labeled form of BLM would present the optimum choice since it mimics the behavior of the analyte, but since it is not available at the market, several alternative compounds were tested as potential internal standards, including methotrexate, vancomycin, and epirubicin [11]. Unfortunately, none of them provided a correction to linearity or reproducibility. Hence, the optimal alternative seems to be using any of its fractions, absent (or present in negligible quantities) in the reference standard and the clinically administered mixture. The A5 fraction was chosen for this purpose due to its commercial availability in a relatively pure form. We monitored its copper complex (BLM-A5-Cu). The exact masses of its protonated form and its characteristic fragments were first determined with a high-resolution mass spectrometer (quadrupole-time-of-flight MS) and then transferred to a low-resolution MS/MS setting. The MRM transitions are stated in Table 1. BLM-A5 was added to the samples at the concentration of 600 ng/mL and proved to provide an improvement in the method performance as seen in improved linearity (r^2=0.9997 *vs* r^2=0.9926 without normalization) and precision (RSD = 3.4% *vs* RSD = 16.1% without normalization for three replicates).

LC-MS method validation

To achieve reliable results, accurately reflecting concentrations of the analyte in the samples, the performance of the method was carefully evaluated. Validation was performed according to the EMA [21] guidelines, evaluating its selectivity, linearity, LLOQ, precision, accuracy error, and measurement uncertainty. Ascertained by using the exact BLM-A2-Cu and BLM-B2-Cu mass data, reported by Kosjek et al. [11] and by precisely determining the mass of newly introduced BLM-A5-Cu in the same way, the method exhibits good selectivity. The mass spectrum of the BLM-A5-Cu complex is presented in Fig. S - 4. Selectivity was then demonstrated by showing the response in blank samples, which were all well below the set limits (20% of the mean LLOQ analyte peak area for the analyte or 5% of the average IS peak area for the internal standard).

Quantification was based on the more abundant BLM-A2-Cu complex taking into account that A2 and B2 fractions are present in the same ratio in both reference standard and clinically used bleomycin. The exhibited response was linear in the whole analytical range (15–1500 ng/mL) with r^2 values exceeding 0.99 for each calibration performed. LLOQ determined as the lowest calibration point with an accuracy error ≤20% was established at 15.0 ng/mL. The method proved to be accurate and repeatable, exhibiting errors within 10% of the nominal value for over 75% of the standards at each performed calibration. Method repeatability, assessed by measuring three replicates of samples at method LLOQ (15 ng/mL) as well as high (600 ng/mL) concentration, exhibited values up to 18.9% RSD and 16.8% RSD, respectively. The results are presented in Table S - 4.

Calibration samples were prepared in a serum matrix and were applicable for quantification in both serum and plasma samples, proving beforehand the matrix effect does not differ among the two in a way that would significantly impact the responses/results (Fig. S - 3). Two-sample *t*-tests assuming equal variances were performed at two concentration levels (15 and 600 ng/mL), comparing results obtained in both matrices and proving the absence of any significant differences. Some day-to-day variability in the slopes and intercepts, observed in the calibration curves, however, necessitates preparation and measuring of fresh calibration standards along with every sample batch.

Inter-day precision in accuracy: long-term performance of the analytical method Monitoring method performance over a longer time period was conducted by preparing multiple fresh calibration curves and quality control samples at different time points (approximately monthly intervals) by different analysts. The data, obtained from the QC samples, is displayed in form of a control chart for the LLOQ (15 ng/mL, Fig. 3) and high (600 ng/mL, Fig. 4) concentrations. The limits were calculated from the first 12 measured results, obtained within the first year, and were kept so for the reported time period. They are to be recalculated on an annual basis. The central line represents the average of all measurements as well as the upper and lower warning (UWL, LWL) and action (UAL, LAL) limits. These were established using the formulas:

$$WL = \bar{x} \pm 2 \cdot STDEV$$
$$AL = \bar{x} \pm 3 \cdot STDEV$$

where $\bar{x}$ stands for the average value of all the measurements and STDEV is the standard deviation between the daily averages, all applying to results, obtained at the first 12 measurements. Plotted on the charts are the average values, measured

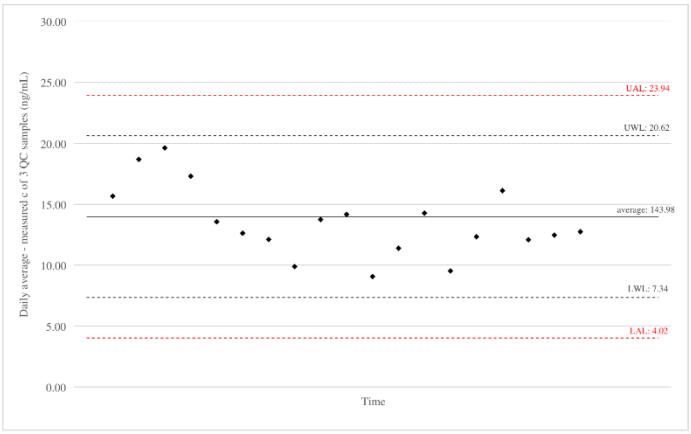


Fig. 3 Control chart of quality control samples at low (15 ng/mL) concentrations of bleomycin

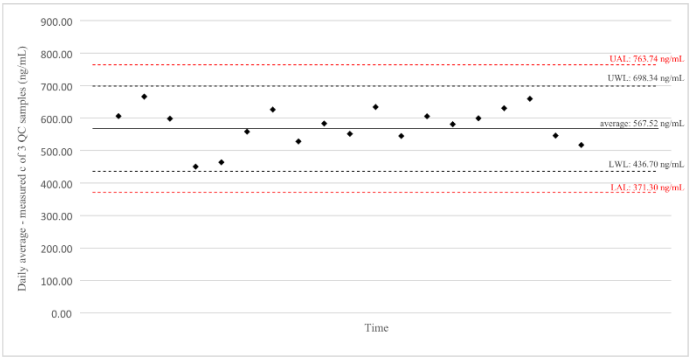


Fig. 4 Control chart of quality control samples at medium (600 ng/mL) concentrations of bleomycin

on each day along with the established limits, showing the scatter and accuracy of the results. As seen on the chart, values fall within said control limits, reflecting good method performance over the time period of 17 months. Variations in instrument signal strength and the resulting peak area variability across individual measurement days are reported in the Supplementary material Figure S - 5.

Dispersion of obtained measurement results can be explained with measurement uncertainty, an important parameter of the performance of an analytical method. To increase the confidence in produced results, evaluation of measurement uncertainty should therefore also be considered as a part of analytical validation. That is performed either by identifying individual uncertainty sources and evaluating the contribution of each one or, as a simpler alternative, by calculating it from validation data as described in guide ISO 21748 [28–31]. Once the uncertainty has been evaluated for a method in a particular laboratory, it may be applied to subsequently acquired results (if there is relevant QC data provided) [28].

The extended measurement uncertainty was calculated for two different concentration levels of bleomycin by following the Nordtest method [32]. The calculation is described in detail in Supplementary material 2.5.2. It was estimated to be 26% at high (600 ng/mL) and 50% at low (15 ng/mL) concentration of analyte at a 95% confidence interval.

Traceability Among the validation parameters, th trueness of the measurements is the most challenging to demonstrate. It should ideally be assessed by relating the values to (internationally recognized) reference standards through

an unbroken chain of calibrations with stated uncertainties, which describes traceability, a fundamental concept in metrology. Matching the real samples in matrix, concentration, and chemical form of the analyte, certified reference materials (CRMs) are considered to provide the highest level of accuracy, uncertainty, and traceability to an SI unit of measurement. Using such materials as quality control samples in method evaluation is the most straightforward way of establishing traceability. In case the market does not supply CRMs for a specific analyte/matrix, true traceability is impossible to achieve. Other measures can and should however be considered to demonstrate the accuracy of the results and increase confidence in them. One possibility is introducing external testing in the form of inter-laboratory studies provided there exist laboratories, performing analyses on the same type of samples. If this is not the case, other solutions, performed within one laboratory, must be resorted to.

Our approach was to compare the primary standard, used for the preparation of calibration samples, to a standard from a different producer. Results, shown in Fig. S - 6, show there is no significant difference between the two standards, which demonstrated a certain level of confidence in the quantification of results, at least regarding the adequacy of the applied primary standard.

Bleomycin stability study

Information on the stability of the analyte in all relevant matrices, concentrations, and storage conditions is of fundamental importance to analytical science as it is the basis for determining the appropriate handling of samples and standards. When stability information for the relevant conditions is not previously reported, a stability study should be conducted along with bioanalytical method validation. The results of quantitative analyses which are seldom performed straight after sample collection can only accurately reflect analyte concentrations at sampling time if it has not degraded in the meantime. No less important is the data on analyte stability in standard solutions used for method calibration and quality control. There is limited information available regarding the stability of bleomycin; what does exist focuses mostly on its photolability and the consequent need for protection from exposure to light [24]. Hence, data on its long-term stability in biological matrices will be of added value for more accurate guidance in clinical workflows.

Bleomycin stability was investigated for biological matrices (plasma and serum) and injection solution at storage-relevant conditions. Data on its stability in biological samples (long-term freezer stability and freeze-thaw stability) provided useful information for sample handling from collection to analysis whereas the data for its long-term freezer and cooler stability in the physiological solution provided information useful for creating/establishing storage recommendations for prepared injection solutions.

Recoveries of the measurements for long-term and freeze-thaw stability experiments are displayed in Figs. S - 7 and 8, each point presenting the average recovery of two aliquots. Results for all measurements were within ± 14.0% of the initial value. Considering the calculated extended measurement uncertainty of the method at the relevant concentration range is higher than this percentage (26.2% at high 600 ng/mL), these results suggest bleomycin remains stable in the two matrices under the applied conditions for the investigated time.

The stability of BLM in injection solution was investigated to explore the possibility of preparing BLM solutions in advance and storing them before use. The results shown in Fig. S - 9 indicate that BLM remains stable over the given time period both when stored in a cooler or in a freezer with the results varying no more than 5% within the period of 140 days. In Fig. S - 10, the results of a freeze-thaw experiment are presented. The measured values indicate its stability throughout the six freeze-thaw cycles, the deviations from the initial value all falling well within the calculated measurement uncertainty of the method.

Conclusions

Through an example of the development, optimization, and establishment of quality assurance protocols for two analytical methods, this study describes a quantitative analysis of a complex polar analyte on the example of bleomycin, addressing several of the challenges that can be faced in such analyses. For the quantification of BLM in blood-derived biological samples, an existing LC-MS method [11] was taken as the basis and was improved by modifying the sample preparation procedure as well as transferring the instrumental part to a more sensitive and accessible instrument. The final method comprises a considerably simpler and more time-efficient sample preparation protocol and analysis on a UHPLC-MS/MS system. Efficient and accurate analysis of large sample sizes is essential in routine clinical practice. Our method provides a simple, sensitive, and reliable approach that can produce high-quality results, making it ideal for patient monitoring, established therapy regimes, and potential therapy optimization studies. With the possibility of mitigating the severe side effects and improving efficacy through combination with other drugs or therapies, bleomycin treatment warrants further investigation, and our method offers a promising platform for such studies.

For the purpose of quantifying BLM in its clinically used form, an injection solution that represents an entirely different sample type, a simple HPLC-based method, was

developed and validated. Separation of BLM's main fractions was, unlike in many previously published methods, achieved in a rapid manner and without the addition of ion-pairing reagents. Full validation, performed for both methods, included assessment of measurement uncertainties and demonstration of the analyte stability.

This work supports enhanced integration of metrological concepts in analytical chemical methods to assure good quality and control of measurement results, highlighting the utmost importance of this, especially when dealing with challenging and complex analyses. It considers the issues of traceability and supports the applicability of measurement uncertainty as well as other important metrological concepts that are most often underreported in scientific articles. This study is also an explanatory example of how the performance of any complex method should be, in addition to initial validation, controlled over time in order to constantly assure an acceptable quality of results. Data, acquired in regular QC checks are visually presented in the form of a control chart, allowing easy tracking of the accuracy and dispersion of QC sample results as well as any trends that might emerge.

While this method covers the analysis of blood-derived samples, its application could be extended to other biological samples with additional modifications to the sample preparation procedure and instrumental analysis. These include tissue samples with even more complex matrices such as cell culture samples, used in ECT studies. For the latter, special efforts should be directed towards achieving lower LLOQ limits indicating the need for (at least) a more sensitive instrument.

Supplementary Information The online version contains supplementary material available at https://doi.org/10.1007/s00216-023-04675-x.

Acknowledgements We would like to thank Dusan Zigon (Department of Environmental Sciences, Jozef Stefan Institute), Mira Lavric (Institute of Oncology Ljubljana, Ljubljana, Slovenia), and Spela Golcar (University of Pharmacy, University of Ljubljana, Ljubljana, Slovenia) for all the valuable work they contributed to this research.

Funding Open access publishing supported by the Slovenian Research Agency and Central Technical Library in Ljubljana. The authors received financial support from the state budget by the Slovenian Research Agency (P1-0143, J1-6744, J4-2546, J3-9269).

Declarations

Conflict of interest The authors declare no competing interests.

Open Access This article is licensed under a Creative Commons Attribution 4.0 International License, which permits use, sharing, adaptation, distribution and reproduction in any medium or format, as long as you give appropriate credit to the original author(s) and the source, provide a link to the Creative Commons licence, and indicate if changes were made. The images or other third party material in this article are included in the article's Creative Commons licence, unless indicated otherwise in a credit line to the material. If material is not included in the article's Creative Commons licence and your intended use is not permitted by statutory regulation or exceeds the permitted use, you will need to obtain permission directly from the copyright holder. To view a copy of this licence, visit http://creativecommons.org/licenses/by/4.0/.

References

1. Claussen CA, Long EC. Nucleic acid recognition by metal complexes of bleomycin. Chem Rev. 1999;99(9):2797–816. https://doi.org/10.1021/cr980449z.
2. McMorrow L, Shaikh M, Kessell G, Muir T. Bleomycin electrosclerotherapy: new treatment to manage vascular malformations. Br J Oral Maxillofac Surg. 2017;55(9):977–9. https://doi.org/10.1016/j.bjoms.2017.10.002.
3. Murray V, Chen JK, Chung LH. The interaction of the metalloglycopeptide anti-tumour drug bleomycin with DNA. Int J Mol Sci. 2018;19(5):1372. https://doi.org/10.3390/ijms19051372.
4. Crnovcic I, Gan F, Yang D, Dong LB, Schultz PG, Shen B. Activities of recombinant human bleomycin hydrolase on bleomycins and engineered analogues revealing new opportunities to overcome bleomycin-induced pulmonary toxicity. Bioorg Med Chem Lett. 2018;28(16):2670–4. https://doi.org/10.1016/j.bmcl.2018.04.065.
5. Campana LG, Clover AJP, Valpione S, Quaglino P, Gehl J, Kunte C, et al. Recommendations for improving the quality of reporting clinical electrochemotherapy studies based on qualitative systematic review. Radiol Oncol. 2016;50(1):1–13. https://doi.org/10.1515/raon-2016-0006.
6. Groselj A, Bosnjak M, Krzan M, Kosjek T, Bottyán K, Plesnik H, et al. Bleomycin concentration in patients' plasma and tumors after electrochemotherapy. A study from InspECT Group. Pharmaceutics. 2021;13(9):1324. https://doi.org/10.3390/pharmaceutics13091324.
7. Racnik J, Svara T, Zadravec M, Gombac M, Cemazar M, Sersa G, et al. Electrochemotherapy with bleomycin of different types of cutaneous tumours in a ferret (Mustela putorius furo). Radiol Oncol. 2018;52(1):98–104. https://doi.org/10.1515/raon-2017-0057.
8. O'Farrell PA, Gonzalez F, Zheng W, Johnston SA, Joshua-Tor L. Crystal structure of human bleomycin hydrolase, a self-compartmentalizing cysteine protease. Structure. 1999;7(6):619–27. https://doi.org/10.1016/s0969-2126(99)80083-5.
9. Cheng S, Khan M, Luo L, Wang L, Liu S, Ping J, et al. Detection of bleomycin and its hydrolase by the cationic surfactant-doped liquid crystal-based sensing platform. Anal Chim Acta. 2021;1150:338247. https://doi.org/10.1016/j.aca.2021.338247.
10. Bleomycin sulphate. In: European pharmacopoeia. 5th ed. Council of Europe; p. 1114–5.
11. Kosjek T, Krajnc A, Gornik T, Zigon D, Groselj A, Sersa G, et al. Identification and quantification of bleomycin in serum and tumor tissue by liquid chromatography coupled to high resolution mass spectrometry. Talanta. 2016;1(160):164–71. https://doi.org/10.1016/j.talanta.2016.06.062.
12. Mabeta P, Dippenaar N, Shelver G. A validated hplc method for the simultaneous determination of bleomycin a2 and b2 in human plasma. Int J Pharm Biomed Res. 2012;1(3):191–4.
13. Mahdadi R, Kenani A, Pommery N, Pommery J, Hénichart JP, Lhermitte M. High-performance liquid chromatography assay of bleomycin in human plasma and rat hepatocytes in culture. Cancer Chemother Pharmacol. 1991;28(1):22–6. https://doi.org/10.1007/bf00684951.

14. Umezawa H, Takita T. The bleomycins: antitumor copper-binding antibiotics. In: Biochemistry. Berlin: Springer; 1980. p. 73–99. (Structure and Bonding). https://doi.org/10.1007/BFb0025287.
15. Shiu GK, Goehl TJ, Pitlick WH. Rapid high-performance liquid chromatographic determination of bleomycin A2 in plasma. J Pharm Sci. 1979;68(2):232–4. https://doi.org/10.1002/jps.2600680228.
16. Shiu GK, Goehl TJ. High-performance paired-ion liquid chromatographic determination of bleomycin A2 in urine. J Chromatogr B Biomed Sci Appl. 1980;181(1):127–31. https://doi.org/10.1016/s0378-4347(00)81281-5.
17. Broughton A. Radioimmunoassay of bleomycin. Methods in Enzymology; 1982. p. 463–470. https://doi.org/10.1016/0076-6879(82)84034-2.
18. Fiedler HP, Wachter J. High-performance liquid chromatographic determination of bleomycins. J Chromatogr A. 1991;1(536):343–7. https://doi.org/10.1016/s0021-9673(01)89268-2.
19. Aszalos A, Crawford J, Vollmer P, Kantor N, Alexander T. High-performance liquid chromatographic determination of components of bleomycin preparations. J Pharm Sci. 1981;70(8):878–80. https://doi.org/10.1002/jps.2600700811.
20. Galba J, Veizerova L, Piešťanský J, Mego M, Novotny L, Dokupilova S, et al. HPLC-QTOF-MS method for identification and determination of Bleomycin A2 and B2 fractions. J Liq Chromatogr Relat Technol. 2015;20:38. https://doi.org/10.1080/10826076.2014.908783.
21. Guideline on bioanalytical method validation [Internet]. European medicines agency; [cited 2022 Nov 14]. Available from: https://www.ema.europa.eu/en/documents/scientific-guideline/guideline-bioanalytical-method-validation_en.pdf.
22. Lal AS, Begum SK, Bharadwaj SS, V L, J V, Paul SFD, et al. Bleomycin-induced genotoxicity in vitro in human peripheral blood lymphocytes evidenced as complex chromosome- and chromatid-type aberrations. Toxicol In Vitro. 2019;54:367–74. https://doi.org/10.1016/j.tiv.2018.10.013
23. Summary of product characteristics: Bleomedac 15000 IU [Internet]. 2022 [cited 2022 Dec 20]. Available from: https://www.medac.eu/fileadmin/user_upload/medac-eu/SPCs/common_SPCs/Bleomedac-spc-common.pdf
24. Thakrar N, Douglas KT. Photolability of bleomycin and its complexes. Cancer Lett. 1981;13:265–8. https://doi.org/10.1016/0304-3835(81)90027-6.
25. Bioanalytical Method Validation Guidance for Industry [Internet]. Food and Drug Administration; 2018 [cited 2022 Dec 20]. Available from: https://www.fda.gov/regulatory-information/search-fda-guidance-documents/bioanalytical-method-validation-guidance-industry
26. Albertini JP, Garnier-Suillerot A. Formation of copper-bleomycin complexes: evidence of a three-step process. J Inorg Biochem. 1985;25(1):15–24. https://doi.org/10.1016/0162-0134(85)83003-8.
27. Linder M. Ceruloplasmin and other copper binding components of blood plasma and their functions: an update. Metallomics. 2016;18:8. https://doi.org/10.1039/c6mt00103c.
28. Ellison SLR, Williams A. Eurachem/CITAC guide: quantifying uncertainty in analytical measurement [Internet]. 2012 [cited 2022 Nov 14]. Available from: https://www.eurachem.org/images/stories/Guides/pdf/QUAM2012_P1.pdf
29. ISO 21748:2017: guidance for the use of repeatability, reproducibility and trueness estimates in measurement uncertainty evaluation. International Organization for Standardization; 2017.
30. Saffaj T, Ihssane B. Uncertainty profiles for the validation of analytical methods. Talanta. 2011;85(3):1535–42. https://doi.org/10.1016/j.talanta.2011.06.042.
31. Farrance I, Frenkel R. Uncertainty of measurement: a review of the rules for calculating uncertainty components through functional relationships. Clin Biochem Rev. 2012;1(33):49–75.
32. Handbook for calculation of measurement uncertainty in environmental laboratories (NT TR 537 - Edition 4) [Internet]. NORDTEST. 2017 [cited 2023 Feb 3]. Available from: http://www.nordtest.info/wp/2017/11/29/handbook-for-calculation-of-measurement-uncertainty-in-environmental-laboratories-nt-tr-537-edition-4/

Publisher's note Springer Nature remains neutral with regard to jurisdictional claims in published maps and institutional affiliations.

3.3.2 Quantitative analysis of trace-level bleomycin in complex matrices: application to in vitro electrochemotherapy

Published: Plešnik, H., Vižintin, A., Miklavčič, D., Steed, J., Stahl-Zheng J., Kosjek, T., Journal of Pharmaceutical and Biomedical Analysis, 2025

This paper extends the pharmacotherapy and method-development part of the thesis by addressing the analytical requirements that arise when drug action is studied at the intracellular level rather than in conventional clinical matrices. Whereas the previous bleomycin study focuses on quantitative analysis in plasma and serum, this work shifts the analytical problem into a substantially more demanding domain: the determination of trace-level intracellular drug concentrations in a complex cell matrix. In doing so, it engages directly with Hypothesis 2, which concerns the feasibility and practical limits of quantitative analysis for extremely polar and low-abundance therapeutics in complex biological systems.

The work is motivated by the need to support in vitro electrochemotherapy studies, where bleomycin uptake is enhanced through electroporation and where biologically relevant concentrations are several orders of magnitude lower than those encountered in clinical samples. From a thesis perspective, the paper is not primarily concerned with electrochemotherapy as a therapeutic modality, but with the analytical consequences of studying drug delivery under such conditions. The study therefore provides a structured example of how analytical workflows must be adapted when sensitivity requirements approach the realistic limits of current instrumentation and sample preparation strategies.

Method development focused on maximizing sensitivity within a chemically and biologically complex matrix. This required careful optimization of cell lysis conditions, solid-phase extraction, and instrumental parameters, while explicitly accounting for bleomycin's polarity, metal-binding behavior, and susceptibility to losses during sample handling. The resulting UHPLC–MS/MS method, implemented on a QTrap 7500 system, was applied to compare intracellular bleomycin levels following two electroporation protocols, serving as a practical demonstration of the method's applicability rather than as a definitive evaluation of electroporation efficacy.

This work addresses Hypothesis 2, but does not confirm it. While the method enables detection of exceptionally low bleomycin concentrations in cell matrices, the analytically achievable limits remain above the biologically relevant intracellular levels, which are on the order of a few hundred molecules per cell. This gap delineates a current boundary of quantitative bioanalysis rather than reflecting a failure of method design. In this sense, the study defines the realistic sensitivity limits of state-of-the-art LC–MS/MS when applied to extreme cases of intracellular trace analysis.

Within the overall thesis narrative, this study illustrates how HILIC–MS/MS workflows can be extended beyond clinical bioanalysis to support mechanistic and delivery-focused research. The methodological principles developed here are transferable to other intracellular quantification challenges and thus contribute to a broader analytical framework for investigating targeted cancer therapies.

Journal of Pharmaceutical and Biomedical Analysis 263 (2025) 116927

Contents lists available at ScienceDirect

Journal of Pharmaceutical and Biomedical Analysis

journal homepage: www.journals.elsevier.com/journal-of-pharmaceutical-and-biomedical-analysis

Quantitative analysis of trace-level bleomycin in complex matrices: Application to in vitro electrochemotherapy

Helena Plešnik [a,b], Angelika Vižintin [c], Damijan Miklavčič [c], Jack Steed [d], Jianru Stahl-Zeng [d], Tina Kosjek [a,b,*]

[a] Department of Environmental Sciences, Jožef Stefan Institute, Jamova 39, Ljubljana 1000, Slovenia
[b] International Postgraduate School Jožef Stefan, Jamova 39, Ljubljana 1000, Slovenia
[c] Faculty of Electrical Engineering, University of Ljubljana, Tržaska 25, Ljubljana 1000, Slovenia
[d] AB Sciex Germany GmbH, Landwehrstraße 54, Darmstadt 64293, Germany

ARTICLE INFO

Keywords:
Electroporation
Electrochemotherapy
Bleomycin
Trace level
Tandem mass spectrometry
Sensitivity

ABSTRACT

Bleomycin, a cytotoxic antibiotic, poses substantial challenges for mass spectrometry-based analysis due to its extreme polarity, chelating properties, heterogeneity of fractions, and propensity to form multiple charged species during electrospray ionization. As one of the few effective drugs used in electrochemotherapy, the ability to quantify trace levels of bleomycin is critical for evaluating treatment efficacy, often requiring sensitivity beyond the capabilities of existing analytical methods. Such precise quantification would facilitate the evaluation of electrochemotherapy efficacy, such as comparing the in vitro effects of nanosecond electric pulses with conventional microsecond pulses. To address these challenges, we integrated cell viability assays with a robust chemical analytical approach. This approach employed solid-phase extraction for sample preparation, combined with HILIC-LC-MS/MS, achieving exceptional sensitivity with LLOQ of 0.075 μg/L and overcoming analyte and matrix complexity. Although a significant reduction in cell survival was confirmed when combining nanosecond pulses (25 × 400 ns) with bleomycin, chemical analysis revealed discrepancies, underscoring the complex interaction between electric pulse parameters and drug action. These findings highlight the need for further refinement of treatment protocols and the development of advanced analytical techniques.

1. Introduction

Bleomycin (BLM) represents a group of structurally related metallo-glycopeptide compounds with both antimicrobial and cytotoxic properties. Clinically used in chemotherapy for treating lymphomas as well as squamous and testicular carcinomas, its application has more recently been expanded to sclerotherapy, proving effective in the treatment of vascular malformations [1,2]. BLM's cytotoxic effect is attributed to its ability to cleave DNA, which is driven by both intracellularly generated activated BLM species and by free radicals formed upon their interaction with molecular oxygen [3]. Reaching the DNA inside the cell nucleus requires transition of BLM molecules through cell membrane, a process, severely hindered by its size and considerable hydrophilicity (logP: −7.5; computed by XLogP3 3.2.2) [4]. Achieving a sufficient concentration of the drug in the nucleus, which is critical for its cytotoxic effect, is therefore a challenge that cannot be tackled by increasing the administered dose as doing so would exacerbate the adverse side effects. Expressed due to BLM's lack of specificity towards tumor cells, these are already quite prevalent. Of particular concern is pulmonary toxicity with reported incidence rates as high as 46 % [5].

To address the challenge of membrane impermeability for intracellularly acting therapeutics, considerable advancements have been achieved using electroporation. This innovative procedure relies on facilitating mass transport across the plasma membrane by electroporation. Delivery of short electric pulses to cells, either in vitro or in vivo in tissue causes transient membrane permeabilization [6]. By appropriately adjusting the parameters, electroporation can be conducted in a reversible manner for applications such as electrochemotherapy or irreversibly for applications such as tissue ablation. Utilized in oncological treatments, they both induce cell death reducing tumor burden and are locally very efficient [7].

In electrochemotherapy (ECT), reversible electroporation acts as a physical delivery method for chemotherapeutic agents, exploiting the transient increase in membrane permeability to facilitate

* Corresponding author at: Department of Environmental Sciences, Jožef Stefan Institute, Jamova 39, Ljubljana 1000, Slovenia.
E-mail address: tina.kosjek@ijs.si (T. Kosjek).

https://doi.org/10.1016/j.jpba.2025.116927
Received 20 January 2025; Received in revised form 22 April 2025; Accepted 24 April 2025
Available online 30 April 2025
0731-7085/© 2025 The Authors. Published by Elsevier B.V. This is an open access article under the CC BY-NC-ND license (http://creativecommons.org/licenses/by-nc-nd/4.0/).

transmembrane transport of otherwise impermeant cytotoxic molecules [8]. Other than membrane permeability increase and intracellular drug accumulation, effects such as vascular disruption, vascular lock and immune response triggering have been observed to arise when applying electrical pulses and are considered to enhance the efficacy of electrochemotherapy [9].

The most common chemotherapeutic agents used in ECT, BLM and cisplatin [10–13], both show significantly potentiated cytotoxicity when combined with electroporation. This has been demonstrated in vitro as well as in vivo and led to the implementation of ECT into clinical practice in 2006, its use steeply rising since [14]. However, nerve stimulation, muscle contractions, and pain experienced in patients remains a significant limiting factor in an otherwise effective therapy. Exploring innovative therapeutic approaches to mitigate these side effects, conventionally employed ECT protocols have been modified by shortening the applied pulses significantly; from micro- to nanosecond range. Nanosecond pulsed electric field as a novel therapeutic strategy indeed promises to induce less contractions explained by the fact that electroporation by nanosecond pulses often occurs below the excitation threshold [15–17]. The effectiveness of these protocols, extensively evaluated using BLM and cisplatin, has confirmed their efficacy to be comparable to longer pulses [12,18,19]. However, Vižintin et al. demonstrated that higher concentrations of BLM were necessary to attain equivalent decreases in cell survival when employing nanosecond pulses, as opposed to the conventional 8 × 100 μs pulses [12]. They suggest this to be due to the smaller membrane pores formed and the resulting diminished cellular BLM uptake when applying nanosecond pulses.

To support the research of these new treatment regimens reliable quantitative analytical methods are of crucial importance. There are but few published methods for the determination of BLM, which is likely a result of the numerous challenges, accompanying its analysis. Two most recent LC-MS-based methods, published by our group, addressed determination of BLM in biological samples, including plasma, serum and tumor tissue [20,21] and present straightforward sample preparation protocols, suitable for simpler matrices, focusing on the applicability in clinical environment with sizeable sample batches. These methods provide a practical approach, emphasizing simplicity and time efficiency, which are critical for clinical settings. Lower limit of quantification (LLOQ) values for BLM in blood-derived samples reach 15 μg/L [20,21]. Studies such as electroporation-mediated transition of BLM into cells however require a different approach, mainly on the account of a different, more complex matrix as well as the extremely low analyte concentrations utilized in the experiments, which fall well below the LLOQ of the said methods.

The objective of this study was to investigate the effect of pulse duration and BLM concentration on cell survival after electrochemotherapy, using murine melanoma (B16F1) cell lines as the experimental model. The efficiency of applied conditions was assessed by both monitoring cell death rates along with the quantification of the intracellular BLM in B16F1 and Chinese hamster ovary (CHO) cells via LC-MS-based analysis. The developed sample preparation included solid-phase extraction-based purification with prior cell lysis to release BLM from the cells. The instrumental analytical method was developed on an ultra-high-performance liquid chromatograph coupled with a hybrid quadrupole-linear ion trap mass spectrometry analyzer QTRAP 7500.

2. Experimental

2.1. Chemicals and materials

Reference standard: Bleomycin sulfate salt (CAS No.: 9041–93–4, cat. no. sc-200134) was purchased in a metal-free form with a declared purity of 95.7 % (C55H84N17O21S3 × H2SO4) from Santa Cruz Biotechnology, Inc. (Dallas, TX, USA). Bleomycin A5 hydrochloride (C57H89N19O21S2 × HCl, CAS: 55658–47–4, cat. no. B4517) used as an internal standard was purchased from LKT Laboratories, Inc. (St. Paul, MN, USA) in a metal-free form and had a declared purity of ≥ 90 %. Agent for control of metal complex formation was CuSO4 × 5H2O, purchased from Alkaloid AD Skopje (Skopje, North Macedonia). Mobile phase additives ammonium formate (≥99.0 %) and formic acid (99 %) were purchased at Sigma-Aldrich Corp. (St. Louis, MO, USA) and Carlo Erba Reagents S.r.l. (Val de Reuil, France), respectively, both were of LC-MS purity grade. Buffers for cell lysis were prepared using the following buffering agents: 4-(2-hydroxyethyl)-1-piperazineethanesulfonic acid (HEPES; cat. no. 1101100250), purchased from Merck & Co., Inc. (Rahway, NJ, USA), 3-(N-morpholino) propanesulfonic acid (MOPS), purchased at ≥ 99.5 % purity from Sigma-Aldrich Corp., and tromethamine (TRIS; cat. no. 5429.1) purchased from Carl Roth GmbH + Co. KG (Karlsruhe, Germany). Sodium hydroxide for pH adjustment was purchased at Merck & Co., Inc. (Rahway, NJ, USA) and sodium dodecyl sulfate (SDS; cat. no. L3771) detergent from Sigma-Aldrich Corp. Acetonitrile (MeCN) and water used as the mobile phases were of LC-MS purity, and all solvents used in sample prep (methanol, water, MeCN) were of analytical grade purity.

The chromatographic column used was ACQUITY PRM BEH Amide (1.7 μm, 2.1 mm×50 mm) (Waters Corp., Milford, MA, USA). For solid-phase extraction, Oasis HLB 1cc (30 mg) extraction cartridges (Waters Corp., Milford, MA, USA) were used. Filtering of the samples was performed on GVS Centrex 0.45 μm cellulose acetate centrifuge filters (Centrex, Oilville, VA, USA) and on 0.2 μm PhenexTM regenerated cellulose membrane syringe filters (Phenomenex Inc., Torrance, CA, USA). The software used included Sciex OS 3.3.1 (Sciex, Framingham, MA, USA), ChemDraw 14.0 (Perkin-Elmer Cp., Norwalk, CT, USA), Microsoft Excel (Microsoft Corp., WA, USA), MATLAB R2020a (MathWorks, MA, USA) and Python programming language (v3.10.0), utilizing the Pingouin (v0.5.3) [22] and the StatsModels library (v0.14.0) [23].

For cell culture, CHO-K1 Chinese hamster ovary cell line, obtained directly from the European Collection of Authenticated Cell Cultures (ECACC, cat. no. 85051005, mycoplasma free), mouse skin melanoma cell line B16F1 (ECACC, cat. no. 92101203, mycoplasma free), Nutrient Mixture F-12 Ham (cat. no. N6658, Sigma-Aldrich), Dulbecco's Modified Eagle Medium (DMEM, cat. no. D5671, Sigma-Aldrich), fetal bovine serum (cat. no. F9665, Sigma-Aldrich), L-glutamine (cat. no. G7513, Sigma-Aldrich), penicillin/streptomycin (cat. no. P0781, Sigma-Aldrich), gentamycin (cat. no. G1397, Sigma-Aldrich), trypsin-EDTA (cat. no T4174, Sigma-Aldrich), Hank's basal salt solution (cat. no. H4641, Sigma-Aldrich) and bleomycin sulphate (Medac, Germany) were used.

2.2. Preparation of standard and working solutions

The lysis buffers HEPES (50 mM HEPES with 0.5 % SDS, pH 7.4), TRIS (50 mM Tris-HCl, 0.5 % SDS, pH 8) and MOPS (50 mM MOPS, 0.5 % SDS, pH 7.4) were freshly prepared prior to analyses by first diluting 1.1915 g of HEPES, 0.6055 g of TRIS or 1.046 g of MOPS in water, respectively, adjusting the pH to 7.4 with 1 M NaOH solution (prepared from NaOH pellets purchased at Merck & Co., Inc., cat. no. 1.06498.1000), adding 5 mL 10 % SDS solution and finally MilliQ water to 100 mL.

The stock solution of BLM was prepared by dissolving 10 mg of BLM sulfate reference standard in 10 mL of methanol and MilliQ water mixture (8:2) and was stored at –18 °C. The working solution at BLM concentrations 0.25, 2 and 20 μg/L were freshly prepared before the analysis by diluting the BLM stock solution with 0.1 % formic acid in MilliQ water. The internal standard (bleomycin A5) stock solution was prepared by dissolving 5 mg of bleomycin A5 in in 5 mL of methanol and MilliQ water mixture (8:2) and was stored at –18 °C. Each time before analysis, a fresh working standard was prepared by diluting the internal standard stock solution to 500 μg/L. This prepared standard was then

added to the samples, resulting in a final concentration of 10 μg/L.

Preparation of calibration and quality control standards:

Calibration standards were prepared as matrix-matched standards by spiking BLM working solutions (concentration range: 0.05 μg/L – 2.5 μg/L; 8 concentration points) into the cell matrix (blank CHO and B16F1 cell pellets in MeOH) prior to the addition of lysis buffer, IS at 10 μg/L and CuSO4 at 3.5 μg/L.

Quality control samples were prepared at low (0.075 μg/L) and high (7.5 μg/L) concentrations in two aliquots, by spiking BLM working solutions into the cell matrix in the same way as calibration standards. Both calibration and quality control standards were prepared like the actual samples (see 2.4 Sample preparation).

$CuSO_4$ was used to drive metal complex formation and was prepared by dissolving 1.22 mg of $CuSO_4$ 5H2O in 20 mL of MilliQ water and was further diluted to 3.05 μg/mL. This solution was then added in excess to the calibration standards, quality control and real samples.

The aqueous mobile phase for the LC-MS method (20 mM ammonium formate with 0.1 % formic acid) was prepared by dissolving 1.261 g of ammonium formate in 100 mL of MilliQ water, and then by 10-times further diluting it. Finally, 0.1 % formic acid was added before degassing.

2.3. Electroporation

Cell culture and measurement of cell survival after electroporation and electrochemotherapy were described previously [12,24]. Briefly, cell survival of B16F1 cells after ECT with BLM was measured by the clonogenic assay. Cells were exposed either to 0, 1, 20, 40 nM BLM and/or 8 × 100 μs electric pulses at 0.9 kV/cm, 1 Hz pulse repetition rate were delivered by a laboratory prototype pulse generator (University of Ljubljana), based on H-bridge digital amplifier with 1 kV MOSFETs (DE275–102N06A, IXYS, Milpitas, California, USA) or 0, 60, 100 and 140 nM BLM and/or 25 × 400 ns electric pulses at 3.9 kV/cm, 10 Hz repetition rate delivered by the CellFX System (Pulse Biosciences, Hayward, California, USA).

For determination of intracellular BLM concentration, CHO cells were treated with 140 nM BLM alone, 25 × 400 ns pulses (at 3.9 kV/cm, 10 Hz repetition rate) alone, the combination of 60, 100 or 140 nM BLM and 25 × 400 ns pulses or the combination of 5, 10 or 40 nM BLM and 8 × 100 μs pulses (at 1.1 kV/cm, 1 Hz pulse repetition rate), while B16F1 cells were treated with 140 nM BLM alone, 25 × 400 ns pulses (at 3.9 kV/cm, 10 Hz repetition rate) alone, the combination of 60, 100 or 140 nM BLM and 25 × 400 ns pulses or the combination of 1, 20 or 40 nM BLM and 8 × 100 μs pulses (at 0.9 kV/cm, 1 Hz pulse repetition rate) following the same protocol as in the previous electrochemotherapy experiments. After treatment, the cell suspension was transferred from the electroporation cuvette to a 1.5 mL centrifuge tube. 25 min after electroporation (or addition of BLM for non-electroporated controls), 530–570 μL of the cell suspension was diluted in 15 mL of complete growth medium in 15 mL centrifuge tubes purchased from TPP Techno Plastic Products AG (Trasadingen, Switzerland) and centrifuged for 5 min at 900 rcf at room temperature. The number of cells was in the range of approximately 1.5 – 3.5 × 106 cells; it was determined with Countess Automated Cell Counter (Invitrogen, Thermo Fisher Scientific) following manufacturer's instructions. The supernatant was discarded and the pellet was washed with 4 mL saline and then centrifuged again for 5 min at 900 rcf at room temperature. The supernatant was discarded and 100 μL of methanol purchased from Sigma-Aldrich Corp. was added to the pellet. The pellets were stored at −20 °C until sample analysis. The experiments were repeated 3 – 4 times per treatment.

Samples for calibration curve and blanks were prepared by putting the cell suspension of CHO or B16F1 in their respective growth medium in a 15 mL centrifuge tube so that the number of cells was in the same range as of the samples for measurements of intracellular BLM concentration. Then, they were processed the same way as the samples for measurements of intracellular BLM concentration.

Stringent measures were implemented to prevent contamination of samples not treated with BLM during the in vitro electrochemotherapy procedure. Fresh electroporation cuvettes, pipette tips, tubes, and other cell culture consumables were utilized for each individual sample.

2.4. Sample preparation

To the cell pellet in methanol, lysis buffer was added in two steps; each time 150 μL. Upon adding the buffer, the cell aggregate was broken up by aspirating it into a pipette. Samples were then sonicated for 15 minutes to aid the cell lysis. 20 μL of internal standard (IS) (500 μg/L) and 600 μL of $CuSO_4$ working solutions (3.05 μg/L) were added to each sample and mixed thoroughly. This was followed by centrifugation at 12900 × g for 15 minutes. Supernatants were then transferred into centrifuge filters (CENTREX, cellulose acetate membrane filters, 0.45 μm pores) and filtered by centrifugation at 1500 x g for 15 minutes. The subsequent solid-phase extraction was carried out on HLB cartridges (Oasis HLB, 30 mg, 1cc), using the following procedure: sorbent was first conditioned with 1 mL of methanol and 0.1 % formic acid in MilliQ water, respectively. The samples were transferred onto the preconditioned cartridges to pass the sorbent under vacuum, which was then dried under vacuum for five minutes. Elution was performed with 2 × 0.5 mL MeCN and MQ water mixture (7:3). Eluates were filtered (regenerated cellulose membrane, 0.2 μm pores) and transferred into vials. Measures have been taken during all sample preparation steps to avoid direct light exposure as BLM has been shown to be light-sensitive [25].

2.5. Instrumental analysis

Instrumental analysis was conducted using an ultra-high-performance liquid chromatograph (UHPLC, Waters, Milford, MA, USA) coupled with a hybrid quadrupole-linear ion trap mass spectrometry analyzer SCIEX 7500 system (Sciex, Framingham, MA, USA) employing positive electrospray ionization (ESI+). Separation was achieved with an ACQUITY PRM BEH Amide (1.7 μm, 2.1 ×50 mm) column. The chromatographic approach was adapted from our group's previously published method, with the only modification being the concentration of the mobile phase modifier. Mobile phase A consisted of MeCN, while mobile phase B comprised 20 mM ammonium formate with 0.1 % formic acid. The gradient program initiated at 5 % B, increased to 50 % at 2 min, further elevated to 60 % at 4 min, and then reverted to 5 %, maintaining this composition until 6 min. The total mobile phase flow rate was 0.3 mL/min, and the column temperature was held at 40 °C. An injection volume of 1.0 μL was used.

The ion source parameters were maintained as follows: ion spray voltage + 2500 V; source temperature 350 °C; Collision Gas (CAD) 15 psi, curtain gas (CUR) 40 psi; ion source gas 1 (GS1) 40 psi; ion source gas 2 (GS2) 50 psi. Ions were acquired in multiple reaction monitoring (MRM) mode; the transitions are together with the compound-specific parameters presented in Table 1. Molecular weight of the BLM-A2-Cu complex being 1475.4, the monitored transitions were from double charged parent ions; two isotopic ions of the analyte BLM-A2-Cu (BLM-

Table 1
MRM parameters for the LC-MS/MS method.

	Q1 *m/z* (Da)	Q3 *m/z* (Da)	Dwell time (ms)	EP (V)	CE (V)	CXP (V)
BLM-A2-Cu	738.4	707.3	75.0	10.0	24.0	14.0
BLM-A2-Cu	739.4	708.2	75.0	10.0	23.0	4.0
BLM-A5-Cu	751.2	706.2	75.0	10.0	40.0	21.0
BLM-A5-Cu	751.2	714.7	75.0	10.0	34.0	24.0

A2-^{63}Cu and BLM-A2-^{65}Cu) and two for the internal standard BLM-A5-Cu.

2.6. Validation protocols

In adherence to the European Medicines Agency (EMA) guidelines [26], we assessed the performance parameters of the method. Selectivity was evaluated by examining blanks (matrix spiked with the internal standard but lacking the analyte), required to show analyte peak areas $\leq$ 20 % of the mean peak area at the LLOQ level. Carryover, defined as the residual signal in solvent blanks obtained immediately after the highest calibrator (2.5 μg/L), needed to be less than 20 % of the peak area in the LLOQ for the analyte and less than 5 % of the mean peak area of the internal standard. Linearity was assessed using calibration curves prepared from matrix-matched calibration standards that consisted of seven points within the range of 0.075 μg/L – 2.5 μg/L in the final extract, which corresponds to 0.075 ng – 2.5 ng of the analyte per one cell pellet. The relationship between the peak area ratio and BLM concentration was determined through linear regression, taking into account that EMA criteria require at least 75 % of the calibrators to fall within ± 15 % (or 20 % for the LLOQ) of their expected concentrations. The determined LLOQ concentration was examined by analyzing multiple (n = 3) replicates of the estimated LLOQ concentration with the calibration curve. The average of these replicates was expected to fall within ± 20 % of the nominal concentration for a minimum of 50 % of the replicates. QC standards were prepared along with each batch of samples in duplicates at 0.075 μg/L to determine accuracy of the method, defined by trueness and precision. Precision was described by assessing injection (n = 3) and method repeatability (n = 3). Extraction efficiency (excluding the lysis efficiency) was evaluated by comparing the analyte peak areas of pre-spiked (spiked with the analyte before the sample preparation process) against the post-spiked (spiked prior to the instrumental analysis) calibration standards, without IS normalization.

2.7. Statistical analysis

Cell survival of B16F1 cells after electrochemotherapy measured by the clonogenic assay was compared to the untreated control with Welch's *t*-test ($\alpha = 0.05$). Non-detects in the measured BLM concentrations were replaced by 0, then the measured BLM concentrations were normalized by dividing them by the number of cells in the sample. Subsequently, samples below the method detection limit and outliers identified by the interquartile range method were excluded. A significance level of $p < 0.05$ was set. The Shapiro-Wilk test assessed normal distribution, with only the CHO cells electroporated with nanosecond pulses showing a violation of this assumption. For these samples, log-transformed normalized BLM concentrations, which demonstrated a normal distribution, were utilized. The Brown-Forsythe test examined the assumption of equal variances for the one-way analysis of variance (ANOVA) and independent *t*-test used to compare differences between the mean measured BLM concentrations among sample groups. In cases of violation, Welch's ANOVA or Welch's *t*-test was employed. Upon detecting a statistically significant difference with the (Welch's) ANOVA, Tukey post hoc test was used to determine which specific groups exhibited significant differences.

3. Results and discussion

3.1. Cell survival

As expected, cell survival of B16F1 was mostly unaffected by the electric pulses or BLM alone, while their combination drastically reduced cell survival (Fig. 1). In accordance with the observations by Vižintin et al. [12] on CHO cells, the decrease in cell survival of B16F1 following electrochemotherapy (i.e., the concurrent application of electric pulses and BLM) was notably more significant with the standard

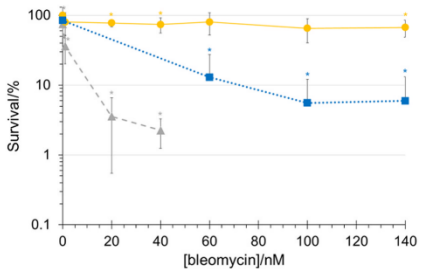


Fig. 1. Cell survival of B16F1 cells measured by the clonogenic assay 7 days after treatment with different bleomycin (BLM) concentrations and/or electroporation. Cells were exposed to either 8 × 100 μs pulses (grey triangles), 25 × 400 ns pulses (blue squares) or no pulses (yellow circles). Asterisks (*) represent a statistically significant difference ($p < 0.05$) in cell survival compared to control cells that were not exposed to either BLM or electric pulses. Note that the y-axis is on a logarithmic scale.

8 × 100 μs pulses than with the 25 × 400 ns pulses. Moreover, cell survival was more reduced when cells were subjected to 8 × 100 μs pulses at lower BLM concentrations compared to treatment with 25 × 400 ns pulses at higher BLM concentrations. However, also the BLM concentrations at which reduction of cell survival was achieved with ns pulses are significantly lower than the therapeutic doses used in clinical practice and from the measured BLM amounts in clinical samples after ECT [20,27]. In contrast, when cisplatin was employed as the chemotherapeutic agent in in vitro electrochemotherapy, both the standard 8 × 100 μs pulses and the 25 × 400 ns pulses demonstrated equal efficacy in reducing cell survival for both CHO and B16F1 cells. Additionally, they both led to a comparable increase in cellular cisplatin uptake [12,24]. The observed discrepancy in the effectiveness of electrochemotherapy with nanosecond pulses when using these two drugs may stem from differences in molecular size. BLM (approximately 1500 Da) is larger than cisplatin (approximately 300 Da), and it is suggested that the pores created by nanosecond pulses are smaller compared to those produced by longer electroporation pulses [28–30]. Therefore, at the same extracellular BLM concentration, more BLM molecules might have penetrated cells through the pores generated by the 8 × 100 μs pulses than through nanopulse-induced pores, as the micro-second pulses might have created more pores of sufficient size to allow BLM entry.

3.2. Chemical analysis of BLM

3.2.1. Cell lysis: procedure development and modifications

Cell lysis constitutes a pivotal step in the sample preparation procedure aimed at quantifying intracellular BLM to evaluate electroporation efficiency. The lysis procedure involved chemical disruption of membranes through the addition of a pH-adjusted solution of a detergent in a buffer, followed by sonication. A buffer was only considered suitable if it supported effective lysis and did not negatively affect the subsequent analysis. Evaluation of the efficacy of three commonly utilized buffers (TRIS, HEPES, and MOPS) was conducted through a two-part experimental approach, aiming to measure the efficiency of cell lysis but also to investigate any potential effects or interferences these buffers might have on the analyte. Blank CHO cell pellets in methanol were spiked with BLM (5 μg/L) and were prepared in triplicates using each of the buffers (pH-adjusted, with the addition of SDS) with the same protocol from this point onwards. While sufficient cell lysis (evaluated by observation under an inverted microscope) was demonstrated regardless of the buffer used, some notable differences were observed in the analyte recovery rates. Results, outlined in Fig. 2 show

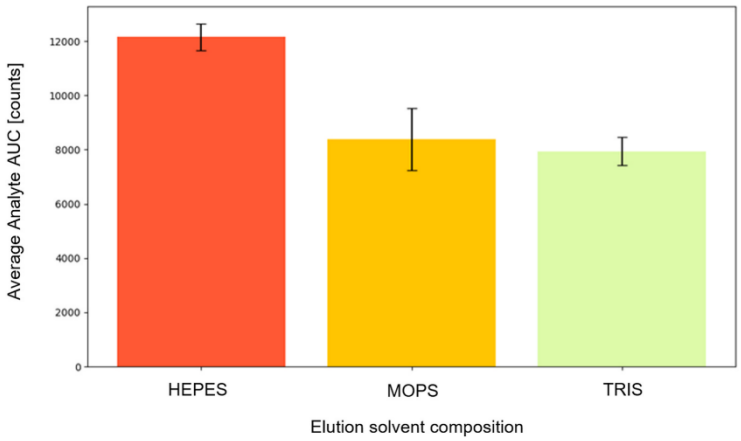


Fig. 2. Abundance of the analyte at 5 μg/L using different lysis buffers (n = 3).

that the recoveries for samples treated with TRIS exhibit lower recoveries compared to the rest, as indicated by lower analyte peak areas. This was interpreted to likely happen due to TRIS' metal-complexing properties [31]. The formation of BLM-Cu complex (the analyte) is in this case constrained due to limited availability of Cu ions in the presence of TRIS, causing an apparent reduction of the analyte inevitably leading to lower signals. HEPES and MOPS, both exhibiting weaker complexing properties [31], proved more suitable, with HEPES showcasing superior peak shapes as well as higher signals, solidifying its selection as the optimal choice for the method.

In the final protocol, the cell aggregate is disrupted by repeated pipette aspiration after introducing the buffer. An additional practical modification of the protocol included adding the lysis buffer in two steps (2 × 150 μL) rather than the entire volume at once, to enhance the efficiency of the cell pellet break-up and subsequently the lysis.

3.2.2. Solid-phase extraction

Sample clean-up was performed using solid-phase extraction, with the final method being an adaptation of a previously developed in-house protocol aimed at quantifying BLM in tissue and blood-derived matrices [20,21]. This adaptation was driven by the need for substantial reduction of LLOQ to make it suitable for trace level analysis of BLM in electroporated cell samples. In pursuit of optimizing the protocol, efforts were focused on enhancing the efficiency of sample preparation. This involved evaluating the impact of various parameters, including the mass of HLB sorbent per cartridge (30 mg and 60 mg), the choice of elution solvents, and the possible post-extraction drying and reconstitution.

The initial method employed 30 mg of HLB sorbent per sample. A comparative study was performed to determine if using a larger amount of sorbent (60 mg per cartridge) could improve recovery rates, given the extremely weak interactions between BLM and HLB sorbent which can be disrupted already by water itself, where the increase of the sorbent mass theoretically counteracts for these losses during extraction [32]. For this purpose, blank CHO cell pellets were spiked with 5 ng of BLM per sample and processed in triplicate using each cartridge type, adjusting solvent volumes as necessary. A statistical evaluation employing a *t*-test to compare the analyte response areas derived from each sample revealed no statistically significant difference in recovery rates between the two sorbent amounts. This indicates that an increase in the sorbent mass does not confer a performance advantage and was therefore not adopted.

Suitability of various elution solvents was assessed with respect to extraction recovery as well as the similarity to the initial LC mobile phase composition, finding that MeCN:water (7:3) was the optimum one (Fig. 3). Building upon prior research [20,27] that established a solid-phase extraction protocol using HLB 96-well plates for blood-derived samples, this study navigates a more complex matrix and lower analyte concentrations, which is the reason for further solvent optimization. Elution solvent selection was guided by stringent criteria, considering that complete drying and reconstitution post-SPE, driven by analyte losses due to vial surface adsorption, should be avoided. This selection was corroborated by an extraction efficiency of 52 % at 2.5 μg/L and 73 % at 7.5 μg/L, determined through a comparison between the peak areas of the analytes before and after extraction. Despite extensive optimization efforts, it is important to acknowledge that the improvements achievable through modifications to the solvent composition are inherently limited and though the extraction efficiency remains suboptimal, it represents the best-case scenario achievable by modifying the elution solvents.

3.2.3. Instrumental analysis

The optimization of chromatographic conditions was conducted through experiments, focusing on the evaluation of mobile phase composition. The combination exhibiting optimal peak shapes and responses involved MeCN as the organic and ammonium formate as the aqueous mobile phase. Notably, detector responses were maximized at the salt concentration of 20 mM, exhibiting a 20 % improvement over the responses observed at 10 mM. Conversely, the introduction of ammonium formate to the MeCN mobile phase was observed to negatively impact peak shape and response.

The SCIEX 7500 mass spectrometer was employed aiming to reach the sensitivity required for determining extremely low concentrations in complex matrices. Detection was carried out in Multiple Reaction Monitoring (MRM) mode with MS operating parameters (electrospray voltage, source temperature, gases, collision energies and exit potentials for individual transitions, etc., see Table 1) automatically optimized. We selected the transitions for BLM-A2-Cu (analyte) based on the understanding that our analyte tends to form chelate with copper, and that copper has two stable isotopes (^{63}Cu and ^{65}Cu), which are clearly distinguishable in mass spectrum. Consequently, two distinct complexes with BLM-A2 are identified, i.e. BLM-A2-^{63}Cu and BLM-A2-^{65}Cu. M^{2+}

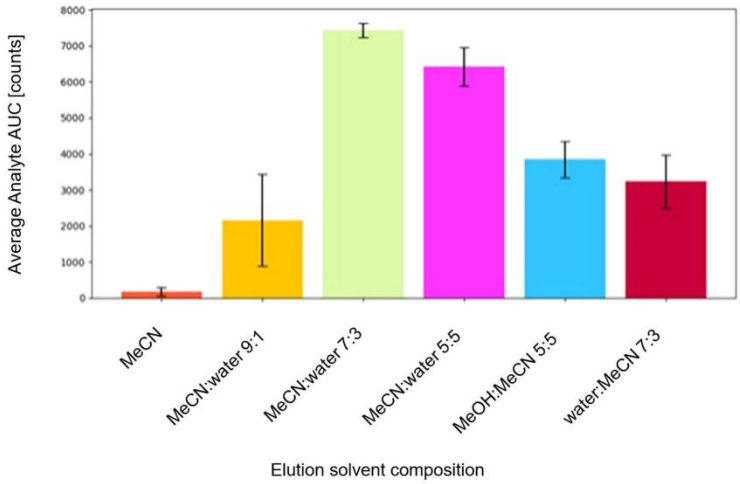


Fig. 3. Comparison of the analyte signal after modifying elution solvent composition (c(BLM) = 5 µg/L; n = 2).

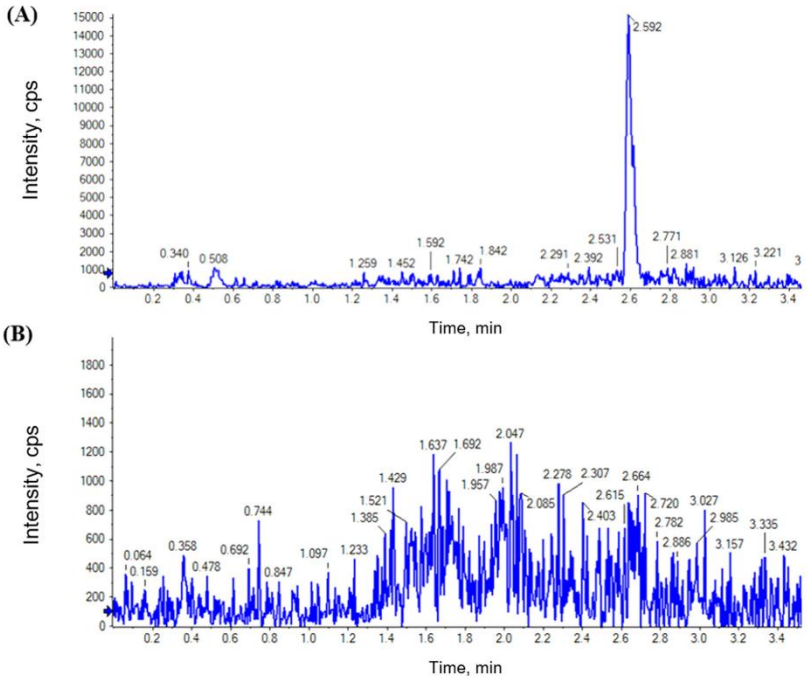


Fig. 4. Extracted ion chromatogram of BLM-A2-Cu at LLOQ concentration (A) and the chromatogram of the same species in a blank matrix (B).

ions of these isotopes correspond to m/z 738.7 and m/z 739.7, respectively. The ratio between ^{63}Cu and ^{65}Cu is 69.17–30.83 %, which leaves the less abundant m/z corresponding to BLM-A2-^{65}Cu complex as a confirming transition, increasing its analytical reliability.

3.2.4. Method validation

The method's performance was evaluated through partial validation procedures aligned with EMA guidelines [26] to ensure the reliability of the obtained results. This validation encompassed an assessment of selectivity, linearity, lower limit of quantification (LLOQ), and accuracy.

Selectivity was ascertained via the two transitions of BLM-A2-^{63}Cu and BLM-A2-^{65}Cu species at the chromatographic retention time of 2.6 min, along with the check-up of a blank matrix extract, which displayed noise intensities significantly lower than 20 % of those for the lowest calibrator (0.05 μg/L). Fig. 4 (top) illustrates the LLOQ signal for BLM-A2-^{63}Cu and the absence of the signal in a blank cell matrix (bottom).

Linearity was investigated across the concentration range of 0.075 μg/L – 2.5 μg/L for both CHO and B16F1 tumor cells to evaluate the method's ability to produce results, directly proportional to the analyte concentration, while also examining matrix effects. The calibration curve for CHO cell matrix indicated satisfactory linearity, with a correlation coefficient R of 0.994. Conversely, the calibration with B16F1 cells exhibited a dispersed profile with a lower R of 0.907, suggesting notable variances that could be attributed to the intrinsic differences in cell pellet structure, constraining the sample preparation. Despite these variances, the matrix effect was found to be consistent in both cell types, as demonstrated by the near-identical linear regression formulae, justifying the use of the CHO cell-derived calibration curve for subsequent sample measurements to maintain analytical consistency. To accommodate samples with concentrations below the LLOQ of the initially prepared calibration curve, an additional curve spanning from 0.005 μg/L to 2.5 μg/L was established post-extraction. This curve demonstrated a commendable linear response with an R of 0.993, extending the (instrumental) method's applicability to lower concentrations.

Accuracy was assessed using calibration samples prepared from CHO cells. The guidelines permit a maximum deviation of 15 % from the nominal value for more than 75 % of the calibration standards above the LLOQ. In our study, we achieved this criterion for 60 % of the calibrators, indicating a performance that, while not fully aligning with the standards, we determined as acceptable considering the constraints encountered. The LLOQ was determined to be 0.075 μg/L, a level at which the EMA guidelines [26] allow for a permissible error margin of up to 20 %. QC samples were prepared at this concentration in duplicate for each batch. They were used to evaluate the method's repeatability (values up to 25 % RSD) and accuracy with 43 % samples at LLOQ concentration falling within ± 20 % of the nominal concentration (while the required limit is 50 %). Additionally, a concentration of 7.5 μg/L was tested, despite being above the highest calibrator used in the calibration curve, to provide supplementary data on method performance. The method validation results are summarized in Table 2.

It is acknowledged that these results, though not fully meeting the EMA guidelines [26] criteria, represent the optimum achievable performance under the existing methodological conditions. This deviation from the guidelines, albeit suboptimal, does not substantially compromise the method's overall utility and reliability. Our findings underscore the method's consistent performance and its potential applicability in the field, highlighting the balance struck between methodological rigor and the practical limitations inherent in such analytical endeavors.

Table 2
Analytical method validation results.

	N = 3 at 0.075 μg/L BLM (LLOQ)	N = 3 at 2.5 μg/L BLM (highest cal. measured with samples)	N = 3 at 7.5 μg/L BLM
Extraction efficiency (%)	117	52	73
Method repeatability (% RSD)	24	5.0	9.0
Inj. repeatability (% RSD)	19	3.8	4.0
Accuracy (all data) in %	88.9, 137, 95.9	80.4, 76.3, 72.8	112, 112, 95.4

3.3. Results of EP cell samples analyses

In the absence of electric pulses, BLM exhibits limited permeability across the cell membrane, primarily entering cells via receptor-mediated endocytosis mechanisms [33]. However, the cytotoxicity of BLM undergoes a potent increase of several hundred to thousandfold with electrochemotherapy [9]. Consequently, we anticipated that non-electroporated cells would exhibit minimal BLM uptake. Therefore, we measured intracellular BLM concentrations in non-electroporated cells solely at the highest concentration utilized in this study (i.e., 140 nM).

Contrary to our expectations, (Welch's) t-tests revealed no significant differences in BLM uptake between CHO cells or B16F1 cells exposed to 140 nM BLM with or without electroporation using 25 × 400 ns pulses (Fig. 5 (B) and Fig. 6 (B)). While ANOVA indicated a statistically significant difference only in B16F1 cells electroporated with 25 × 400 ns pulses between those not exposed to BLM and those incubated with 140 nM of BLM, a trend can be observed that a higher BLM concentration was measured for cells that were incubated with higher BLM concentrations, regardless of the electroporation protocol (Fig. 5 (A) and Fig. 6 (A)). These observations may be attributed to the detection of residual BLM from the treatment, which was not internalized by the cells, thereby potentially masking the actual signal originating from internalized BLM.

The detection of signals in the non-spiked samples is not entirely unexpected in a highly sensitive method. Such low concentrations, as they fall below the determined LLOQ, would normally be disregarded. However, given the extremely low concentrations observed in many samples, it was deemed reasonable to also report these sub-LLOQ values to avoid excluding a substantial portion of the data, which explains the traces of BLM, detected (and reported) in non-spiked cell samples.

4. Conclusions

The primary objective of this study was developing an LC-MS-based analytical method for quantifying bleomycin at ultra-trace levels in electroporated cells. This effort was driven by the need to support findings from cell survival assays, which suggest that nanosecond pulses can permeabilize cell membranes similarly to traditional microsecond pulses, albeit at higher concentrations. The optimization and application of this analytical method are shown in the study.

We demonstrated the capability of state-of-art analytical equipment to determine trace levels of highly complex analytes. However, the limitation is still the significant divergency between the capacity of state-of-art equipment, i.e. what can be measured, and on the other edge, the trace level concentration that can kill the cell, which is a few hundred BLM molecules per cell (translating to 1×10^{-6} ng per 1000 cells). Despite advancements, this low level is still unachievable and demonstrates the need for further improving the equipment and analytical methods sensitivity. One important constraint is also the losses during sample preparation and an immense impact of matrix on electrospray ionization, which requires further innovations in analytical practices, especially when it comes to such demanding and thus important analytical challenges. Another solely analytical and interesting finding was the choice of lysis buffer to enable the analysis of intracellular chelating agents.

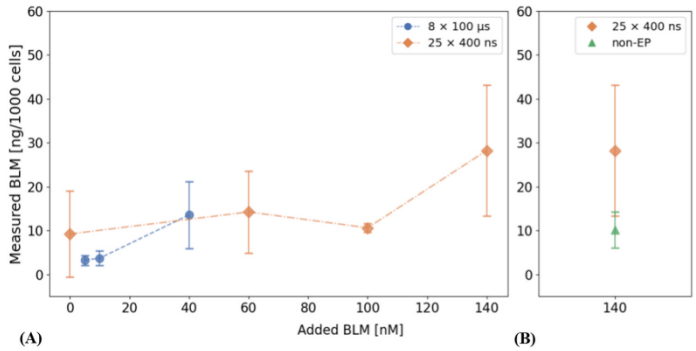


Fig. 5. The arithmetic mean and standard deviation of bleomycin (BLM) concentration normalized by the number of cells in the samples plotted against the initial BLM concentration applied to CHO cells prior to electric pulse delivery. CHO cells were exposed to 8 × 100 µs pulses (blue circles) or 25 × 400 ns pulses (orange diamonds) (A). The measured BLM concentration in cells exposed to 140 nM BLM, comparing results between cells electroporated with 25 × 400 ns pulses (orange diamond) and non-electroporated CHO cells (green triangle) is shown on (B).

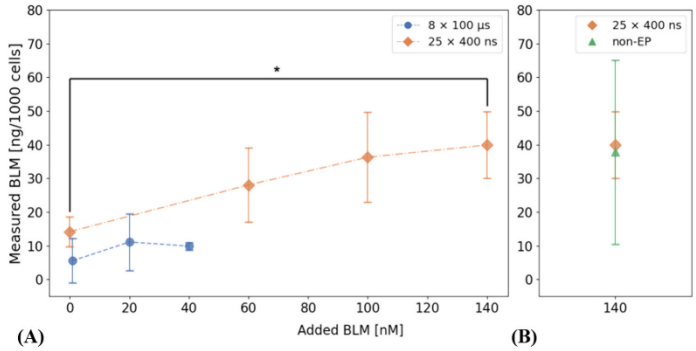


Fig. 6. The arithmetic mean and standard deviation of bleomycin (BLM) concentration normalized by the number of cells in the samples plotted against the initial BLM concentration applied to B16F1 cells prior to electric pulse delivery. B16F1 cells were exposed to 8 × 100 µs pulses (blue circles) or 25 × 400 ns pulses (orange diamonds) (A). The measured BLM concentration in B16F1 cells exposed to 140 nM BLM, comparing results between cells electroporated with 25 × 400 ns pulses (orange diamond) and non-electroporated cells (green triangle) is shown on (B). Asterisk (*) represents a statistically significant difference ($p < 0.05$) in the measured BLM concentration.

We found contradictory results for nonpermeabilized B16F1 cells showing highest concentration of BLM, however this is not in line with the finding for CHO cells that in nonpermeabilized form exhibited lowest concentration, which may be explained by externally deposited BLM that was insufficiently washed off during the pellet washing. Previous studies have demonstrated that BLM binds to and interacts with cell membranes [34,35] suggesting that this washing step might be more critical than previously thought. However, further intensification of the washing procedure could potentially lead to cell lysis and compromise subsequent analyses. Therefore, our approach maintains a careful balance between efficient washing and preserving cell integrity.

Further research should explore the mechanistic differences in membrane permeabilization between pulse durations and investigate the potential for combining nanosecond pulses with other therapeutic agents to enhance clinical outcomes. The utility of our developed analytical method, however, reaching extremely low LLOQs compared to existing methods, could be extended to various targeted delivery studies beyond electroporation, including alternative delivery methods like nanoparticles and liposomes, and can guide other chemotherapeutic quantifications, offering valuable insights for pharmacokinetic and cellular uptake studies. This versatility underscores the method's broader utility in advancing targeted cancer therapy research.

Funding

The authors acknowledge the financial support from the state budget by the Slovenian Research Agency (P1–0143, J1–6744, J4–2546, J3–9269).

CRediT authorship contribution statement

Vižintin Angelika: Writing – original draft, Visualization, Methodology, Investigation, Data curation. **Plešnik Helena:** Writing – review & editing, Writing – original draft, Visualization, Methodology, Investigation, Conceptualization. **Miklavčič Damijan:** Writing – review & editing, Supervision, Funding acquisition. **Stahl-Zeng Jianru:** Writing –

review & editing. **Steed Jack:** Supervision, Investigation. **Kosjek Tina:** Writing – review & editing, Writing – original draft, Visualization, Supervision, Project administration, Methodology, Funding acquisition, Conceptualization.

Declaration of Competing Interest

The authors declare that they have no known competing financial interests or personal relationships that could have appeared to influence the work reported in this paper.

References

[1] L. McMorrow, M. Shaikh, G. Kessell, T. Muir, Bleomycin electrosclerotherapy: new treatment to manage vascular malformations, Br. J. Oral. Maxillofac. Surg. 55 (2017) 977–979, https://doi.org/10.1016/j.bjoms.2017.10.002.

[2] C.A. Claussen, E.C. Long, Nucleic Acid recognition by metal complexes of bleomycin, Chem. Rev. 99 (1999) 2797–2816, https://doi.org/10.1021/cr980449z.

[3] V. Murray, J.K. Chen, L.H. Chung, The INteraction of the Metallo-glycopeptide Anti-tumour Drug Bleomycin with DNA, Int. J. Mol. Sci. 19 (2018) 1372, https://doi.org/10.3390/ijms19051372.

[4] XLOGP3 (v3.2.2), (n.d.). http://www.sioc-ccbg.ac.cn/skins/ccbgwebsite/software/xlogp3/ (accessed April 2, 2024).

[5] I. Crnovcic, F. Gan, D. Yang, L.-B. Dong, P.G. Schultz, B. Shen, Activities of recombinant human bleomycin hydrolase on bleomycins and engineered analogues revealing new opportunities to overcome bleomycin-induced pulmonary toxicity, Bioorg. Med. Chem. Lett. 28 (2018) 2670–2674, https://doi.org/10.1016/j.bmcl.2018.04.065.

[6] T. Kotnik, L. Rems, M. Tarek, D. Miklavčič, Membrane Electroporation and Electropermeabilization: Mechanisms and Models, Annu. Rev. Biophys. 48 (2019) 63–91, https://doi.org/10.1146/annurev-biophys-052118-115451.

[7] B. Geboers, H.J. Scheffer, P.M. Graybill, A.H. Ruarus, S. Nieuwenhuizen, R.S. Puijk, P.M. van den Tol, R.V. Davalos, B. Rubinsky, T.D. de Gruijl, D. Miklavčič, M. R. Meijerink, High-voltage electrical pulses in oncology: irreversible electroporation, electrochemotherapy, gene electrotransfer, electrofusion, and electroimmunotherapy, Radiology 295 (2020) 254–272, https://doi.org/10.1148/radiol.2020192190.

[8] X. Gong, Z. Chen, J.J. Hu, C. Liu, Advances of electroporation-related therapies and the synergy with immunotherapy in cancer treatment, Vaccines 10 (2022) 1942, https://doi.org/10.3390/vaccines10111942.

[9] D. Miklavčič, B. Mali, B. Kos, R. Heller, G. Serša, Electrochemotherapy: from the drawing board into medical practice, Biomed. Eng. OnLine 13 (2014) 29, https://doi.org/10.1186/1475-925X-13-29.

[10] L.M. Mir, J. Gehl, G. Sersa, C.G. Collins, J.-R. Garbay, V. Billard, P.F. Geertsen, Z. Rudolf, G.C. O'Sullivan, M. Marty, Standard operating procedures of the electrochemotherapy: Instructions for the use of bleomycin or cisplatin administered either systemically or locally and electric pulses delivered by the CliniporatorTM by means of invasive or non-invasive electrodes, Eur. J. Cancer Suppl. 4 (2006) 14–25, https://doi.org/10.1016/j.ejcsup.2006.08.003.

[11] O. Michel, J. Kulbacka, J. Saczko, J. Mączyńska, P. Błasiak, J. Rossowska, A. Rzechonek, Electroporation with cisplatin against metastatic pancreatic cancer: *In Vitro* study on human primary cell culture, BioMed. Res. Int. 2018 (2018) e7364539, https://doi.org/10.1155/2018/7364539.

[12] A. Vižintin, S. Marković, J. Ščančar, D. Miklavčič, Electroporation with nanosecond pulses and bleomycin or cisplatin results in efficient cell kill and low metal release from electrodes, Bioelectrochemistry 140 (2021) 107798, https://doi.org/10.1016/j.bioelechem.2021.107798.

[13] G. Serša, M. Čemažar, D. Miklavčič, Antitumor effectiveness of electrochemotherapy with cis-diamminedichloroplatinum(II) in mice1, Cancer Res 55 (1995) 3450–3455.

[14] L.G. Campana, A.J.P. Clover, S. Valpione, P. Quaglino, J. Gehl, C. Kunte, M. Snoj, M. Cemazar, C.R. Rossi, D. Miklavcic, G. Sersa, Recommendations for improving the quality of reporting clinical electrochemotherapy studies based on qualitative systematic review, Radiol. Oncol. 50 (2016) 1–13, https://doi.org/10.1515/raon-2016-0006.

[15] A.G. Pakhomov, O.N. Pakhomova, The interplay of excitation and electroporation in nanosecond pulse stimulation, Bioelectrochemistry 136 (2020) 107598, https://doi.org/10.1016/j.bioelechem.2020.107598.

[16] G. Long, P.K. Shires, D. Plescia, S.J. Beebe, J.F. Kolb, K.H. Schoenbach, Targeted Tissue Ablation With Nanosecond Pulses, IEEE Trans. Biomed. Eng. 58 (2011) 2161–2167, https://doi.org/10.1109/TBME.2011.2113183.

[17] E. Gudvangen, V. Kim, V. Novickij, F. Battista, A.G. Pakhomov, Electroporation and cell killing by milli- to nanosecond pulses and avoiding neuromuscular stimulation in cancer ablation, Sci. Rep. 12 (2022) 1763, https://doi.org/10.1038/s41598-022-04868-x.

[18] M. Scuderi, J. Dermol-Cerne, J. Scancar, S. Markovic, L. Rems, D. Miklavcic, The equivalence of different types of electric pulses for electrochemotherapy with cisplatin – an in vitro study, Radiol. Oncol. 58 (n.d.) 51–66. https://doi.org/10.2478/raon-2024-0005.

[19] A. Vižintin, J. Vidmar, J. Ščančar, D. Miklavčič, Effect of interphase and interpulse delay in high-frequency irreversible electroporation pulses on cell survival, membrane permeabilization and electrode material release, Bioelectrochemistry 134 (2020) 107523, https://doi.org/10.1016/j.bioelechem.2020.107523.

[20] T. Kosjek, A. Krajnc, T. Gornik, D. Zigon, A. Groselj, G. Sersa, M. Cemazar, Identification and quantification of bleomycin in serum and tumor tissue by liquid chromatography coupled to high resolution mass spectrometry, Talanta 160 (2016) 164–171, https://doi.org/10.1016/j.talanta.2016.06.062.

[21] H. Plesnik, M. Bosnjak, M. Cemazar, G. Sersa, T. Kosjek, An effective validation of analytical method for determination of a polar complexing agent: the illustrative case of cytotoxic bleomycin, Anal. Bioanal. Chem. 415 (2023) 2737–2748, https://doi.org/10.1007/s00216-023-04675-x.

[22] R. Vallat, Pingouin: statistics in Python, J. Open Source Softw. 3 (2018) 1026, https://doi.org/10.21105/joss.01026.

[23] S. Seabold, J. Perktold, Statsmodels: econometric and statistical modeling with python, Proc. 9th Python Sci. Conf. (2010) 92–96, https://doi.org/10.25080/Majora-92bf1922-011.

[24] A. Vizintin, S. Markovic, J. Scancar, J. Kladnik, I. Turel, D. Miklavcic, Nanosecond electric pulses are equally effective in electrochemotherapy with cisplatin as microsecond pulses, Radiol. Oncol. 56 (2022) 326–335, https://doi.org/10.2478/raon-2022-0028.

[25] N. Thakrar, K.T. Douglas, Photolability of bleomycin and its complexes, Cancer Lett. 13 (1981) 265–268, https://doi.org/10.1016/0304-3835(81)90027-6.

[26] Bioanalytical method validation: scientific guideline, (2011). ⟨https://www.ema.europa.eu/en/bioanalytical-method-validation-scientific-guideline⟩ (accessed November 14, 2022).

[27] A. Groselj, M. Bosnjak, M. Krzan, T. Kosjek, K. Bottyán, H. Plesnik, C. Jamsek, M. Cemazar, E. Kis, G. Sersa, Bleomycin Concentration in Patients' Plasma and Tumors after Electrochemotherapy. A Study from InspECT Group, Pharmaceutics 13 (2021) 1324, https://doi.org/10.3390/pharmaceutics13091324.

[28] A.G. Pakhomov, J.F. Kolb, J.A. White, R.P. Joshi, S. Xiao, K.H. Schoenbach, Long-lasting plasma membrane permeabilization in mammalian cells by nanosecond pulsed electric field (nsPEF), Bioelectromagnetics 28 (2007) 655–663, https://doi.org/10.1002/bem.20354.

[29] A.G. Pakhomov, A.M. Bowman, B.L. Ibey, F.M. Andre, O.N. Pakhomova, K. H. Schoenbach, Lipid nanopores can form a stable, ion channel-like conduction pathway in cell membrane, Biochem. Biophys. Res. Commun. 385 (2009) 181–186, https://doi.org/10.1016/j.bbrc.2009.05.035.

[30] P.T. Vernier, Y. Sun, M.A. Gundersen, Nanoelectropulse-driven membrane perturbation and small molecule permeabilization, BMC Cell Biol. 7 (2006) 37, https://doi.org/10.1186/1471-2121-7-37.

[31] C.-Q. Xiao, Q. Huang, Y. Zhang, H.-Q. Zhang, L. Lai, Binding thermodynamics of divalent metal ions to several biological buffers, Thermochim. Acta 691 (2020) 178721, https://doi.org/10.1016/j.tca.2020.178721.

[32] T. Kosjek, S. Perko, D. Zigon, E. Heath, Fluorouracil in the environment: Analysis, occurrence, degradation and transformation, J. Chromatogr. A 1290 (2013) 62–72, https://doi.org/10.1016/j.chroma.2013.03.046.

[33] G. Pron, N. Mahrour, S. Orlowski, O. Tounekti, B. Poddevin, J. Belehradek, L. M. Mir, Internalisation of the bleomycin molecules responsible for bleomycin toxicity: a receptor-mediated endocytosis mechanism, Biochem. Pharm. 57 (1999) 45–56, https://doi.org/10.1016/S0006-2952(98)00282-2.

[34] A. Cort, T. Ozben, A. Sansone, S. Barata-Vallejo, C. Chatgilialoglu, C. Ferreri, Bleomycin-induced trans lipid formation in cell membranes and in liposome models, Org. Biomol. Chem. 13 (2015) 1100–1105, https://doi.org/10.1039/C4OB01924E.

[35] Z. Yu, R. Paul, C. Bhattacharya, T.C. Bozeman, M.J. Rishel, S.M. Hecht, Structural features facilitating tumor cell targeting and internalization by bleomycin and its disaccharide, Biochemistry 54 (2015) 3100–3109, https://doi.org/10.1021/acs.biochem.5b00277.

3.3.3 Support to TDM in clinical study attempting to reduce the dosage of API and thus reduce adverse effects: bleomycin concentration in patients' plasma and tumors after electrochemotherapy. A study from InspECT group

Published: Groselj, A., Bosnjak, M., Krzan, M., Kosjek, T., Bottyán, K., Plesnik, H., Jamsek, C., Cemazar, M., Kis, E., Sersa, G., Pharmaceutics, 2021

This paper contributes to the pharmacotherapy section of the thesis by extending the analytical work on bleomycin from method development to clinical application in patients undergoing electrochemotherapy. The study investigates bleomycin concentrations in plasma and tumor tissue with the clinical aim of optimizing treatment timing and dosing, while within the thesis its main relevance lies in demonstrating how validated LC–MS/MS analysis of this highly polar drug can support pharmacokinetic interpretation under real clinical conditions.

Rather than focusing further on analytical optimization, the study shows how quantitative plasma data can be translated into clinically relevant concentration–time profiles. The results revealed substantial interindividual variability in bleomycin pharmacokinetics, particularly age-related differences in elimination, indicating that identical dosing does not result in comparable systemic exposure across patients. This directly illustrates the importance of reliable quantitative analysis when defining therapeutic exposure windows.

Tumor tissue analysis added a second clinically relevant dimension by showing highly variable intratumoral bleomycin concentrations, independent of tumor size. This suggests that local drug distribution is influenced by biological factors such as vascularization and sampling location, and that plasma kinetics alone cannot fully explain tissue exposure.

My contribution focused on quantitative analysis of bleomycin in patient plasma samples using LC–MS/MS. These analytical results formed the basis for pharmacokinetic interpretation in the study and directly connect the methodological work presented earlier in the thesis with clinically actionable conclusions.

Overall, this paper places the preceding analytical developments into a clinical pharmacotherapy context and shows how robust quantification of a polar cytostatic supports treatment interpretation beyond the analytical laboratory.

pharmaceutics

MDPI

Article

Bleomycin Concentration in Patients' Plasma and Tumors after Electrochemotherapy. A Study from InspECT Group

Ales Groselj [1,2,†], Masa Bosnjak [3,4,†], Mojca Krzan [5], Tina Kosjek [6,7], Kriszta Bottyán [8], Helena Plesnik [6,7], Crt Jamsek [1,2], Maja Cemazar [3,9], Erika Kis [8,*] and Gregor Sersa [3,10,*]

1 Department of Otorhinolaryngology and Cervicofacial Surgery, University Medical Centre Ljubljana, Zaloska 2, SI-1000 Ljubljana, Slovenia; ales.groselj@kclj.si (A.G.); crt.jamsek@kclj.si (C.J.)
2 Faculty of Medicine, University of Ljubljana, Vrazov trg 2, SI-1000 Ljubljana, Slovenia
3 Department of Experimental Oncology, Institute of Oncology Ljubljana, Zaloska 2, SI-1000 Ljubljana, Slovenia; mbosnjak@onko-i.si (M.B.); mcemazar@onko-i.si (M.C.)
4 Faculty of Pharmacy, University of Ljubljana, Aškerčeva 7, SI-1000 Ljubljana, Slovenia
5 Department of Pharmacology and Experimental Toxicology, Faculty of Medicine, University of Ljubljana, Korytkova 2, SI-1000 Ljubljana, Slovenia; mojca.limpel@mf.uni-lj.si
6 Department of Environmental Sciences, Jozef Stefan Institute, Jamova 39, SI-1000 Ljubljana, Slovenia; tina.kosjek@ijs.si (T.K.); helena.plesnik@ijs.si (H.P.)
7 Jozef Stefan International Postgraduate School, Jamova 39, SI-1000 Ljubljana, Slovenia
8 Department of Dermatology and Allergology, University of Szeged, 6721 Szeged, Hungary; krisztabottyan@gmail.com
9 Faculty of Health Sciences, University of Primorska, Polje 42, SI-6310 Izola, Slovenia
10 Faculty of Health Sciences, University of Ljubljana, Zdravstvena pot 5, SI-1000 Ljubljana, Slovenia
* Correspondence: kis.erika.gabriella@med.u-szeged.hu (E.K.); gsersa@onko-i.si (G.S.); Tel.: +386-1-5879-434 (G.S.)
† These authors contributed equally to this work.

Abstract: The plasma concentration profile of bleomycin in the distribution phase of patients younger than 65 years is needed to determine the suitable time interval for efficient application of electric pulses during electrochemotherapy. Additionally, bleomycin concentrations in the treated tumors for effective tumor response are not known. In this study, the pharmacokinetic profile of bleomycin in the distribution phase in 12 patients younger than 65 years was determined. In 17 patients, the intratumoral bleomycin concentration was determined before the application of electric pulses. In younger patients, the pharmacokinetics of intravenously injected bleomycin demonstrated a faster plasma clearance rate than that in patients older than 65 years. This outcome might indicate that the lowering of the standard bleomycin dose of 15,000 IU/m^2 with intravenous bleomycin injection for electrochemotherapy is not recommended in younger patients. Based on the plasma concentration data gathered, a time interval for electrochemotherapy of 5–15 min after bleomycin injection was determined. The median bleomycin concentration in tumors 8 min after bleomycin injection, at the time of electroporation, was 170 ng/g. Based on collected data, the reduction of the bleomycin dose is not recommended in younger patients; however, a shortened time interval for application of electric pulses in electrochemotherapy to 5–15 min after intravenous bleomycin injection should be considered.

Keywords: electrochemotherapy; electroporation; bleomycin; pharmacokinetics; blood samples; tumor samples; drug delivery

check for updates

Citation: Groselj, A.; Bosnjak, M.; Krzan, M.; Kosjek, T.; Bottyán, K.; Plesnik, H.; Jamsek, C.; Cemazar, M.; Kis, E.; Sersa, G. Bleomycin Concentration in Patients' Plasma and Tumors after Electrochemotherapy. A Study from InspECT Group. *Pharmaceutics* **2021**, *13*, 1324. https://doi.org/10.3390/pharmaceutics13091324

Academic Editors: Neal M. Davies and Dong Hyun Kim

Received: 16 July 2021
Accepted: 19 August 2021
Published: 24 August 2021

Publisher's Note: MDPI stays neutral with regard to jurisdictional claims in published maps and institutional affiliations.

Copyright: © 2021 by the authors. Licensee MDPI, Basel, Switzerland. This article is an open access article distributed under the terms and conditions of the Creative Commons Attribution (CC BY) license (https://creativecommons.org/licenses/by/4.0/).

1. Introduction

Electrochemotherapy is a local cancer ablative therapy that is currently performed in numerous cancer centers throughout Europe. Drug delivery into cells in electrochemotherapy is based on a physical delivery method called electroporation. Tumor tissue is exposed to an external electric field and delivered through electrodes with different geometries that correspond to different sizes and shapes of the treated tumors. Different malignancies, such

as melanoma, basal cell carcinoma, cutaneous squamous cell carcinoma, breast cancer, Kaposi sarcomas, and others, are effectively treated with electrochemotherapy. The objective response rate of skin tumors is approximately 80% [1–4]. Nevertheless, electrochemotherapy has been shown to have different effectiveness in tumors of different histotypes; basal cell carcinomas have proven to be the most responsive, with an objective response rate of up to 95%, while melanomas have an objective response rate of approximately 70%. Studies have demonstrated that the response to electrochemotherapy is also dependent on the size of the tumors and eventual previous treatment(s) either with chemotherapy, radiotherapy, or surgery [5]. The most recent analysis of electrochemotherapy effectiveness in cutaneous malignancies in 987 patients with 2482 treated lesions was published in 2020 [6]. For the smallest lesions (less than 5 mm), the analysis showed 82% complete and 91% objective response rates after a single therapy. Not only cutaneous lesions but also deep-seated tumors, such as hepatocellular carcinoma or liver metastases of colorectal carcinoma, could be effectively treated with electrochemotherapy, and different response rates were observed, with hepatocellular carcinoma being more responsive [7,8].

The underlying mechanisms of therapeutic effectiveness have not yet been clearly elucidated. A preclinical search for the biological markers of tumor response to electrochemotherapy has already been performed. Intrinsic sensitivity to chemotherapeutic drugs, the immunophenotype of tumors and immunocompetence of the host, and vascularization of tumors partially determine the response to electrochemotherapy [9–12]. In addition, BRAF mutation was found to be a biological marker of synergistic effects with BRAF inhibitors and electrochemotherapy [13]. Olaparib, which is a DNA repair inhibitor, and electrochemotherapy have synergistic effects in *BRCA*-mutated breast cancer cells [14]. Viral infection, such as HPV infection, can also predispose tumor cells to a better response to electrochemotherapy [15].

For better planning and performing clinical studies using electrochemotherapy, a research roadmap for the investigation of biological factors of tumor response to electrochemotherapy has been published [16]. One of the predictive factors could also be bleomycin concentrations in plasma and tumors. The pharmacokinetics of bleomycin in patients has been defined by radioimmunoassay and high-pressure liquid chromatography but not by liquid chromatography mass spectrometry [17,18]. The first report of bleomycin pharmacokinetics in patients older than 65 years treated with electrochemotherapy was published by our group in 2016 [19] after the method for detection of bleomycin in serum and tumor samples was established [20]. The results demonstrated that the bleomycin dose in elderly patients can be reduced by one-third. No significant difference in long-term disease-free survival was observed in elderly patients treated with a reduced dose of bleomycin compared to those treated with a standard dose of bleomycin [21]. We also observed less intensive post electrotherapy reactions, shorter healing times, and better cosmetic outcomes in elderly patients treated with a reduced dose of bleomycin [22]. Other groups have also demonstrated a good antitumor response after reducing the bleomycin dose in elderly patients [23].

Based on the mentioned studies, we formulated one of our main questions as follows: what is the time course of bleomycin plasma concentration in patients younger than 65? Can we reduce the dose of bleomycin also in this age group, or is the time course of bleomycin plasma concentration profile significantly different from the 65 years old and older patients that were already published? In relation to the pharmacokinetic profile in patients younger than 65 years, the time interval for electrochemotherapy, i.e., time between the intravenous bleomycin injection and application of electric pulses, was compared to that of the older patient population.

Moreover, the concentrations of bleomycin in tumors have not yet been determined. Therefore, in this study, we wanted to determine the correlation between concentrations of bleomycin in tumors and response to the treatment. Furthermore, we also wanted to determine the minimal effective dose in tumors needed for a good antitumor response.

Altogether, we aimed to determine bleomycin pharmacokinetic aspects upon a physically mediated drug delivery method, electroporation, which would serve us to better understand the efficacy and safety aspects of electrochemotherapy and its application in younger and older patients' populations.

2. Patients and Methods

2.1. Patients

The study was conducted as a prospective, interventional study between October 2017 and December 2019 within the International Network for Sharing Practices of electrochemotherapy (InspECT) (www.insp-ect.org, accessed 15 March 2021). All patients who presented with skin cancers, recurrent disease (and/or metastatic disease) or a second primary tumor in the head and neck region were either not suitable for conventional treatments or refused them. The patients were treated with electrochemotherapy at the Department of Otorhinolaryngology and Cervicofacial Surgery, University Medical Centre Ljubljana, Slovenia or the Department of Dermatology and Allergology, University of Szeged, Hungary. The study was approved by the National Ethics Committee of the Republic of Slovenia (0120-296/2017-3, 25 March 2017) and the Regional and Institutional Review Board of Human Investigations at the University of Szeged, Hungary (4129-223/2017, 20 November 2017). The study was registered in the ISRCTN database (ISRCTN74054653). Treatment with electrochemotherapy was previously agreed upon by a multidisciplinary board, and written informed consent was obtained from all eligible patients. The selection of patients was performed according to the NICE guidelines. The included patients were older than 18 years and presented with different histologies of cutaneous tumors (basal cell carcinoma, squamous cell carcinoma, melanoma, and others). The exclusion criteria were as follows: (a) patients not suitable for electrochemotherapy according to the NICE guidelines and (b) patients who did not comply with requirements for blood collection, tumor biopsy or tissue sampling according to the SOP for blood collection or tissue sampling. In the study, altogether 25 patients were included; 8 patients younger than 65 for blood sample collection, 4 patients younger than 65 for blood and tumor sample collection and 13 patients for tumor sample collection with no age limitation.

2.2. Procedure

Electrochemotherapy was performed according to the updated standard operating procedures [24]. Briefly, bleomycin (bleomycin medac, Medac, Wedel, Germany) was injected intravenously (bolus in 2 min) at a dose of 15,000 IU/m^2 body surface area (1000 IU is equal to 1 mg of bleomycin activity), and 8 min after the injection, electric pulses were applied. Electric pulses for electrochemotherapy were generated by a Cliniporator pulse generator (IGEA, s.r.l., Carpi, Italy) and delivered by fixed geometry electrodes, i.e., mainly electrodes with eight needles arranged in two rows of four needles each with a distance of 4 mm between the rows. In one application of electric pulses, eight pulses with a voltage of 400 V, a pulse duration of 100 µs and a frequency of 5000 Hz were applied. The number of applications was adjusted to the size of the treated tumors.

2.3. Blood Samples Collection

For blood collection, 12 patients younger than 65 years were eligible. Two milliliters of arterial blood samples were collected at predetermined time points (0, 5, 10, 20, 30, and 40 min after bleomycin administration, where 0 is considered the time immediately before bleomycin injection) into blood collection tubes (BD Vacutainer, Franklin Lakes, NJ, USA). Samples were centrifuged at 1882× *g* for 10 min at room temperature. Plasma was carefully transferred to a new Eppendorf tube and stored at −20 °C until analysis.

2.4. Tumor Samples Collection

For tumor tissue collection, 17 patients either younger or older than 65 years (4 were the same patients as for blood collection) were eligible. Eligible patients should have had enough tumor volume for 3-mm punch biopsy and further electrochemotherapy procedures. A one-time punch biopsy was performed just before application of electric pulses, 8 min after intravenous bleomycin injection. Multiple biopsies were not taken because of relatively small tumor volumes. The tumor samples were taken from the visibly viable tumor section, and the sample was taken throughout the tumor thickness. The samples were placed into cryotubes (Corning Incorporated, Corning, NY, USA) and stored at −80 °C until further analysis.

2.5. Chemical Analysis

Plasma samples were prepared for analysis by protein precipitation and phospholipid removal using Ostro™ 96-well plates (Waters Corp., Milford, MA, USA). A 200-µL plasma sample was added to the 2-mL well, followed by 600 µL acetonitrile with 0.1% formic acid and internal standard epirubicin at a final concentration of 0.05 µg/mL. The mixture was then aspirated three times with a pipette and pushed through the Ostro^{TM} sorbent at 60 psi N_2 for 5 min. The extract was finally filtered through a 0.2-µm regenerated cellulose filter and analyzed by liquid chromatography coupled to tandem mass spectrometry (LC-MS/MS).

Tumor samples were ground to a fine powder under liquid nitrogen, suspended in 6 mL 0.1% HCOOH, sonicated for 60 min, centrifuged at 12,900 RCF for 20 min and filtered through 0.45-µm cellulose acetate filters before solid-phase extraction using Oasis HLB 1 cc/30 mg cartridges. After the sample filtrates were loaded onto the cartridges, the sorbent was dried under vacuum for 30 min and subsequently eluted using 0.5 mL of Milli-Q water/methanol (6/4) twice with 0.5 mL acetonitrile solution. As follows, the sample extracts were blown down to 1 mL using N_2 and were then kept frozen until LC-MS/MS analysis, which was performed within one month.

LC-MS/MS analysis was performed with a Nexera ultrahigh-performance LC (Shimadzu Corp., Kyoto, Japan) coupled to a QTRAP® 4500 MS/MS system (AB Sciex, Framingham, MA, USA). Separation was achieved at room temperature using a 5-cm-long Acquity UPLC BEH Amide (Waters Corp., Milford, MA, USA) column with a 1.7-µm particle size and 2.1-mm internal diameter. The mobile phases were 10 mM ammonium formate with 0.1% formic acid and acetonitrile. The flow rate was 0.3 mL/min. The mass spectrometer was operated in positive electrospray ionization with the multiple reaction monitoring acquisition mode. The data station operating software used was Analyst® v1.6.3 (AB Sciex, Framingham, MA, USA).

The method linearity range was 0.006 µg/mL to 1.5 µg/mL at R^2 of 0.995. The method detection limit was 0.045 µg/mL and the quantification limit 0.14 µg/mL. The intraday variation was 12% at low (0.02 µg/mL) and 2% at medium (0.60 µg/mL) BLM levels. The interday variations were 19% and 16% for low and medium levels, respectively.

2.6. Pharmacokinetic Data Analysis

Bleomycin plasma concentrations versus the time of each patient and the combined data of all 12 patients were analyzed. We determined the following pharmacokinetic parameters: the area under the plasma concentration-time curve (AUC), which was calculated using the trapezoid method from time 0 to 40 min after single bolus intravenous injection ($AUC\ 0 \rightarrow 40$), and plasma clearance (Cl) was calculated as follows:

$$Cl = \frac{dose}{AUC\ 0 \rightarrow 40} \quad (1)$$

The elimination rate constant k_{el} was determined from the slope of ln (concentration) versus the time curve, and half-life was calculated using the following:

$$t = \frac{\ln 2}{k_{el}} \quad (2)$$

and volume of distribution (Vd)

$$Vd = \frac{t}{\ln 2} \times Cl \quad (3)$$

2.7. Tumor Response Analysis

The tumor volumes were calculated according to the SOP, i.e., $a \times b^2 \times \pi/6$. Tumor response 2 months after electrochemotherapy was evaluated with a clinical exam according to RECIST 1.1 criteria [25].

2.8. Statistical Analysis

The values in this study are represented as arithmetic mean (AM) ± standard error of the mean (SE) unless otherwise stated. Comparisons between two groups were performed using unpaired 2-tailed Student's *t*-test. A *p*-value of less than 0.05 was considered to be statistically significant. GraphPad Prism (GraphPad, San Diego, CA, USA) was used for statistical analysis and graphical representation.

3. Results

3.1. Bleomycin Pharmacokinetics in Plasma of Younger Patients

The time course of the plasma concentration of bleomycin was determined in 12 patients younger than 65 years. The patients were treated with a standard dose of bleomycin, i.e., 15,000 IU/m^2 bleomycin in bolus injection. The patients' demographics are presented in Table 1, and their median age was 52.2 years, with a range from 35 to 64. Patients presented with cutaneous tumors eligible for electrochemotherapy. The predominant tumor types were SCC (n = 6) and BCC (n = 5). The median dose of bleomycin used in electrochemotherapy was 27,404 ± 2637 IU. In all, except for three patients who were either off study or lost to follow-up, the complete response (CR) of the treated tumors was achieved.

Blood samples were drawn at several time points, i.e., 5, 10, 20, 30, and 40 min after bleomycin intravenous injection, and bleomycin concentration was determined in the plasma of these patients. Bleomycin concentrations were determined using liquid chromatography coupled to tandem mass spectrometry. Based on the measurements, the pharmacokinetic parameters of bleomycin elimination were determined. The plasma concentration-time profile following intravenous bolus injection of bleomycin is shown in Figure 1. For comparison, the same graph shows the pharmacokinetic profile of plasma concentration-time profile in the patients who were older than 65 years, which is information taken from our previous publication [19].

In patients younger than 65 years, following a single bolus intravenous injection of bleomycin (24,000–30,000 IU, mean dose 27,404 ± 2637 IU) plasma concentration 5 min after injection was 2.219 ± 0.391 mg/L. The concentration of bleomycin declined gradually with an elimination constant (k_{el}) of 0.068 ± 0.059 min^{-1} and reached a value of 0.915 ± 0.173 mg/L at 40 min after injection (Figure 1).

The apparent volume of distribution (Vd), area under the curve (AUC), plasma clearance (Cl) and elimination half-life of bleomycin were calculated and are shown in Table 2. In the same table are also the pharmacokinetic parameters of the previously published data on patients older than 65 years, which were determined and calculated the same way as in this study [19].

Table 1. Characteristics of patients eligible for blood collection, according to the tumor histotype, initial tumor volume, age and bleomycin dose given in treatment with electrochemotherapy and tumor response after 2 months according to RECIST 1.1 criteria.

Patient No.	Gender	Age at ECT (Years)	Localization	Histology	Number of Treated Lesions	Bleomycin Dose (IU)	Response at 2 Months	Tumor Volume (cm^3)
1	M	45	Skin	SCC	1	30,000	CR	0.6
2	M	59	Skin	SCC	1	24,000	Lost to FU	20.5
3	M	35	Skin	BCC	1	30,000	PR	17.7
4	F	39	Skin	BCC	1	24,000	CR	3.5
5	M	49	Skin	SCC	4	30,000	CR	0.3, 14.1, 12.8, 6.3
6 *	M	58	Skin	SCC	6	30,000	CR	30.0, 5.6, 0.4, 0.2, 0.2, 19.3
7 *	M	49	Skin	BCC	1	26,000	CR	3.8
8	M	59	Skin	SCC	1	30,000	CR	5.2
9	F	50	Skin	BCC	1	25,000	CR	10.6
10	F	55	Skin	BCC	1	26,000	Lost to FU	0.2
11 *	M	63	Skin	Melanoma	3	29,100	CR	0.5, 1.0, 3.8
12 *	M	64	Skin	SCC	7	24,750	Off study	0.2, 0.6, 0.8, 0.7, 0.6, 0.9, 0.8
Total = 12	3 F/9 M	Median = 52.2 Range = 35–64				Mean dose = 27,404 ± 2637		

BCC—basal cell carcinoma, CR—complete response, FU—follow-up, PR—partial response, SCC—squamous cell carcinoma, * patients also eligible for tumor sample collection.

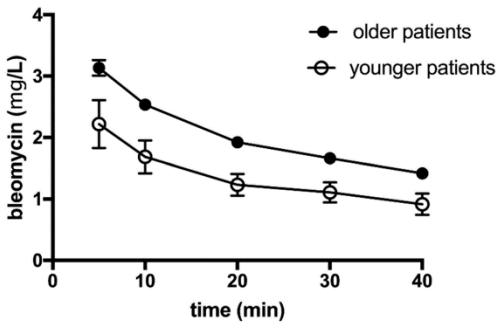


Figure 1. The elimination of bleomycin from the plasma of patients younger and older than 65 years after intravenous bolus injection of 15,000 IU/m^2 bleomycin dose. The points represent the mean +/− SEM value determined in 12 patients. The graph for older patients has already been published, but due to direct comparison, we present the data on the same graph (with permission).

Although the half-life of bleomycin was not significantly different from that in older patients, significant differences were observed in AUC, plasma clearance and volume of distribution. The AUC in younger patients was significantly lower than that in older patients, which is consistent with significantly increased plasma clearance in younger patients compared to older patients. In addition to increased clearance, the increased volume of distribution of bleomycin was determined in younger patients in comparison with older patients. A possible explanation for these two observations is that older patients have age-related decreases in kidney function and different body compositions regarding the water/fat ratio. Therefore, these results indicate that the bleomycin dose in patients younger than 65 years could not be decreased unless their kidney function was impaired.

The ideal time interval for electrochemotherapy in older patients was determined at 8–40 min after intravenous bleomycin bolus injection. From the elimination curves in this study, it was calculated that the plasma clearance of bleomycin in younger patients is much more abundant than the plasma clearance of bleomycin in older patients. Specifically, the plasma concentration that has been determined in older patients at 40 min after bleomycin injection (trough concentration) has already been reached at 15 min after bleomycin injection in younger patients. Moreover, the peak plasma concentration was reached in 5 min in younger patients compared to 8 min after bleomycin injection in older patients. We can conclude that the ideal time interval for electrochemotherapy being at peak-trough levels of bleomycin in systemic circulation lies between 5 and 15 min in younger patients and between 8 and 40 min in older patients.

Table 2. Comparison of pharmacokinetic parameters, obtained in 40 min post-bleomycin intravenous injection, of patients younger and older than 65 years treated by electrochemotherapy with 15,000 IU/m^2 bleomycin.

Sub-Groups of Patients	Number of Patients	$t_{1/2}$ (min)		*AUC* 0 → 40 (µg min/mL)		Plasma Clearance *Cl* (mL/min)		*Vd* (L)	
Younger Patients	12								
AVG		24.84	n.s.	50.83	$p < 0.0001$	999.1	$p = 0.0007$	32.17	$p = 0.0083$
SEM		2.10		7.90		261.0		6.24	
Lower 95% CI of mean		20.22		33.44		424.6		18.44	
Upper 95% CI of mean		29.46		68.22		1574.0		45.90	
Older Patients	24								
AVG		29.4		86.02		311.3		15.9	
SEM		1.79		7.899		15.83		2.65	
Lower 95% CI of mean		25.69		79.55		278.6		10.42	
Upper 95% CI of mean		33.10		92.49		344.1		21.37	

n.s.—not statistically significant.

3.2. *Bleomycin Dose Distribution in Tumor Samples*

Tumor tissue was obtained with punch tumor biopsies of tumors treated by electrochemotherapy from 17 patients regardless of the age at the time of electrochemotherapy. Patients were predominantly older than 65 years ($n = 12$), and the median age of the patients was 72.8 years (range = 49–85 years). All patients were treated with electrochemotherapy using 15,000 IU/m^2 intravenous bleomycin bolus injection, and biopsies were taken from one tumor per patient 8 min after bleomycin administration, just before the application of electric pulses (Table 3).

The predominant samples were biopsies from BCC ($n = 9$) and SCC ($n = 5$) and one sample each from porocarcinoma, melanoma, and angiosarcoma. The bleomycin concentrations determined ranged from 14 ng/g of tumor to 1534 ng/g of tumor (Figure 2a). The median concentration was 174 ng/g of tumor, regardless of tumor histology. No significant differences in bleomycin concentration between the BCC and SCC were determined ($p = 0.917$) (Figure 2b). The tumor complete response rate 2 months after therapy was 89% (8/9) in BCC and 80% (4/5) in SCC. There was no correlation between the volume of the tumor and the concentration determined in the punch biopsy sample (Figure 2c).

Table 3. Characteristics of patients eligible for one tumor sample collection, according to the tumor histotype, age of patients, bleomycin dose given in treatment with electrochemotherapy and tumor response after 2 months according to RECIST 1.1 criteria.

Patient No.	Gender	Age at ECT (Years)	Localization	Histology	Number of Treated Lesions	Bleomycin Dose (IU)	Tumor Response (All Tumors)	Tumor Response (Tumor with Biopsy)	Bleomycin Concentration per 1 g of Tumor (ng/g)	Tumor Volume (cm^3)
1	F	85	Skin	BCC	3	24,000	1 CR, 2 PR	PR	133	47.1
2	M	65	Skin	BCC	1	30,000	CR	CR	123	3.3
3	F	85	Skin	BCC	2	25,000	2 CR	CR	359	12.6
4 *	M	49	Skin	BCC	1	26,000	CR	CR	464	3.8
5	M	81	Skin	BCC	5	27,000	4 CR, 1 SD	CR	250	6.0
6	F	82	Skin	BCC	1	24,000	CR	CR	112	65.4
7	F	76	Skin	BCC	5	24,000	5 CR	CR	18	1.5
8	F	79	Skin	BCC	1	29,850	CR	CR	422	3.8
19	F	78	Skin	BCC	16	21,900	11 CR, 5 PR	CR	1466	30.2
10	M	76	Skin	SCC	1	27,000	CR	CR	147	2.6
11 *	M	58	Skin	SCC	6	30,000	6 CR	CR	14	19.3
12	M	85	Skin	SCC	1	24,000	CR	CR	174	4.7
13	M	62	Skin	SCC	1	26,000	CR	CR	142	0.2
14 *	M	64	Skin	SCC	7	24,750	Off study	/	1534	0.2
15 *	M	63	Skin	Melanoma	3	29,100	3 CR	CR	71	0.5
16	F	70	Skin	Angiosarcoma	1	28,650	PD	PD	819	4.0
17	M	81	Skin	Porocarcinoma	2	29,850	2 CR	CR	327	3.8
Total = 19	7 F/10 M	Median = 72.8 Range = 49–85				Mean dose = 26,535 ± 2631			Median = 174 Range = 14–1534	

BCC—basal cell carcinoma, CR—complete response, PR—partial response, SCC, squamous cell carcinoma, SD—stable disease, PD—progressive disease, * patients also eligible for blood sample collection.

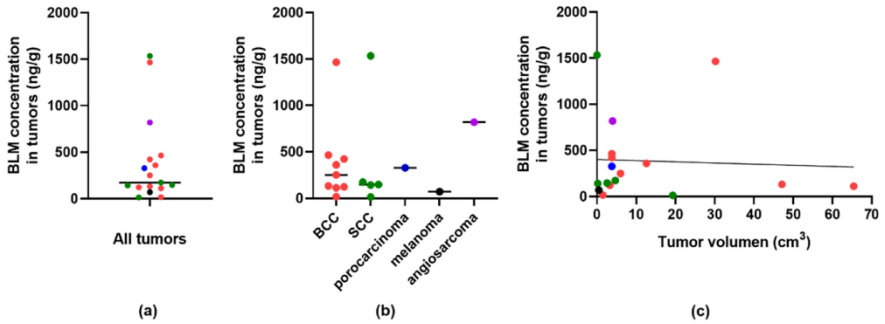


Figure 2. Median bleomycin concentrations in tumor samples. (**a**) Bleomycin (BLM) concentrations normalized to 1 g of the tumor sample in all analyzed tumors. (**b**) Bleomycin (BLM) concentrations normalized to 1 g of the tumor sample in correlation to tumor type. (**c**) Correlation of bleomycin (BLM) concentrations in tumor and tumor volume with linear curve fit analysis.

4. Discussion

This study is the first to determine the pharmacokinetic profile of bleomycin in the distribution phase after intravenous bolus injection in patients younger than 65 years. The bleomycin was eliminated from plasma with an elimination constant of 0.068 min^{-1}. The study also provides preliminary data about the minimal bleomycin concentration in tumors of 14–18 ng/g to induce complete responses of electrochemotherapy-treated tumors. Furthermore, the data also indicate that there is no significant difference in bleomycin tumor concentration between BCC and SCC tumors and no correlation between intratumoral bleomycin concentration and tumor size. Based on the plasma concentration data, a time interval for electrochemotherapy of 5–15 min after intravenous bolus bleomycin injection is recommended for patients younger than 65.

This is a preliminary study due to its limitations, such as the low number of included patients. The data on younger patients were compared to the data collected in previous study on older patients, but still within the same clinical study. This was due to slow recruitment of younger patients. Another obstacle was that in some patients, blood and tumor tissue collection was not possible, due to their physical condition or tumor size or location. To overcome these drawbacks of the study a broader multicentric study is needed as well to obtain more data on bleomycin concentrations in tumors and correlate them with tumor size and tumor type.

Our previous study determined the effective time interval for electrochemotherapy of 8–40 min after bleomycin administration in older patients [19]. The slow elimination rate of bleomycin from systemic circulation in older patients implies slow bleomycin elimination due to the physiological specificities of the older population and age-related decline in kidney function. In younger patients, i.e., less than 65 years of age, bleomycin is eliminated faster than in elderly patients. These differences in plasma concentration and elimination rate are important, since they indicate that the physiological parameters related to patient age need to be considered to ensure safe and effective treatment of electrochemotherapy using bleomycin that is given intravenously.

Can we conclude that lowering the therapeutic dose of bleomycin in electrochemotherapy in patients younger than 65 years is not indicated? The data provided in this manuscript suggest that lowering the dose might not be recommended. However, a correlation between the age and pharmacokinetics of bleomycin in different age groups is needed to confirm the indication for a lower dose. Furthermore, we would need to have a correlation between the plasma bleomycin concentration and tumor concentration, which our study could not

demonstrate. Only three patients had both data points, which is not sufficient to draw any conclusions. In the standard operating procedures, it is also stated that lowering the dose is indicated upon demonstration of impaired kidney function. Creatinine levels might not be the sole indicator of kidney impairment, especially in the elderly population, where production of creatinine is decreased due to age-related reduction in skeletal muscle mass and there would also be a need for other factors upon which the indications of lowering the dose are needed [19]. Furthermore, the study of Rotunno et al. demonstrated that lowering the dose by more than 30% could be effective in electrochemotherapy [23]. Therefore, further studies are needed to explore this possibility more in depth. Nevertheless, this study provides preliminary data on bleomycin pharmacokinetics for treatment with electrochemotherapy using intravenously administered bleomycin, and further studies can build upon these data.

Intratumoral bleomycin determination in patients treated with electrochemotherapy has not yet been performed, except for murine tumors [11]. In electrochemotherapy the bleomycin dose is so low that without electroporation it does not have antitumor effectiveness. This was demonstrated in preclinical studies and in early clinical trials as well [26,27]. To study in more detail pharmacokinetics of bleomycin in electrochemotherapy we used recently developed liquid chromatography coupled to tandem mass spectrometry method to explore the following three questions [20]. What is the minimal drug concentration in tumors for the complete response of tumors? Is there a difference in drug concentration between different tumor types? Is there a correlation between the tumor size and drug concentration? Based on the small amount of data, all three questions were partially answered. In this study, we had 17 tumor samples of predominantly BCC and SCC tumors. We determined the approximate tumor concentration of bleomycin in these two tumor types, with a median concentration of 174 ng/g of tumor. In these two tumor types, a minimal bleomycin concentration of 14–18 ng/g of tumor was needed to provide the complete response of the tumors to electrochemotherapy. However, BCC at 133 ng/g responded only partially to electrochemotherapy. Thus, contrary to the results obtained in murine tumors where the correlation between intratumoral bleomycin concentration at the time of electroporation and antitumor effectiveness was obtained, this was not confirmed in clinical samples. Further preclinical and clinical studies are needed to determine the parameters that affect the accumulation and distribution of drugs in tumors. Additionally, we did not show a correlation between bleomycin concentration in the tumor and tumor size. The concentration of bleomycin is most likely dependent on the site of punch biopsy sampling and vascularization of the tumors. Interestingly, in angiosarcoma, where the bleomycin concentration was among the highest, the tumor progressed while not responding to electrochemotherapy. This observation might be explained by the differences in vascularization and perfusion in different histological types of tumors.

In this study, we evaluated the bleomycin concentration in tumors after intravenous drug administration. However, studies on drug accumulation in tumors after intratumoral administration are needed. The drug concentration and drug distribution might be different from intravenous administration. Intratumoral drug administration is quite rare in clinical studies; however, with more evidence, it might be more frequently used. A recent study in a senior population showed that older patients can also be treated with electrochemotherapy, and in such cases, local anesthesia and intratumoral drug administration are recommended [16,22]. Other studies that address the drug distribution within tumors are also needed. To date, a suitable method has been developed for the distribution of cisplatin [28]. In that study, high spatial resolution imaging of cisplatin distribution in spheroids of tumor cells was determined using two different approaches, namely, fluorescently labeled cisplatin determined by confocal fluorescence microscopy and laser ablation isotope dilution inductively coupled plasma mass spectrometry. The results demonstrated satisfactory agreement in terms of the spatial distribution between the two methods, and the intensity of the fluorescence matched well with the concentrations of platinum obtained by laser ablation isotope dilution inductively coupled plasma mass spectrometry; thus, this

technique could be used reliably for human tumor samples. Therefore, studies comparing the pharmacodynamics of bleomycin between intravenous and intratumoral administration are needed. The needed concentrations of the drug for good antitumor effectiveness would enable better treatment approaches.

5. Conclusions

Lower plasma concentrations of bleomycin and faster elimination rate of bleomycin in patients younger than 65 years treated with electrochemotherapy than in patients older than 65 years might indicate that lowering the standard bleomycin dose of 15,000 IU intravenous bleomycin injection for electrochemotherapy is not recommended in younger patients. Based on the bleomycin plasma concentration data gathered in this study, the suggested time interval for electrochemotherapy is 5–15 min after the intravenous bleomycin injection for patients younger than 65 years.

Author Contributions: Conceptualization, G.S., M.C., A.G.; methodology, T.K., H.P.; software, M.K.; validation, A.G., M.K., K.B.; formal analysis, M.K.; investigation, A.G. and C.J., E.K., K.B.; resources, G.S., E.K.; data curation, M.B.; writing—original draft preparation, M.B. and A.G.; writing—review and editing, G.S., M.C. and E.K.; visualization, M.B., M.K.; supervision, G.S. and E.K.; project administration, G.S.; funding acquisition, G.S., M.K., E.K., T.K. All authors have read and agreed to the published version of the manuscript.

Funding: The authors acknowledge the financial support from the state budget by the Slovenian Research Agency (program no. P3-0003, P1-0143, P3-0067, P3-0307; J3-9269).

Institutional Review Board Statement: The study was conducted according to the guidelines of the Declaration of Helsinki and approved by the National Ethics Committee of the Republic of Slovenia (0120-296/2017-3) and the Regional and Institutional Review Board of Human Investigations at the University of Szeged, Hungary (4129-223/2017).

Informed Consent Statement: Written informed consent was obtained from the patients to publish this paper.

Data Availability Statement: The data presented in this study are available on request from the corresponding author. The data are not publicly available due to the privacy of the patients.

Acknowledgments: We would like to thank Mira Lavric (Institute of Oncology Ljubljana, Ljubljana, Slovenia) and Biserka Veberic (Department of Otorhinolaryngology and Cervicofacial Surgery, University Medical Centre Ljubljana) for all the valuable work they contributed to this research.

Conflicts of Interest: The authors declare no conflict of interest.

References

1. Mali, B.; Jarm, T.; Snoj, M.; Sersa, G.; Miklavcic, D. Antitumor effectiveness of electrochemotherapy: A systematic review and meta-analysis. *Eur. J. Surg. Oncol.* **2013**, *39*, 4–16. [CrossRef] [PubMed]
2. Campana, L.G.; Miklavčič, D.; Bertino, G.; Marconato, R.; Valpione, S.; Imarisio, I.; Dieci, M.V.; Granziera, E.; Cemazar, M.; Alaibac, M.; et al. Electrochemotherapy of superficial tumors—Current status: Basic principles, operating procedures, shared indications, and emerging applications. *Semin. Oncol.* **2019**, *46*, 173–191. [CrossRef] [PubMed]
3. Matthiessen, L.W.; Keshtgar, M.; Curatolo, P.; Kunte, C.; Grischke, E.-M.; Odili, J.; Muir, T.; Mowatt, D.; Clover, J.P.; Liew, S.H.; et al. Electrochemotherapy for Breast Cancer—Results From the INSPECT Database. *Clin. Breast Cancer* **2018**, *18*, e909–e917. [CrossRef] [PubMed]
4. Bertino, G.; Sersa, G.; De Terlizzi, F.; Occhini, A.; Plaschke, C.C.; Groselj, A.; Langdon, C.; Grau, J.J.; McCaul, J.A.; Heuveling, D.; et al. European Research on Electrochemotherapy in Head and Neck Cancer (EURECA) project: Results of the treatment of skin cancer. *Eur. J. Cancer* **2016**, *63*, 41–52. [CrossRef]
5. Campana, L.G.; Mali, B.; Sersa, G.; Valpione, S.; Giorgi, C.A.; Strojan, P.; Miklavcic, D.; Rossi, C.R. Electrochemotherapy in non-melanoma head and neck cancers: A retrospective analysis of the treated cases. *Br. J. Oral Maxillofac. Surg.* **2014**, *52*, 957–964. [CrossRef]
6. Clover, A.; de Terlizzi, F.; Bertino, G.; Curatolo, P.; Odili, J.; Campana, L.; Kunte, C.; Muir, T.; Brizio, M.; Sersa, G.; et al. Electrochemotherapy in the treatment of cutaneous malignancy: Outcomes and subgroup analysis from the cumulative results from the pan-European International Network for Sharing Practice in Electrochemotherapy database for 2482 lesions in 987 patients (2008–2019). *Eur. J. Cancer* **2020**, *138*, 30–40. [CrossRef]

7. Djokic, M.; Cemazar, M.; Bosnjak, M.; Dezman, R.; Badovinac, D.; Miklavcic, D.; Kos, B.; Stabuc, M.; Stabuc, B.; Jansa, R.; et al. A Prospective Phase II Study Evaluating Intraoperative Electrochemotherapy of Hepatocellular Carcinoma. *Cancers* **2020**, *12*, 3778. [CrossRef]
8. Edhemovic, I.; Brecelj, E.; Cemazar, M.; Boc, N.; Trotovsek, B.; Djokic, M.; Dezman, R.; Ivanecz, A.; Potrc, S.; Bosnjak, M.; et al. Intraoperative electrochemotherapy of colorectal liver metastases: A prospective phase II study. *Eur. J. Surg. Oncol. EJSO* **2020**, *46*, 1628–1633. [CrossRef]
9. Čemažar, M.; Miklavčič, D.; Serša, G. Intrinsic Sensitivity of Tumor Cells to Bleomycin as an Indicator of Tumor Response to Electrochemotherapy. *Jpn. J. Cancer Res.* **1998**, *89*, 328–333. [CrossRef]
10. Sedlar, A.; Dolinsek, T.; Markelc, B.; Prosen, L.; Kranjc, S.; Bosnjak, M.; Blagus, T.; Cemazar, M.; Sersa, G. Potentiation of electrochemotherapy by intramuscular IL-12 gene electrotransfer in murine sarcoma and carcinoma with different immunogenicity. *Radiol. Oncol.* **2012**, *46*, 302–311. [CrossRef]
11. Grošelj, A.; Kranjc, S.; Bosnjak, M.; Kržan, M.; Kosjek, T.; Prevc, A.; Čemažar, M.; Sersa, G. Vascularization of the tumours affects the pharmacokinetics of bleomycin and the effectiveness of electrochemotherapy. *Basic Clin. Pharmacol. Toxicol.* **2018**, *123*, 247–256. [CrossRef]
12. Ursic, K.; Kos, S.; Kamensek, U.; Cemazar, M.; Miceska, S.; Markelc, B.; Bucek, S.; Staresinic, B.; Prevodnik, V.K.; Heller, R.; et al. Potentiation of electrochemotherapy effectiveness by immunostimulation with IL-12 gene electrotransfer in mice is dependent on tumor immune status. *J. Control. Release* **2021**, *332*, 623–635. [CrossRef] [PubMed]
13. Dolinsek, T.; Prosen, L.; Cemazar, M.; Potocnik, T.; Sersa, G. Electrochemotherapy with bleomycin is effective in BRAF mutated melanoma cells and interacts with BRAF inhibitors. *Radiol. Oncol.* **2016**, *50*, 274–279. [CrossRef] [PubMed]
14. Bosnjak, M.; Jesenko, T.; Markelc, B.; Janzic, L.; Cemazar, M.; Sersa, G. PARP inhibitor olaparib has a potential to increase the effectiveness of electrochemotherapy in BRCA1 mutated breast cancer in mice. *Bioelectrochemistry* **2021**, *140*, 107832. [CrossRef] [PubMed]
15. Brezar, S.K.; Prevc, A.; Zakelj, M.N.; Brozic, A.; Cemazar, M.; Strojan, P.; Sersa, G. Synergistic effect of cisplatin chemotherapy combined with fractionated radiotherapy regimen in HPV-positive and HPV-negative experimental pharyngeal squamous cell carcinoma. *Sci. Rep.* **2020**, *10*, 1563–1569. [CrossRef]
16. Sersa, G.; Ursic, K.; Cemazar, M.; Heller, R.; Bosnjak, M.; Campana, L.G. Biological factors of the tumour response to electrochemotherapy: Review of the evidence and a research roadmap. *Eur. J. Surg. Oncol. EJSO* **2021**, *47*, 1836–1846. [CrossRef] [PubMed]
17. Hall, S.W.; Strong, J.E.; Broughton, A.; Frazier, M.L.; Benjamin, R.S. Bleomycin clinical pharmacology by radioimmunoassay. *Cancer Chemother. Pharmacol.* **1982**, *9*, 22–25. [CrossRef]
18. Alberts, D.; Chen, H.-S.; Woolfenden, J.; Moon, T.; Chang, S.; Hall, J.; Himmelstein, K.; Gross, J.; Salmon, S. Pharmacokinetics of bleomycin in man—III. Bleomycin 57Co Vs Bleomycin. *Cancer Chemother. Pharmacol.* **1979**, *3*. [CrossRef]
19. Groselj, A.; Krzan, M.; Kosjek, T.; Bosnjak, M.; Sersa, G.; Cemazar, M. Bleomycin pharmacokinetics of bolus bleomycin dose in elderly cancer patients treated with electrochemotherapy. *Cancer Chemother. Pharmacol.* **2016**, *77*, 939–947. [CrossRef]
20. Kosjek, T.; Krajnc, A.; Gornik, T.; Zigon, D.; Groselj, A.; Sersa, G.; Cemazar, M. Identification and quantification of bleomycin in serum and tumor tissue by liquid chromatography coupled to high resolution mass spectrometry. *Talanta* **2016**, *160*, 164–171. [CrossRef]
21. Jamsek, C.; Sersa, G.; Bosnjak, M.; Groselj, A. Long term response of electrochemotherapy with reduced dose of bleomycin in elderly patients with head and neck non-melanoma skin cancer. *Radiol. Oncol.* **2020**, *54*, 79–85. [CrossRef]
22. Groselj, A.; Bosnjak, M.; Strojan, P.; Krzan, M.; Cemazar, M.; Sersa, G. Efficiency of electrochemotherapy with reduced bleomycin dose in the treatment of nonmelanoma head and neck skin cancer: Preliminary results. *Head Neck* **2018**, *40*, 120–125. [CrossRef]
23. Rotunno, R.; Campana, L.G.; Quaglino, P.; De Terlizzi, F.; Kunte, C.; Odili, J.; Gehl, J.; Ribero, S.; Liew, S.; Marconato, R.; et al. Electrochemotherapy of unresectable cutaneous tumours with reduced dosages of intravenous bleomycin: Analysis of 57 patients from the International Network for Sharing Practices of Electrochemotherapy registry. *J. Eur. Acad. Dermatol. Venereol.* **2018**, *32*, 1147–1154. [CrossRef]
24. Gehl, J.; Sersa, G.; Matthiessen, L.W.; Muir, T.; Soden, D.; Occhini, A.; Quaglino, P.; Curatolo, P.; Campana, L.G.; Kunte, C.; et al. Updated standard operating procedures for electrochemotherapy of cutaneous tumours and skin metastases. *Acta Oncol.* **2018**, *57*, 874–882. [CrossRef] [PubMed]
25. Eisenhauer, E.A.; Therasse, P.; Bogaerts, J.; Schwartz, L.; Sargent, D.; Ford, R.; Dancey, J.; Arbuck, S.; Gwyther, S.; Mooney, M.; et al. New response evaluation criteria in solid tumours: Revised RECIST guideline (version 1.1). *Eur. J. Cancer* **2009**, *45*, 228–247. [CrossRef] [PubMed]
26. Byrne, C.M.; Thompson, J.; Johnston, H.; Hersey, P.; Quinn, M.J.; Hughes, T.; McCarthy, W.H. Treatment of metastatic melanoma using electroporation therapy with bleomycin (electrochemotherapy). *Melanoma Res.* **2005**, *15*, 45–51. [CrossRef]
27. Sersa, G.; Kotnik, V.; Čemažar, M.; Miklavčič, D.; Kotnik, A. Electrochemotherapy with bleomycin in SA-1 tumor-bearing mice—Natural resistance and immune responsiveness. *Anti-Cancer Drugs* **1996**, *7*, 785–791. [CrossRef]
28. Marković, S.; Uršič, K.; Cemazar, M.; Sersa, G.; Starešinič, B.; Milačič, R.; Ščančar, J. High spatial resolution imaging of cisplatin and Texas Red cisplatin in tumour spheroids using laser ablation isotope dilution inductively coupled plasma mass spectrometry and confocal fluorescence microscopy. *Anal. Chim. Acta* **2021**, *1162*, 338424. [CrossRef] [PubMed]

Chapter 4

Conclusions and Future Perspectives

The state of the art in analytical sciences shows a persistent gap in the detection and characterization of highly polar compounds. While reversed-phase chromatography continues to dominate LC–MS workflows, its physicochemical properties inherently limit access to the most hydrophilic domain of chemical space. However, many human metabolites, environmental contaminants, clinically relevant pharmaceuticals, and other organic compounds (not specifically addressed in this thesis) fall precisely within this polarity range. Over the past decade, HILIC has emerged as a complementary solution that allows for the expansion of analytical coverage and is being widely implemented, although its performance remains strongly method-dependent and sensitive to operational conditions. Its routine implementation still lags behind its demonstrated analytical capability despite increasing interest. The full analytical potential of HILIC therefore remains underexploited in practice, particularly in complex real-world studies where broad polarity coverage is essential. The main contribution of this thesis is the systematic demonstration of how the chemical space coverage of LC-MS-based analytical workflows can be significantly expanded towards polar chemical space by integrating HILIC-based analyses. Presenting both targeted and untargeted applications, this work shows that HILIC serves as a versatile chromatographic strategy with broad applicability—including, but not limited to, metabolomics, exposure science, and pharmacotherapy—the domains specifically explored in this thesis. By addressing method development, validation, QC procedures, and data processing considerations, the thesis provides a practical foundation that can be adapted to diverse analytical studies involving polar compounds.

Novel contributions to science from this research were reported in four first-author publications and presented at three international conferences. The publications address key analytical challenges associated with hydrophilic compounds, demonstrated through the developments and applications of HILIC-based methods in biological, environmental, and pharmaceutical contexts. The specific novel contributions can be summarized as follows:

(i) Development of a complete non-targeted LC–HRMS exposure science workflow for urine samples, encompassing sample preparation, RP and HILIC instrumental analysis, data processing, and annotation procedures. The workflow is designed specifically for non-targeted screening of biomarkers of exposure and is characterized and validated to the extent feasible for a non-targeted method.

(ii) Application of the developed urine NTS workflow to a cohort of women with ovarian cancer, resulting in the annotation of BoEs that differ between diseased and control groups.

(iii) Integrated metabolomic and exposure-oriented non-targeted study in a PCOS cohort, combining complementary RP/HILIC serum metabolomics with exposure biomarker screening in matched samples, demonstrating chromatographic complementarity and

revealing both metabolomic and exposure-related differences between PCOS patients and healthy controls, thereby providing further empirical support for the combined use of RP and HILIC in complex biological studies.

(iv) Development and validation of highly sensitive analytical methods for quantification of bleomycin in multiple biological matrices (serum, plasma, and cell lines), achieving lower limits of quantification than previously reported and addressing analytical challenges specific to highly polar, structurally complex, and metal-complexing analytes.

(v) Systematic treatment of QA/QC and validation challenges for complex polar analytes in the absence of certified reference materials, using bleomycin as a case study to propose practical, transferable strategies for assessing accuracy, precision, and long-term method performance under constrained conditions.

Among these contributions, the findings most likely to generalize beyond the individual applications are the demonstrated complementarity of RP and HILIC for extending accessible chemical space, the workflow-level principles for incorporating HILIC into non-targeted analyses, systematic application and discussion of QA/QC strategies developed for analytically challenging compounds under conditions in which conventional reference materials are unavailable. These are not restricted to the biological matrices, cohorts, or analytes examined here and can be adapted to other studies in which highly polar compounds represent an analytically relevant part of the chemical space.

Adding HILIC to non-targeted workflows extends accessible chemical space, particularly toward highly polar analytes, but at the cost of greater analytical and computational complexity. In the workflows investigated here, dual RP/HILIC analysis approximately doubled primary LC–MS acquisition time and the number of raw data files, while also requiring separate preprocessing, QC evaluation, feature filtering, and annotation. In the presented urinary exposure-screening application, addition of HILIC resulted in 28% increase in coverage compared with RP alone. This value is specific to the investigated matrix, workflow, and chemical space and should therefore be considered an illustrative example rather than a generally expected gain from adding HILIC. Dual RP/HILIC analysis is therefore not necessarily warranted for every study. Its implementation should depend on whether the additional chemical-space coverage justifies the associated increase in analytical effort and data-processing complexity.

Future work should focus on simplifying and standardizing workflows designed for broad polarity coverage to facilitate their routine application and reduce the additional analytical burden associated with dual-mode analysis. At the same time, the trade-off between additional coverage and resource requirements should be evaluated for the specific analytical objective. Dual RP/HILIC analysis is particularly justified in initial exploratory or non-targeted screening, where relevant analytes may not yet be known and broad chemical-space coverage is desirable. Once compounds or compound classes of interest have been identified, subsequent targeted, validation, or routine studies can be streamlined by selecting the chromatographic mode best suited to those analytes.

Established complementary techniques such as capillary electrophoresis–MS, ion chromatography–MS, and supercritical fluid chromatography–MS should also be considered, as they may extend analytical access to compound classes that remain insufficiently represented even in combined RP/HILIC workflows. Their integration into exposure biomarker screening deserves systematic evaluation, particularly for analytes located at polarity extremes or exhibiting poor retention under conventional LC conditions.

While these perspectives concern broad analytical coverage in screening workflows, highly polar compounds also remain analytically demanding in targeted applications, particularly when ultra-trace quantification is required. This was also evident in the

bleomycin-focused part of this thesis, where substantial sensitivity improvements were achieved through dedicated sample preparation and LC–MS/MS optimization, yet the lower limits of quantification remained above the levels required for some experimentally relevant intracellular concentrations. In the case of bleomycin (or other heteroatom-rich or metal-complexing analytes), coupling LC separations with element-selective detection (e.g. ICP-MS) could represent a viable strategy, particularly because the metal-associated signal can be monitored independently of molecular ionization efficiency. This approach could provide better selectivity and robustness in cases where ESI-based detection is compromised by ion suppression or complexation equilibria. Its applicability, however, depends on stable and well-defined metal speciation throughout sample preparation and chromatographic separation.

Taken together, these perspectives indicate that further progress in polar analysis will depend both on broader methodological integration and on analyte-specific solutions for particularly demanding compounds. Overall, this thesis demonstrates that expanding the analytical reach toward polar chemical space is both feasible and scientifically valuable. By showing how HILIC-based LC–MS can be deployed across metabolomics, exposomics, and pharmacotherapy, the work provides a practical contribution to the field and lays the groundwork for future analyses that demand broader and more representative chemical coverage.

References

[1] L. Ruddigkeit, R. van Deursen, L. C. Blum, and J.-L. Reymond, "Enumeration of 166 Billion Organic Small Molecules in the Chemical Universe Database GDB-17," *J. Chem. Inf. Model.*, vol. 52, no. 11, pp. 2864–2875, Nov. 2012, doi: 10.1021/ci300415d.

[2] T. Hulleman, V. Turkina, J. W. O'Brien, A. Chojnacka, K. V. Thomas, and S. Samanipour, "Critical Assessment of the Chemical Space Covered by LC–HRMS Non-Targeted Analysis," *Environ. Sci. Technol.*, vol. 57, no. 38, pp. 14101–14112, Sep. 2023, doi: 10.1021/acs.est.3c03606.

[3] G. Black *et al.*, "Exploring chemical space in non-targeted analysis: a proposed ChemSpace tool," *Anal. Bioanal. Chem.*, vol. 415, no. 1, pp. 35–44, Jan. 2023, doi: 10.1007/s00216-022-04434-4.

[4] M. Krauss, H. Singer, and J. Hollender, "LC–high resolution MS in environmental analysis: from target screening to the identification of unknowns," *Anal. Bioanal. Chem.*, vol. 397, no. 3, pp. 943–951, Jun. 2010, doi: 10.1007/s00216-010-3608-9.

[5] E. Schymanski *et al.*, "Identifying Small Molecules via High Resolution Mass Spectrometry: Communicating Confidence," *Environ. Sci. Technol.*, vol. 48, Jan. 2014, doi: 10.1021/es5002105.

[6] Q. Hu, H. Tang, and Y. Wang, "Challenges in Analysis of Hydrophilic Metabolites Using Chromatography Coupled with Mass Spectrometry," *J. Anal. Test.*, vol. 4, no. 3, pp. 140–162, Jul. 2020, doi: 10.1007/s41664-020-00126-z.

[7] D. S. Wishart, "Emerging applications of metabolomics in drug discovery and precision medicine," *Nat. Rev. Drug Discov.*, vol. 15, no. 7, pp. 473–484, Jul. 2016, doi: 10.1038/nrd.2016.32.

[8] T. Kosjek *et al.*, "Identification and quantification of bleomycin in serum and tumor tissue by liquid chromatography coupled to high resolution mass spectrometry," *Talanta*, vol. 160, pp. 164–171, Nov. 2016, doi: 10.1016/j.talanta.2016.06.062.

[9] O. Salamin, L. Ramic, R. Nicoli, S. Rudaz, D. Guillarme, and T. Kuuranne, "Identification of Candidate Blood Biomarkers of Recombinant Human Erythropoietin Administration Using Targeted Polar Metabolomics by HILIC-MS/MS," *Drug Test. Anal.*, vol. 17, no. 12, pp. 2323–2332, 2025, doi: 10.1002/dta.3943.

[10] D.-Q. Tang, L. Zou, X.-X. Yin, and C. N. Ong, "HILIC-MS for metabolomics: An attractive and complementary approach to RPLC-MS," *Mass Spectrom. Rev.*, vol. 35, no. 5, pp. 574–600, 2016, doi: 10.1002/mas.21445.

[11] Y. Kawachi, T. Ikegami, H. Takubo, Y. Ikegami, M. Miyamoto, and N. Tanaka, "Chromatographic characterization of hydrophilic interaction liquid

chromatography stationary phases: hydrophilicity, charge effects, structural selectivity, and separation efficiency," *J. Chromatogr. A*, vol. 1218, no. 35, pp. 5903–5919, Sep. 2011, doi: 10.1016/j.chroma.2011.06.048.

[12] A. J. Alpert, "Hydrophilic-interaction chromatography for the separation of peptides, nucleic acids and other polar compounds," *J. Chromatogr. A*, vol. 499, pp. 177–196, Jan. 1990, doi: 10.1016/S0021-9673(00)96972-3.

[13] Y. Guo, "Recent progress in the fundamental understanding of hydrophilic interaction chromatography (HILIC)," *The Analyst*, vol. 140, no. 19, pp. 6452–6466, Oct. 2015, doi: 10.1039/c5an00670h.

[14] P. Jandera, "Stationary and mobile phases in hydrophilic interaction chromatography: a review," *Anal. Chim. Acta*, vol. 692, no. 1, pp. 1–25, Apr. 2011, doi: 10.1016/j.aca.2011.02.047.

[15] C. Kulsing *et al.*, "Insights into the Origin of the Separation Selectivity with Silica Hydride Adsorbents," *J. Phys. Chem. B*, vol. 119, no. 7, pp. 3063–3069, Feb. 2015, doi: 10.1021/jp5103753.

[16] P. Hemström and K. Irgum, "Hydrophilic interaction chromatography," *J. Sep. Sci.*, vol. 29, no. 12, pp. 1784–1821, 2006, doi: 10.1002/jssc.200600199.

[17] M. Flasch, V. Fitz, E. Rampler, C. N. Ezekiel, G. Koellensperger, and B. Warth, "Integrated Exposomics/Metabolomics for Rapid Exposure and Effect Analyses," *JACS Au*, vol. 2, no. 11, pp. 2548–2560, Nov. 2022, doi: 10.1021/jacsau.2c00433.

[18] K. A. Dill, "The mechanism of solute retention in reversed-phase liquid chromatography," *J. Phys. Chem.*, vol. 91, no. 7, pp. 1980–1988, Mar. 1987, doi: 10.1021/j100291a060.

[19] J. L. Rafferty, L. Zhang, J. I. Siepmann, and M. R. Schure, "Retention mechanism in reversed-phase liquid chromatography: a molecular perspective," *Anal. Chem.*, vol. 79, no. 17, pp. 6551–6558, Sep. 2007, doi: 10.1021/ac0705115.

[20] Y. Guo, D. Baran, and L. Ryan, "Quantitative Assessment of Retention Mechanisms for Ionized Compounds in Hydrophilic Interaction Chromatography (HILIC)," *Anal. Chem.*, vol. 97, no. 7, pp. 4057–4065, Feb. 2025, doi: 10.1021/acs.analchem.4c05880.

[21] T. Hanai, "Definition of HILIC System and Quantitative Analysis of Retention Mechanisms," *Curr. Chromatogr.*, vol. 5, no. 1, pp. 43–52, doi: 10.2174/2213240605666180207093716.

[22] Y. Guo, "A survey of polar stationary phases for hydrophilic interaction chromatography and recent progress in understanding retention and selectivity," *Biomed. Chromatogr.*, vol. 36, no. 4, p. e5332, 2022, doi: 10.1002/bmc.5332.

[23] H. A. Al Saoud, M. Szumski, M. Sprynskyy, S. Bocian, and B. Buszewski, "Biosilica as a New Stationary Phase in HILIC Mode," *Chromatographia*, vol. 86, no. 10, pp. 641–647, Oct. 2023, doi: 10.1007/s10337-023-04275-y.

[24] M. A. Guarducci, A. Fochetti, A. Ciogli, and G. Mazzoccanti, "A Compendium of the Principal Stationary Phases Used in Hydrophilic Interaction Chromatography: Where Have We Arrived?," *Separations*, vol. 10, no. 1, p. 22, Jan. 2023, doi: 10.3390/separations10010022.

[25] J. C. Linden and C. L. Lawhead, "Liquid chromatography of saccharides," *J. Chromatogr. A*, vol. 105, no. 1, pp. 125–133, Feb. 1975, doi: 10.1016/S0021-9673(01)81096-7.

[26] B. Buszewski and S. Noga, "Hydrophilic interaction liquid chromatography (HILIC)—a powerful separation technique," *Anal. Bioanal. Chem.*, vol. 402, no. 1, pp. 231–247, 2012, doi: 10.1007/s00216-011-5308-5.

[27] P. Bonini, T. Kind, H. Tsugawa, D. K. Barupal, and O. Fiehn, "Retip: Retention Time Prediction for Compound Annotation in Untargeted Metabolomics," *Anal. Chem.*, vol. 92, no. 11, pp. 7515–7522, Jun. 2020, doi: 10.1021/acs.analchem.9b05765.

[28] J. Ruta, S. Rudaz, D. V. McCalley, J.-L. Veuthey, and D. Guillarme, "A systematic investigation of the effect of sample diluent on peak shape in hydrophilic interaction liquid chromatography," *J. Chromatogr. A*, vol. 1217, no. 52, pp. 8230–8240, Dec. 2010, doi: 10.1016/j.chroma.2010.10.106.

[29] J. K. Nicholson, J. C. Lindon, and E. Holmes, "'Metabonomics': understanding the metabolic responses of living systems to pathophysiological stimuli via multivariate statistical analysis of biological NMR spectroscopic data," *Xenobiotica Fate Foreign Compd. Biol. Syst.*, vol. 29, no. 11, pp. 1181–1189, Nov. 1999, doi: 10.1080/004982599238047.

[30] G. J. Patti, O. Yanes, and G. Siuzdak, "Metabolomics: the apogee of the omics trilogy," *Nat. Rev. Mol. Cell Biol.*, vol. 13, no. 4, pp. 263–269, Apr. 2012, doi: 10.1038/nrm3314.

[31] O. Fiehn, "Metabolomics--the link between genotypes and phenotypes," *Plant Mol. Biol.*, vol. 48, no. 1–2, pp. 155–171, Jan. 2002.

[32] A. V. Aderemi, A. O. Ayeleso, O. O. Oyedapo, and E. Mukwevho, "Metabolomics: A Scoping Review of Its Role as a Tool for Disease Biomarker Discovery in Selected Non-Communicable Diseases," *Metabolites*, vol. 11, no. 7, p. 418, Jun. 2021, doi: 10.3390/metabo11070418.

[33] C. H. Johnson, J. Ivanisevic, and G. Siuzdak, "Metabolomics: beyond biomarkers and towards mechanisms," *Nat. Rev. Mol. Cell Biol.*, vol. 17, no. 7, pp. 451–459, Jul. 2016, doi: 10.1038/nrm.2016.25.

[34] C. P. Wild, "Complementing the genome with an 'exposome': the outstanding challenge of environmental exposure measurement in molecular epidemiology," *Cancer Epidemiol. Biomark. Prev. Publ. Am. Assoc. Cancer Res. Cosponsored Am. Soc. Prev. Oncol.*, vol. 14, no. 8, pp. 1847–1850, Aug. 2005, doi: 10.1158/1055-9965.EPI-05-0456.

[35] X. Han and R. W. Gross, "Global analyses of cellular lipidomes directly from crude extracts of biological samples by ESI mass spectrometry: a bridge to lipidomics," *J. Lipid Res.*, vol. 44, no. 6, pp. 1071–1079, Jun. 2003, doi: 10.1194/jlr.R300004-JLR200.

[36] J. Szpunar, "Metallomics: a new frontier in analytical chemistry," *Anal. Bioanal. Chem.*, vol. 378, no. 1, pp. 54–56, Jan. 2004, doi: 10.1007/s00216-003-2333-z.

[37] S. Alseekh *et al.*, "Mass spectrometry-based metabolomics: a guide for annotation, quantification and best reporting practices," *Nat. Methods*, vol. 18, no. 7, pp. 747–756, Jul. 2021, doi: 10.1038/s41592-021-01197-1.

[38] C. Martias *et al.*, "Optimization of Sample Preparation for Metabolomics Exploration of Urine, Feces, Blood and Saliva in Humans Using Combined NMR and UHPLC-HRMS Platforms," *Molecules*, vol. 26, no. 14, p. 4111, Jul. 2021, doi: 10.3390/molecules26144111.

[39] A. B. Eshawu, T. J. Gunda, B. Kumar, and S. Matta, "Advancements in sample preparation and extraction techniques for metabolomic analysis of animal fluids," *Microchem. J.*, vol. 218, p. 115259, Nov. 2025, doi: 10.1016/j.microc.2025.115259.

[40] H. Gika and G. Theodoridis, "Sample Preparation Prior to The LC–MS-Based Metabolomics/Metabonomics of Blood-Derived Samples," *Bioanalysis*, vol. 3, no. 14, pp. 1647–1661, Jul. 2011, doi: 10.4155/bio.11.122.

[41] S. Naz, D. C. Moreira dos Santos, A. García, and C. Barbas, "Analytical Protocols Based on LC–MS, GC–MS and CE–MS for Nontargeted Metabolomics of Biological Tissues," *Bioanalysis*, vol. 6, no. 12, pp. 1657–1677, Jun. 2014, doi: 10.4155/bio.14.119.

[42] J. Sarkar, R. Singh, and S. Chandel, "Understanding LC/MS-Based Metabolomics: A Detailed Reference for Natural Product Analysis," *PROTEOMICS – Clin. Appl.*, vol. 19, no. 1, p. e202400048, 2025, doi: 10.1002/prca.202400048.

[43] S. Rakusanova and T. Cajka, "Tips and tricks for LC–MS-based metabolomics and lipidomics analysis," *TrAC Trends Anal. Chem.*, vol. 180, p. 117940, Nov. 2024, doi: 10.1016/j.trac.2024.117940.

[44] B. Zhou, J. F. Xiao, L. Tuli, and H. W. Ressom, "LC-MS-based metabolomics," *Mol. Biosyst.*, vol. 8, no. 2, pp. 470–481, Feb. 2012, doi: 10.1039/c1mb05350g.

[45] D. Vuckovic and J. Pawliszyn, "Systematic Evaluation of Solid-Phase Microextraction Coatings for Untargeted Metabolomic Profiling of Biological Fluids by Liquid Chromatography−Mass Spectrometry," *Anal. Chem.*, vol. 83, no. 6, pp. 1944–1954, Mar. 2011, doi: 10.1021/ac102614v.

[46] C. D. Broeckling *et al.*, "Current Practices in LC-MS Untargeted Metabolomics: A Scoping Review on the Use of Pooled Quality Control Samples," *Anal. Chem.*, vol. 95, no. 51, pp. 18645–18654, Dec. 2023, doi: 10.1021/acs.analchem.3c02924.

[47] C. Coman, F. A. Solari, A. Hentschel, A. Sickmann, R. P. Zahedi, and R. Ahrends, "Simultaneous Metabolite, Protein, Lipid Extraction (SIMPLEX): A Combinatorial Multimolecular Omics Approach for Systems Biology *," *Mol. Cell. Proteomics*, vol. 15, no. 4, pp. 1435–1466, Apr. 2016, doi: 10.1074/mcp.M115.053702.

[48] R. A. Zenati *et al.*, "Evaluation of Two Simultaneous Metabolomic and Proteomic Extraction Protocols Assessed by Ultra-High-Performance Liquid Chromatography Tandem Mass Spectrometry," *Int. J. Mol. Sci.*, vol. 24, no. 2, p. 1354, Jan. 2023, doi: 10.3390/ijms24021354.

[49] F. M. Geier, E. J. Want, A. M. Leroi, and J. G. Bundy, "Cross-Platform Comparison of Caenorhabditis elegans Tissue Extraction Strategies for Comprehensive Metabolome Coverage," *Anal. Chem.*, vol. 83, no. 10, pp. 3730–3736, May 2011, doi: 10.1021/ac2001109.

[50] C. Gonzalez-Riano, A. Garcia, and C. Barbas, "Metabolomics studies in brain tissue: A review," *J. Pharm. Biomed. Anal.*, vol. 130, pp. 141–168, Oct. 2016, doi: 10.1016/j.jpba.2016.07.008.

[51] J. D. Mosley *et al.*, "Metabolomics 2023 workshop report: moving toward consensus on best QA/QC practices in LC–MS-based untargeted metabolomics," *Metabolomics*, vol. 20, no. 4, p. 73, Jul. 2024, doi: 10.1007/s11306-024-02135-w.

[52] C.-J. Chen, D.-Y. Lee, J. Yu, Y.-N. Lin, and T.-M. Lin, "Recent advances in LC-MS-based metabolomics for clinical biomarker discovery," *Mass Spectrom. Rev.*, vol. 42, no. 6, pp. 2349–2378, 2023, doi: 10.1002/mas.21785.

[53] J. Sun and Y. Xia, "Pretreating and normalizing metabolomics data for statistical analysis," *Genes Dis.*, vol. 11, no. 3, p. 100979, May 2024, doi: 10.1016/j.gendis.2023.04.018.

[54] C. J. Sands *et al.*, "Representing the Metabolome with High Fidelity: Range and Response as Quality Control Factors in LC-MS-Based Global Profiling," *Anal. Chem.*, vol. 93, no. 4, pp. 1924–1933, Feb. 2021, doi: 10.1021/acs.analchem.0c03848.

[55] D. S. Wishart *et al.*, "HMDB 5.0: the Human Metabolome Database for 2022," *Nucleic Acids Res.*, vol. 50, no. D1, pp. D622–D631, Jan. 2022, doi: 10.1093/nar/gkab1062.

[56] R. Schmid *et al.*, "Integrative analysis of multimodal mass spectrometry data in MZmine 3," *Nat. Biotechnol.*, vol. 41, no. 4, pp. 447–449, Apr. 2023, doi: 10.1038/s41587-023-01690-2.

[57] S. Grijseels, T. Vasskog, P. J. Heinsvig, T. N. Myhre, T. Hansen, and M. Mardal, "Validation of two LCHRMS methods for large-scale untargeted metabolomics of serum samples: Strategy to establish method fitness-for-purpose," *J. Chromatogr. A*, vol. 1732, p. 465230, Sep. 2024, doi: 10.1016/j.chroma.2024.465230.

[58] W.-C. Wang, N. Amini, C. Huber, M. Kull, and A. Kruve, "Active Learning Improves Ionization Efficiency Predictions and Quantification in Nontargeted LC/HRMS," *Anal. Chem.*, vol. 97, no. 25, pp. 13131–13139, Jul. 2025, doi: 10.1021/acs.analchem.5c00816.

[59] H. G. Gika, G. A. Theodoridis, and I. D. Wilson, "Hydrophilic interaction and reversed-phase ultra-performance liquid chromatography TOF-MS for metabonomic analysis of Zucker rat urine," *J. Sep. Sci.*, vol. 31, no. 9, pp. 1598–1608, May 2008, doi: 10.1002/jssc.200700644.

[60] H. Idborg, L. Zamani, P.-O. Edlund, I. Schuppe-Koistinen, and S. P. Jacobsson, "Metabolic fingerprinting of rat urine by LC/MS: Part 1. Analysis by hydrophilic interaction liquid chromatography–electrospray ionization mass spectrometry," *J. Chromatogr. B*, vol. 828, no. 1, pp. 9–13, Dec. 2005, doi: 10.1016/j.jchromb.2005.07.031.

[61] M. Navarro-Reig, J. Jaumot, A. Baglai, G. Vivó-Truyols, P. J. Schoenmakers, and R. Tauler, "Untargeted Comprehensive Two-Dimensional Liquid Chromatography Coupled with High-Resolution Mass Spectrometry Analysis of Rice Metabolome Using Multivariate Curve Resolution," *Anal. Chem.*, vol. 89, no. 14, pp. 7675–7683, Jul. 2017, doi: 10.1021/acs.analchem.7b01648.

[62] W. Shi *et al.*, "Integrative serum metabolomic analysis for preventive effects of Yaobitong capsule in adjuvant-induced rheumatoid arthritis rat based on RP/HILIC-UHPLC-Q-TOF MS," *Anal. Biochem.*, vol. 637, p. 114474, Jan. 2022, doi: 10.1016/j.ab.2021.114474.

[63] X. Yuan *et al.*, "Integrated metabolomic analysis for intervention effects of Gushudan on glucocorticoid-induced osteoporostic rat plasma based on RP/HILIC-UHPLC-Q-Orbitrap HRMS," *Anal. Biochem.*, vol. 591, p. 113559, Feb. 2020, doi: 10.1016/j.ab.2019.113559.

[64] E. Rampler, H. Schoeny, B. M. Mitic, Y. E. Abiead, M. Schwaiger, and G. Koellensperger, "Simultaneous non-polar and polar lipid analysis by on-line combination of HILIC, RP and high resolution MS," *Analyst*, vol. 143, no. 5, pp. 1250–1258, 2018, doi: 10.1039/C7AN01984J.

[65] "Eurostat, 2024." Accessed: Jan. 12, 2026. [Online]. Available: https://ec.europa.eu/eurostat/statistics-explained/index.php?title=Chemicals_production_and_consumption_statistics

[66] S. M. Rappaport, "Genetic Factors Are Not the Major Causes of Chronic Diseases," *PLOS ONE*, vol. 11, no. 4, p. e0154387, Apr. 2016, doi: 10.1371/journal.pone.0154387.

[67] G. W. Miller and D. P. Jones, "The nature of nurture: refining the definition of the exposome," *Toxicol. Sci. Off. J. Soc. Toxicol.*, vol. 137, no. 1, pp. 1–2, Jan. 2014, doi: 10.1093/toxsci/kft251.

[68] N. Brucker, S. N. do Nascimento, L. Bernardini, M. F. Charão, and S. C. Garcia, "Biomarkers of exposure, effect, and susceptibility in occupational exposure to traffic-related air pollution: A review," *J. Appl. Toxicol. JAT*, vol. 40, no. 6, pp. 722–736, Jun. 2020, doi: 10.1002/jat.3940.

[69] L. Gilles *et al.*, "HBM4EU combines and harmonises human biomonitoring data across the EU, building on existing capacity - The HBM4EU survey," *Int. J. Hyg. Environ. Health*, vol. 237, p. 113809, Aug. 2021, doi: 10.1016/j.ijheh.2021.113809.

[70] "The European Human Biomonitoring Initiative (HBM4EU): Human biomonitoring guidance values for selected phthalates and a substitute plasticizer - ScienceDirect." Accessed: Aug. 22, 2024. [Online]. Available: https://www.sciencedirect.com/science/article/pii/S1438463921000377

[71] P. Marx-Stoelting *et al.*, "A walk in the PARC: developing and implementing 21st century chemical risk assessment in Europe," *Arch. Toxicol.*, vol. 97, no. 3, pp. 893–908, Mar. 2023, doi: 10.1007/s00204-022-03435-7.

[72] M. Pourchet *et al.*, "Suspect and non-targeted screening of chemicals of emerging concern for human biomonitoring, environmental health studies and support to risk assessment: From promises to challenges and harmonisation issues," *Environ. Int.*, vol. 139, p. 105545, Jun. 2020, doi: 10.1016/j.envint.2020.105545.

[73] J. Feldmann, H. R. Hansen, T. M. Karlsson, and J. H. Christensen, "ICP-MS As a Contributing Tool to Nontarget Screening (NTS) Analysis for Environmental Monitoring," *Environ. Sci. Technol.*, vol. 58, no. 29, pp. 12755–12762, Jul. 2024, doi: 10.1021/acs.est.4c00504.

[74] K. E. Manz *et al.*, "Non-targeted analysis (NTA) and suspect screening analysis (SSA): a review of examining the chemical exposome," *J. Expo. Sci. Environ. Epidemiol.*, vol. 33, no. 4, pp. 524–536, Jul. 2023, doi: 10.1038/s41370-023-00574-6.

[75] P. Tolani, S. Gupta, K. Yadav, S. Aggarwal, and A. K. Yadav, "Chapter Four - Big data, integrative omics and network biology," in *Advances in Protein Chemistry and Structural Biology*, vol. 127, R. Donev and T. Karabencheva-Christova, Eds., in Proteomics and Systems Biology, vol. 127. , Academic Press, 2021, pp. 127–160. doi: 10.1016/bs.apcsb.2021.03.006.

[76] J. Arrebola *et al.*, "Adipose tissue concentrations of persistent organic pollutants and prevalence of type 2 diabetes in adults from Southern Spain," *Environ. Res.*, vol. 122, Jan. 2013, doi: 10.1016/j.envres.2012.12.001.

[77] G. V. Iyengar and A. Rapp, "Human placenta as a 'dual' biomarker for monitoring fetal and maternal environment with special reference to potentially toxic trace elements. Part 3: Toxic trace elements in placenta and placenta as a biomarker for these elements," *Sci. Total Environ.*, vol. 280, no. 1, pp. 221–238, Dec. 2001, doi: 10.1016/S0048-9697(01)00827-0.

[78] Y. Gu, J. T. Peach, and B. Warth, "Sample preparation strategies for mass spectrometry analysis in human exposome research: Current status and future perspectives," *TrAC Trends Anal. Chem.*, vol. 166, p. 117151, Sep. 2023, doi: 10.1016/j.trac.2023.117151.

[79] M. Musatadi *et al.*, "The role of sample preparation in suspect and non-target screening for exposome analysis using human urine," *Chemosphere*, vol. 339, p. 139690, Oct. 2023, doi: 10.1016/j.chemosphere.2023.139690.

[80] E. L. Schymanski and S. Neumann, "The Critical Assessment of Small Molecule Identification (CASMI): Challenges and Solutions," *Metabolites*, vol. 3, no. 3, pp. 517–538, Jun. 2013, doi: 10.3390/metabo3030517.

[81] E. Eckert, H. Drexler, and T. Göen, "Determination of six hydroxyalkyl mercapturic acids in human urine using hydrophilic interaction liquid chromatography with tandem mass spectrometry (HILIC-ESI-MS/MS)," *J. Chromatogr. B Analyt. Technol. Biomed. Life. Sci.*, vol. 878, no. 27, pp. 2506–2514, Oct. 2010, doi: 10.1016/j.jchromb.2009.09.003.

[82] K. Sterz, G. Scherer, J. Krumsiek, F. J. Theis, and J. Ecker, "Identification and quantification of 1-hydroxybutene-2-yl mercapturic acid in human urine by UPLC-HILIC-MS/MS as a novel biomarker for 1,3-butadiene exposure," *Chem. Res. Toxicol.*, vol. 25, no. 8, pp. 1565–1567, Aug. 2012, doi: 10.1021/tx3002862.

[83] R. Jagani *et al.*, "Multiclass Assays for Measuring Environmental Chemical Mixture Exposure: Analytical Methodologies and Applications in Exposomics Research," *Metabolites*, vol. 15, no. 11, p. 742, Nov. 2025, doi: 10.3390/metabo15110742.

[84] H. L. Röst *et al.*, "OpenMS: a flexible open-source software platform for mass spectrometry data analysis," *Nat. Methods*, vol. 13, no. 9, pp. 741–748, Sep. 2016, doi: 10.1038/nmeth.3959.

[85] C. A. Smith, E. J. Want, G. O'Maille, R. Abagyan, and G. Siuzdak, "XCMS: Processing Mass Spectrometry Data for Metabolite Profiling Using Nonlinear Peak

Alignment, Matching, and Identification," *Anal. Chem.*, vol. 78, no. 3, pp. 779–787, Feb. 2006, doi: 10.1021/ac051437y.

[86] H. Tsugawa *et al.*, "A lipidome atlas in MS-DIAL 4," *Nat. Biotechnol.*, vol. 38, no. 10, pp. 1159–1163, Oct. 2020, doi: 10.1038/s41587-020-0531-2.

[87] L. L. Hohrenk, F. Itzel, N. Baetz, J. Tuerk, M. Vosough, and T. C. Schmidt, "Comparison of Software Tools for Liquid Chromatography–High-Resolution Mass Spectrometry Data Processing in Nontarget Screening of Environmental Samples," *Anal. Chem.*, vol. 92, no. 2, pp. 1898–1907, Jan. 2020, doi: 10.1021/acs.analchem.9b04095.

[88] S. Lennon *et al.*, "Harmonized quality assurance/quality control provisions to assess completeness and robustness of MS1 data preprocessing for LC-HRMS-based suspect screening and non-targeted analysis," *TrAC Trends Anal. Chem.*, vol. 174, p. 117674, May 2024, doi: 10.1016/j.trac.2024.117674.

[89] A. Rafiei and L. Sleno, "Comparison of peak-picking workflows for untargeted liquid chromatography/high-resolution mass spectrometry metabolomics data analysis," *Rapid Commun. Mass Spectrom.*, vol. 29, no. 1, pp. 119–127, 2015, doi: 10.1002/rcm.7094.

[90] H. Hupatz, I. Rahu, W.-C. Wang, P. Peets, E. H. Palm, and A. Kruve, "Critical review on in silico methods for structural annotation of chemicals detected with LC/HRMS non-targeted screening," *Anal. Bioanal. Chem.*, vol. 417, no. 3, pp. 473–493, Jan. 2025, doi: 10.1007/s00216-024-05471-x.

[91] H. Oberacher, V. Reinstadler, M. Kreidl, M. A. Stravs, J. Hollender, and E. L. Schymanski, "Annotating Nontargeted LC-HRMS/MS Data with Two Complementary Tandem Mass Spectral Libraries," *Metabolites*, vol. 9, no. 1, p. 3, Dec. 2018, doi: 10.3390/metabo9010003.

[92] R. Chaleckis, I. Meister, P. Zhang, and C. E. Wheelock, "Challenges, progress and promises of metabolite annotation for LC–MS-based metabolomics," *Curr. Opin. Biotechnol.*, vol. 55, pp. 44–50, Feb. 2019, doi: 10.1016/j.copbio.2018.07.010.

[93] A. David *et al.*, "Towards a comprehensive characterisation of the human internal chemical exposome: Challenges and perspectives," *Environ. Int.*, vol. 156, p. 106630, Nov. 2021, doi: 10.1016/j.envint.2021.106630.

[94] I. Blaženović, T. Kind, J. Ji, and O. Fiehn, "Software Tools and Approaches for Compound Identification of LC-MS/MS Data in Metabolomics," *Metabolites*, vol. 8, no. 2, p. 31, Jun. 2018, doi: 10.3390/metabo8020031.

[95] N. Caballero-Casero *et al.*, "Towards harmonised criteria in quality assurance and quality control of suspect and non-target LC-HRMS analytical workflows for screening of emerging contaminants in human biomonitoring," *TrAC Trends Anal. Chem.*, vol. 136, p. 116201, Mar. 2021, doi: 10.1016/j.trac.2021.116201.

[96] N. Alygizakis *et al.*, "Towards a harmonized identification scoring system in LC-HRMS/MS based non-target screening (NTS) of emerging contaminants," *TrAC Trends Anal. Chem.*, vol. 159, p. 116944, Feb. 2023, doi: 10.1016/j.trac.2023.116944.

[97] J. Hollender *et al.*, "NORMAN guidance on suspect and non-target screening in environmental monitoring," *Environ. Sci. Eur.*, vol. 35, no. 1, p. 75, Sep. 2023, doi: 10.1186/s12302-023-00779-4.

[98] B. Rochat, "Proposed Confidence Scale and ID Score in the Identification of Known-Unknown Compounds Using High Resolution MS Data," *J. Am. Soc. Mass Spectrom.*, vol. 28, no. 4, pp. 709–723, Apr. 2017, doi: 10.1007/s13361-016-1556-0.

[99] J. Liigand, T. Wang, J. Kellogg, J. Smedsgaard, N. Cech, and A. Kruve, "Quantification for non-targeted LC/MS screening without standard substances," *Sci. Rep.*, vol. 10, no. 1, p. 5808, Apr. 2020, doi: 10.1038/s41598-020-62573-z.

[100] L. Malm *et al.*, "Quantification Approaches in Non-Target LC/ESI/HRMS Analysis: An Interlaboratory Comparison," *Anal. Chem.*, vol. 96, no. 41, pp. 16215–16226, Oct. 2024, doi: 10.1021/acs.analchem.4c02902.

[101] D. Broadhurst *et al.*, "Guidelines and considerations for the use of system suitability and quality control samples in mass spectrometry assays applied in untargeted clinical metabolomic studies," *Metabolomics*, vol. 14, no. 6, p. 72, May 2018, doi: 10.1007/s11306-018-1367-3.

[102] W. B. Dunn, I. D. Wilson, A. W. Nicholls, and D. Broadhurst, "The importance of experimental design and QC samples in large-scale and MS-driven untargeted metabolomic studies of humans," *Bioanalysis*, vol. 4, no. 18, pp. 2249–2264, Sep. 2012, doi: 10.4155/bio.12.204.

[103] K. T. Peter *et al.*, "Nontargeted Analysis Study Reporting Tool: A Framework to Improve Research Transparency and Reproducibility," *Anal. Chem.*, vol. 93, no. 41, pp. 13870–13879, Oct. 2021, doi: 10.1021/acs.analchem.1c02621.

[104] W. B. Dunn *et al.*, "Procedures for large-scale metabolic profiling of serum and plasma using gas chromatography and liquid chromatography coupled to mass spectrometry," *Nat. Protoc.*, vol. 6, no. 7, pp. 1060–1083, Jul. 2011, doi: 10.1038/nprot.2011.335.

[105] E. Adua *et al.*, "Multi-block data integration analysis for identifying and validating targeted N-glycans as biomarkers for type II diabetes mellitus," *Sci. Rep.*, vol. 12, no. 1, p. 10974, Jun. 2022, doi: 10.1038/s41598-022-15172-z.

[106] T. Downing and N. Angelopoulos, "A primer on correlation-based dimension reduction methods for multi-omics analysis," *J. R. Soc. Interface*, vol. 20, no. 207, p. 20230344, doi: 10.1098/rsif.2023.0344.

[107] A. Singh *et al.*, "DIABLO: an integrative approach for identifying key molecular drivers from multi-omics assays," *Bioinforma. Oxf. Engl.*, vol. 35, no. 17, pp. 3055–3062, Sep. 2019, doi: 10.1093/bioinformatics/bty1054.

[108] J. A. Westerhuis *et al.*, "Assessment of PLSDA cross validation," *Metabolomics*, vol. 4, no. 1, pp. 81–89, Mar. 2008, doi: 10.1007/s11306-007-0099-6.

[109] R. A. van den Berg, H. C. J. Hoefsloot, J. A. Westerhuis, A. K. Smilde, and M. J. van der Werf, "Centering, scaling, and transformations: improving the biological information content of metabolomics data," *BMC Genomics*, vol. 7, p. 142, Jun. 2006, doi: 10.1186/1471-2164-7-142.

[110] M. D. Wilkinson *et al.*, "The FAIR Guiding Principles for scientific data management and stewardship," *Sci. Data*, vol. 3, no. 1, p. 160018, Mar. 2016, doi: 10.1038/sdata.2016.18.

[111] European Union, "Regulation (EU) 2016/679 of the European Parliament and of the Council of 27 April 2016 on the protection of natural persons with regard to the

processing of personal data and on the free movement of such data, and repealing Directive 95/46/EC (General Data Protection Regulation) (Text with EEA relevance)." Official Journal of the European Union, Apr. 27, 2016. Accessed: Jan. 20, 2026. [Online]. Available: http://data.europa.eu/eli/reg/2016/679/oj

[112] A. Mueller-Schoell *et al.*, "Therapeutic drug monitoring of oral targeted antineoplastic drugs," *Eur. J. Clin. Pharmacol.*, vol. 77, no. 4, pp. 441–464, Apr. 2021, doi: 10.1007/s00228-020-03014-8.

[113] S. Velghe, S. Deprez, and C. P. Stove, "Fully automated therapeutic drug monitoring of anti-epileptic drugs making use of dried blood spots," *J. Chromatogr. A*, vol. 1601, pp. 95–103, Sep. 2019, doi: 10.1016/j.chroma.2019.06.022.

[114] S. G. Wicha, M. G. Kees, A. Solms, I. K. Minichmayr, A. Kratzer, and C. Kloft, "TDMx: A novel web-based open-access support tool for optimising antimicrobial dosing regimens in clinical routine," *Int. J. Antimicrob. Agents*, vol. 45, no. 4, pp. 442–444, Apr. 2015, doi: 10.1016/j.ijantimicag.2014.12.010.

[115] M. Deppenweiler *et al.*, "Towards therapeutic drug monitoring of everolimus in cancer? Results of an exploratory study of exposure-effect relationship," *Pharmacol. Res.*, vol. 121, pp. 138–144, Jul. 2017, doi: 10.1016/j.phrs.2017.04.029.

[116] M. Briki *et al.*, "Liquid chromatography coupled to tandem mass spectrometry (LC-MS/MS) methods for the therapeutic drug monitoring of cytotoxic anticancer drugs: An update," *J. Chromatogr. B*, vol. 1236, p. 124039, Apr. 2024, doi: 10.1016/j.jchromb.2024.124039.

[117] S. Ishida, J. Lee, D. J. Thiele, and I. Herskowitz, "Uptake of the anticancer drug cisplatin mediated by the copper transporter Ctr1 in yeast and mammals," *Proc. Natl. Acad. Sci. U. S. A.*, vol. 99, no. 22, pp. 14298–14302, Oct. 2002, doi: 10.1073/pnas.162491399.

[118] L. H. Matherly, Z. Hou, and Y. Deng, "Human reduced folate carrier: translation of basic biology to cancer etiology and therapy," *Cancer Metastasis Rev.*, vol. 26, no. 1, pp. 111–128, Mar. 2007, doi: 10.1007/s10555-007-9046-2.

[119] M. Molina-Arcas *et al.*, "Human equilibrative nucleoside transporter-1 (hENT1) is required for the transcriptomic response of the nucleoside-derived drug 5′-DFUR in breast cancer MCF7 cells," *Biochem. Pharmacol.*, vol. 72, no. 12, pp. 1646–1656, Dec. 2006, doi: 10.1016/j.bcp.2006.07.036.

[120] G. Pron *et al.*, "Internalisation of the bleomycin molecules responsible for bleomycin toxicity: a receptor-mediated endocytosis mechanism," *Biochem. Pharmacol.*, vol. 57, no. 1, pp. 45–56, Jan. 1999, doi: 10.1016/S0006-2952(98)00282-2.

[121] C. A. Claussen and E. C. Long, "Nucleic Acid recognition by metal complexes of bleomycin," *Chem. Rev.*, vol. 99, no. 9, pp. 2797–2816, Sep. 1999, doi: 10.1021/cr980449z.

[122] V. Murray, J. K. Chen, and L. H. Chung, "The Interaction of the Metallo-Glycopeptide Anti-Tumour Drug Bleomycin with DNA," *Int. J. Mol. Sci.*, vol. 19, no. 5, p. 1372, May 2018, doi: 10.3390/ijms19051372.

[123] S. M. Mohammed *et al.*, "Mechanisms of Bleomycin-induced Lung Fibrosis: A Review of Therapeutic Targets and Approaches," *Cell Biochem. Biophys.*, vol. 82, no. 3, pp. 1845–1870, Sep. 2024, doi: 10.1007/s12013-024-01384-9.

[124] L. G. Campana *et al.*, "Recommendations for improving the quality of reporting clinical electrochemotherapy studies based on qualitative systematic review," *Radiol. Oncol.*, vol. 50, no. 1, pp. 1–13, Mar. 2016, doi: 10.1515/raon-2016-0006.

[125] A. Vižintin, S. Marković, J. Ščančar, and D. Miklavčič, "Electroporation with nanosecond pulses and bleomycin or cisplatin results in efficient cell kill and low metal release from electrodes," *Bioelectrochemistry*, vol. 140, p. 107798, Aug. 2021, doi: 10.1016/j.bioelechem.2021.107798.

[126] I. Crnovcic, F. Gan, D. Yang, L.-B. Dong, P. G. Schultz, and B. Shen, "Activities of recombinant human bleomycin hydrolase on bleomycins and engineered analogues revealing new opportunities to overcome bleomycin-induced pulmonary toxicity," *Bioorg. Med. Chem. Lett.*, vol. 28, no. 16, pp. 2670–2674, Sep. 2018, doi: 10.1016/j.bmcl.2018.04.065.

[127] "Bleomycin sulphate," in *European pharmacopoeia*, 10th ed., vol. 2020, Council of Europe, pp. 1114–1115.

[128] N. Thakrar and K. T. Douglas, "Photolability of bleomycin and its complexes," *Cancer Lett.*, vol. 13, no. 3, pp. 265–268, Aug. 1981, doi: 10.1016/0304-3835(81)90027-6.

[129] L. M. Mir, S. Orlowski, J. Belehradek, and C. Paoletti, "Electrochemotherapy potentiation of antitumour effect of bleomycin by local electric pulses," *Eur. J. Cancer Clin. Oncol.*, vol. 27, no. 1, pp. 68–72, Jan. 1991, doi: 10.1016/0277-5379(91)90064-K.

[130] G. Pron *et al.*, "Internalisation of the bleomycin molecules responsible for bleomycin toxicity: a receptor-mediated endocytosis mechanism," *Biochem. Pharmacol.*, vol. 57, no. 1, pp. 45–56, Jan. 1999, doi: 10.1016/S0006-2952(98)00282-2.

[131] G. Ciarimboli, "Membrane transporters as mediators of Cisplatin effects and side effects," *Scientifica*, vol. 2012, p. 473829, 2012, doi: 10.6064/2012/473829.

[132] M. Visentin, R. Zhao, and I. D. Goldman, "The Antifolates," *Hematol. Oncol. Clin. North Am.*, vol. 26, no. 3, pp. 629–ix, Jun. 2012, doi: 10.1016/j.hoc.2012.02.002.

[133] R. Zhao and I. D. Goldman, "Resistance to antifolates," *Oncogene*, vol. 22, no. 47, pp. 7431–7457, Oct. 2003, doi: 10.1038/sj.onc.1206946.

[134] S. R. Munnangi *et al.*, "Drug complexes: Perspective from Academic Research and Pharmaceutical Market," *Pharm. Res.*, pp. 1–22, May 2023, doi: 10.1007/s11095-023-03517-w.

[135] J. Nagaj, P. Kołkowska, A. Bykowska, U. K. Komarnicka, A. Kyzioł, and M. Jeżowska-Bojczuk, "Interaction of methotrexate, an anticancer agent, with copper(II) ions: coordination pattern, DNA-cleaving properties and cytotoxic studies," *Med. Chem. Res.*, vol. 24, no. 1, pp. 115–123, Jan. 2015, doi: 10.1007/s00044-014-1074-1.

[136] V. A. Rao, "Iron Chelators with Topoisomerase-Inhibitory Activity and Their Anticancer Applications," *Antioxid. Redox Signal.*, vol. 18, no. 8, pp. 930–955, Mar. 2013, doi: 10.1089/ars.2012.4877.

Bibliography

Publications Related to the Thesis

Journal Articles

Plešnik, H., Omerzel, M., Čemažar, M., Serša, G., & Kosjek, T. (2023). An effective validation of analytical method for determination of a polar complexing agent: The illustrative case of cytotoxic bleomycin. Analytical and Bioanalytical Chemistry, 415(14), 2737–2748. doi:10.1007/s00216-023-04675-x

Grošelj, A., Bošnjak, M., Krzan, M., Kosjek, T., Bottyán, K., Plešnik, H., Jamšek, Č., Čemažar, M., Kis, E., & Serša, G. (2021). Bleomycin concentration in patients' plasma and tumors after electrochemotherapy: A study from InspECT Group. Pharmaceutics, 13(9), 1324–1324. doi:10.3390/pharmaceutics13091324

Plešnik, H., Vižintin, A., Miklavčič, D., Steed, J., Stahl-Zeng, J., & Kosjek, T. (2025). Quantitative analysis of trace-level bleomycin in complex matrices: Application to in vitro electrochemotherapy. Journal of Pharmaceutical and Biomedical Analysis, 263, 116927. doi:10.1016/j.jpba.2025.116927

Plešnik, H., Rekar, Ž., Stevanović, S., Virant-Klun, I., Imamović Kumalić, S., Sladić, M., Mazej, D., Snoj Tratnik, J., Horvat, M., & Kosjek, T. (2025). Nontargeted urinary profiling strategy for endocrine-disrupting chemicals in women with ovarian malignancies. Environmental Science & Technology, 59(17), 8380-8390. doi:10.1021/acs.est.4c13290

Pasković, I., Andlovic, M., Plešnik, H., Vavpetič, P., Žurga, P., Popović, L., Šala, M., Franić, M., Dlačić, I., Goreta Ban, S., Polić Pasković, M., Kosjek, T., & Pongrac, P. (2026). Foliar application of protein hydrolysates promotes growth and affects leaf ionome in olive. Horticulturae, 12(2), 151. doi:10.3390/horticulturae12020151

Moufawad, T., Ayeni, K., Baira, E., Baudry, C., Belova, L., Chaker, J., Chalet, C., Covaci, A., Damont, A., David, A., Fernandez, M. F., Habchi, B., Huber, C., Jadé, G., Kosjek, T., Krauss, M., Laurentie, M., Ndaw, S., Nijssen, R., Oberacher, H., Plešnik, H., Rekar, Ž., Rizzo, S., Salamanca-Fernandez, E., Termentzi, A., Vorkamp, K., Warth, B., Zhu, L., Kasiotis, K. M., Le Bizec, B., Lamoree, M., & Antignac, J.-P. (submitted, 2026). Comparing non-targeted screening workflows for perinatal chemical exposome analysis: A European interlaboratory study from the PARC EU project.

Habchi, B., Martin Remy, A., Belova, L., Covaci, A., Damont, A., Kosjek, T., Huber, C., Grova, N., Antoine, G., Moufawad, T., Baira, E., Baudry, C., Chalet, C., Dervilly, G., Duca, R. C., Fenaille, F., Fernández, M. F., Gabriel, C., Huet, C., Jadé, G.,

Kajtazi, A., Kärkkäinen, O., Kasiotis, K. M., Kevrekidou, A., Koudelka, Š., Kozlowska, L., Lamoree, M., Iamiceli, A. L., Laurentie, M., Le Bizec, B., Nieuwenhuyse, A., Nijssen, R., Oberacher, H., Plešnik, H., Price, E. J., Rekar, Ž., Rodriguez-Carrillo, A., Santo, R., Sarigiannis, D., Savignac, J.-M., Stelmasiak, M., Sunnarborg, K., Termentzi, A., Vuillaume, R., Schymanski, E. L., Rutledge, D. N., Antignac, J.-P., & Ndaw, S. (submitted, 2026). Comparative assessment of suspect / non-target screening workflows for characterizing occupational human internal chemical exposure: Results of a European interlaboratory study from the EU-PARC project.

Rekar, Ž., Plešnik, H., Tkalec, Ž., Srnovršnik, T., Virant-Klun, I., Pinter, B., Mazej, D., Horvat, M., & Kosjek, T. (in preparation). Integrated non-targeted exposomics and metabolomics reveal elevated endocrine-disrupting chemical burden and altered steroid metabolism in women with PCOS.

Other Publications

Journal Articles

Zugan, M., Plešnik, H., Rijavec, T., Kosjek, T., & Lapanje, A. (in preparation). Unleashing Nature's Recycling Power: Paraburkholderia sp. L4 strain converts lignin into valuable resources.

Rekar, Ž., De Santo, R., Stevanović, S., Plešnik, H., Moufawad, T., Antignac, J.-P., Habchi, B., Ndaw, S., Vorkamp, K., Zhu, L., Jamin, E. L., Iamiceli, A. L., & Kosjek, T. (in preparation). Supramolecular solvent (SUPRAS)-based extraction as a complementary strategy for extended urinary exposome profiling.

Conference Papers

Plešnik, H., & Kosjek, T. (2021). Bias in analytical methods: Bleomycin case study. In Throughout Knowledge Towards a Green New World: 13th Jožef Stefan International Postgraduate School Students' Conference and 15th Young Researchers' Day (pp. 19–20). Ljubljana, Slovenia.

Plešnik, H., Tkalec, Ž., Zugan, M., Lapanje, A., & Kosjek, T. (2022). Determination of the products of bacterial lignin degradation: Targeted and non-targeted screening. In Proceedings of the 22nd European Meeting on Environmental Chemistry (p. 106). Ljubljana, Slovenia.

Plešnik, H., Tkalec, Ž., Zugan, M., Lapanje, A., & Kosjek, T. (2022). LC-MS/MS determination of the products of bacterial lignin degradation. In Week of Microbial Technologies: Book of Abstracts (pp. 74–75).

Plešnik, H., Tkalec, Ž., Zugan, M., Lapanje, A., & Kosjek, T. (2022). LC-MS/MS determination of the products of bacterial lignin degradation. In Metabolomics 2022: 18th Annual Conference of the Metabolomics Society (p. 251).

Plešnik, H., Omerzel, M., Čemažar, M., Serša, G., & Kosjek, T. (2023). LC-MS determination of bleomycin in biological and pharmaceutical specimens. In Proceedings of the 71st ASMS Conference on Mass Spectrometry and Allied Topics. Houston, TX, USA.

Plešnik, H., Rekar, Ž., & Kosjek, T. (2024). Comprehensive non-targeted UHPLC-HRMS analysis of urinary exposome using integrated HILIC and reversed-phase approaches. In Proceedings of the 4th Nordic Metabolomics Conference (p. 71). Turku, Finland.

Plešnik, H., Rekar, Ž., Stevanović, S., Virant-Klun, I., Imamović Kumalić, S., Sladić, M., Mazej, D., Snoj Tratnik, J., Horvat, M., & Kosjek, T. (2025). Non-Targeted Screening of Urinary Biomarkers Identifies Endocrine Disruptors Linked to Ovarian Malignancies. In Metabolomics 2025: 21st Annual Conference of the Metabolomics Society (p. 254).

Biography

Education and research activities:

- 2020 - present: Jožef Stefan International Postgraduate School, Ljubljana: PhD student of Ecotechnology
- 2014 - 2020: University of Ljubljana, Faculty of Pharmacy, Master' s degree in Pharmacy

Foreign work and study experience:

- 2017: Eberhard-Karls Universität Tübingen, study exchange (6 months)
- 2023 (1 week): AB Sciex UK
- 2026 (1 month): LABERCA, France

Research projects:

- J4-2546: Monitoring the clinical and immune response to improve the outcome of combined electrochemotherapy and IL-12 gene therapy in dogs with spontaneous peripheral tumours
- J3-9269: Clinical pharmacological approach to optimization of therapeutic concentration of bleomycin treatment with electrochemotherapy
- P2-0249: Electroporation in biology, biotechnology and medicine
- UIA02-228: Alien PLAnt SpEcies - from harmful to useful with citizens' led activities (APPLAUSE)
- 101057014: Partnership for the Assessment of Risks from Chemicals (PARC):
    - 4.3.2.a_Y1: H01 Perinatal exposure, 4.3.2.b_Y2: H02 Occupational exposure,
    - 4.3.2.c_Y3: H03 Complementary developments, 4.2.1.a_Y1 ENVMonitoringPilotSurvey
- J7-4635: Preclinical development of new Mitochondrial ion channel inhibitors for Cancer therapy (MitoCan)
- J4-2550: Identifying the genetic determinants of chemical toxicity in the green alga Chlamydomonas reinhardtii
- J3-2530: Effect of endocrine disruptors (bisphenols, parabens, triclosan) and potentially toxic and essential chemical elements on the birth, infertility and ovarian cancer in Slovenia
- I0-0005 Infrastructure program of Jožef Stefan Institute
- J7-50230 Building Efficient NCDs (NonCommunicable Diseases) Early Warning Tools (BE NEWT)

Conferences:

- 13th Jožef Stefan International Postgraduate School Students' Conference and 15th Young Researchers' Day, online, 2021
- 17th RECETOX Summer School 2021, 2021, Online
- Metabolomics 2022 Conference, Valencia, Spain
- ASMS Annual Conference, Houston, TX, USA
- The first Slovenian Congress on Electroporation, 2023, Bled, Slovenia
- The European Meeting on Environmental Chemistry, 2022, Ljubljana
- Week of Microbial Technologies, 2022, online
- The fourth Nordic Metabolomics Conference, 2024, Turku, Finland
- Metabolomics 2025 Conference, Prague, Czech Republic

Awards

- Excellent in science award (ARIS), Plešnik, H., Rekar, Ž., Stevanović, S., Virant-Klun, I., Imamović Kumalić, S., Sladić, M., Mazej, D., Snoj Tratnik, J., Horvat, M., & Kosjek, T. (2025). Nontargeted urinary profiling strategy for endocrine-disrupting chemicals in women with ovarian malignancies. Environmental Science & Technology, 59(17), 8380-8390. doi:10.1021/acs.est.4c13290

Research interests: non-targeted screening, exposomics, environmental health, metabolomics, polar compounds analysis, pharmacotherapy analysis